Molecular Genetics of Dupuytren´s Disease

Inaugural-Dissertation

zur

Erlangung des Doktorgrades

der Mathematisch-Naturwissenschaftlichen Fakultät

der Universität zu Köln

vorgelegt von

Kerstin Becker

aus Köln

2012

Berichterstatter: Prof. Dr. Peter Nürnberg

(Gutachter) Prof. Dr. Angelika A. Noegel

Tag der mündlichen Prüfung: 22.01.2013

Abstract

Dupuytren's disease (DD) is a fibromatosis of connective tissue within the palm of the hands. It is characterised by progressive collagen deposition that leads to hardening and thickening of the connective tissue and results in permanent contraction of affected fingers. The aetiology of Dupuytren's disease is so far unknown and the pathogenesis is favoured by ageing, genetic predisposition, mechanic trauma and possibly other risk factors. Blood and tissue samples of over 850 German and Swiss DD patients were collected in order to analyse the genetics, gene expression patterns and the *in vitro* behaviour of disease tissue derived fibroblast in 2-D and 3-D models.

A genome wide association study (GWAS) with 565 unrelated DD patients and 1,219 controls was performed. Data for 5,204,451 single-nucleotide polymorphisms (SNPs; 186 cases genotyped with Affymetrix Genome-Wide Human SNP Array 6.0 and 379 cases, 1219 controls genotyped with Axiom CEU 1 Array; data imputed with HapMap CEU reference panel) were analyzed for association with DD. SNP rs2290221 on chromosome 7p14, showed the strongest association signal with a p-value of 2.2×10^{-10} and odds ratio of 2.13. SNP rs2290221 is located intronic of the genes secreted frizzled-related protein 4 (SFRP4) and ependymin related protein 1 (zebrafish) (EPDR1).

In addition an integrative replication study with 2,325 Dutch, English and German DD cases and 11,562 controls was performed. It identified nine different susceptibility loci that showed genome-wide significance. Six of these loci contain genes known to be involved in the Wnt/β-catenin signalling pathway. Again the strongest association was seen for the 7p14 locus.

Consistent with GWAS findings, a whole genome expression analysis with 12 DD primary disease tissue samples and 12 normal fascia controls revealed upregulation of the Wnt/β-catenin signalling pathway and also changes in mitochondrial function and oxidative stress response in disease tissue. The Wnt signalling pathway is therefore likely to be a key player in the fibromatosis process observed in DD. Primary disease tissue derived fibroblasts at least in part retained their disease associated characteristics *in vitro*, they exhibited higher proliferation rates and generated strong contraction forces in 3-D collagen gels, and thus present an excellent model for investigating the mechanisms of DD in the context of aging and aging associated diseases.

Zusammenfassung

Bei der Dupuytren´schen Erkrankung (DD) handelt es sich um eine Fibromatose des Bindegewebes in der Handinnenfläche und der Innenseite der Finger. Im Verlauf der Krankheit verhärtet und verdickt sich das Bindegewebe aufgrund progressiver Kollagenablagerungen. Dies führt zu einer dauerhaften Kontraktion von betroffenen Fingern. Die Ursache des Morbus Dupuytren ist bisher unbekannt. Der Krankheitsverlauf wird durch Alter, genetische Veranlagung, mechanische Traumata und möglicherweise weitere Risikofaktoren begünstigt. Von über 850 deutschen und Schweizer DD-Patienten wurden Blut und Gewebeproben gesammelt, um die Genetik, Genexpression und das *In-vitro*-Verhalten von Fibroblasten in 2-D und 3-D-Modelle zu analysieren.

In einer genomweiten Assoziations-Studie (GWAS) wurden 565 DD-Patienten und 1.219 Kontrollen miteinander verglichen. Dabei wurden 5.204.451 genetische Marker (single-nucleotide polymorphisms (SNPs)) untersucht. SNP rs2290221 auf Chromosom 7p14, zeigte das stärkste Assoziationssignal mit einem P-Wert von $2,2 \times 10^{-10}$ und eine Odds Ratio von 2,13. SNP rs2290221 befindet sich im Intron der beiden Gene secreted frizzled-related protein 4 (SFRP4) und ependymin related protein 1 (zebrafish) (EPDR1).

Parallel dazu wurde eine integrative Replikations-Studie mit 2325 Niederländisch, Deutsch und Englisch DD Patienten und 11.562 Kontrollen durgeführt. Diese identifizierte neun verschiedene Loci, die mit genomweiter Signifikanz mit DD assoziierten. Sechs dieser Loci enthalten Gene, die im Wnt/β-catenin-Signalweg eine Rolle spielen.

In Übereinstimmung mit den GWAS Erkenntnisse ergab eine genomeweite Expressions-Analyse, bei der 12 DD- und 12 Kontroll-Gewebeproben miteinander verglichen wurden, eine Hochregulation des Wnt/β-Catenin-Signalweges in den DD Proben. Außerdem wurden Veränderungen in der oxydative Stressreaktion festgestellt. Der Wnt-Signalweg stellte daher wahrscheinlich eine wichtige Komponente im Krankheitsprozess dar. Primäre Fibroblasten, die aus DD Gewebe gewonnen wurden, behielten zum Teil ihre mit der Krankheit verbundenen Eigenschaften *in vitro*. Sie zeigten eine höhere Proliferationsrate und erzeugt starke Kontraktionskräfte in 3-D Kollagengelen. Sie stellen somit ein hervorragendes Modell dar für die Untersuchung der Krankheitsmechanismen im Kontext des Alterns und alters-assoziierter Krankheiten.

Table of Content

1 Introduction

1.1 Aging and Aging Associated Diseases

Aging is a progressive process that leads to death. It is characterised by decline in body functions and loss of fertility. Aging occurs in many organisms although bacteria and some multicellular organisms e.g. Hydra do not age. In general all organisms with clear separation of soma and germline are thought to undergo aging. On the cellular level the loss of replicative capacity is called senescence.

There are several theories that try to explain aging from an evolutionary point of view. Kirkwood and Austad (2000) argued that animals in the wild mostly die early in life of extrinsic hazards, e.g. infection, predation or starvation and only very few animals live long enough to die of old age. Consequently evolutionary aging theories explain the aging process not as a trait under natural selection but as a by-product of life. In the "mutation accumulation" theory, first developed by P.B. Medawar (1952), delirious mutations that affect late stages in life but have no impact on the earlier phases (e.g. reproduction) accumulate over generations because there is no selection against them (Martin *et al*. 1996, Kirkwood and Austad 2000, Charlesworth 2001). One human example for this may be Huntington's disease, which is caused by a dominant mutation that was not selected against because the disease manifests only after the onset of reproduction (Partridge and Gems 2002). The "pleiotropy" or "trade-off" theory (Williams 1957) states that a mutation with positive effect early in life is favoured by selection regardless of possible deleterious effects the same mutation has late in life if the probability of surviving to be affected is small. Support for this theory is thought to come from experiments with Drosophila melanogaster where early reproducing flies were short lived compared to late reproducing ones (Partrigde and Gems 2002). One consistent observation in humans was that women who lived to the age of 100 years were four times more likely to have had children while in their forties than women who survived to age 73 (Perls *et al*. 1997). The "disposable soma" theory (Kirkwood 1977), is based on optimal allocation of limited metabolic resources between somatic maintenance and reproduction. Because metabolic resources are limited investment in e.g. reproduction at the expense of repair allows damage to accumulate with age (Kirkwood and Austad 2000).

All these theories are based on the observation that death in wild living animals is primarily caused by extrinsic factors at a young age. But looking at survival curves (Kirkwood and Austad 2000) may only reveal part of the age-structure of populations. Another point of view

is offered by mortality curves. Especially in larger animals (mammals) mortality by extrinsic hazards is high in newborn animals and may peak again when offspring leave their parental care and e.g. try to establish a territory. Only individuals that live beyond this point may reproduce. At the same time these individuals also have a higher chance to reach old age. Therefore the aging process may have a larger effect on the population subgroup that reproduces than on the whole population itself.

Although aging is not an ordered process under natural selection like development, it is still a common process that is regulated through common mechanisms in different (model) animals (Partrigde and Gems 2002). That is because aging is affected by common genetically controlled processes, reproduction and damage repair that are conserved in animals. Several studies from Drosophila melanogaster and Caenorhabditis elegans show that fecundity and lifespan are inversely connected (Sgrò and Partridge 1999, Friedman and Johnson 1988). In humans extrinsic hazards have been greatly reduced in developed countries resulting in proportionately more and older old people. Aging associated diseases are therefore more common forming serious health and resource (cost) issues. The arising interest in aging and aging associated diseases results mainly from the questions how we age, and how healthy aging can be achieved. To answer these questions one has to study the mechanisms of aging on cellular and molecular level downstream of its evolutionary origin.

1.1.1 Free Radical Theory of Aging

Again several theories were developed that try to explain the molecular mechanisms that drive the aging process. Most prominent among these is the Free Radical Theory of Aging (also termed Mitochondrial Free Radical Theory of Aging (MFRTA) or Oxidative Stress Theory of Aging (OSTA)). It states that the damage of reactive oxygen species (ROS) accumulates over time and that this damage to macromolecules and cells underlies the aging process. Since it was first proposed (Harman 1956) this theory was much discussed because it remains difficult to prove. Long lived species show reduced ROS production compared to short lived species (Sanz *et al*. 2010, Lambert *et al*. 2007, Sohal *et al*. 1995, Ku and Sohal 1993), with exceptions (Andziak *et al*. 2005). But experimental manipulations to reduce or increase ROS production rather did not result in increased or reduced lifespan, respectively (Sanz *et al*. 2010, Pérez *et al*. 2009, and Doonan *et al*. 2008). Nevertheless the production of ROS is a complex process whose disruption in disease and aging leads to oxidative damage (de Magalhães and Church 2006). Other theories were developed highlighting other important processes that get deregulated with age and that may be associated with

(disrupted) ROS production. The immune system may play an important role in the aging process. The Immune oxidation-inflammation theory of aging tries to link oxidative damage in cells of the immune system to aging (De la Fuente 2008). Most age-related diseases are associated with a low level of chronic inflammation (De la Fuente and Miquel 2009) and the immune system is a source of ROS. Neutrophils, macrophages, dendritic cells and monocytes release ROS (oxidative burst), as part of their innate immune function towards different pathogens (Cannizzo *et al*. 2011, Cathcart 2004, Park 2003). Another line of argument highlights that protein aggregates accumulated in aging cells. These are removed by autophagy and lysosomal degradation (Terman *et al*. 2006). Lysosoms are especially sensitive to ROS and may therefore also play an important part in the aging process. The mechanisms of ROS function in conjunction with oxidative stress shall be discussed in greater detail in chapter 1.3 of this introduction.

1.1.2 Insulin/IGF Signalling and Aging

The best studied signalling pathway involved in aging is the Insulin signalling pathway. C. elegans strains with mutations in components of this pathway have extended lifespans (Ogg *et al*. 1997, Kimura *et al*. 1997, Kenyon *et al*. 1993, Friedman *et al*. 1988). In the worm food stimulates the secretion of insulin-like hormones by chemosensory neurons. These bind to the neuronal receptor Daf-2. Upon receptor binding intracellular signalling leads to the inhibition of Daf-16, a transcription factor that regulates e.g. the transcription of genes involved in ROS reduction (superoxide dismutase (SOD2, SOD3) and catalase) (Honda and Honda 1999, Murphy *et al*. 2003, Lee *et al*. 2003). In mammals there are three related receptors: the insulin receptor (Insr), the insulin-like growth factor 1 (Igf1) receptor and the insulin receptor-related receptor (Insrr). A decrease in insulin/Igf1 signalling has been shown to extend longevity in mice (Brown-Borg *et al*. 1996, Coschigano *et al*. 2000, Flurkey *et al*. 2001). Mutations in these mice affect the activities of the multiple components of these signalling pathways, i.e. phosphatidylinositol-3-phosphate (PI3K), Akt and Forkhead proteins (FOXO) (Blüher *et al*. 2003; Holzenberger *et al*. 2003) which are also targets of the ROS-mediated redox pathways (Papaconstantinou 2009).

These last findings come from research on model organisms (yeast, worm, fly, and mouse). Another approach to access aging mechanisms is the study of aging associated diseases. In the developed countries aging was proposed to be the major risk factor for diseases and death in humans after the age of 28 (Harman 2006). Therefore studying aging associated diseases is one important approach to access healthy aging in humans.

1.2   Dupuytren´s Disease

Dupuytren's disease (DD) (OMIM 126900) is one of the most common genetic disorders of connective tissue (CT). Patients develop non-malignant (benign) CT tumours in the palm of the hand and in the fingers (fibromatosis). The fibromatosis is characterised histological by the proliferation of fibroblasts and the massive deposition of collagen. The tumour shows an aggressive clinical behaviour with frequent local recurrence.

Connective Tissue (CT) is one of the four traditional classes of tissues (the others being epithelial, muscle, and nervous tissue). It is found throughout the body and consists mostly of extracellular matrix (ECM) that can be either loosely or densely packed. Collagen is the main component of connective tissue in animals and also the most abundant protein in mammals, making up about 25% of the total protein content. There are also specialised CT subtypes which include cartilage, bone, blood, adipose, haematopoietic and lymphatic tissue.

A prominent CT structure in the palm of the hand that is affected by DD is the superficial palmar fascia (palmar aponeurosis), which forms a thin triangular layer of connective tissue underlying the dermis in the palm of the hand and extending into the fingers (see figure 1 and 2). It is attached to the undersurface of the skin above it and the bones and muscle coverings below it. The superficial palmar fascia acts as scaffolding which anchors palm skin to the bones in the hand and maintains the shape of the skin. The fascia is a normally unnoticeable layer, with few resident cells. In DD it thickens and contracts causing permanent bending of affected fingers.
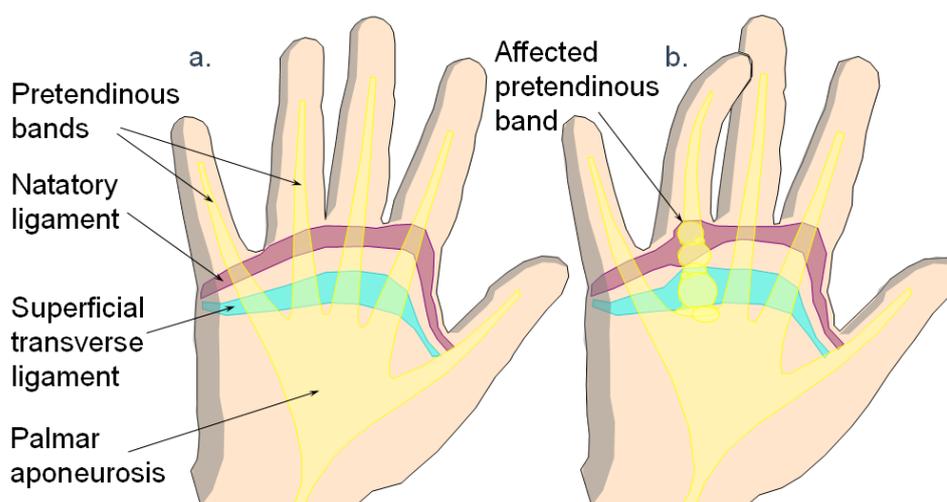
**Figure 1. Schematic representation of three main structures of the palmar fascia.
a. normal anatomy, b. Dupuytren's contracture.**

Palmar aponeurosis
dense fibrous connective tissue
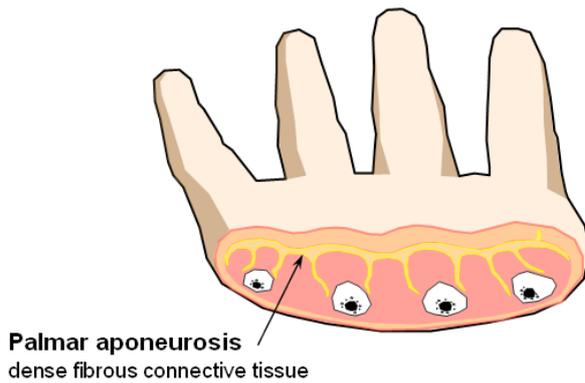
**Figure 2. Cross-section of the hand. Highlighted in yellow
is the palmar aponeurosis that partly extends into the overlying
dermis and underlying muscle layer.**

In the early stages DD affects the bands of aponeurotic fascial fibres that run longitudinally in the palm (Luck 1959) (figure 1). In the course of DD first one or more small tender lumps form in the palm of the hand, these are called nodules. These nodules are characterised by high content of proliferating fibroblasts and relatively low amounts of collagen. The skin can become attached to the nodules and invaginated (figure 4). In the progresses of the disease hard cords do form along the fascial fibres. These cords consist mostly of collagen fibres and few proliferating fibroblasts. As cords form or extent into fingers, these get contracted bending permanently towards the palm. Once contracture develops, the fingers get in the way affecting simple everyday tasks such as face washing (poking the eye with affected digit), combing hair, putting the hand in a pocket or glove, driving or playing sports. Dupuytren's disease often develops in both hands and most commonly affects the ring fingers and the little fingers, followed by the index, the middle fingers and the thumbs (Bayat and McGrouther 2006). Contractures often span several adjacent joints. For affected joints, if bending one joint allows the adjacent joint to be fully straightened and vice versa, the contracture is referred to as a "composite contracture". If an affected joint cannot be fully straightened in any hand position, the result is called a "fixed contracture". The disease may cause deformity of the affected hand, limiting hand function and diminishing the patient's quality of life (figures 3 and 4).

Figure 3. Clinical photograph showing the hands of two patients with advanced stage DD showing severe deformity. First picture (white background) from: Couto-Gonzalez *et al*. 2010. Second picture (green background) from: Howard *et al*. 2003.

Figure 4. Photograph showing a patients hand with Dupuytren's disease in digit 4. Photo: Frank C. Müller.

Three different stages of disease tissue can be defined: proliferative, involutional and residual (Luck 1959). The first stage in characterised by proliferating fibroblasts in the nodules. Cells, rather than collagen, make up a large portion of the tissue, and the nodules are likely to be vascular. In the involutional stage, fibroblasts within the nodules align along the major lines of stress, predominately in the longitudinal axes of the hand (Luck 1959). As the contracture progresses, the nodules become smaller and increasingly ill-defined. In the residual stage, the nodules disappear, leaving a hypocellular and tendon-like fibrous cord (Luck 1959). The progression through these stages varies greatly in different individuals (Shih and Bayat 2010) from an aggressive course were the disease progresses to severe contraction in a few years to mild progression with no apparent change over many years. Nodules and cords can be found simultaneously in affected tissue from one patient.

1.2.1 The Myofibroblast

The myofibroblast is the celltype thought to be responsible for the contraction on cellular level. Myofibroblasts differentiate from fibroblasts. Myofibroblasts differentiate after tissue injury. They are involved in normal wound healing and organ development (Tomasek *et al*. 2002). They synthesise ECM components, remodel the ECM and exhibit great contraction forces responsible for wound contraction leading to wound closure (Hinz *et al*. 2007).
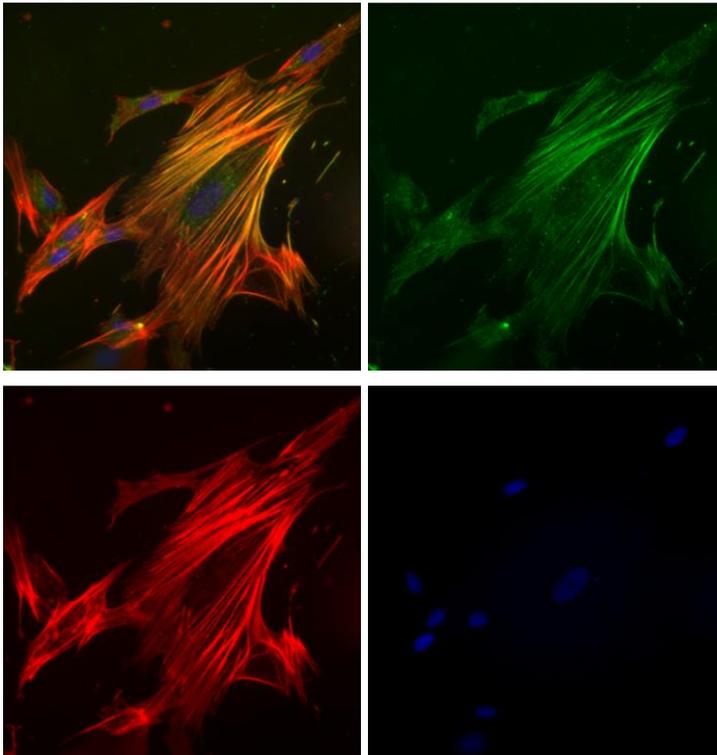
Figure 5. Immunohistological staining of a myofibroblast.
The actin filaments arrayed in parallel sheets (stress fibers)
are stained in red (phalloidin), the nucleus is stained in blue
(DAPI) and αSMA is stained in green. 40x magnification.

Unchallenged fibroblasts exhibit few or no actin-associated cell-cell and cell-matrix contacts and little ECM production (Tomasek *et al*. 2002). After tissue injury, they become activated to migrate into the damaged tissue by cytokines locally released from inflammatory cells (Werner and Grose 2003). Macrophages and T lymphocytes have been observed in DD tissue (Baird *et al*. 1993). Fibroblasts are normally shielded from mechanical stress through the ECM. Disruption of the ECM in tissue injury results in mechanic stress, which also activates fibroblasts. In response to mechanical challenge, fibroblasts produce contractile stress fibres. These are composed of cytoplasmic actins (Tomasek *et al*. 2002). Stress fibres are connected to fibrous ECM proteins at sites of integrin-containing cell-matrix junctions (Hinz 2006) and between cells via *de novo* established N-cadherin-type adherents' junctions (Hinz *et al*. 2004). Additionally differentiated myofibroblasts are defined by their *de novo*

expression of alpha smooth muscle actin (αSMA) (figure 5), which localises to stress fibres. In culture fibroblasts generate stress fibres when grown on normal plastic or glass surface. To stimulate αSMA expression fibroblast must be additionally treated with transforming growth factor beta 1 (TGFβ1) (Hinz 2006, Hinz *et al*. 2007). *In vitro* αSMA positive fibroblasts show twofold stronger contraction forces than αSMA negative fibroblasts (Hinz *et al*. 2001). At the end of tissue repair, the reconstructed ECM again takes over the mechanical load and myofibroblasts are released from stress and disappear by massive apoptosis (Tomasek *et al*. 2002).

1.2.2 History and Prevalence

DD was first described by the Swiss physician Felix Plater in 1614 and was later named after Baron Guillaume Dupuytren, a French physician, who in 1831 extensively lectured on the subject (Brenner and Rayan 2003). DD is common in the north of Europe. It is present in Germany (Brenner *et al*. 2001, Loos *et al*. 2006), Scandinavia (Bergenudd *et al*. 1993), Iceland (Guğmundsson *et al*. 2000), the UK (Gerber *et al.* 2011), and Ireland and has also been described in white populations in Northern America and Australia and in parts of Japan. It is rare in other populations, e. g. from Africa were only sporadic cases without family history are reported (Mitra and Goldstein 1994), or Asia (except Japan) (Slattery 2010). DD is significantly more frequent in the north than in the south of France (Maravic *et al*. 2005).

DD is a common disease. Estimative more than 2.3% of the German population are affected (Brenner *et al*. 2001). In UK the prevalence is about 4% in men and 2% in women (Early 1962). The prevalence of DD increases with age (Hindocha *et al*. 2009). In Iceland it increased from 7.2% in men aged 46-49 years to 39.5% in men >70 years old (Guğmundsson *et al*. 2002). Patients treated surgically for DD have an increased risk for cancer and cancer associated death (Wilbrand *et al*. 2000, Guğmundsson *et al*. 2002).

1.2.3 Treatment

There are a variety of classification systems (Rayan 1998, Woodruff *et al*. 1998, Falter *et al*. 1991, Tubiana 1986) to group disease severity. Tubiana's system (figure 6) grades the contracture into one of four stages based on the combined angles of contracture of the joints of the finger (metacarpal phalangeal (MCP) and proximal interphalangeal (PIP)). The contraction degree at each finder joint is measured and classified. Classifications from each finger can be added for one hand resulting in a maximal value of twenty.
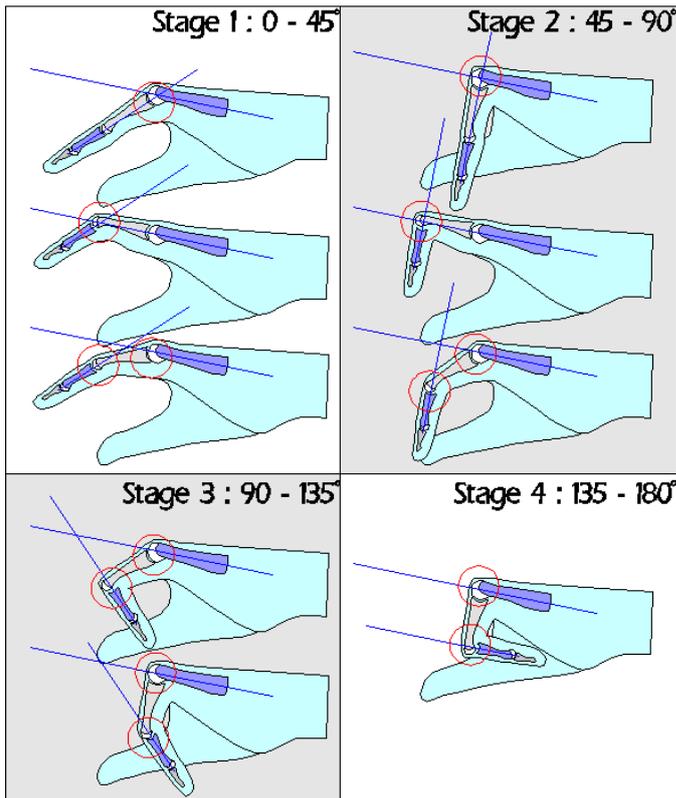
Figure 6 Tubiana's classification. It grades the contracture into one of four stages based on the combined angles of contracture of the MCP and PIP joints, and may be applied to both composite and fixed contractures: This angle is illustrated by the blue lines in this diagram. MCP: metacarpal phalangeal; PIP: proximal interphalangeal. From *www.handcenter.org*.

There is no cure for DD so far. When disease hampers finger movement corrective surgical treatment becomes necessary. Roughly two different approaches are frequently applied. The more non-invasive method involves the cutting across tight bands of diseased fascia, letting the edges gape apart and heal back at or closer to their natural length to restore the area's original flexibility (fasciotomy). This can be done without opening the affected area, by inserting a small-gauge needle through the skin along the length of the cord (needle fasciotomy). The cord is incised, using sweeping motions. Thus the cord is weakened and allows an extension force over the finger to rupture it (Desai and Hentz 2011). Most common is the surgical removal of affected tissue (limited fasciectomy) (figure 7). This procedure involves careful dissection and excision of the involved diseased fascia. After surgery, the hand is splinted, with the MCP and PIP joints in an extended position. Short- and long-term effectiveness of splinting following surgery was only poorly evaluated (Larson and Jerosch-Herold 2008). A resent non-surgical approach is based on the injection of collagenases into the affected tissue in order to resolve the collagen deposits (Hurst *et al*. 2009). Collagenase is injected directly into a Dupuytren cord, leading to lysis of the collagen

found within the diseased tissue. The patient returns the following day for joint manipulation in an attempt to rupture the cord (Desai and Hentz 2011).

Postoperative complications include haematoma, skin necrosis, infection, nerve injury, vascular injury, prolonged oedema, reflex sympathetic dystrophy and, rarely, finger loss. The most common complication is postoperative joint stiffness and loss of pre-operative flexion. Regardless of the technique, there is a high rate of recurrence following surgical correction (Bayat and McGrouther 2006, Denkler 2010). For needle fasciotomy it was in the range of 65% after 33 months (van Rijssen *et al*. 2006).
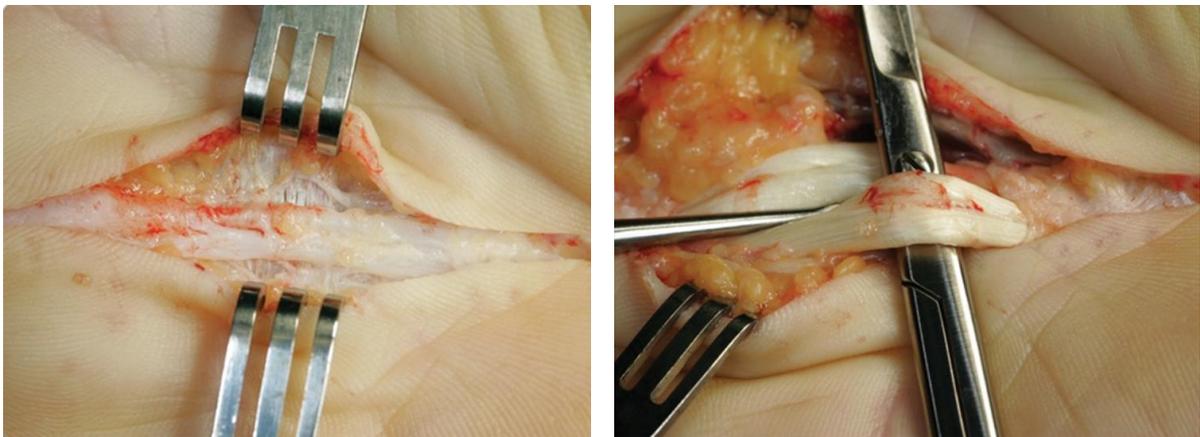
Figure 7. A. Exposure of Dupuytren's cord in the palm of the hand. From Rozen *et al*. 2012.

1.2.4 Genetics and other Risk Factors

DD is clearly an aging associated disease with onset from the fourth and fifth decade of life. A strong risk factor is male gender. Women are less severe affected and develop the disease later in live. In men the time of first surgical treatment peaks around the fifth decade of live while women mostly present for surgery approximately one decade later.

Frequent familial occurrence of DD indicates a genetic basis for the disease. Studies have determined a family predisposition in 12.5% (Brenner *et al*. 2001) and 27% of cases (Coert *et al*. 2006). Several extended pedigrees were identified particularly in Scandinavia, pointing to an autosomal dominant inheritance with reduced penetrance (Burge 1999). There is one report so far describing a whole genome approach to identifying an underlying gene in an extended Swedish family (Hu *et al*. 2005). They found linkage to an interval on chromosome 16 with a lod score value of 3.2, assuming 90% penetrance in family members over 45 years of age. Another small genome wide association study (GWAS) has been conducted with 40 cases and 40 controls (Ojwang *et al*. 2010). But no candidate genes have been identified so

far. Reduced penetrance in several pedigrees and the large number of apparently sporadic cases indicate that Dupuytren disease is a complex disease in which genetic and environmental risk factors are involved. Several environmental factors have been proposed to contribute to DD development. Smoking and alcohol consumption have been associated with DD (e.g. Burge *et al*. 1997, Godtfredsen *et al*. 2004, Guğmundsson *et al*. 2000). Elevated blood glucose levels, low body weight, and low BMI (body mass index) have also been associated with DD (Guğmundsson *et al*. 2000). Heavy manual labour and exposure to vibrations probably contribute to the disease (Liss and Stock 1996, Descatha *et al*. 2011).

DD is common among diabetes mellitus type 2 patients, but they may be in general less severe affected (Noble *et al*. 1984). In a study with epilepsy patients 56% had DD (Critchley *et al*. 1976). The authors proposed that this association is probably due to epileptic drug intake and subsequent stimulation of tissue growth factors. DD is common in patients with frozen shoulder, another fibrotic disorder (Smith *et al*. 2001). DD is rare among patients with rheumatoid arthritis (Arafa *et al*. 1984) and DD patients had less frequently stiff joints and rheumatic disorders (Guğmundsson *et al*. 1999).

1.2.5 Social Relevance and Civic Impact

DD is a common complex disorder. High prevalence rates result in considerable economic burden for treatment of this disease (Maravic *et al*. 2005, Gerber *et al.* 2011). Although DD is not life threatening it affects a constantly used tool, the hand. Finger contraction hampers already small tasks in the daily routine e.g. handshake. And patients may additionally experience pain in the affected hand. There is no cure for DD. High reoccurrence rates are observed after surgical treatment and the risk of complications is even higher at repeated surgery (Denkler 2010).

1.2.6 Other related Diseases

There are a number of clinically related conditions that occur less frequent and manifest in different parts of the body. Patients that present with one of these conditions often also have DD. In some DD patients connective tissue depots form at the dorsum of the proximal interphalangeal finger joints, the so called knuckle pads. In plantar fibromatosis (Ledderhose´s disease, LD) the sole of the feet is affected. Often the fibromatosis manifests in the part of the sole that is not in contact with the ground and thus does not hamper walking but in extreme cases the toes can contract.

Penile contracture (Peyronie's disease, PD) is characterized by the formation of thickened fibrous plaques on the dorsum of the penis. Comparison of gene expression profiles indicates

that Dupuytren´s disease and Peyronie's disease share a common pathophysiology (Qian *et al*. 2004). PD was described as a genetic disorder with autosomal dominant inheritance (Bias *et al*. 1982). It was also linked to trauma (Carrieri *et al*. 1998). In this study it will be evaluated how many DD patients additionally suffer from these related conditions.

1.3   Mitochondrial Dysfunction and Oxidative Stress

In the following section recent knowledge of mitochondrial dysfunction and oxidative stress in the context of aging is discussed briefly. Mitochondrial dysfunction was implicated in the aetiologies of type 2 diabetes (Patti *et al*. 2003, Petersen *et al*. 2004, Lowell and Shulman 2005) and age related neurodegenerative disorders (Bowling and Beal 1995), e.g. Alzheimer's disease (Swerdlow and Khan 2004), Parkinson's disease (Langston *et al*. 1983, Schapira *et al*. 1989, Bindoff *et al*. 1989), and Huntington's disease (e.g. Kuwert *et al*. 1990, Kim *et al*. 2010).

1.3.1 Mitochondrial Dysfunction

The main function of mitochondria is ATP production, which occurs during mitochondrial oxidative phosphorylation. During oxidative phosphorylation, electrons from reduced substrates are transferred to O_2 through a chain of respiratory electron transporters including the complex I, III, and IV proton (H^+) pumps, which in turn generate a proton gradient across the mitochondrial inner membrane. The electrochemical energy of this gradient is then used by the ATP synthesis (complex V) which couples H^+ reuptake with ADP phosphorylation in the matrix to generate ATP (Feissner *et al*. 2009). Proteins of the electron transport chain are downregulated with aging (Ghosh *et al*. 2011). Electrons leak from reduced sites in the respiratory chain and react with oxygen to form reactive oxygen species (ROS) which play an important role in cell signalling, but are better known for creating oxidative stress (Brookes *et al*. 2002). In mitochondria ROS cause mutations of mitochondrial DNA (mtDNA) which affect the electron transport chain function triggering increased ROS generation and accumulation of mtDNA damage over time (Mammucari and Rizzuto 2010). During aging, giant non-functional mitochondria, defective in ATP production together with aberrant macromolecules, accumulate especially in post-mitotic organs, such as the nervous system and the cardiac and skeletal muscle. These are removed by autophagy, which also declines with aging (Bergamini *et al*. 2007) accelerating the accumulation of these large aggregates with age (Mammucari and Rizzuto 2010).

1.3.2 ROS Production in Mitochondria

ROS is implied in the aetiology of a number of diseases such as diabetes (Newsholme *et al*. 2007) and hypertension (Paravicini and Touyz 2006). In the mitochondrial respiratory chain, the transport of electrons is coupled with the formation of ROS. In particular, the redox reactions at respiratory complexes I and III generate superoxide ($O_2^{\bullet-}$) (Rigoulet *et al*. 2011). Under physiologic conditions, the superoxide production is around 0.1% of the respiratory rate (Tahara *et al*. 2009). $O_2^{\bullet-}$ in solution is short lived and rapidly converted into hydrogenperoxid (H_2O_2) e.g. by the mitochondrial superoxide dismutase (SOD2). H_2O_2 is not a free radical (one or two unpaired electrons in the outer electron orbital) and is a more-stable molecule that is able to diffuse across biologic membranes. By the so called Fenton reaction H_2O_2 generates the highly reactive hydroxyl radicals $^\bullet$OH and $H^\bullet$ in the presence of metals such as Fe, which is a co-factor of many proteins. Other proteins in mitochondria are able to produce ROS, e.g. dehydrogenases, a-ketoglutarate dehydrogenase complex (aKGDHC) and glycerol-3-phosphate dehydrogenase (GPDH) and uncoupling proteins (UCPs) (Tahara *et al*. 2009) and monoamine oxidase (MAOA) in the outer mitochondrial membrane (Peña-Silva *et al*. 2009).

1.3.3 ROS Production at the Plasma Membrane

Mitochondria are the main side of ROS production. Another source of ROS are cells of the immune system. Neutrophils, macrophages, dendritic cells and monocytes release ROS in response to pathogens (Cannizzo *et al*. 2011). ROS in these cells is generated by NADPH oxidases (NOXs) located in the plasma membrane. They catalyze the production of superoxide by the one-electron reduction of oxygen, using NADPH as the electron donor (Babior 1999): $2\,O_2 + NADPH \rightarrow 2\,O_2^- + NADP^+ + H^+$.

$O_2^{\bullet-}$ is then converted into H_2O_2 by the cytosolic superoxide dismutase (SOD1) (Cannizzo *et al*. 2011). The NOX gene family includes seven members. They are expressed in a variety of different tissues (Krause 2004). NOX4 is most widely expressed and was associated with transforming growth factor β (TGFβ1) induced fibroblast to myofibroblast differentiation (Cucoranu *et al*. 2005).

1.3.4 Mitochondrial Dysfunction without enhanced ROS Production

The Mitochondrial Free Radical Theory of Aging predicts that a normal metabolism causes ROS production in mitochondria. ROS cause damage to lipids, proteins, and mtDNA. ROS-induced mtDNA mutations lead to the synthesis of functionally impaired respiratory chain subunits, causing respiratory chain dysfunction which in turn enhances ROS production.

This cycle over time promotes aging (Harman 2006) and involves an exponential increase of mtDNA mutations over time. But the formation of ROS in the course of normal metabolism does not necessarily increase significantly with age (Barja 1999). Trifunovic *et al*. (2005) used a mouse model that accumulates mtDNA mutations over time because of a defect mitochondrial polymerase lacking proofreading 3'-exonuclease activity (Trifunovic *et al*. 2004) and found no increase in ROS and oxidative damage and at the same time severely impaired respiratory chain function. The authors concluded from these findings that mtDNA mutations rather than ROS initially drive the aging process. But absolute mutation levels (deletions) have been argued to be too low to drive premature aging in these mice (Kraytsberg *et al*. 2009).

1.4   WNT/β-catenin Signalling Pathway

Wnts are secreted glycoproteins that act as short range signals in multiple processes. They are expressed in spatially restricted and dynamic patterns during development (Cadigan and Nusse 1997) and in the adult organism (Moon *et al*. 2004). Wnt signalling has been implicated in the pathogenesis of cancer (van de Wetering *et al*. 2002, Giles *et al*. 2003, Uematsu *et al*. 2003), cardiovascular disease (van Gijn *et al*. 2002), and Alzheimer's disease (De Ferrari and Inestrosa 2000) and upregulation of Wnt signalling was associated with aging (Marchand *et al*. 2011, Brack *et al*. 2007, Liu *et al*. 2007). The Wnt protein family comprises 19 members in mammals which can trigger different pathways in the signal receiving cell (Veeman *et al*. 2003, Sugimura and Li 2010). One extensively studied pathway involves the stabilisation of β-catenin which then translocates into the nucleus and acts on the expression of target genes. Wnt signalling is activated during fibroblast proliferation (Cheon *et al*. 2004) and elevated levels of β-catenin were found in pulmonary fibrosis (Chilosi *et al*. 2003), aggressive fibromatosis (Cheon *et al*. 2002), and also in DD (Varallo *et al*. 2003). Expression profile of human lung fibroblasts treated with Wnt3a revealed that among genes differentially expressed in response to Wnt stimulation, where genes that play a role in differentiation of fibroblasts to a myofibroblast or smooth muscle phenotype (Klapholz-Brown *et al*. 2007).

1.4.1 Wnt/β-catenin Signalling

In the absence of Wnt, β-catenin is targeted to a multimeric protein complex called the destruction complex, which includes the scaffolding protein axin and the tumour suppressor protein adenomatous polyposis coli (Apc). β-catenin is then phosphorylated by casein kinase 1 (Ck1, CSNK1A1) and subsequent glycogen synthase kinase 3β (Gsk3β) (Liu *et al*. 2002).

This phosphorylation targets β-catenin for ubiquitination and subsequent degradation by the proteasome (figure 8). In the nucleus prospective target genes of the pathway are kept in a repressed state by T-cell factor (Tcf) and lymphoid enhancer-binding protein (Lef) transcription factors and associated co-repressors (Gordon and Nusse 2006, Logan and Nusse 2004).
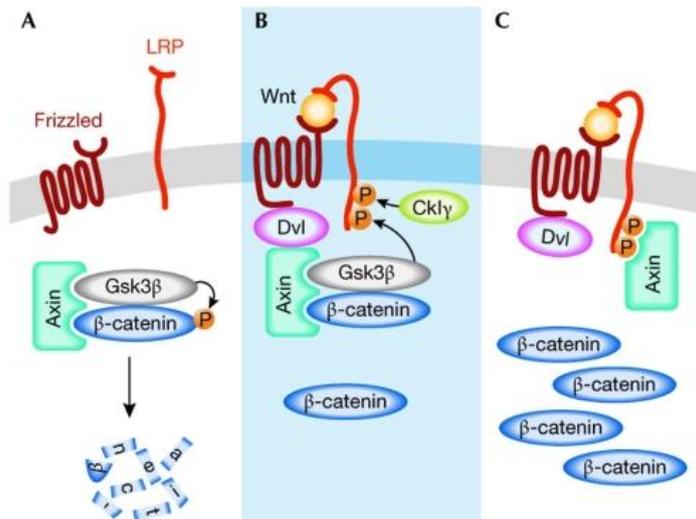
Figure 8 Model for the activation of the Wnt/β-catenin pathway. (A) **In the absence of a Wnt signal, β-catenin is phosphorylated and targeted for proteasome-mediated degradation by a destruction complex that contains axin and Gsk3β among other proteins.** (B) **On binding of Wnt to the receptors Fzd and LRP, Dvl binds to Fzd and recruits the destruction complex through interaction with axin. Subsequently, Gsk3β phosphorylates critical sites on LRP, which, together with residues phosphorylated by CkIγ, act as docking sites for axin.** (C) **Binding of axin to LRP leads to inhibition of the destruction complex and stabilization of β-catenin. CkIγ, casein kinase Iγ; Dvl, dishevelled; Fz, Frizzled; Gsk3β, glycogen synthase kinase 3β. From Fuerer** *et al*. **Wnt signalling in development and disease. Max Delbrück Center for Molecular Medicine meeting on Wnt signalling in Development and Disease. EMBO Rep. 2008 Feb;9(2):134-8.**

Two cell-surface receptors cooperate to transmit Wnt signals across the plasma membrane to activate β-catenin signalling. Wnts bind to the seven transmembran domains containing receptor frizzeld (Fzd 1-10) and the low density lipoprotein receptor-related protein (Lrp 5 and 6). Ternary ligand-receptor complexes form ribosome-sized aggregates in the cell membrane. The binding of Wnt to Fzd/Lrp leads to the phosphorylation of Lrp6 by Gsk3β and Ck1 (Rao and Kühl 2010). Axin and the phosphoprotein dishevelled (Dvl) then bind to the cytoplasmic tails of Lrp and Fzd, respectively. The destruction complex is disrupted and axin is degraded. The activation of Dvl also leads to the inhibition of Gsk3β. Both effects increase the post-translational stability of β-catenin. As the β-catenin level rise in the cytoplasma, β-catenin also translocates into the nucleus, where it interacts with DNA-bound Tcf and Lef family members to act on the transcription of target genes (Moon *et al*. 2004).

1.4.2 Wnt Signalling: Modifications, Antagonists and Activators

Wnts are modified before secretion by the addition of two fatty acids, palmitic acid on the first conserved cysteine and palmitoleic acid on a highly conserved serine residue (Willert *et al*. 2003; Takada *et al*. 2006). These modifications render Wnt proteins hydrophobic and Heparan sulfate proteoglycans (Hspgs) prevent Wnts from aggregating in the extracellular matrix (Fuerer *et al*. 2010). Members of the Hspg family were shown to act as a reservoir or modulator for several growth factors and signalling molecules (e.g. Bernfield *et al*. 1999; Whitelock and Iozzo 2005). Sulphated proteoglycan levels were elevated in DD primary tissue (Tunn *et al*. 1988).

Telomerase directly modulates Wnt/β-catenin signalling by serving as a cofactor in a beta-catenin transcriptional complex. The telomerase protein component TERT (telomerase reverse transcriptase) interacts with BRG1 (also called SMARCA4), a SWI/SNF-related chromatin remodelling protein, and activates Wnt-dependent reporters in cultured cells and *in vivo* (Park *et al*. 2009).

In addition to its function in the Wnt signalling pathway, β-catenin also binds tightly to the cytoplasmic domain of type I cadherins and plays an essential role in the structural organization and function of cadherins by linking cadherins through α-catenin to the actin cytoskeleton (Jamora and Fuchs 2002, Gumbiner 2000).

There are several inhibitors and activators that either inhibit or promote Wnt signalling extracellular. One example for an inhibitor is the family of dickkopf proteins (DKK) (Glinka *et al*. 1998). DKK1 binds to LRP5/6 and the transmembrane protein Kremen (Mao *et al*. 2002). This interaction inactivates LRP5/6. R-Spondins (RSPOs) promote Wnt signalling by antagonizing DKK1-mediated interaction with LRP and Kremen (Kim *et al*. 2008). Sclerosteosis (SOST) and sclerostin domain containing 1 (SOSTDC1) are also secreted Wnt inhibitors that bind to and inactivate LRP (Semënov *et al*. 2005, Itasaki *et al*. 2003). Wnt inhibitory factor (WIF) proteins and secreted frizzled related proteins (SFRP1,2-5) act by directly binding Wnt molecules and can function as Wnt inhibitors, but may also stabilize Wnt's and facilitate Wnt signalling (Hsieh *et al*. 1999, Hoang *et al*. 1996). Connective-tissue growth factor (CTGF) modulates Wnt signalling and interacts with LRP6 (Mercurio *et al*. 2004). Dapper, antagonist of beta-catenin, homolog (DACT1-3) promotes Wnt/β-catenin signalling by binding intracellulary to Dvl (Gloy *et al*. 2002).

In colorectal cancer Wnt/β-catenin is commonly dysregulated in colorectal cancer (Pálmer *et al*. 2001). Vitamin D acts protective against colorectal cancer (Garland *et al*. 1989).The most

active vitamin D metabolite, 1alpha,25-dihydroxyvitamin D3 (D3) inhibits β-catenin transcriptional activity by promoting vitamin D receptor (VDR) binding to β-catenin and the induction of E-cadherin expression. Vitamin D3 has been shown to regulate two genes encoding the extracellular Wnt inhibitors DKK-1 and DKK-4. By an indirect transcriptional mechanism, D3 increases the expression of DKK-1 RNA and protein, which acts as a tumour suppressor in human colon cancer cells harbouring endogenous mutations in the Wnt/beta-catenin pathway (González-Sancho *et al*. 2005). In contrast, vitamin D3 represses DKK-4 transcription by inducing direct VDR binding to its promoter. DKK-4 is a target of the Wnt/β-catenin pathway and is up-regulated in colorectal tumours (Pendás-Franco *et al*. 2008). Several vitamin D target genes have been characterized including tenascin-C, fibronectin, laminin and its receptor, apolipoprotein D, insulin-like growth factor binding protein 3, cyclin C, and several members of the transforming growth factor family and their receptors (Freedman, 1999).

Mice overexpressing SFRP4, aWnt inhibitor had significant higher serum and urine levels of vitamin D (Cho *et al*. 2010). The connection between Wnt/β-catenin signalling and viamin D signalling could be causative for the observed north-south decrease in the prevalence of DD.

1.4.3 Wnt/β-catenin Signalling and Aging

Wnt/β-catenin signalling is increased and leads to an enhanced fibrosis in aging muscle (Brack *et al*. 2007). During aging the regenerative potential of muscle declines (Goldspink *et al*. 1994). Muscle tissue is replaced by fibrous connective tissue and adipose tissue. Brack *et al*. (2007) examined muscle tissue and cells derived from muscles of young (~6-month-old) and aged (~24-month old) mice. Axin2 (target of Wnt/β-catenin signalling) transcript levels were increased in aged muscle and a progressive increase in Wnt signalling in myogenic cells during aging with an increase in β-catenin and decrease of GSK3β was noted. Increased β-catenin was also found in aged muscle tissue in response to injury compared with young tissue. The injection of Wnt3A into young muscle after injury resulted in increased connective tissue deposition phenotypically similar to regenerating aged muscle. Exogenous Wnt also reduced cellular proliferation in young regenerating muscles. Reduced fibrosis was seen in aged muscle after the injection of Wnt inhibitors (DKK1 and SFRP3). The authors concluded that the fibrotic aging phenotype in muscle is promoted by Wnt's (or Wnt-like proteins) present in the aging serum (Brack *et al*. 2007).

Liu *et al*. (2007) determined reduced number of stem cells in the klotho mouse, a model for accelerated aging (Kuro-o *et al*. 1997) that lacks klotho, a secreted protein found to decline

in the serum of mouse and human during aging (Xiao *et al*. 2004). Liu *et al*. noted that klotho and Wnt were co-expressed in transfected cells. They showed by immunoprecipitation that klotho binds to Wnt3A, Wnt1, Wnt4 and Wnt5A. In their cell-culture model klotho inhibited Wnt-signalling and the mouse model lacking klotho expression had enhanced expression of Wnt target genes (Axin2). In cultured fibroblasts (mouse embryonic and human) continuous exposure to Wnt3A first increased proliferation (BrdU incorporation) but over time proliferation decreased while the level of apoptosis was not increased. The authors concluded that chronic Wnt stimulation may contribute to stem cell depletion and aging.

Marchand *et al*. (2011) compared the expression profiles of middle old (43-60 years, N = 8) and older patients (75-83 years, N = 7) in mammary artery media and found target genes of the Wnt/β-catenin signalling pathway upregulated in the older group (e.g. SPP1, WISP1, versican and IGFBP2). B-catenin mRNA was not significantly upregulated but β-catenin phosphorylation at serine 675 was significantly increased in the older group. This phosphorylation induces β-catenin nuclear localization and transcriptional activity, suggesting that β-catenin is activated during aging. Cyclin D2 mRNA and protein levels were unchanged as were mRNA levels of catalase and SOD2. Wnt3A treatment of vascular smooth muscle cells (VSMC) from old rats (8 month old) did not induce proliferation and cyclin D1 expression as it did in VSMCs derived from young rats (6 weeks old) while β-catenin was activated in young and old cells. The authors concluded that β-catenin pathway is activated during human vascular aging but that the proliferative response to Wnt is altered downstream of β-catenin activation (Marchand *et al*. 2011).

Together these findings hint that Wnt/β-catenin signalling plays an important role during aging and that its function in aged tissue differs from that of young tissue.

1.5   Objectives and Hypotheses

Dupuytren´s disease is a complex disease with a strong genetic basis. The aim of this study was to identify loci in the human genome that are associated with Dupuytren´s disease. Therefore a genome wide association study (GWAS) was conducted with a case control study design. This study design should allow for the identification of some of the genetic factors that promote pathogenesis. Because DD is a complex genetic disease several genetic loci are expected to be associated, each contributing in small part to the susceptibility of this disease.

Expression profiles of primary tissue and tissue derived fibroblasts differ between DD patients and matched controls (Pan *et al*. 2002, Qian *et al*. 2004, Rehman *et al*. 2008, Satish *et al*. 2008, Zang *et al*. 2008). A range of genes identified from these studies were proposed to play a causative role in the pathogenesis of DD. But no signalling pathways have been attributed to DD so far. A whole genome expression analysis was conducted in order to identify major signalling pathways involved in DD pathogenesis. Results from this experiment may possibly support and confirm findings from the GWAS. As DD is an aging associated disease identified pathways may lead to the identification of links between DD and aging.

DD fibroblasts *in vivo* are characterised by high proliferative and contractile activity. Disease tissue derived primary fibroblasts were cultured and characterised in comparison to control tissue derived fibroblasts. These experiments should help to establish and characterise a simple *in vitro* model, desirable to test hypotheses from the GWAS in the future.

A questionnaire based elevation of known risk factors and other parameters was conducted in order to characterise DD patients sampled for DNA and disease tissue epidemiologically.

Integration of data from all these approaches should help to pave the way to a comprehensive understanding of the molecular pathology of this poorly understood aging-related disease.

2 Materials and Methods

2.1 Sample Collection, Storage and Handling

2.1.1 Subjects

Between 2007 and 2011 760 DD patients were recruited through the outpatient clinics of the plastic surgery departments of nine hospitals in Germany and one in Switzerland. Additionally a number of patients were recruited through the German Dupuytren Society (Dupuytren e.V.).

Genotype data from 1618 German controls were already available, 1164 of these were part of the Popgen study (University of Kiel, Germany) (project number: BSP+SPC/110217/83), and 454 were from KORA (Helmholtz Center Munich, Neuherberg, Germany) (project number: K26/11). These samples were genotyped with the Affymetrix 6.0 chip. In addition genotype data for 1219 Popgen controls that were typed on the Affymetrix Axiom 2.0 chip was also available. Participants provided written informed consent and the study was approved by the Ethics Committee of the MathNat Faculty of the University of Cologne. 282 control DNAs with European background were provided by the University of Essen.

2.1.2 Questionnaire

For each participant a one-sided questionnaire was completed by the attending physician. The recorded parameters are given in Table 1. The questionnaire was changed twice during the study, when minor adjustments or additional questions became eligible. All versions of the questionnaire are listed in figures 68-70 of the appendix. A separate questionnaire was used for control individuals, which is also given in the appendix.

Table 1. Parameters enquired in questionnaire survey for DD patients

parameter	factors
name	
date of birth	
gender	male, female
age at first surgery	
affected hand	right, left, both
degree after Tubiana	0, 1, 2, 3, 4
recurrence	recurrence, extension
preceding complications	trauma, sudeck dystrophy
ectopic manifestations	e.g. knuckle pads, plantar fibromatosis
affected family members	no, yes, who

Table 1 continued:

parameter	factors
other diseases	diabetes mellitus, rheumatoid arthritis, epilepsy, other
medication	antiarrhythmia, antihypertensive, antiepileptic drugs, other
for women:	
age at menopause	
hormone intake	yes, no
ovarian surgery	yes, no
profession	
smoking habits	0, <5, <20, >20 cigarettes per day
year subject stopped smoking	
alcohol intake	never, occasional, regular

The age at first surgery is likely to reflect a combination of the age of onset and progression of disease. Both, patients with an early age of onset or an aggressive course of disease will potentially present earlier for surgery than patients who are affected late in life or are mildly affected. The age at first surgery was therefore selected as a variable to compare different patient subgroups. Two tailed student´s t-test was applied to test whether groups differed significantly in their ages at first surgery. Statistical analyses were done with excel. Associations were considered significant if the p-value was <0.05.

2.2 DNA Extraction

DNA was extracted for 565 patients from either whole blood samples or primary fibroblasts.

2.2.1 DNA Extraction from Blood

For DNA extraction peripheral blood was sampled in EDTA containing S-Monovette tubes (Sarstedt, Nümbrecht, Germany). Samples contained 2 to 10ml of whole blood. Blood samples were shipped at room temperature and frozen upon arrival at -20°C (short term storage) or -80°C (long time storage).

A number of 12 to 24 samples were extracted simultaneously. For extraction the frozen blood sample was thawed at room temperature. The thawed sample was transferred to a 50ml falcon tube (BD Bioscience, USA). Possible blood clots were solved by adding 500µl Proteinase K (10mg/ml) and 10 minutes incubation at room temperature. Blood volume was then recorded and four times the volume of cell lysis buffer (solution A: 0.01mol/l Tris, 0.005mol/l $MgCl_2$, 0.32mol/l saccharose, 1% Triton X 100; pH 8) was added. The sample

was incubated for 10 min at room temperature on a Stuart table tube roller (Bibby Scientific Limited, UK). The sample was then centrifuged at 2500rpm and 4°C for 10 minutes (Megafuge, rotor 8155). Subsequently the supernatant was carefully decanted without losing the cell nucleus pellet at the bottom of the tube.

Then 2ml solution B (0.4mol/l Tris, 0.15mol/l NaCl, 1%SDS, 0.06mol/l EDTA; pH 8) was added and transferred with the pellet to a 15ml falcon tube. The sample was vortexed briefly for a few seconds then incubated at room temperature on the tube roller till the pellet was completely resolved. After that 500µl of solution C (5mol/l perchlorate) was added to the sample. The tube was inverted ten times and spun down briefly to collect the liquid at the bottom of the tube. 2ml of cold (4°C) chloroform was added and the sample mixed by shaking the tube. The sample was then spun at 4°C for 10 minutes. Phase separation resulted in upper aqueous layer containing the DNA and lower whitish phase containing halogen and coagulated proteins. The upper phase was transferred to new 15ml tube. Again a volume of 500µl solution C or less was added and mixed with the sample followed by the addition of 2ml chloroform and centrifugation as before. After centrifugation the upper phase was again collected in a fresh 15ml tube. If the upper phase was clear the sample was further processed, if not solution C and chloroform were added for a third time. As soon as the DNA containing phase was clear of proteins an equal amount of icecold isopropanol was added to the sample to precipitated the DNA. The tube was inverted slowly ten times till white strands of DNA were visible. The DNA coil was fished with a glass rod and transferred to a 1.5ml tube containing 1ml of 99% ethanol. The DNA was pelleted at 13000rpm in a refrigerable table microcentrifuge for 10 min at +4°C the ethanol was decanted and the DNA pellet air dried. When the pellet was dry 500µl of DNase free water were added to the sample and the DNA was resolved for days on a tube roller at 4°C. The solved DNA sample was stored at -20°C till further processing.

2.2.2 DNA Extraction from primary Fibroblasts

In some cases, where no blood sample existed, DNA was extracted from primary patient fibroblasts. Fibroblasts were cultured in $225cm^2$ cell culture flasks. Upon reaching confluence cells were harvested as described below (see chapter: Cell culture). The samples were centrifuged to pellet cells and the supernatant was aspirated.

The cell pellets were stored at -20°C till further processing. To isolated DNA cell pellets were lysed in 1ml solution B (0.4mol/l Tris, 0.15mol/l NaCl, 1%SDS, 0.06mol/l EDTA; pH

8) and DNA was extracted as described above (see chapter: DNA extraction from blood). Extracted DNA was dissolved in DNase free water and stored at 4°C.

2.2.3 DNA Quality control and Quantification

1 to 10 dilutions of the DNA stocks were made. DNA dilutions were analysed with a ND-1000 Spectrophotometer (Wilmington, USA). 1.5µl of well mixed DNA dilutions were loaded onto the ND-1000 Spectrophotometer. DNA light absorbance at 260nm and 280nm was measured trice for every sample and DNA concentration and purity were calculated directly by the provided software.

2.3   Whole Genome Association Study

Completion of the sequencing of the human genome in 2001 (Venter *et al*. 2001, Lander *et al*. 2001) and the International HapMap Project (International HapMap Consortium 2003 and 2005), a catalogue of common genetic variants in humans, resulted in crucial insights into human genetic diversity (Hakonarson and Grant 2011). Genetic variants that are near each other tend to be inherited together. They are in linkage disequilibrium with each other. Individuals who carry a particular allele at one site often predictably carry specific alleles at other nearby variant sites. It is therefore possible to infer genotypes of genetic variants through linkage disequilibrium without genotyping them directly. The HapMap project aims to identify a set of common genetic variants (minor allele frequency (MAF) $\geq$ 5%) with which the other common variants can be inferred.

Together with advances in single-base extension biochemistry and hybridization/detection to synthetic oligonucleotides these insights have made it possible to accurately and cost effectively genotype hundreds of thousands of single nucleotide polymorphisms (SNPs) (Steemers *et al*. 2006).

In the first step genomic DNA is fragmented and amplified. Fragmentation can be accomplished for example with digestion enzymes or mechanically. Adapters are annealed to the fragments. The adapters function as primer binding sites for whole-genome amplification (WGA) which generates sufficient DNA for subsequent hybridization to the array chip. Amplified DNA is again fragmented ($\sim$300–600 base pairs) and resuspended at low-picomolar target concentration to drive hybridization to the array. The array contains beads that each carries copies of allele-specific oligonucleotides for one SNP. As the DNA fragments hybridise to the array the oligonucleotids bind to a 50bp sequence directly adjacent to the SNP. After hybridisation the oligo-probes are extended with labelled ddNTPs. Dependent on the present allele a different label is incorporated. Signals from

different labels are then amplified and captured with a bead array reader (Gunderson *et al*. 2005, Steemers *et al*. 2006).

2.3.1 DNA Sample Preparation for Affymetrix Chips

DNAs with concentrations above 50ng/µl were transferred to 96-well plates, subsequent called mother plates. Mother plates were normalised to 50ng/µl with a Microlab starlet robot (Hamilton, Bonaduz, Switzerland). 100ng of each DNA sample was loaded onto 2% agarose gels to check for DNA integrity.

2.3.2 Affymetrix 6.0 Chip

In this study 186 patient DNA samples were analysed with the Genome-Wide Human SNP Array 6.0 (Affymetrix UK Ltd, UK), which features 1.8 million genetic markers, including more than 906,600 single nucleotide polymorphisms (SNPs) and more than 946,000 probes for the detection of copy number variation. Affymetrix' GeneChip™ technology applies a combination of photolithography and combinatorial chemistry to directly synthesise oligonucleotides on a glass surface. Up to 6.5 million different oligonucleotides are synthesised on a 1.7 cm² surface. DNA samples (200–500ng) were processed and hybridized according to the manufacturer's instructions by ATLAS Biolabs GmbH, Berlin. Data was then processed and analyzed by Prof. Dr. Michael Nothnagel, Christian-Albrechts University, Institute of Medical Informatics and Statistics, Kiel.

2.3.3 Axiom CEU 1 Chip

379 additional samples were genotyped with the Axiom Genome-Wide CEU 1 Array Plate which features more than 587,000 SNPs and 11,000 single base insertions/deletions (in/dels). SNP content and insertions/deletions (in/dels) for the Axiom™ Genome-Wide CEU 1 Array were selected from the Axiom Genomic Database. These validated markers were derived from various public sources, including the International HapMap Project (~464,000 SNPs), the Single Nucleotide Polymorphism Database (dbSNP), and 1000 Genomes Project content already in dbSNP (~122,000 SNPs and in/dels).

The Axiom genotyping platform is a two color, ligation-based assay utilizing 30-mer oligonucleotide probes synthesized in situ on a microarray substrate, with automated, parallel processing of 96 samples per plate. Features are 3µm squares, at a pitch of 5µm center-to-center, with a total of ~ 1.38 million features available for experimental content. Each SNP feature contains a unique oligonucleotide sequence complementary to the genomic sequence flanking the SNP site on either the forward or reverse strand. Solution

probes bearing attachment sites for one of two dyes, depending on the 3' (SNP-site) base (A or T, versus C or G) hybridize to the glass probe/target complex, and are then ligated for specificity. Features are typically replicated twice on the array, so that each SNP is interrogated by two features; A/T and C/G SNPs require four features, because the two alleles match the same dye and therefore distinct probe sequences in different physical locations on the array are required to distinguish them. A maximum of ~ 690,000 SNPs may be accommodated by this format; this number is reduced if A/T or C/G SNPs are included, or if additional features are used to improve the resolution of specific SNPs, but may also be increased if high resolution SNPs are tiled with a single feature. The platform can be leveraged for designing arrays at previously unattainable levels of SNP density with respect to customization of variant selection.

Sample preparation

DNA samples were brought onto 96-well plates (mother plates) as described above. Plates were then normalized to 15ng/µl. 5µl were of each normalized sample was loaded onto 1% agarose gels (E-Gel® 48 1% Life Technologies) and run in EG mode on E-base devices (Life Technologies) for 12 minutes. Thus DNA integrity was visualized. Only samples with a distinct band directly below the gel pocket, which constitutes intact genomic DNA were used for whole genome genotyping (see figure 9 for an example). Degraded DNA samples were replaced. Four 96-well plates with 94 Dupuytren Patient DNA samples each were prepared. In addition each of the four plates contained a reference DNA sample (Axiom Reference Genomic DNA 103).
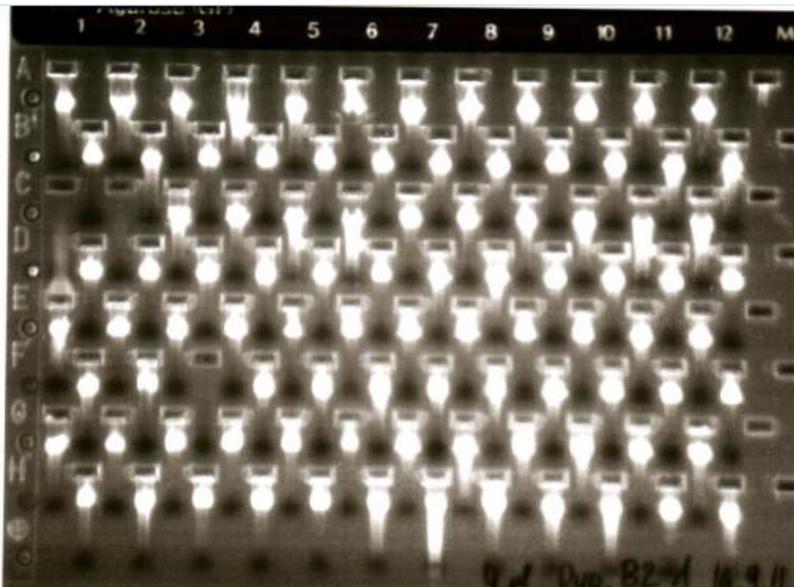
Figure 9. Gel image of DNA samples for whole genome genotyping.

Axiom Genotyping

20ul (~300ng) per sample were brought onto 96-deep-well plates (Beckman Deep Well Titer, polypropylene; P/N 267007). The Affymetrix Axiom version 2.0 assay was preformed as described in the user manual. The protocol consists of the following steps: 1. Whole genome amplification, 2. Fragmentation, 3. Resuspension and quality control step, 4. Hybridisation, staining and detection. All pipetting steps in the first three steps were carried out with Biomek FX robot (Beckman Coulter). Hybridisation and subsequent washing, staining and detection steps were carried out with the GeneTitan instrument (Affymetrix UK Ltd, United Kingdom).

1. Whole Genome Amplification

All reagents (Denaturation Solution, Neutralizing Solution, Amplification Solution and water) were thawed on the benchtop at room temperature for one hour. The 10x Denaturation solution was diluted with water and 20μl of the dilution were transferred to the sample. Genomic DNA samples were denatured 37°C for 10 min. 130μl of neutralizing solution was then added to each well. The amplification master mix was prepared from amplification solution and enzyme mix and 230μl of the mastermix were pipetted onto each sample. The samples were then incubated for 23±1 hours in an oven at 37°C.

2. Fragmentation

Enzymatic fragmentation was carried out. Axiom Frag Enzyme, Axiom 10X Frag Buffer, Axiom Precip Soln 1 and 2, Axiom Frag Diluent, Axiom Frag Rxn Stop solution and Isopropanol (99.5%) were used in this step. Axiom 10X Frag Buffer and Axiom Precip Soln 2 were thawed to room temperature on the benchtop. In order to inactivate the amplification enzymes the sample plate was incubated at 65°C and then at 45°C for 20 min each. Then 47.5μl of fragmentation buffer was added to the sample. Fragmentation enzymes and Fragmentation diluent was mixed and 11.3μl of the mixture added to each sample. The sample was then incubated for 30 min at 40°C. Then 19μl of stop solution were added to the sample. The precipitation solutions were mixed and 240μl of the solution and 600μl of isopropanol were added to the sample. The fragmented DNA was precipitated over night at -20°C.

3. Resuspension and hybridization preparation and quality control

On the following day the sample plate was centrifuged for 40 min at 4 °C at 3200xg in order to pellet the DNA. The plate was then inverted to remove the liquid and placed upside down on a tissue for 5 min. the plate was then dried in an oven at 37°C for 20 min. Axiom Hyb Buffer, Axiom Hyb Soln 1, Axiom Resusp Buffer and Axiom Hyb Soln 2 were used in the next step. The resuspension buffer was placed on the benchtop at room temperature for one hour prior to usage. 35µl of resuspension buffer was added to the sample and the sample was mixed by pipetting up and down. The hybridization mastermix was prepared from hybridization buffer and hybridization solutions 1 and 2. 80µl of the hybrisation mastermix was added to the sample. 115µl of the sample hybridization mixture were then transferred onto the hybridization reaction plate. The sample was diluted 1:5 by pipetting 5µl of sample in a plate with 55µl water. The diluted sample was the diluted further by adding 10µl of diluted sample to 90µl of water for optical density (OD) measurement of sample DNA concentration. Additionally 3µl of diluted sample were mixed with 120µl of TrackIt Gel Loading Buffer (diluted 1000-fold) in the gel QC plate.

Quality control was then preformed. 4% agarose gels (E-Gel® 48 1% Life Technologies) were run in EG mode on E-base devices (Life Technologies). 20µl of sample from the gel QC plate and 15µl of diluted TrackIt 25bp ladder were loaded onto the gel. The gel picture was taken after 20 min. For an example see figure 10. Fragmentation should result in DNA fragments of 25 to 125 base pairs.
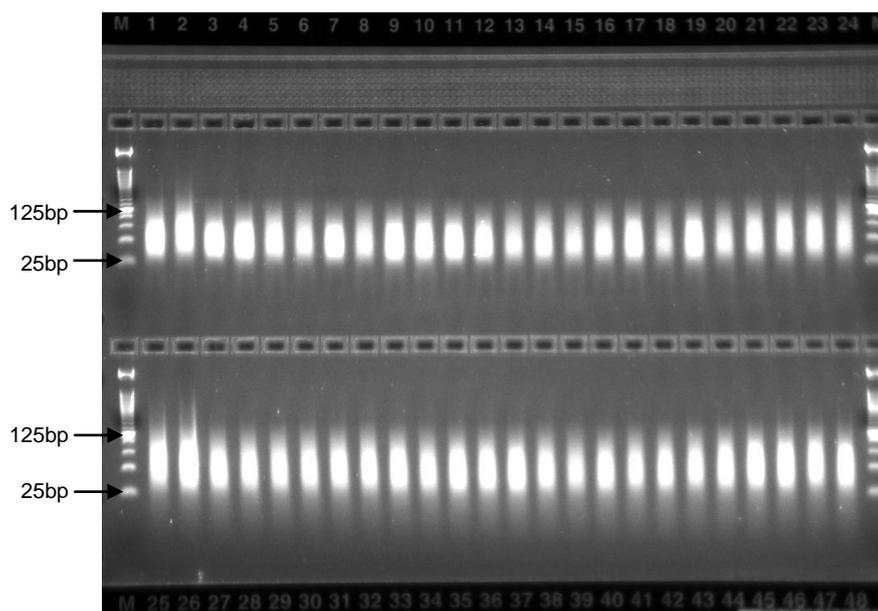
Figure 10. Gel image example of 48 fragmented samples.

For OD measurement at 260, 280 and 320nm a DTX 880 Multimode Detector with Genomic Filter Slide (Beckman Coulter) was employed. DNA concentrations were calculated by the provided software. Total sample concentrations should range between 1000 and 1600µg.

4. Preparation for the GeneTitan Instrument Hybridisation, Staining and Scanning

The hybridisation plate is covered with a metallic lid. The sample is then incubated in a thermal cycler (PTC200) at 95°C for 10 min and then at 48°C for 3 min to denature the samples. 105µl of the samples is then transferred to the hybridisation tray and loaded onto the GeneTitan instrument. The array plate is simultaneous loaded. Hybridisation lasts 23.5 hours.

On the following day the washing and staining solutions for the washing and staining of the hybridised array are prepared with the biomek instrument. Five different 96-well plates are prepared. One contains stabilising solution, two plates contain stain 1, one plate contains stain 2 and one plate contains ligate solution. All five plates are loaded onto the GeneTitan instrument after hybridisation. The samples on arrays are then ligated, washed, stained and stabilized during 5 hours. After this the array is scanned by the GeneTitan instrument during 7.5 hours. The data is then imported into the Genotyping Console software (Affymetrix).

Dish quality control (QC) and Genotype calling

The Genotyping Console software (Affimetrix) software was used to perform dish QC and for subsequent genotype calling. Before performing genotyping analysis on any samples, the quality of each individual sample should be determined. Dish QC (DQC) is the recommended sample quality QC metric for the Axiom™ Arrays. DQC operates by measuring signal at a collection of non-polymorphic sites in the genome (i.e., sites that do not vary in sequence from one individual to the next). DQC monitors non-polymorphic locations where it is known which of the two channels in the assay represents the allele present in the genome; therefore, which channel should have a signal intensity above the background signal, and which channel's signal should be indistinguishable from the background are known. DQC is a measure of the extent to which the distribution of signal values for the two channels are separated from the signal values for the background, with 0 indicating no separation and 1 indicating perfect separation. Samples with a DQC value less than the default DQC threshold of 0.82 were dropped from the study.

DQC is a useful single-sample performance metric, and under normal circumstances it correlates well with genotyping performance. One exception to these circumstances is the case of sample mixing—a sample consisting of different individuals mixed together can still have a good DQC score since the signals at non-polymorphic locations will remain the same in a mixture. Such samples can generally be identified by having the combination of good DQC values and abnormally low sample call rates. No such samples were found.

With the GTC software Dish QC was preformed per plate and the genotypes were called for all four patient and 13 control plates (Popgen controls genotyped on the same platform) together with the algorithm AxiomGT1: Axiom 2.0. The confidence threshold was set to 0.15. The prior models file Axiom_GW_Hu_SNP.r4.AxiomGT1.models was used. Genotype data was then exported to PLINK format (Purcell *et al.* 2007).

Data analysis

Data analysis was conducted with the PLINK software package (version 1.07; http://pngu.mgh.harvard.edu/purcell/plink/) following protocols by Anderson *et al.* (2010) and Clarke *et al.* (2011). Data files were recoded in binary file format. Sex was imputed from the X chromosome genotypes with the "--impute-sex" option and checked against recorded gender information from the questionnaires. (This reference check was done in cases only.) 51 individuals with call rates below 97% were removed. Of these 7 were cases. For the remaining individuals the mean heterozygosity rate was calculated in order to identify samples with an excessive or reduced proportion of heterozygote genotypes, which may be indicative of DNA sample contamination or inbreeding, respectively. 10 samples were removed that had a heterozygosity rate greater than ± 3 standard derivations from the mean (see figure 11). Three duplicated control samples and two related cases were also excluded. For the remaining 359 cases and 1173 controls SNP quality control was preformed. 587,299 SNPs and small in/dels were genotyped. All markers with call rates of less than 97%, a minor-allele frequency of less than 0.01, or a deviation from Hardy-Weinberg equilibrium (P>0.00001) were excluded.

Multidimensional scaling analysis was conducted to identify genetic differences in cases and controls, as cases originated from different locations in Germany and Switzerland while all controls came from the north of Germany. The allele frequencies between cases and controls were compared with the use of a basic chi-square allelic test with 1 degree of freedom and the overdispersion factor of association test statistic (genomic control inflation factor, λgc;

Devlin and Roeder1999) was calculated with the use of observed versus expected values for all SNPs. In order to correct for population stratification association testing was conducted with logistic regression and the first four covariates.
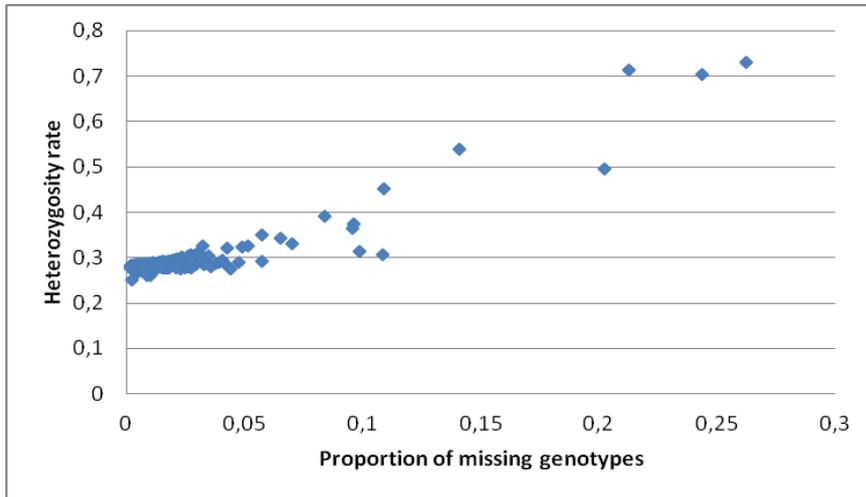
Figure 11. Genotype failure rate versus heterozygosity across all individuals genotyped with Axiom. N=1590
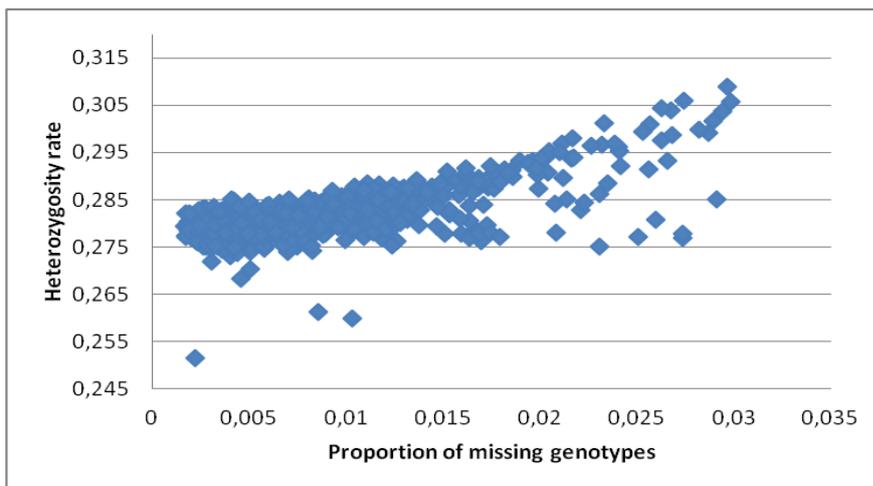
Figure 12. Genotype failure rate versus heterozygosity across individuals with genotype call rates >97% and and/or a heterozygosity rate ± 3 s.d. from the mean. N=1559

2.3.4 Imputation

The data from 186 cases genotyped on the Affymetrix 6.0 chip and 379 cases and 1219 controls genotyped on the Axiom genotyping platform were imputed with the Beagle v.3.3.2 software (Browning and Browning 2009) using the HapMap Phase3 reference panel (including 180 Utah residents with Northern and Western European ancestry from the CEPH collection (CEU) genotyped for about 3.1 million SNPs) (The International HapMap Consortium 2010). Imputation was done by Prof. Dr. Michael Nothnagel and Dr. Sabine Siegert, Christian-Albrechts University, Institute of Medical Informatics and Statistics, Kiel.

5,204,451 SNPs were included in the subsequent association test with a Bonferroni level of 9.6E-09 and an imputations score (Beagle's r2) of >0.8. Data was adjusted for the first six components (covariates) of a multidimensional scaling (MDS) analysis in order to correct for genomic inflation (also see chapter 2.3.3).

2.3.5 SNPstream Genotyping

The Genome Lap SNPstream 48-plex Genotyping System (Beckman Coulter GmbH, Germany) was used to genotype selected SNPs in replication and verification of GWA results. The SNPstream Genotyping System is based on single nucleotide primer extension, where the 3'-ends of tagged extension primers are complementary to the sequence strictly adjacent to the SNP site (Denomme and Van Oene 2005). The extension primer binds to the afore amplified sequence and one of two different fluorescent labelled dideoxynucleotides is added to the primer sequence depending on which SNP allele is present in the sequence. The tagged extension primers can be directed toward a specific location in each well (containing a 4 x 4 oligonucleotide array) of the 384 SNPware plate, because of the presence of a tag at the 5'-terminus of the extension primer, complementary to the arrayed oligonucleotides. In a multiplex reaction 465 new patient samples and 282 controls (provided through the University of Essen) were analysed for 48 SNPs.

The annotation of each SNP and its frequency in populations of European ancestry were assessed in dbSNP NCBI and ENSEMBL (http://www.ensembl.org/index.html) databases. Tagged SNPs were used when SNPs proofed incompatible with either primer panel. The liquid handling in all the reaction protocols was done with Biomek FX Workstation (Beckman Coulter, GmbH, Germany). 48 PCR primer pairs and 48 extension primers were designed with the online software of Beckman&Coulter (www.autoprimer.com). PCR primers were designed to amplify a short sequence (90–175bp) surrounding the polymorphic site for each SNP of interest. The single-strand tagged extension primers were designed to be complementary to a 30 nucleotide sequence flanking the SNP site.

Multiplex PCR reaction and clean up

Multiplex PCR was performed in a GeneAmp 9700 thermocycler (Applied Biosystems GmbH, Germany) according to the recommended PCR conditions: one denaturation cycle at 94°C for 1min, 40 cycles with denaturation at 94°C for 30 s, annealing at 55°C for 30 s, and extension at 72°C for 1 min, followed by cooling the reaction to 4°C. The reaction was performed in a final volume of 5µl with 6ng genomic DNA, 75µM dNTP mix, 50nM primer

pool, 5mM MgCl$_2$, and 1U AmpliTaq Gold polymerase (Applied Biosystems GmbH, Germany) in water. PCR products were purified by Exo-Sap reaction (0.67U exonuclease I and 0.33U shrimp alkaline phosphatase in 3µl added to the 5µl PCP product), performed in a GeneAmp 9700 thermocycler to degrade unincorporated PCR primers and dNTPs, following the recommended conditions: first step at 37°C for 30 min and final incubation at 96°C for 10 min.

Primer extension reaction

After SBE Clean-Up PCR products were divided to two 384 well plates by transferring 4µl of the original plate to a new 384 well plate. Extension protocol was performed using an appropriate mix containing TAMRA and Bodipy-fluorescein labelled dideoxynucleotides (ddNTPs) and a pool of allele-specific tagged extension primers. One of the 384 well plates was used for the TCAG primer extension reaction, whereas the other plate was used for the CGAT primer extension reaction. This separation is necessary because only two instead of four fluorescent dyes are used to label the four different dideoxynucleotides (ddNTPs). E.g. in the TCAG reaction SNPs with the allele combination T/C, A/G, and T/G can be distinguished because T and A are labelled with one dye and C and G with the other. For this reaction the extension primer panel includes only primer that bind to SNPs sequences with either T/C, A/G, or T/G allele combinations. The extension reaction was performed in a GeneAmp 9700 thermocycler according to the recommended extension conditions with a cycle at 96°C for 3 min, 60 cycles with a first step at 94°C for 20 sec and a second step at 40°C for 11 sec, and final hold at 4°C. The reaction was performed in a final volume of 7.5µl with 1.50µl water, 1.88µl Extension Mix Diluent, 0.04µl each of the two extension mixes (containing the dye-labelled dideoxynucleotides) for each reaction (TC and AG for TCAG primer extension reaction, CG and AT for the CGAT primer extension reaction), 0.01µl of SNPware primer panel 1 (and 2 for the other reaction), and 0.01µl of DNA polymerase.

Hybridisation

After the primer extension the two reaction plates were pooled together again. 7µl Hybridization Solution were added into each well of one of the primer extension reaction plates, mixed and everything was transferred onto the second primer extension reaction plate. 16µl from each well of the pooled plate was then transferred to a prewashed SNPware plate. The SNPware plate with the hybridization mix was incubated at 42°C for 2 h in a humid chamber. Thereafter, the SNPware plate was washed three times, adding 1 x SNPware Wash Buffer II to each well to remove the probes not arrayed. The SNPware plate was

placed face down on a soft tissue in a centrifuge and spun for 2 min at 1.500 rpm to dry the plate.

Data analysis

The SNPware plate was analyzed with the GenomeLab SNPStream array imager. Blue and green lasers (488 and 532 nm, respectively) detected the fluorescent colour of the extended base for each spot. Genotype data were generated on the basis of the relative fluorescent intensities for each SNP with the GetGenos software. The software converted the numbers and sample position data into scatter plots which were then automatically separated into statistical genotype clusters. Graphical review and operator adjustment of the genotype clusters were performed to refine fluorescent cutoff values and the genotypes were exported into a result excel file. Data was analysed with PLINK v1.07 (Purcell *et al.* 2007) (http://pngu.mgh.harvard.edu/purcell/plink/). To test for allel based association the chi-square test and the Fischer's exact test were applied.

2.3.6 PCR and Sequencing reaction of Candidate Genes

Direct Sanger sequencing of selected candidate genes was performed on a 3730 sequencer with 48 capillaries (Applied Biosystems Foster City, USA). The device uses capillary electrophoresis of fluorescent-labelled DNA-fragments.

Polymerase chain reaction (PCR) and clean up

Prior to the sequencing reaction PCR products were amplified with specific primers. Primers were designed to encompass 400-500bp of the exon sequence of target genes. Primer specificity was tested by blasting the primer sequence against the human reference sequence with NCBI blast tools (http://www.ncbi.nlm.nih.gov/). Primers were obtained through Sigma-Aldrich Chemie GmbH, Germany. PCR reactions were carried out in a total volume of 10µl using 5ng DNA, 1µM of each, forward and reverse primer, 1µM dNTPs, 1µl PCR buffer 1 and 0.1µl InnuTag polymerase (5U/µl) (Analytikjena, Germany). PCR was performed in a Tetrad2 thermocycler (Bio-Rad Laboratories, Inc., Germany). PCR parameters consisted of an initial step at 94°C for 1min, followed by 33 cycles each with 30sec at 94°C, 30sec at the appropriate primer annealing temperature and 1min at 72°C, and followed by a final hold at 16°C.

Subsequent residual nucleotides were removed in a cleanup reaction with Exonuclease I (Exo I, 15000U) (Neo Lab) and Shrimps Phosphatase Alkali (SAP, 500U) (Promega). In a

final volume of 4µl 0.32µl SAP (1U/µl) and 0.09µl Exo I (20U/µl) were added to the PCR product. Reactions were incubated at 37°C for 25 min and then at 72°C for 15 min.

Gel Electrophoresis

All PCR products were analysed by electrophoresis using 2% agarose gels. These were made by melting 2g agarose in 100ml 1x TAE buffer (89mM Tris HCl, 89mM boric acid, 10mM EDTA) by heating in a microwave oven for 2 minutes and then adding 5µl ethidium bromide solution. The electrophoresis was performed in gel tanks containing 1x TAE buffer. 1.5µl of each PCR was loaded onto the gel and electrophoresis was carried out at 120V for 20-30 minutes. SmartLadder (Eurogentec, Seraing, Belgium) was co-loaded to specify PCR product sizes and estimate product quantity. Agarose gels were analyzed under UV-light and photographed.

Sequencing reaction

In the sequencing reaction either the forward or the reverse primer is used. In addition to unlabelled dNTPs the reaction also contains fluorescence labelled ddNTPs. When incorporated into the growing DNA sequence these labelled ddNTPs terminate the elongation of the DNA because they don't have a 3'-hydroxy group. This leads to amplified DNA fragments with different sizes that can be separated by capillary electrophoresis and detected after excitation by a laser. Sequences were viewed with the program SeqMan which is part of the DNASTAR software package (DNASTAR, Inc. Madison, USA).

Sequencing reactions contained the following in a final volume of 10µl: 2-4µl clean up reaction product, 0.25µl ABI Big Dye version1.1 (Applied Biosystems GmbH, Germany), 1µM primer, and 1.75µl sequencing buffer (Applied Biosystems GmbH, Germany). The sequencing reaction was performed in a Tetrad2 thermocycler (Bio-Rad Laboratories, Inc., Germany). Parameters consisted of 33 cycles each with 10sec at 96°C, 5sec at 55°C and 4min at 60°C, followed by a final hold at 16°C. Purification of sequencing reactions (CleanSEQ) and the subsequent sequencing run were performed by the CCG sequencing facility.

2.4 RNA Extraction, Quality Control and Quantification

RNA was extracted from primary tissue samples and from disease tissue derived fibroblasts for whole genome and single gene expression analysis.

2.4.1 RNA Extraction from primary Tissue

Tissue samples were taken from Dupuytren Patients undergoing surgery and normal palmar fascia was obtained from persons having carpal tunnel release. Patient consent and ethical approval was confirmed prior to surgery. Tissue samples were placed in RNAlater and shipped at room temperature. Upon arrival samples were stored at -20°C till RNA extraction. Per sample approximately 150mg of tissue was removed from RNAlater stabilising reagent and cut into very small pieces with a sterile scalpel on a petri dish at room temperature. The sample was then placed in a 2ml round bottom eppendorf tube containing one 7mm stainless steel ball.1 ml RLT (Qiagen GmbH, Germany) buffer, containing guanidine thiocyanate and beta-mecaptoethanol or 1ml trizol (QIAzol, Qiagen GmbH, Germany) was added to the sample. In the following samples were kept on ice between steps if not otherwise mentioned. The tissue samples were minced in a bead mill (Tissue Lyser 2, Qiagen GmbH, Germany) for 2-6 min at $30s^{-1}$ and room temperature. Homogenised samples were spun in a table centrifuge (microcentrifuge) at room temperature at maximum speed (14000 rpm) for 5 minutes to remove cell debris. The supernatant was transferred to one or distributed equally to two fresh 2ml eppendorf tubes. If the sample was homogenised in RLT buffer, an equal amount of phenol (Carl Roth GmbH & Co. KG, Germany) was added to the sample. The trizol reagent already contains phenol so that no further addition of phenol to samples homogenised in trizol is necessary. One-fifth volume of chloroform (Carl Roth GmbH & Co. KG, Germany) was then added to the lysate. Samples were vortexed for two to five times with one minute incubation one ice between steps. Samples were spun at maximum speed (13000rmp) in a refrigerable table microcentrifuge for 30 min at +4°C.

Phase separation results in an upper aqueous phase containing the RNA, a whitish interphase consisting mostly of DNA and a red phenol phase containing proteins. The clear upper phase (approximately 500µl) was transferred to a new tube. Again an equal amount of phenol and one-fifth volume of chloroform were added and the samples were spun at 13000rmp for 30 min at +4°C. The aqueous phase was carefully transferred into a new 1.5ml eppendorf tube minimizing chloroform carryover. An equal amount of 99% ethanol (Merck) was added, samples were vortexed briefly and immediately spun at 14000rpm at room temperature. The precipitated RNA formed a tiny whitish pellet at the bottom of the tube. The RNA pellet was washed ones in 80% ethanol and then dried briefly on ice. The dry pellet was dissolved in RNase free water. According to pellet size 5 to 80 µl of water were added to the RNA pellet. The pellet was dissolved by pipetting up and down for a couple of times and then stored at -20°C or -80°C.

2.4.2 RNA Extraction from Primary Fibroblasts

For total RNA extraction from cultured fibroblasts the Qiagen RNeasy Midi Kit (Qiagen GmbH, Germany) was used. The procedure is based on columns with a silica membrane that selectively binds RNA molecules. In brief, RNA is bound to the membrane, washed and then eluted with water. The silica membrane absorbs RNA molecules that are longer than 200 bases, which excludes smaller RNAs from this isolation method. The protocol was followed as provided in the kit's handbook (Chapter: Isolation of total RNA from Animal Cells). All steps were performed at room temperature. All centrifugations were done at 40000rpm.

For each sample cells were grown in T225 cell culture flasks till confluence (approximately $1x10^7$ cells). Media was removed and cells were washed ones with 25ml of PBS. Cells were trypsinised with 15ml 0.5% Trypsin-EDTA (Invitrogen GmbH, Germany) during incubation for five minutes at 37°C. Digestion was monitored with a light microscope and cells were further loosened through gently tapping the flask. Upon debonding of cells the digestion process was stopped by adding 15ml of media. The cells were transferred to a 50ml falcon tube and centrifuged at 1600rpm and 4°C for 3 minutes. Media was removed and 2ml of RLT buffer (Qiagen GmbH, Germany), containing guanidine thiocyanate and beta-mecaptoethanol (~1%) was added to the cell pellet. Guanidine thiocyanate is highly denaturing and inactivates RNases in the lysate while β-mecaptoethanol is used to prevent the reformation of the intra-molecular disulphide bridges. The sample was vortexed vigorously to lyse cells and then stored at -20°C or -80°C till further processing.

A minimum of 8 and a maximum of 12 samples were extracted simultaneously. Thawed to room temperature each sample was mix with 2ml of 70% ethanol and transferred immediately to an RNeasy midi column placed in a 15ml centrifuge tube. The sample was centrifuged for 5 minutes till the lysate had passed completely through the column. The flow-through was discarded and 2ml of wash buffer was added to the column (the first wash step). The sample was again centrifuged for 5 minutes. After that a DNA digestion was preformed. Therefore the RNase free DNase Set (Qiagen GmbH, Germany) was used. In preparation the lyophilized DNase 1 pellet (1500 Kunitz units) was solved in 550µl of RNase-free water. Then 20µl DNase stock was added to 140µl of buffer provided in the set. The DNase mix was pipetted onto the membrane and the sample was incubated for 15 minutes. This was followed by the second wash step. Another volume of 2ml wash buffer was added to the sample. To inactivate the DNase, the sample was incubated for 5 minutes before centrifugation for 5 minutes. In the third wash step 2.5ml of the second wash buffer (RPE) was added to the column and the sample was centrifuged for 3 minutes. This wash

step was repeated ones with a 5 minutes centrifugation. The RPE buffer contains ethanol in order to dry the silica membrane. The dry column was transferred to a fresh 15ml tube and 150µl of RNase-free water were pipetted onto the membrane. The sample was centrifuged for 3 minutes and a second volume of 150µl RNase-free water was added to the column. The sample was again centrifuged for 3 minutes and ~300µl of eluate were transferred to a 1.5ml eppendorf tube. The sample was stored at -20°C or -80°C.

2.4.3 RNA Quantification with NanoDrop Spectrophotometer

Absorbance at 260nm was measured with a NanoDrop ND-8000 Spectrophotometer (Wilmington, USA). 1µl of well mixed RNA sample was loaded onto the ND-1000 Spectrophotometer. Light absorbance at 230nm, 260nm and 280nm was measured and concentration and purity were calculated directly by the provided software.

Absorption at 230nm is caused by contamination with phenol, thiocyanates, and other organic compounds. For a pure RNA sample, the ratio of absorbance at 260 and 230nm ($A_{260/230}$) should be around 2. If the RNA sample is heavily contaminated with proteins, the $A_{260/280}$ will be less than the ideal value of 2. RNA samples were diluted as required for downstream applications.

2.4.4 RNA Quality Control with Bioanalyzer Instrument

While a spectrophotometer measures the concentration of nucleic acids, it gives no information about the integrity of the RNA (or DNA) in the sample. Highly degraded RNA can be unsuitable for downstream applications. Therefore the 2100 Bioanalyzer (Agilent Technologies GmbH, Germany) was used to access RNA integrity. In addition the Bioanalyzer offers a more accurate method to determine purity and quantity of a RNA sample. The Bioanalyzer is a microfluidics-based platform for separating RNA with a capillary electrophoresis system. The associated software program estimates the integrity of the RNA based on the entire electrophoretic trace of the sample (Schroeder *et al.* 2006). This includes the presence or absence of degradation products and is independent of sample concentration. The software automatically assigns an integrity number (RIN) to an eukaryote total RNA sample. The RIN ranges from 1 to 10, with 10 describing a completely non-degraded RNA sample. The RIN is dependable on isolation method with which the RNA sample was extracted. RNA purification over silica based columns bias towards larger RNAs overestimating RNA quality (Schroeder *et al.* 2006). Figure 13 and 14 give examples for electrophoretic traces separated with the Bioanalyzer instrument.
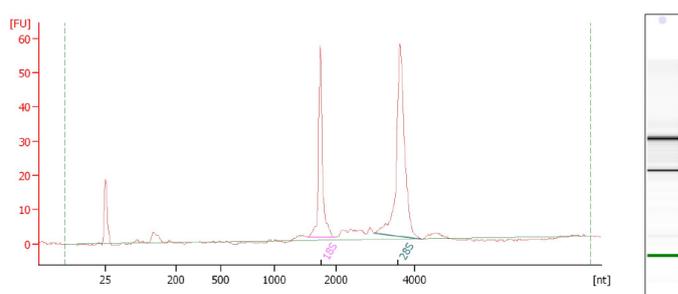
Figure 13. Example for an electrophoretic trace of a total RNA sample with RIN 9.8.
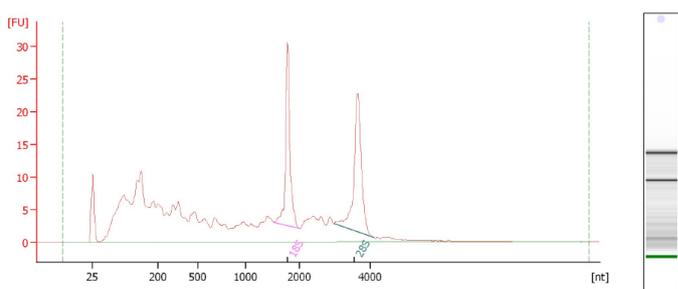
Figure 14. Example for an electrophoretic trace of a total RNA sample with RIN 6.7.

The Agilent RNA 6000 Nano Kit was applied to analyse RNA samples with the bioanalyzer instrument. The Agilent RNA 6000 Nano Assay Protocol (Edition April 2007) was followed for the procedure. 12 RNA samples can be loaded onto one RNA 6000 Nano chip. In preparation 1.5µl of RNA samples was pipetted into 0.2ml PCR tube-stripes. RNA samples were denatured at 70°C for 2 minutes in a PCR cycle machine and transferred on ice afterwards. The RNA 6000 Nano gel matrix was filtered prior to use. 1µl of dye concentrate was added to 65µl of filtered gel. The bioanalyzer instrument comes with a priming station for loading the gel dye mix into the chip. 18µl of gel dye mix was loaded onto the chip as described in the manual. Then 5µl of RNA 6000 Nano marker were loaded into all 12 sample wells and an additional marker well on the chip. Finally 1µl of denatured RNA sample was loaded in each of the 12 sample wells. The chip was vortexed for 1 minute at 2400rpm and then run on the bioanalyzer instrument. Data analysis was done automatically on the associated desk top computer.

2.5   Whole Genome Gene Expression Analysis

The Illumina HumanHT-12 v3 Expression BeadChip was used for whole genome expression analysis of DD samples and controls. Each array on the HumanHT-12 v3 Expression BeadChip targets more than 25,000 annotated genes with more than 48,000 probes derived from the National Center for Biotechnology Information Reference Sequence (NCBI) RefSeq (Build 36.2, Rel 22) and the UniGene (Build 199) databases. The BeadChip is

designed to support highly efficient genome-wide association studies (GWAS). 12 samples can be processed per BeadChip. 12 DD primary tissue samples were compared with 12 matched controls. Control connective tissue samples were obtained during trigger finger or carpal tunnel release. All participating subjects were of European origin. The mean age of DD patients was 65±10 years. While the average age of the control subjects was 61±13 years. Table 2 gives an overview over analysed samples. For the whole genome gene expression analysis only RNA samples with RIN≥6.9 were used.

Table 2. Whole Genome Expression Analysis Samples.

NR	sample	sample ID	status	gender	birth yr	familial	source	conc.	260/280	260/230	RIN
1	7509601	7509601	control	f	1930	no	TVS III	209	1.98	1.86	7.4
2	7511401	7511401	control	f	1938	no	KTS	323	1.93	1.96	7.5
3	7510801	7510801	control	f	1954	no	KTS	311	1.92	2.24	7.9
4	7512601	7512601	control	f	1960	no	KTS	224	2.06	2.07	7.8
5	7012201	7012201	patient	f	1934	no	DD	408	2.08	1.87	7.1
6	3012101	3012101-2	patient	f	1937	no	DD	533	2.10	1.96	8.3
7	7001501	7001501	patient	f	1941	no	DD	65	2.01	2.08	9.5
8	3015701	3015701-2	patient	f	1952	yes	DD	116	1.96	1.89	8.2
9	7509901	7509901-2	control	m	1930	no	TVS IV	74	1.93	2.09	7.1
10	7512101	7512101	control	m	1934	no	KTS	169	1.89	2.23	7.3
11	7510401	7510401	control	m	1946	no	TVS V	186	1.94	1.96	6.9
12	7513101	7513101	control	m	1950	no	KTS	196	2.05	2.08	7.0
13	7512501	7512501	control	m	1956	no	KTS	118	2.07	2.13	9.1
14	7510001	7510001	control	m	1961	no	KTS	125	1.89	2.23	7.6
15	7511101	7511101	control	m	1965	no	KTS	150	1.94	1.75	7.3
16	7509501	7509501	control	m	1966	no	KTS	169	2.01	2.02	8.5
17	7301801	7301801-2	patient	m	1932	no	DD	99	2.03	2.01	9.8
18	7002601	7002601-2	patient	m	1942	yes	DD	263	2.00	1.99	8.5
19	7020901	7020901	patient	m	1946	yes	DD	440	2.00	2.24	7.8

Samples used in the Whole-Genome Gene Expression Analysis. NR: sample number in order of appearance on the expression chip (samples 1-12: chip 1, samples 13-24: chip 2); gender: f: female, m: male; birth yr: year of birth of the proband, familial: yes, if family members of the subject were affected by DD, source: source of the analysed tissue: DD: Dupuytren, TVS: trigger finger, KTS: carpal tunnel; conc.: RNA concentration (ng/µl) in the original sample as determined with the bioanalyzer instrument, 260/280: absorbance ratio at 260nm and 280nm measured with NanoDrop ND-8000 Spectrophotometer, 260/230: absorbance ratio at 260nm and 230nm measured with NanoDrop ND-8000 Spectrophotometer, RIN: RNA integrity number.

Table 2 continued:

NR	sample	sample ID	status	gender	birth yr	familial	source	conc.	260/280	260/230	RIN
20	7514101	7514101-2	patient	m	1948	no	DD	526	2.09	2.03	8.6
21	7000501	7000501-1	patient	m	1936	yes	DD	491	2.07	2.00	7.3
22	3012901	3012901-2	patient	m	1953	no	DD	49	1.97	1.97	9.4
23	7001901	7001901-1	patient	m	1958	no	DD	254	1.97	1.76	8.8
24	7005901	7005901-1	patient	m	1964	no	DD	69	1.98	1.73	9.0

Samples used in the Whole-Genome Gene Expression Analysis. NR: sample number in order of appearance on the expression chip (samples 1-12: chip 1, samples 13-24: chip 2); gender: f: female, m: male; birth yr: year of birth of the proband, familial: yes, if family members of the subject were affected by DD, source: source of the analysed tissue: DD: Dupuytren, TVS: trigger finger, KTS: carpal tunnel; conc.: RNA concentration (ng/µl) in the original sample as determined with the bioanalyzer instrument, 260/280: absorbance ratio at 260nm and 280nm measured with NanoDrop ND-8000 Spectrophotometer, 260/230: absorbance ratio at 260nm and 230nm measured with NanoDrop ND-8000 Spectrophotometer, RIN: RNA integrity number.

2.5.1 RNA Amplification for Array Analysis

The Illumina TotalPrep RNA Amplification Kit (Ambion Inc., USA) was applied for generating biotinylated, amplified RNA for hybridisation with the Illumina HumanHT-12 v3 Expression BeadChip. The protocol comprises three oligonucleotide synthesis steps and two column purification steps. In the **first step** (**Reverse Transcription**) the mRNA in the sample is used as a template by the reverse transcriptase (ArrayScript) to generate single stranded cDNAs. The oligo-dT primer in this reaction binds to the poly-A tails of the mRNAs. In addition the primer contains a T7 promoter sequence that gets thus incorporated into the cDNA.

In the **second step** the single stranded cDNA is converted into double-stranded DNA (**Second Strand Synthesis**). This reaction employs DNA polymerase and RNase H to simultaneously synthesize second strand cDNA and degrade the RNA. The cDNA is purified in **the third step** to remove RNAs, primer and enzymes. In the following ***in vitro transcription*** antisense RNA (cRNA) copies of the original mRNA are generated from the double-stranded cDNA template by a T7 RNA polymerase. The cRNAs are biotin-labelled through the incorporation of biotin-UTP. This is the amplification step of the procedure. In the **last step** the cRNA is purified over a silica membrane column.

Eight samples were processed simultaneously. Appropriate master mixes were prepared for each reaction. All centrifugations were carried out at 10000rpm and room temperature. Per sample 500ng total RNA in 11µl of nuclease-free water was placed in 0.2ml sterile PCR tube-stripes. 9µl of reverse transcription master mix was added to the sample. The master

mix consisted of 1µl T7 Oligo(dT) primer, 2µl 10x first strand buffer, 4µl dNTP mix, 1µl RNase inhibitor and 1µl ArrayScript. Sample and master mix were mixed thoroughly by pipetting up and down 2-3 times and flicking the closed tube-stripe 3-4 times. The tube-stripe was centrifuged briefly to collect the reaction mix at the bottom of the tube and then incubated for 2h at 42°C in a thermal cycler with the lid temperature set to 50°C to prevent condensation.

After 2 h the sample was removed from the cycler und immediately transferred on ice. 80µl of second strand master mix containing 63µl of nuclease-free water, 10µl 10x second strand buffer, 4µl dNTP mix, 2µl DNA polymerase and 1µl RNase H, was added to the sample. The sample was then incubated for 2 h at 16°C. After second strand synthesis the sample was placed on ice and transferred to a 0.5ml reaction tube. 250µl of cDNA binding buffer was mixed with the sample. The sample was then pipetted onto a cDNA filter cartridge sitting in a wash tube. The sample was centrifuged for 1min till the mixture had passed through the filter. The flow-through was discarded. The cDNA sample bound to the filter membrane was washed with 500µl of wash buffer. The wash buffer was passed through the filter during 1min centrifugation. The flow-through was discarded and the sample was placed back in the empty wash tube for another 1min centrifugation to remove the wash buffer completely from the filter before the filter cartridge was placed in an elution tube.

Nuclease-free water was pre-heated to 55°C. 20µl of the water was pipetted onto the filter. The sample was incubated for 2 min and then centrifuged for 1min. Elution resulted in ~17.5µl purified cDNA. The eluate was transferred in a 0.2ml PCR tube-stripe. The *in vitro* transcription (IVT) mater mix was prepared at room temperature. It consisted of 2.5µl T7 10x reaction buffer, 2.5µl T7 enzyme mix and 2.5µl biotin-NTP mix. 7.5µl of the IVT master mix was mixed with the cDNA sample. The sample was then incubated for 14h at 37°C in a thermal cycler with the lid temperature set to 100°C. After 14h the product was cooled to 4°C and incubated for ~16h. The reaction can be held post-IVT for up to 48h at 4°C for convenience. The reaction was stopped by adding 75µl of nuclease-free water to the sample. The sample was then transferred to a 0.5ml reaction tube. 350µl of cRNA binding buffer was mixed with the sample. 250µl of 99% ethanol was added ad the whole mixture was immediately transferred to a cRNA filter cartridge sitting in a wash tube. The sample was centrifuged for 1min and the flow-through was discarded. The sample was then washed with 650µl of wash buffer. After the wash buffer had passed through the filter the flow-through was removed and the filter was placed back in the wash tube and centrifuged for an additional 1min. The filter cartridge was then transferred to a fresh elution tube and 200µl of

preheated (55°C) nuclease-free water was pipetted onto the filter. The sample was incubated in a heat block at 55°C for 10 min. the sample was then centrifuged for 1.5min. Approximately 200µl of cRNA was eluted. CRNA yield was determined with NanoDrop 8000 Spectrometer. For the whole genome gene expression direct hybridisation assay the biotin-labelled cRNA was normalised to 750ng in 5µl. The appropriate amount of sample constituting 750ng was vacuum dried in a vacuum centrifuged (speed rac) and then resuspended in 5µl of water.

2.5.2 Whole Genome Gene Expression Direct Hybridisation Assay

The whole genome gene expression direct hybridisation assay was preformed over two days. On the first day the cRNA sample was dispensed to the BeadChip and then hybridised over night for 14-20h. On the following day the BeadChip was washed, labelled and analysed with the Illumina BeadArray Reader.

In preparation the cRNA sample was heated at 65°C for 5 minutes, vortexed and pulse centrifuged at 250xg. After the sample had cooled again to room temperature it was mixed with 10µl of hybridisation mix (HYB) and loaded onto the BeadChip. The 15µl was pipetted onto the inlet port for each lane on the BeadChip. The liquid was then transported by capillary forces between BeadChip and coverseal. The BeadCip was placed in a humidified hybridisation chamber and incubated in a hybridisation oven at 58°C for 19:20h on a slow moving rocker.

After hybridisation the BeadChip was removed from the hybridisation chamber and submerged face up in wash buffer (E1BC). Then the coverseal was removed while the chip was under the buffer. The BeadChip was placed in a slide-rack submerged in a cuvette containing 250ml wash buffer (E1BC). The rack was the transferred to a wash bath containing high temperature wash buffer. The chip was incubated static at 55°C for 10 minutes in this wash bath. After that the chip in the slide-rack was immediately transferred back into the cuvette containing fresh wash buffer E1BC. The slide-rack was gently moved up and down 5-10 times under the buffer. The cuvette with the slide-rack was then placed on an orbital shaker and shaken at room temperature for 5 minutes. The slide-rack was transferred to a cuvette containing 250ml 99% ethanol and washed for 10 minutes on the orbital shaker. Afterwards the chip was washed again in wash buffer as above, this time with two minutes incubation on the rocker.

In the next step the BeadChip was blocked with block buffer. Therefore the chip was placed in a wash tray, covered with block buffer and incubated on the shaker for 10 minutes.

After the blocking step the BeadChip was transferred to a fresh wash tray containing 2µg Cy3-Streptavidin in 2ml blocking buffer. Streptavidin is a bacterial protein that binds non-covalently to the biotin in the cRNA. Cy3 is a fluorescent dye of the cyanine dye family. The excitation of Cy3 by ~550 nm laser light induces a light emission maximum of ~570 nm. The chip was completely covered with the buffer and incubated for 10 minutes on the shaker at room temperature. After the incubation the chip was washed again in wash buffer E1BC for 5 minutes. Lastly the BeadChip was dried by 4 minutes centrifugation at 1400rpm and room temperature. The chip was then scanned with the Illumina BeadArray Reader.

2.5.3 Expression Data Analysis with Illumina Genome-Studio

The data generated with the BeadArray Reader was visualized with the Illumina GenomeStudio Data Analysis Software. This tool supports the primary analysis of microarray-based data and offers different graphical interface to view results. Differential mRNA expression results were exported as table in Excel (Microsoft).

2.5.4 Expression Data Analysis with Ingenuity Pathway Analysis

With the Ingenuity Pathways Analysis software expression data was further analyzed. The software integrates data from a variety of experimental platforms to analyse protein networks and pathways. The software enables the search for networks and pathways that are altered in expression data sets.

2.6   Quantitative Real-Time PCR

Reverse-transcription quantitative real-time PCR (RT-qPCR) was performed using the LightCycler®480 platform (Roche Diagnostics GmbH, Germany) and corresponding LightCycler® (Roche Diagnostics GmbH, Germany) 480 software release 1.5.0 (version LCS480 1.5.0.39, Roche Diagnostics).

Eleven target genes were selected from the expression chip results for verification with RT-qPCR (TGFβ3, MAFB, RSPO2, SFRP4, WNT2, ACTA2, APP, CASP3, CAT, MAOA and SOD2). Each target gene was compared to four reference genes (EIF3H, EIFC2C, GAPDH and PCDH18). Reference genes were also chosen from the chip results for showing similar expression levels in disease and control fascia.

The experiment was carried out for nine DD patients and nine controls. The patient samples were different ones from the ones used in the expression chip experiment. The control samples were different except two that were used before in the expression chip experiment.

Primer pairs for selected target genes were either designed with the Roche probe primer design tool provided via the Roche homepage or with the web based NCBI primer blast tool. Specificity was tested against the human RNA reference sequence with NCBI and/or ensemble blast tools. Primer sequence and product size are given in table 32 (in the appendix).
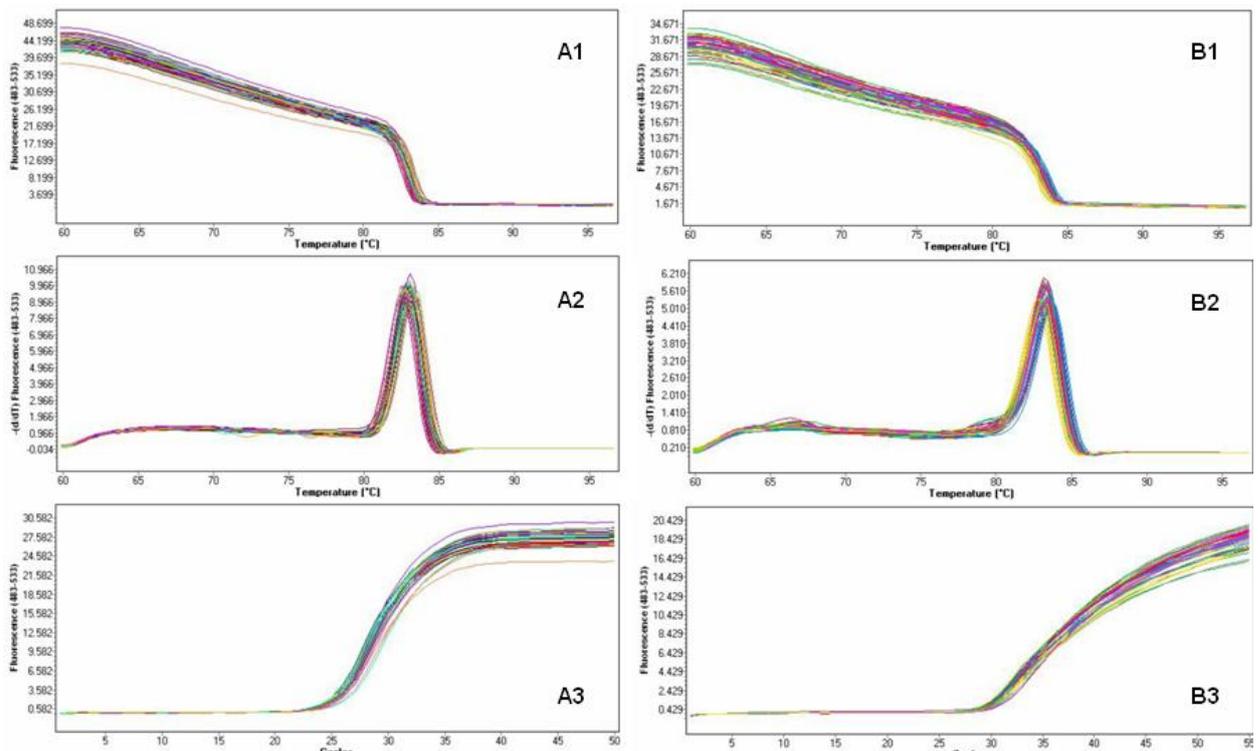
Figure 15. Depicted are two examples for melting and amplification curves generated in RT qPCR. A melting and amplification curves for EIF3H as an example for one reference gene, B melting and amplification curves for FZD4 as an example for one target gene. 1. Melting curve; 2. Negative derivative of the sample fluorescence versus temperature showing one melting peak for all samples. This indicates a pure, homogenous amplification of a single PCR product. 3. Amplification curve.

The SYBR® GreenER™ qPCR reagent system (Invitrogen GmbH, Germany) was applied to perform the RT-qPCR. The SYBR Green dye incorporates into double-stranded DNA, and emits light upon excitation. Thus, as the double-stranded PCR product accumulates, fluorescence increases. The drawback of this relatively simple system is that the dye also binds to any other double-stranded DNA present in the reaction, including primer dimers and other non-specific reaction products. This may result in false positives if primers are not specific. Primer specificity was therefore carefully checked in preparation and confirmed with melting curve analysis. Melting curves were done for all reference and target genes to assure that the same target was amplified in patient and control samples. Figure 15 gives examples for melting and amplification curves for one reference and one target gene.

Each RT-qPCR reaction was carried out in a final volume of 20µl, consisting of 2µl diluted RNA (approximately 10ng RNA), 10µl EXPRESS SYBR GreenER qPCR SuperMix Universal (Invitrogen GmbH, Germany), 0.4µM of forward and reverse primer each (Sigma-Aldrich Co, Germany), 0.5µl of Express SuperScript Mix for One-Step SYBR GreenER (Invitrogen GmbH, Germany), and 6.7µl DNase/RNase-free water (Invitrogen GmbH, Germany). Each reaction was done in duplicate. The reactions were carried out in white 96-well plates (Roche Diagnostics GmbH, Germany).

The RT-qPCR program consisted of the following steps, **1. Reverse transcription (RT):** Firstly the template RNA was transcribed into cDNA. Therefore samples were incubated at 55°C for 5 minutes. **2. Pre-Incubation:** The qPCR reactions were then initiated at 95°C for 2 minutes to activate the Hot Start Taq polymerase. **3. Amplification:** Each of the following 50 amplification cycles consisted of a 10seconds denaturation step at 95°C, a 30 seconds annealing step at 60°C and a 6 seconds elongation step at 72°C. The fluorescence intensity was recorded at the end of the elongation step in each cycle. **4. Melting curve:** After the 50 cycles of amplification a melting curve was recorded in order to test product specificity. This included a 5 seconds step at 95°C, a 1 minute step at 60°C and a final heating of the product to 97°C. **5. Cooling:** The program was concluded with a cooling step at 40°C for 10 seconds.

PCR efficiency (E) was set to two for all target and reference genes, implying that the amount of respective PCR product was doubled in each cycle. However this is rarely the case, because a variety of factors influence PCR efficiency e.g. primer annealing, annealing temperature and sample preparation, and not all may be optimal. So that E is likely to be lower than two and may also differ slightly between target and reference genes. This was borne in mind during data analysis. Target genes that showed low PCR efficiency as evident from complanate amplification curves were exclude from the analysis.

Data analysis

Difference between the gene expression levels of DD and controls was assessed with the quantification cycle (C_q) method (Livak and Schmittgen, 2001) as provided by the Light Cycler 480 software (Roche Diagnostics GmbH, Germany). C_q values were obtained from the qPCR. ΔC_q was calculated by subtracting C_q of the internal controls, which was the averaged C_q of the reference genes, from the C_q of the target genes. Levels of target gene expression normalized using reference genes or relative gene expression levels were represented by $2^{-\Delta C_q}$ (Schmittgen *et al*. 2008). Two-tailed student's t-test on the $2^{-\Delta C_q}$ of DD and controls for all reference and target genes were carried out in excel. The significance

level was set to P = 0.05. If the P-value was below 0.05 the null hypothesis that relative expression levels between DD and controls did not differ was rejected. Fold change of the relative gene expression levels of DD compared to controls were calculated using the $2^{-\Delta\Delta Cq}$ method (Livak and Schmittgen, 2001).

In order to further assess the expression of the eleven target genes in DD, disease and control tissues within the same patient were compared. Therefore the relative expression values of disease tissue were compared with those of macroscopically normal appearing fascia tissue, which was removed from adjacent to the disease tissue. This experiment was carried out for four DD patients. Additionally the gene expression of disease tissue was compared to that of fat tissue from the same patient. The fat tissue also originated from adjacent to disease tissue. This was done for two patients.

In a next step the expression values of the eleven afore mentioned target genes as well as those of additional target genes (THBS4, EPDR1, FZD4, GSK3β; CDH1 and ATP5B) were compared for DD and control derived primary fibroblast cell lines. A slightly different set of reference genes was used in this experiment (EIF3H, EIFC2C, GAPDH, and RN18S1). The analysis was done for eleven patient cell lines and seven control cell lines. Cells were harvested in passage two. To assess the influence of TGFβ1 on target gene expression, the relative expression values of fibroblasts treated with TGFβ1 were compared to the same cell line not treated with TGFβ1. This was done for five DD patients and one control. Data analysis in all RT-qPCR experiments was done as described above.

2.7 Cell Culture of Human Fibroblast Cell Lines

2.7.1 Isolation of Human Fibroblasts from primary Tissue

Primary disease tissue was sampled from Dupuytren´s patients undergoing surgery. Control tissue of unaffected palmar fascia was taken from control persons requiring carpal tunnel release.

Tissue samples were immediately placed in twenty millilitres of transport media containing: 10% FCS, 75µg/ml Amphotericin, 100 IU/ml Penicillin, 100µg/ml Streptomycin and 10 mg/ml Gentamycin in Dulbecco's modified Eagle's medium (DMEM, Invitrogen GmbH, Germany). Samples were sent to the CCG at room temperature. All further processing of samples at the CCG was done under sterile conditions under a Biowizard Xtra XF-130 cell culture fume hood (Kojair Tech Oy, Finland). Upon arrival tissue samples were removed from transport media and washed ones in phosphate-buffered physiological saline solution

(PBS: 136.8mM NaCl, 2.5mM KCl, 0.8mM Na_2HPO_4, 1.47mM KH_2PO_4, 0.9mM $CaCl_2$, 0.5mM $MgCl_2$ ($6H_2O$), Invitrogen GmbH, Germany). Most fat was macroscopically removed. Samples were then cut into small pieces of approximately $0.3cm^3$ with sterile scalpels. Up to ten of those pieces were placed in one round 8cm Petri dish. A small amount of culture medium containing the following: 10% FCS (foetal calve serum, Invitrogen GmbH, Germany), 100 IU/ml Penicillin, 100µg/ml Streptomycin and 2mM Glutamine was carefully added to the Petri dish and samples were incubated in a Heraeus BBD6220 cell culture incubator (Thermo Fisher Scientific Inc., Germany) at 37°C in a humidified atmosphere of 95% air and 5% CO_2 over night. On the following day approximately ten millilitres of culture medium was added to the culture dish. Media was change every two to four days. Outgrow of fibroblasts from the tissue pieces was checked weekly with an Axiovert40CFL light microscope (Carl Zeiss AG, Germany).

2.7.2 Cultivation of Human Fibroblasts

Once the tissue pieces were surrounded by a ring of fibroblasts, the tissue pieces were removed and media was aspired. Cells were washed once with PBS and 5ml of 0.5% Trypsin with 0.53mM EDTA (Invitrogen GmbH, Germany) pre-warmed to 37°C was added to the dish. Cells were incubated at 37°C. Digestion of cells was monitored with a light microscope (Axiovert40CFL, Carl Zeiss AG, Germany). Upon debonding of cells the digestion process was stopped by adding 5ml of culture media. Cells were transferred to a 15ml tube and centrifuged at 1600rpm for 3 minutes. Media was aspirated and the cell pellet was dissolved in 10ml of fresh media. Cells were transferred to a $225cm^2$ cell culture flask in a final volume of 50ml culture medium. Cells were grown till confluence and then harvested by trypsinization: medium was removed; cells were washed once with 20ml of PBS; 15ml of 0.5% Trypsin was added; digestion at 37°C; 15ml of culture medium was added; centrifuged at 1600rpm for 3 minutes. Liquid was aspirated and the cell pellet was dissolved in 4.5ml FCS supplemented with 10% DMSO. Cell content of one $225cm^2$ flask was split to three 2ml cryoconservation tubes. Samples were frozen at -80°C over night followed by long term storage in a liquid nitrogen tank.

2.7.3 Cultivation of Fibroblasts on Coverslips

Human fibroblasts were grown either on poly-L-Lysine, fibronectin, collagen coated or non-coated glass coverslips. One coverslip was placed in each well off six-well cell culture plates. Approximately $1x10^5$ cells were planted per well. Each well contained 2ml of culture

medium. Cells were either untreated or treated with 2ng/ml TGFβ1 and cultivated for 2-5 days.

22mm round fibronectin (human) coated glass coverslips were purchased from BD Bioscience. Poly-L-lysine coated coverslips were prepared as follows. 22x22mm glass coverslips were roughened in 65% nitric acid and 37% hydrochloric acid (2:1) for 2h on a slow moving magnet stirrer. Coverslips were washed in dH$_2$O for 15 minutes. Coverslips were stored in 99% ethanol. Under a cell culture fume hood the appropriate number of coverslips was air dried and one coverslip was transferred to each well of a six well culture dish. Coverslips were covered with 0.01% Poly-L-Lysine solution (Sigma Aldrich GmbH, Germany) and incubated for 10 minutes. Poly-L-lysin solution was aspirated and coverslips were dried ~1h. Coverslips were sterilised with UV-light for 45 minutes. Six well plates were stored at 4°C. For collagen coated coverslips, coverslips were roughen as described above, dispersed to 6-well plates, sterilised with UV-light and then coated with 3% collagen solution (bovine, pH 2) (Advanced BioMatrix). Collagen polymerised at room temperature and 6-well plates were stored at 4°C.

Cells were stained immunohistological as follows. The media was aspirated and cells were washed twice with PBS. Cells were fixed with 4% PFA for 15 minutes at 4°C or room temperature. Fixation agent was removed and cells were washed four times with PBS. Cells were permeabilised with 3% BSA, 1% TritonX in PBS for 10 minutes at room temperature. Cells were washed twice and blocked for 1h with 3% BSA in PBS at room temperature. Blocking solution was removed and primary antibody solution (in PBS containing 1% BSA, 0.025% Triton X-100) was added. The αSMA antibody (ab7817, Abcam plc, UK) was diluted 1:1000. Samples were incubated at 4°C over night or ≥1h at room temperature. Primary antibody solution was aspirated and the cells were washed 3 times in PBS. Cells were incubated with secondary antibody for ≥1h at room temperature protected from light.

As secondary antibody Alexa Fluor 488 goat anti-mouse IgG (Invitrogen GmbH, Germany) was used, in a concentration of 5ng/µl. Cells were washed once with dH$_2$O and then incubated with Alexa Flour 594 phalloidin (Invitrogen GmbH, Germany) for 15 minutes in the dark. Samples were washed ones in dH$_2$O and then stained with DAPI (4´,6-diamidino-2-phenylindole, dilactate, Biotium Inc, USA) for 2-3 minutes. Samples were washed four times in dH$_2$O. Coverslips were removed from the cell culture dish, excess liquid was carefully removed with a tissue and coverslips were placed face down on glass slides in a drop of mounting media (0.05M Tris, 25% glycerine, 10% polyvinyl alcohol, 0.4% phenol, pH 8).

Slides were dried in the dark and then viewed with Leica DM6000 B (Leica Microsystems GmbH, Germany).

2.7.4 Collagen Matrix Contraction Assay

In order to compare contraction properties of disease derived primary fibroblasts with control fibroblast a simple contraction assay was performed. Cells (0.5×10^5 per well) were grown in 3-dimensional collagen gels (1.5mg/ml).

Three parts 3% bovine collagen solution, pH 2 (Advanced BioMatrix) were mixed with one part 10x HBSS (Invitrogen GmbH, Germany). A small amount of NaOH was added to adjust the pH value to ~7. Cells were dispensed in FCS and two parts of FCS were given to the collagen mixture. The ready collagen mixture (3:1:2) was cast into 24 well plates (0.5ml/well) and dried at 37°C in a cell culture incubator for 2 hours. Negative controls were cast without cells. Once the collagen-gel was stiff 1ml of media was added to each well and gels were cultivated for up to 13 days.

Gel-matrices were photographed daily and the weight of the gel was measured. As the gel continues to contract, water is excluded from the matrix and the gel weights less.

2.7.5 Functional Assays: Oxidative Stress Enzyme Function

The Amplex® Red Catalase Assay Kit (Invitrogen GmbH, Germany) was used to measure catalase enzyme activity in patient and control primary fibroblasts. Fibroblasts in passage 3 to 6 were used in this experiment. Fibroblasts were cultivated at 37°C and 40.5°C. Cells were grown in 225cm^2 cell culture flasks to confluence, harvested by trypsinization at 37°C and resuspended with 10ml 20mM phosphate buffer. Cell concentration was measured for each sample with a Z2 Cell Counter instrument (Beckman Coulter GmbH, Germany). Cells were then sonicated in 0.1M tris buffer (pH 7.5). The obtained cell homogenate was centrifuged at 4°C and 17xg for 20 minutes. The supernatant was aliquoted into two 1.5ml eppendorf tubes and shock frosted in liquid nitrogen. Samples were stored at -80°C.

In the assay, the catalase (CAT) in the sample first reacts with H_2O_2 to produce water and oxygen. Next the Amplex Red reagent reacts with a 1:1 stoichometry with any unreacted H_2O_2 in the presence of horseradish peroxidase (HRP) to produce the fluorescent oxidation product, resorufin. As catalase activity increases, the signal from resorufin decreases. The results are plotted by subtracting the observed fluorescence from that of a no-catalase control. Resorufin has absorption and fluorescence emission maxima of approximately 571

nm and 585nm, respectively. Because the absorbance is strong, the assay can be performed either fluorometrically or spectrophotometrically.

Samples were thawed at room temperature and transferred on ice. Samples were then diluted to a cell homogenate of approximately 1000 cells/µl. 25µl of each diluted sample was transferred to a 96-well plate. A standard curve of CAT activity (range from 0.626 to 1U/ml) was simultaneously run for quantification. The analysis was done in triplicate. 25µl of 40µM H_2O_2 solution was added to each well. The reaction was incubated for 30 minutes at room temperature. 50µl of 100µM Amplex Red (Resazurin) containing 0.4U/ml HPR was added to each well. The reaction was incubated at 37°C for 30 minutes in the dark. Fluoresces was measured in a microplate reader using excitation at 558nm and emission detection at 610nm. A standard curve was generated from the standard samples and the curve equation was used to determine catalase activity in the patient and control samples. Student's t-test was applied to access significance of catalase activity differences between cases and controls.

2.8 Functional Assays: RNA interference

Based on the results of GWAS and whole genome expression experiments, three genes were selected for RNA interference assays. For each of the following genes: glycogen synthase kinase 3 beta (GSK3β), nucleoredoxin (NXN) and NADPH oxidase 4 (NOX4) three Stealth RNAi siRNA Duplex Oligoribonucleotides were purchased through Life Technologies (Paisley, GB). Per gene, each of the three siRNAs targets a different sequence of the same mRNA.

For RNAi experiments fibroblasts were seeded onto collagen gels in six-well-plates. For the collagen gel 0.25ml collagen/well were mixed with 10x HBSS (Invitrogen GmbH, Germany). The pH-value was adjusted with NaOH till the color indicator within the HBSS turned pink. OptiMEM (Invitrogen GmbH, Germany) was added to bring the mixture to 1ml per well. The collagen mixture was added to the six-well-plate and the plate incubated at 37°C (incubator without CO_2-connection) till the collagen-gel polymerized.

After polymerization plates were seeded with cells and incubated over night (at 37°C in a humidified atmosphere of 95% air and 5% CO_2). On the next day cells were either treated with target or control (Stealth RNAi siRNA negative control Med GC, Life Technologies, Germany) siRNA. 1µl of Lipofectamine 2000 (Invitrogen GmbH, Germany) was diluted in 50µl OptiMEM. The mixture was incubated for 5 min. The Lipofectamine dilution was then combined with a dilution of either target or control siRNA in OptiMEM. The combined solution was incubated for 20min and then added to the cells. Target or control siRNA were

diluted to a final concentration of 50nM when added to the cells. Cells were incubated for 2-4 hours. Cells were then either left untreated or one of the following stimuli was added: 50ng/ml Wnt3a (Sigma Aldrich GmbH, Germany), 2.5ng/ml TGFbeta1 (Abcam plc, UK), 1µM BIO (Sigma Aldrich GmbH, Germany). Cells were incubated for 70 hours. Cells were then harvested by dispatching the collagen gel from the well. The collagen gel was transferred to a 15ml falcon and pelleted by centrifugation. The media was aspirated and the collagen gel stored at -20°C. RNA was extracted with the InviTrap Spin Universal RNA Mini Kit (Stratec Molecular GmbH, Germany). Relative expression levels of target genes were measured by qPCR on the LightCycler®480 platform (Roche Diagnostics GmbH, Germany). The overall knock-down efficiency ranged from 70-80%.

2.9 Histology of primary Tissue Samples

Primary disease tissue samples of DD patients and connective tissue samples of control individuals were collected in transport media (as described above). Upon arrival at the CCG a portion of the sample was transferred to formalin and incubated at 4°C approximately for one day. The sample was then embedded in paraffin, sectioned and stained immunhistochemical and with Haematoxyilin/Eosin.

2.9.1 Fixation, Paraffin Embedding and Sectioning

Tissue samples were cut into small pieces (approx. $3mm^3$). The pieces were then put in a cell safe capsule. Each cell safe capsule was placed in a processing cassette and fixation was performed with the tissue processor LEICA ASP200S (Leica Microsystems GmbH, Germany) with the protocol shown in table 3.

Table 3. Fixation Protocol.

Step	Time	Reagent	Step	Time	Reagent
1	2 hours	Formalin	7	1 hour	100% Ethanol
2	1,5 hours	Formalin	8	1,5 hours	Xylol
3	1,5 hours	70% Ethanol	9	1,5 hours	Xylol
4	1,5 hours	80% Ethanol	10	1,5 hours	Histowax (62°C)
5	1 hour	100% Ethanol	11	1,5 hours	Histowax (62°C)
6	1 hour	100% Ethanol	12	1,5 hours	Histowax (62°C)

Fixation protocol run on the LEICA ASP200S instrument (Leica Microsystems GmbH, Germany).

After fixation samples were transferred to the paraffin station LEICA EG1150H (Leica Microsystems GmbH, Germany) preheated to 65°C. Samples were then halved with a scalpel and put in a stainless steel base mould with the cutting edge on the downside. The processing cassette was filled with 65°C warm paraffin from the paraffin station. The moulds were left to cool on a cold plate until the paraffin block could be easily retrieved.

5μm thin sections were cut with the fully automated rotary microtome LEICA RM2255 (Leica Microsystems GmbH, Germany) and put in a water bath with 37°C. From there the sections were transferred to poly-L-Lysine coated slides. The slides were left to dry on a heating plate at 37°C for one hour and then transferred to an incubator with 37°C overnight.

2.9.2 Haematoxylin-Eosin (HE) Staining

HE stain is a widely used stain in histology. It consists of haematoxylin which stains cell nuclei blue. This nuclear staining is followed by counterstaining with a solution of eosin. Eosin stains protein structures e.g. collagen fibres red. Prior to staining paraffin sections must be deparaffinised and re-hydrated. Sections of disease and control tissue were incubated in xylol for 20 minutes and then re-hydrated by placing the slides two-times in 100% ethanol, two times in 80% ethanol, two times in 30% ethanol, and two times in deionised water (dH_2O) for 10 seconds each. The slides were then transferred to a glass cuvette containing 250ml haematoxylin solution and incubated for three to five minutes. Slides were washed once with dH_2O and the stain was developed under tap water for up to 10 minutes. Slides were rinse again with dH_2O and then incubated in eosin solution for three minutes. Samples were dehydrated by placing the slides two times in dH_2O, two times in 30% ethanol, two times in 80% ethanol, two times in 100% ethanol. From there slides were transferred back to xylol for 5 minutes. Slides were removed, excess xylol was wiped off with a tissue paper and slides were mounted. Dried slides were viewed under a Leica DM6000 B microscope (Leica Microsystems GmbH, Germany).

2.9.3 Immunohistochemical (IHC) Staining

Sections of disease and control tissue were deparaffinised in xylol for 20 minutes at room temperature. Sections were then re-hydrated by placing the slides in each of eight 250ml cuvettes containing decreasing ethanol concentrations (two-times of each 100%, 80%, 30% and 0% ethanol in dH_2O) for ~5sec. while moving the slide-rack gently up and down under the liquid. After that antigen retrieval was preformed. This is necessary because of the formation of methylene bridges during fixation, which cross-link proteins and therefore mask antigenic sites. Either heat-mediated or enzymatic antigen retrieval was performed as

recommended for the single antibodies in their data sheets. For heat-mediated antigen retrieval 250ml of Sodium citrate buffer (10mM Sodium citrate, 0.05% Tween 20, pH 6.0) was boiled in a standard microwave. The slide-rack with the samples was then placed in the hot but no longer boiling citrate buffer and incubated for 30 minutes.

For enzymatic antigen retrieval 100ml of 0.05% Trypsin-EDTA was heated to 37°C in a water-bath before adding the slides and incubating them for 7 minutes at 37°C. After antigen retrieval slides were transferred to TBST buffer (20mM Tris HCl, 150mM NaCl, 0.04% Tween 20, pH 7.4), washed ones in a new volume of TBST and then submerged in 250ml of blocking solution (10% FCS, 1%BSA in PBS). Sections were blocked for 30 minutes at room temperature. After blocking slides were transferred faces up to a staining chamber. (The staining chamber contains a reservoir for H_2O in order to prevent drying out of the sections during staining.) A volume of 70µl primary antibody dilution (in PBS containing 1% BSA, 0.025% Triton X-100) was applied to each section. The αSMA antibody (ab7817, Abcam plc, UK) was diluted 1:1000, the collagen 4 antibody (ab6586, Abcam plc, UK) was also diluted 1:1000. The lid of the staining chamber was closed and samples were incubated over night at 4°C.

On the next day slides were again placed in a slide-rack, washed twice in TBST and transferred back to the staining chamber. Fluorescence labelled secondary antibody was then applied. As secondary antibody for αSMA either Texas Red goat anti-mouse IgG or Alexa Fluor 488 goat anti-mouse IgG (both Invitrogen GmbH, Germany) each in a concentration of 5ng/µl (~350ng per section) were used. As a secondary antibody for collagen 4 Alexa Fluor 488 rabbit anti-goat IgG (Invitrogen GmbH, Germany) was used. Samples were protected from light with the staining chamber lid and incubated for 1-2h at room temperature. Slides were placed back in the slide-rack, washed once in TBST and then stained with DAPI (10µg/ml) for 3 minutes. Slides were washed four-times in TBST. Slides were placed on tissue paper with sections facing up. Mounting media (0.05M Tris, 25% glycerine, 10% polyvinyl alcohol, 0.4% phenol, pH 8) was pipetted onto each section and coverslips were mounted. Slides were dried over night in the dark. Fluorescence was visualised with Leica DM6000 B (Leica Microsystems GmbH, Germany).

2.10 Statistical Tests

The **chi-square test of goodness-of-fit** was used to compare observed allele frequencies of a single nucleotide polymorphism (SNP) marker with the expected allele frequencies under Hardy-Weinberg equilibrium (1 degree of freedom).

If the frequency of one allele in a population is p and the other allele is q, the null hypothesis is that expected frequencies of the three genotypes are p^2, $2pq$, and q^2.

The test statistic is calculated by taking the observed number (O), subtracting the expected number (E) and squaring the difference. Each difference is divided by the expected number, and these standardized differences are summed. The equation is:

$$chi^2 = \sum \frac{(O - E)^2}{E}$$

The chi-square test of goodness-of-fit was preformed with the computer software Plink (see e.g. chapter 2.3.3).

The **Fisher's exact test** was used to examine the association between two nominal variables in a 2 x 2 table (table 2.1). The null hypothesis for this test is that the relative proportions of one variable are independent of the second variable.

Table 4 Example for a 2x2 table used in Fisher's exact test

a	b	a + b
c	d	c + d
a + c	b + d	n = a + b + c + d

The probability of getting the observed data given in table 2.1 is calculated with the hypogeometric distribution under the null hypothesis that the proportions are the same:

$$P = \frac{\binom{a+b}{a}\binom{c+d}{c}}{\binom{n}{a+c}} = \frac{(a+b)!(c+d)!(a+c)!(b+d)!}{n!a!b!c!d!}$$

The **Student's t-test** was applied to compare the means of two samples. The statistical null hypothesis is that the means are equal for the two categories. The t-test assumes that the

observations within each group are normally distributed and the variances are equal in the two groups. The test statistic, t_s, to test whether the means of two unequal sample sizes are different can be calculated using the t-distribution:

$$t_s = \frac{\overline{X}_1 - \overline{X}_2}{s_{\overline{X}_1 - \overline{X}_2}}$$

$$s_{\overline{X}_1 - \overline{X}_2} = \sqrt{\frac{(n_1 - 1)s_1^2 + (n_2 - 1)s_2^2}{n_1 + n_2 - 2}\left(\frac{1}{n_1} + \frac{1}{n_2}\right)}$$

Where $\overline{X}_1$ and $\overline{X}_2$ are the means of group 1 and 2 and $s_{\overline{X}_1 - \overline{X}_2}$ is the standard error of the difference in the means, which gets smaller as the sample variances decrease or the sample sizes increase. Thus t_s gets larger as the means get farther apart, the variances get smaller, or the sample sizes increase. The probability of getting the observed t_s value under the null hypothesis depends on the number of degrees of freedom. The degrees of freedom for a t-test is the number of observations in each group minus two (n1 + n2 − 2). In the equation above s^2 is the unbiased estimator of the variance of the two samples. All t-tests were performed two-tailed.

The significance level for all tests was set to P = 0.05. If the P-value was below 0.05 the null hypothesis was rejected. Statistical tests were performed with excel and were taken from http://udel.edu/~mcdonald/ (McDonald 2009).

3   Results

3.1   Epidemiology

903 samples were collected from summer 2007 to summer 2012. Of those 51 were control samples and 852 were DD patient samples. 815 patients completed the questionnaire while for 37 patients only name, gender and birth date were recorded by the attending physicians. 14 patients were relatives of other participants. 801 of the DD samples were of unrelated patients who completed the questionnaire (table 5). 143 (17.9%) of these were women, resulting in an overall male/female ratio of 4.6:1. Table 5 gives the age distribution of collected samples for men and women.

Table 5. Male-female ratio in DD patients.

decade of live	all	men	women	ratio	familial	%
29-39	15	11	4	2.8:1	8	53.3
40-49	80	70	10	7.0:1	44	55.0
50-59	191	158	33	4.8:1	84	44.0
60-69	278	225	53	4.2:1	102	36.7
70-79	208	169	39	4.3:1	63	30.3
80-89	29	25	4	6.3:1	5	17.2
all	801	658	143	4.6:1	306	38.2

Given are the numbers of male and female DD patients for each decade of live. Considered was the age at collection date. Familial: number and percentage of cases with a positive family history.

3.1.1 Age at first Surgery

For each patient the age at sample collection and the age at first surgery were recorded. The mean age of patients at the sampling date was 63.5 ± 10.5 years (N = 801). The mean age at first surgery was 59.0 ± 12.2 years for all patients that underwent surgery till the collection date (N=736). Women were on average 61.1 ± 11.4 years old when they first underwent surgery (N = 121, 16.4%) while men were 58.6 ± 12.3 years old (N = 615). Men were therefore on average 2.5 years younger than women at the time of first surgery. 65 patients contributed a blood sample but did not require surgery till the time of sample collection. They were on average 61.2 ± 11.7 years old at collection date. 22 (33.8%) of these were women.

Figure 16 and 17 summarise the age distribution of patients. Shown in figure 16 is the age of first surgery for male and female DD patients grouped in decades. The number of patients in

each age group is given on the y-axis. In each of the seven age classes more men than women underwent surgery for DD. Figure 17 gives the proportion of operated patients for each decade of live separated by sex. 30% of men underwent surgery in their sixth and 28% in their seventh decade of live while the largest proportion of women underwent surgery in their seventh decade of live (37%). The youngest male patient was 22, the oldest 87 years of age when they underwent first surgery. The age of first surgery in women ranged from 27 to 84 years of age.
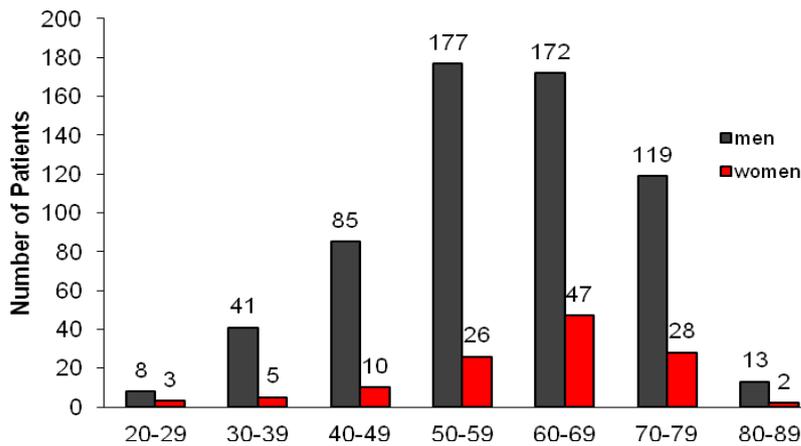
Figure 16. Age distribution of DD patients at the time of first surgery. Given are the numbers of female (dark colour) and male (light colour) patients that underwent first surgery for each decade from 20 to 89 yrs of age.
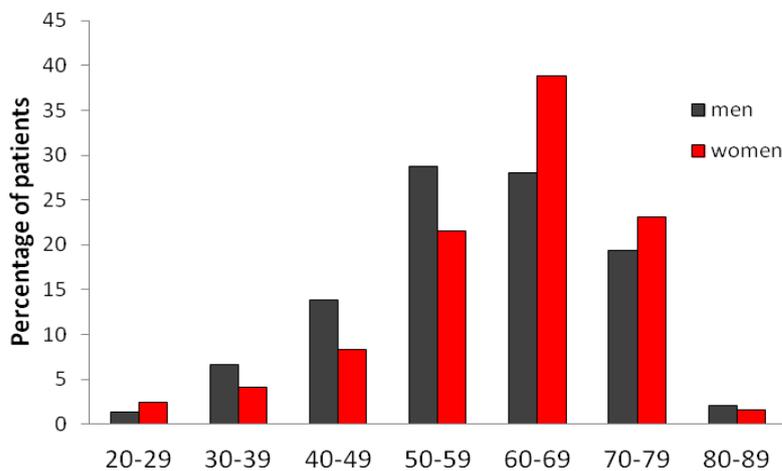
Figure 17. Age distribution of DD patients at first surgery in percent. Given are the percentages of female (dark colour) and male (light colour) patients that underwent first surgery for each decade of live from 20 to 89 yrs. of age.

3.1.2 Affected Hands

In half of the DD patients both hands were affected (see table 6). In 26.9% of cases the right hand and in 22.9% the left hand was affected. For both left and right hand the degree after Tubiana was recorded for each patient. This degree ranged from 0 to 4. Only one affected

finger per hand was taken into account (see introduction). The mean degree for all patients was 2.17 ± 1.13 (N = 711). It was 1.90 ± 1.15 in women (N = 123, 17.3%) and 2.23 ± 1.12 in men (P-value of student´s t-test: 0.00375). 192 (25.0%) of patients had two or more surgeries on the same hand due to recurrence of the disease. Several patients had many surgeries over time.

Table 6. Affected hands in DD patients.

	N	%
hand	767	100
both hands	385	50.2
left hand	176	22.9
right hand	206	26.9
recurrence	192	25.0

3.1.3 Family Predisposition

306 (38.2%) patients reported a family predisposition for DD (see table 7). In 89 (29.1%) cases family members from the maternal line were affected. In 70 (78.6%) of those the mother was affected while in the remaining 19 cases family members other than the mother were affected, e.g. a grandparent or aunt or uncle. 140 patients had affected family members in their paternal line. The father was affected in 134 (95.7%) of those. In three of the remaining six cases the paternal grandfather was affected while the father was not affected.

Table 7 Family predisposition for DD.

familial cases		N	%
total		306	100
lineage known	maternal line	89	29.1
	paternal line	141	45.8
	both	10	3.3
lineage unknown	siblings	43	14.1
	children	4	1.3
	other	19	6.2

Ten patients had affected family members in both maternal and paternal line. Nine of those had both parents affected. For 66 cases the parental line was unknown (siblings or children affected) or not specified (6.2%). 98 (32.0%) patients had more than one affected family member. In 18 cases a grandparent but not the parent was affected by DD. For a number of

additional patients a family predisposition was suggestive but not confirmed e.g. due to the death of relatives (not included in table 7).

DD patients with family predisposition were on average 55.9 ± 12.2 years old when they first underwent surgery for DD (N = 268) compared to patients without family predisposition who were 61.1 ± 11.7 years old (N = 458). This age difference was also evident for males and females separately. Women with family predisposition for DD (N = 48, 17.9%) were 58.8 ± 11.7 years old when they underwent fist surgery while women without family predisposition (N = 71, 15.5%) were 62.9 ± 11.0 years old (Table 8). Men with family predisposition (N = 220) had a mean age of 55.3 ± 12.3 years at first surgery and men without family predisposition (N = 387) were 60.8 ± 11.8 years old.

Table 8. Mean age at first surgery for DD patients with and without familial predisposition.

		N	EDATE	SD	dif	P-value	N	surgery	SD	dif	P-value
All	Non-familial	495	65.1	10.06			458	61.1	11.7		
	Familial	296	61.1	10.6	4.0	1.2E-07	268	55.9	12.2	5.2	2.2E-08
	Maternal and paternal line	10	54.8	10.5	10.3	1.5E-03	10	47.9	12.1	13.2	4.8E-04
Women	Non-familial	82	65.2	9.9			71	62.9	11.0		
	Familial	59	63.0	10.5	2.2	0.2	48	58.8	11.7	4.1	5.4E-02
	Maternal line	23	65.0	10.3			16	61.9	9.4		
	Paternal line	23	58.4	10.2	6.6	3.8E-02	21	54.8	13.2	7.1	8.3E-02
	Line unknown	13	67.8	7.8	2.9	0.4	11	61.9	9.0	0.0	1.0
Men	Non-familial	413	65.1	10.1			387	60.8	11.8		
	Familial	237	60.6	10.6	4.5	1.0E-07	220	55.3	12.3	5.5	1.4E-07
	Maternal line	66	59.6	10.3			63	54.5	13.3		
	Paternal line	118	60.2	10.7	0.6	0.7	108	55.0	12.2	0.5	0.8
	Line unknown	53	62.8	10.4	3.2	0.1	49	56.9	10.8	2.4	0.3

Mean ages at sample collection date (EDATE) and first surgery (surgery) for DD patients with and without familial predisposition for all patients, and women and men separately. P-values are those of student's t-test. Mean ages at first surgery of familiar cases were compared to those of the non-familiar cases within each group ("all", "women" and "men") and paternal line and line unknown were compared to maternal line.

Patients who had affected family members both in their maternal and paternal line (N = 10) were youngest when they first underwent surgery (table 8). Women had an earlier mean age at first surgery when the affected family member was in their paternal line and men had a slightly earlier mean age at first surgery when the affected family member was in their maternal line. For both these categories the standard derivation was larger than in the control group. 101 (34.1%) patients with family predisposition had more than one surgery compared to 102 (20.6%) without family predisposition. Patients with family predisposition had both

hands affected in 59.5% of cases compared to 44.5% in patients without family predisposition (P-value of Fischer's exact test: 0.02). Patients with a family predisposition had a mean stage after Tubiana of 2.2 ± 1.1 compared to 2.2 ± 1.2 in patients without family predisposition.

3.1.4 Ectopic Manifestations and other Diseases

Sample collection was preformed trough eleven different clinics and hospital departments from all over Germany and one in Switzerland. In most centres more than one physician collected the samples and completed the questionnaires. Some recorded parameters varied between centres. E. g. the percentage of patients with family predisposition for DD varied between 24% and 45% (table 9). In contrast the mean ages of sample collection and first surgery differed only slightly between clinics (table 9).

Table 9. Number of samples for the different centers.

Center	N	Familial	%	EDATE	SD	N	Surgery	SD
10	8	3	37.5	61.8	9.5	8	48.5	8.1
30	119	54	45.4	63.5	10.3	118	58.7	12.6
40	29	11	37.9	63.0	8.8	27	56.0	9.8
50	162	54	34.0	65.7	10.9	162	60.4	12.2
60'	16	8	50.0	62.9	9.8	14	56.9	11.7
60"	75	40	53.3	56.8	10.9	52	51.9	13.5
70	110	37	33.6	62.4	9.1	103	58.7	9.9
73	25	8	32.0	66.9	9.0	19	63.1	12.2
75	141	61	43.3	64.8	10.0	119	61.1	12.2
77	73	18	24.7	64.2	9.6	72	60.4	11.8
78	43	12	27.9	62.6	11.4	42	58.5	12.6
all	801	306	38.2	63.5	10.5	736	59.0	12.2

Number of samples and mean ages at sample collection date (EDATE) and first surgery (Surgery) for DD patients collected at different clinics (centres). Number and percentages of familial cases are given for each clinic.

The observed inter-centre variance was especially true for ectopic manifestations of the disease. 102 (12.7%) of all patients had ectopic manifestations. 58 (7.2%) patients showed knuckle pads. The percentage of patients with knuckle pads per centre ranged from 0% to 17.9%. A plantar fibromatosis was present in 41 (5.1%) of all patients. The percentage of plantar fibromatosis ranged from 0% to 11.3% between centres. Two patients had both plantar fibromatosis and knuckle pads. One patient suffered from frozen shoulder and four patients did not specify the location of the ectopic manifestation.

Patients were asked for the presence of other diseases, namely diabetes, rheumatoid arthritis and epilepsy. Most common were hypertension, diabetes, arrhythmia and respiratory

diseases (e.g. asthma, bronchitis, COPD (chronic obstructive pulmonary disease)). Not uncommon were e.g. cancer, thyroid dysfunction, cataract and elevated uric acid levels (or gout). For 135 (16.9%) patients arterial hypertension was recorded while 279 (34.8%) patients took antihypertensive drugs. 108 (13.5%) patients had diabetes type 2. 18 (2.2%) patients had rheumatoid arthritis while 11 additional patients suffered from arthritis (not specified). 3 (0.4%) patients had epilepsy and 6 (0.7%) patients took antiepileptic drugs.

Again prevalence for diseases varied between clinics. Recorded hypertension cases per clinic are given in table 10 as an example for inter-centre variance.

Table 10. Hypertension and antihypertensive drug intake of DD patients from different centres.

Centre	N	Hypertension	%	Antihypertensivies	%
10	8	0	0,0	1	12,5
30	119	23	19,3	60	50,4
40	29	2	6,9	8	27,6
50	162	13	8,0	56	34,6
60'	16	2	12,5	3	18,8
60"	75	4	5,3	11	14,7
70	110	2	1,8	13	11,8
73	25	1	4,0	6	24,0
75	141	48	34,0	55	39,0
77	73	29	39,7	43	58,9
78	43	11	25,6	23	53,5
all	801	135	16.9	279	34.8

Numbers and percentages of DD patients with hypertension and anti-hypertensive drug intake per clinic (centre). N: total number of DD patients sampled at each centre.

3.1.5 Diabetes Mellitus

Diabetes patients are thought to suffer from a milder form of DD than non-diabetic patients. The age at first surgery was therefore compared between the two groups (table 11). Diabetic patients (N = 102, 13.8% female) were on average 3.5 years older (62.1 ± 11.1 yrs) than non-diabetic patients (58.5 ± 12.3 yrs; N = 634, 18.3% female, P-value student's t-test: 0.007) when they first underwent surgery for DD. The same tendency was true for females and males separately (data not shown). The percentage of familiar cases was higher for both women and men in the non-diabetic subgroups (female: 26.7% vs. 44.2%, male: 34.4% vs. 37.8%). The mean degree after Tubiana for diabetic patients was 2.3 ± 1.1 compared to 2.1 ± 1.1 for non-diabetic patients (P-value student's t-test: 0.2).

Table 11. Diabetes mellitus in DD patients.

	N	EDATE	SD	dif	P (t-test)	N	Surgery	SD	dif	P-value
no diabetes	693	63,0	10,6			634	58,5	12,3		
diabetes	108	66,7	9,1	3,7	5,5E-04	102	62,1	11,1	3,5	6,5E-03
familial no diabetes	270	60,2	10,6			243	55,0	12,4		
familial diabetes	36	65,9	9,3	5,7	2,7E-03	35	60,0	10,9	5,0	2,5E-02
non-familial no diabetes	423	64,8	10,2			391	60,7	11,8		
non-familial diabetes	72	67,2	9,0	2,4	6,1E-02	67	63,2	11,0	2,4	0,1

Mean ages at sample collection date (EDATE) and first surgery (Surgery) for DD patients with and without diabetes and familiar predisposition for DD for all patients, and women and men separately. P-values are those of student's t-test. Mean ages at first surgery of familiar cases were compared to those of the non-familiar cases within each group ("all", "familial" and "non-familial").

3.1.6 Alcohol and Smoking

Alcoholism and heavy smoking were suggested as risk factors for DD. DD patients were asked about smoking behaviour and alcohol consumption. 361 (45.2%) were current or former smokers. Smokers (N = 331, 10.3% women) had a mean age of 58.1 ± 12.3 years at the time of first surgery. Non-smokers (N = 405, 21.5% women) were on average 59.7 ± 12.3 years old (P-value, student's t-test: 0.077). Heavy smokers (N = 81, 4.9% women) who consumed more than twenty cigarettes per day had a mean age of 57.1 ± 11.8 years when they underwent first surgery.

Table 12. Smoking behaviour in DD patients.

		N	EDATE	SD	dif	P-value	N	Surgery	SD	dif	P-value
all	non-smoker	438	64.0	10.6			405	59.7	12.3		
	smoker	361	63.4	10.3	0.6	0.5	331	58.1	12.3	1.6	7.7E-02
	<5	64	63.2	11.0	0.8	0.7	59	58.6	11.3	1.1	0.5
	<20	139	62.2	11.6	1.8	0.2	127	57.3	13.0	2.4	5.6E-02
	>20	87	62.8	9.2	1.2	0.5	81	57.1	11.8	2.7	7.1E-02
non-familial	non-smoker	254	65.9	9.7			236	62.7	10.8		
	smoker	241	64.3	10.3	1.6	7.3E-02	222	59.4	12.4	3.3	2.7E-03
	<5	40	64.6	10.6	1.3	0.4	37	58.9	11.4	3.8	5.1E-02
	<20	95	63.2	11.8	2.7	3.2E-02	88	58.8	13.1	3.8	8.0E-03
	>20	58	64.3	9.1	1.6	0.3	54	59.1	11.3	3.5	3.3E-02
familial	non-smoker	184	61.4	11.0			169	55.6	12.7		
	smoker	120	61.1	10.1	0.2	0.7	109	55.6	11.7	0.0	1.0
	<5	24	60.9	11.3	0.5	0.9	22	58.2	11.1	-2.6	0.4
	<20	44	60.1	10.8	1.3	0.7	39	53.9	12.0	1.8	0.4
	>20	29	59.9	8.7	1.5	0.7	27	52.9	11.8	2.7	0.3

Mean ages at sample collection date (EDATE) and first surgery (Surgery) for DD patients with and without family predisposition for DD for smoker and non-smoker. SD – standard derivation, <5: less than 5 cigarettes per day, <20: less than 20 cigarettes per day, >20: more than 20 cigarettes per day. P-values are those of a two-tailed student's t-test.

When cases were divided into patients with and without familial predisposition (table 12) the age difference between smokers and non-smokers was more pronounced in patients without familial predisposition and non-existent in patients with familial predisposition.

When smokers were further subdivided according to the amount of consumed cigarettes per day, the age difference increased with the amount of consumed cigarettes for patients with family predisposition. Patients with family predisposition who consumed less than 5 cigarettes per day were 2.6 years older than non-smokers with family predisposition. In contrast patients with family predisposition who consumed more than 20 cigarettes per day were on average 2.7 years younger than non-smokers and 6.2 years younger than heavy smokers without family predisposition.

Table 13. Alcohol consumption in DD patients.

	N	%
total	801	100
alcohol consumption	663	82.8
occasional	487	60.8
regular	176	22.0
never	136	17.0
alcoholic	2	0.2

Given are the total numbers and percentages of all, occasional, regular, never and diseased alcohol consumers within the sample collective.

663 (82.8%) of DD patients consumed alcohol (see table 16). They were divided into occasional and regular alcohol consumers. The dosage of regular consumers comprised e.g. 1-3 bottles of beer or 1-3 glasses of wine per day. Alcoholism was recorded for two patients.

3.1.7 Early Menopause

Prof. Dr. Sigrid Tinschert noted that some female patients presenting with DD at the clinic in Dresden had a noticeable early menopause. Therefore the parameters age at menopause, hormone intake and ovarian surgery were included in the questionnaire. 76 women gave details about age at menopause, hormone intake and ovarian surgery. The mean age at menopause for these women was 48.2 ± 5.9 years. 39 (51.3%) were under 50 years of age, 19 (25.0%) were between 50 and 51 years and 18 (23.7%) were older than 50 years. 20

(26.3%) underwent ovarian surgery. The mean age of menopausal onset for women without ovarian surgery (natural menopause, N = 56) was 48.5 ± 4.9 years.

3.1.8 Trauma and Sudeck-Dystrophy

18 patients developed DD after hand trauma (surgery). Nine patients suffered from sudeck-dystrophy after DD operation. All 25 patients (two with both trauma and sudeck-dystrophy) had either one or several of the following characteristics: a family predisposition for DD, ectopic manifestations of DD, an aggressive course of disease or fast recurrence after treatment.

3.1.9 Occupational Exposure

Participants were asked about their profession and hobbies in order to classify occupational exposure in DD patients. 454 patients stated their profession or hobby in the questionnaire. 384 could be grouped into professions or groups of profession consisting of more than five members. Of these 352 underwent surgery for DD. Office workers were taken as control group (table 14).

Table 14. Profession of DD patients.

Profession	N	EDATE	SD	dif	P-value	N	Surgery	SD	dif	P-value
Office worker	128	63.1	11.4			116	60.3	12.0		
Teacher	17	66.9	8.6	-3.8	0.2	17	62.6	9.8	-2.3	1.0
Salesclerk	30	63.0	9.2	0.1	1.0	17	61.9	10.3	-1.6	0.8
Carpenter	8	67.7	11.1	-4.6	0.3	8	65.9	12.1	-5.6	0.4
Laboratory technician	7	69.6	8.3	-6.5	0.1	6	66.5	6.1	-6.2	0.4
Electrician	16	65.1	7.4	-2.0	0.5	15	62.7	8.7	-2.4	1.0
Agriculturist, Gardener	22	68.3	8.4	-5.2	0.0	21	60.1	12.5	0.2	0.4
Cook, Baker, Butcher	6	66.9	9.6	-3.8	0.4	6	56.0	17.2	4.3	0.2
Builder	30	62.9	11.0	0.2	0.9	30	58.9	12.8	1.5	0.1
Engineer[1], Machinist	29	60.4	10.8	2.7	0.2	28	55.3	14.6	5.1	3.5E-03
Heavy labour[2]	9	58.2	11.1	4.9	0.2	8	55.5	12.6	4.8	8.5E-02
Metalworker	59	64.4	9.4	-1.3	0.5	58	59.1	12.0	1.3	4.4E-02
Driver	23	59.2	8.8	3.8	0.1	22	54.8	11.3	5.5	2.8E-03

384 participants who stated their profession in the survey and 352 who also underwent surgery for DD. N: number of workers, EDATE: mean age at sample collection, Surgery: mean age at first surgery, SD: standard derivation, [1] exclusive 7 engineers without work specifications; [2] as stated by participant/ attending physician (not specified); P-values are those of student's t-test, the ages of first surgery of each category were compared to those of office workers as a control group.

Office workers (e.g. secretaries, bankers and computer workers) had a mean age of 60.3 ± 12.0 years of age when they first underwent surgery for DD. The mean ages at first surgery of builders and drivers were significantly lower (table 14). These two groups of profession had a mean stage of disease after Tubiana of 2.6 ± 1.3 and 2.7 ± 1.3, respectively, while office workers had a mean stage of disease after Tubiana of 2.2 ± 1.0. Carpenters and laboratory technicians had a higher mean age of first surgery than office workers. The mean stage after Tubiana was highest in carpenters (3.1 ± 0.6).

Table 15. Profession of DD patients.

Profession	Non-familial					Familial				
	N	surgery	SD	dif	P-value	N	surgery	SD	dif	P-value
Office worker	60	62.6	10.7			56	57.8	12.7		
Teacher	10	64.7	10.8	-2.1	0.6	7	59.7	7.3	-1.9	0.7
Salesclerk	9	64.9	11.4	-2.3	0.6	8	58.5	7.6	-0.7	0.9
Carpenter	8	65.9	12.1	-3.2	0.4	0				
Laboratory technician	5	66.6	6.7	-4.0	0.4	1	66.0	0	-8.2	
Electrician	10	66.3	7.1	-3.7	0.3	5	55.6	7.1	2.2	0.7
Agriculturist, Gardener	12	59.4	14.2	3.2	0.4	9	61.1	9.7	-3.3	0.5
Cook, Baker, Butcher	4	50.8	18.8	11.9	5.0E-02	2	66.5	4.5	-8.7	0.4
Builder	25	58.8	11.9	3.9	0.1	5	59.4	16.3	-1.6	0.8
Engineer[1], Machinist	16	60.9	12.7	1.8	0.6	12	47.8	13.5	10.1	1.8E-02
Heavy labour[2]	4	66.3	8.3	-3.6	0.5	4	44.8	4.3	13.1	4.9E-02
Metalworker	34	60.0	12.7	2.7	0.3	24	57.8	10.9	0.0	1.0
Driver	17	56.3	11.4	6.3	3.9E-02	5	49.6	9.2	8.2	0.2

352 participants who stated their profession in the survey and underwent surgery for DD. Those without and with family predisposition considered separately. N: number of workers, EDATE: mean age at sample collection, Surgery: mean age at first surgery, SD: standard derivation, dif: difference in years between the mean ages of each profession and those of office workers, [1] exclusive 7 engineers without work specifications; [2] as stated by participant/ attending physician (not specified); P-values are those of student's t-test, the ages of first surgery/EDATE of each category were compared to those of office workers as a control group.

Patients were further sub-divided in those with and without familial history (table 15). Only professional drivers had a lower mean age at first surgery than office worker for both familial and non-familial groups. The proportion of familial cases in the group of office workers was about 50% while the percentage of familial cases in the group of builders and drivers was much lower (17% and 22%, respectively).

3.2   Genome wide Association Study

Chronological order of experiments is given in the beginning to clarify experimental design. First a genome wide association study was conducted to identify susceptibility loci for DD. 186 unrelated DD DNA samples were compared with 1618 control samples from the POPGEN and KORA cohorts in a case-control setting (904,440 SNPs). Eight candidate regions on chromosomes 1, 2, 6, 7, 9, 11, 16, and X were identified. Four of these reached genome-wide significance with at least one marker with $P < 5x10^{-8}$. The others showed suggested association. A summary of results for the different loci is given in table 33 of the appendix.

At the same time the group of Prof. Wijmenga at the Department of Genetics, University Medical Center Groningen, the Netherlands conducted a GWAS with 960 Dutch persons with DD and 3117 controls. They genotyped the samples with Illumina HumanCytoSNP-12 arrays, which comprise 301,232 SNPs. These were called with the use of the Illumina algorithm (Genome Studio, version 2.10.1). To test for replication of association, they selected SNPs that showed an association with a P value of less than 10^{-4}.

In order to replicate both the findings from the Netherlands and the initial findings from the small GWAS of the present study a selection of 48 SNPs were genotyped with the SNPstream genotyping platform at the CCG (465 DD patients and 282 control samples provided through the University of Essen). In addition more samples from the Netherlands and samples from the UK were genotyped in the group of Prof Wijmenga for their replication SNPs (32 SNPs). The meta-analysis included 2325 DD cases and 11,562 controls and identified nine loci associated on a genome wide level (Dolmans *et al.* 2011).

The remaining German DD cases that were not genotyped with the Affymetrix 6.0 chip were then genotyped on the Affymetrix Axiom platform at the CCG (587,299 SNPs). To date 379 cases have been genotyped with the Axiom CEU 1 chip. These 379 cases were compared with 1219 POPGEN controls that had been genotyped on the same platform at the CCG. The Affymetrix 6.0 (186 cases) and Axiom 2.0 (379 cases, 1219 controls) data were then imputed with the Beagle v.3.3.2 software using the HapMap Phase3 refernce panel. The subsequent association test considered 5,204,451 SNPs.

3.2.1 GWAS results: Axiom Genome-Wide CEU 1 Array Data

57,084 SNP genotypes were excluded because they did not meet quality-control criteria, leaving 530,215 SNPs typed in 359 patients with DD and in 1173 controls. The call rate for the remaining SNPs was 99.4%. There was moderate evidence for inflation in the test statistic (λgc = 1.199) (see figure 18). Adjustment for differential population stratification with the use of the first four components on the basis of a multidimensional scaling analysis of uncorrelated SNPs reduced the inflation to λgc = 1.00. The inflation was caused by genetic heterogeneity between cases. Patients from Switzerland showed the strongest difference to the control samples from the north of Germany (see figures 19-20). There were no signs of differences in SNP call rates between cases and controls.
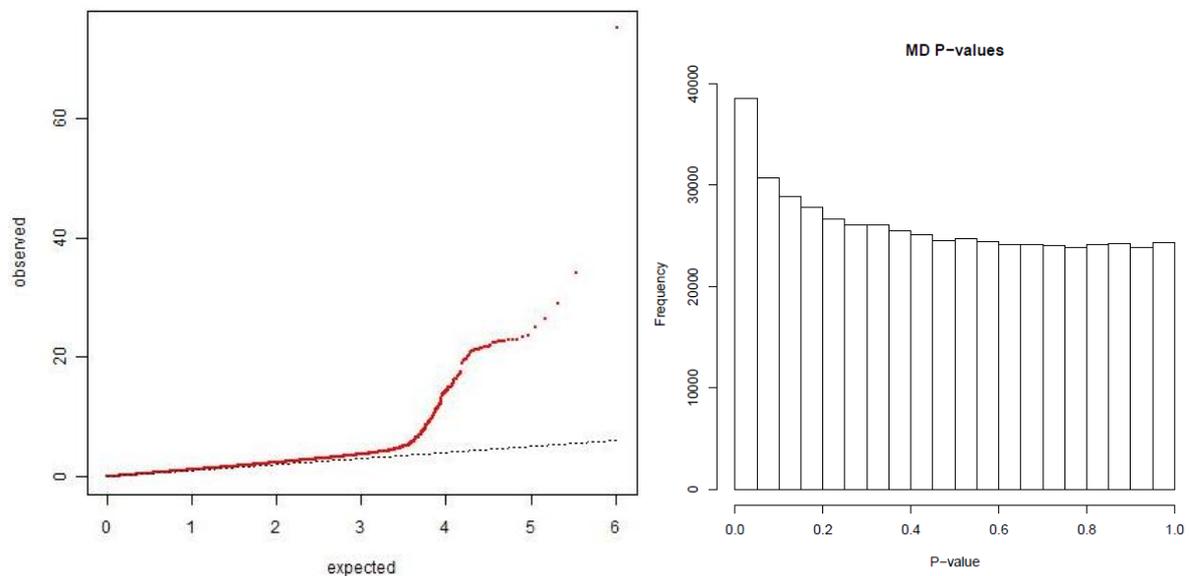
Figure 18. Quantile-quantile plot (qq-plot) of expected vs. observed P-values for a chi-square-test of association (red) before correction for population stratification. Many markers showed P-values of 10^{-3} caused by genetic heterogeneity withing cases.
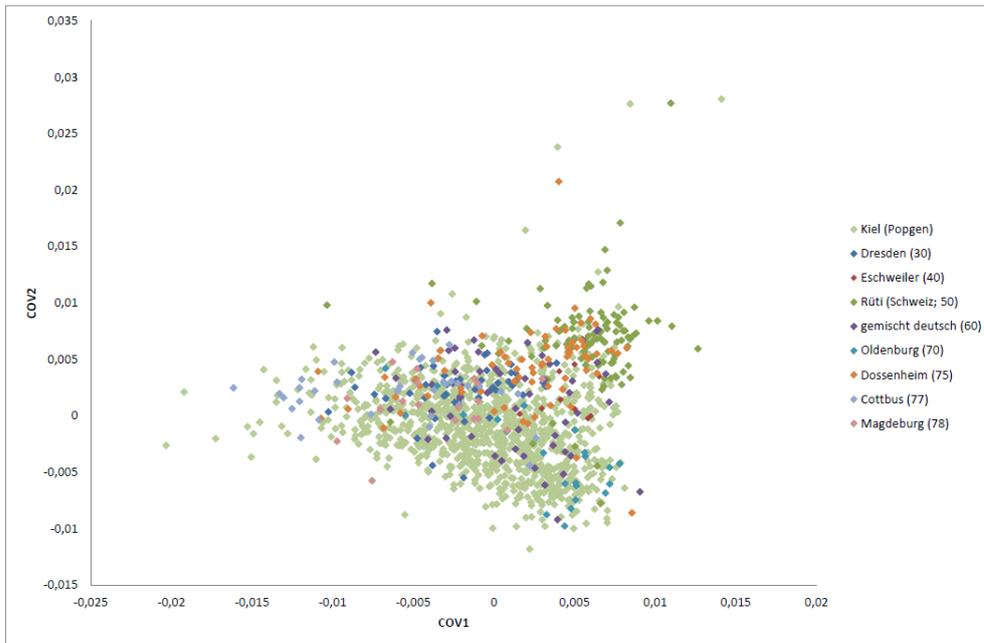
Figure 19. Scatter diagram of the first two principal components (covariates). Visible are the differences between samples from Switzerland (green dots) and the Popgen controls (light green dots).
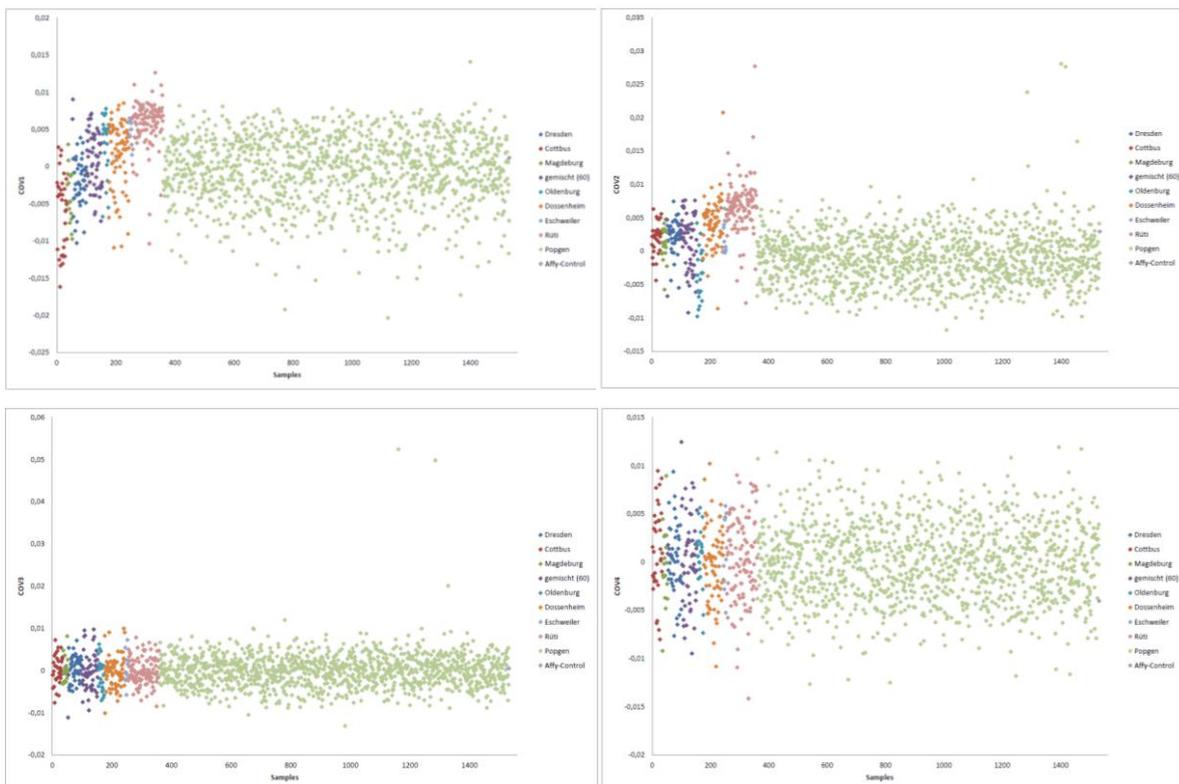
Figure 20. The first four covariates plotted against all samples. Samples are sorted after their geographical origin on the x-axis. Differences are visible between the cases from different geographical origins. The greatest differences can be observed between samples from the east of Germany (red and green coloured dots) and from the Switzerland's (salmon coloured dots). No genetic differences are seen in the sample collective from the third covariate onwards. Three outliers are present in the control sample set.
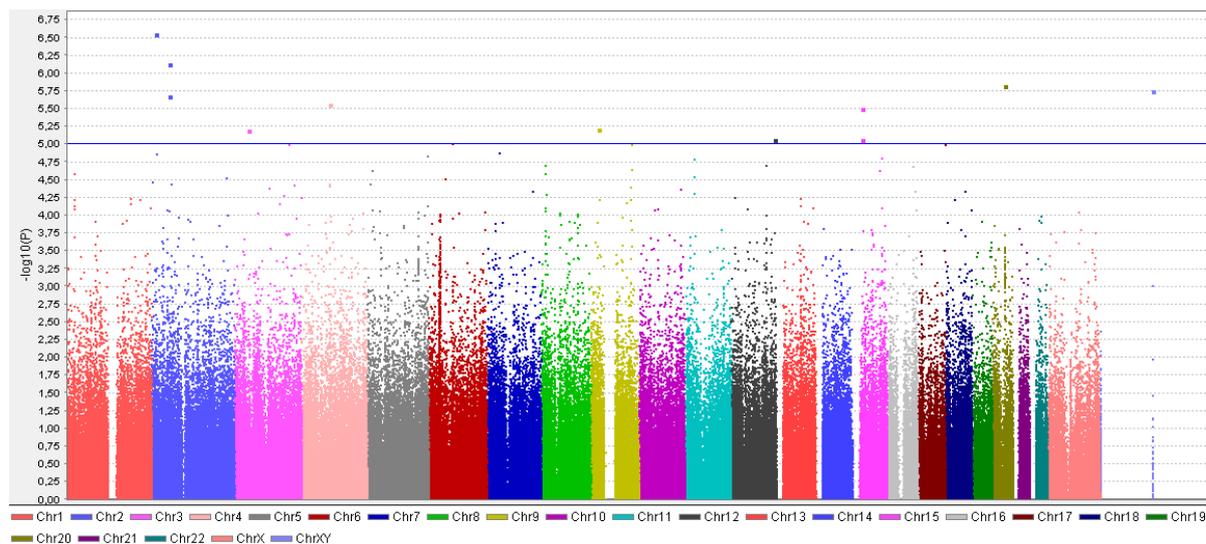
Figure 21. Manhattan plot showing the genomewide P-values (-log10) plotted against their respective chromosomal position. The horizontal blue line shows the suggestive genomewide significance threshold of $1x10^{-5}$. The plot includes 359 DD cases and 1173 controls tested for 530,215 SNPs. P-values are those of a 2df test of logistic regression, which involves two variables representing an additive effect of allele dosage and a dominance deviation. The association test was corrected for the first four covariates of a multidimensional scaling analysis conducted with a selection of uncorrelated SNPs.

Figure 21 shows a manhattan plot for the GWAS data from the Axiom genotyping experiment. The genomewide P-values were obtained with the use of a test of association with 2 degrees of freedom, which involves two variables representing an additive effect of allele dosage and a dominance deviation. This test was used in order to correct for genomic inflation. No SNP tested for association reached genomewide significance of $5.0x10^{-8}$. Some SNPs showed suggestive association and reached P-values below $1.0x10^{-5}$. The noticeable structure on chromosome six corresponds to the HLA region. A manhattan plot for chromosome 20 is given in figure 23. Regional plots for all loci of interest (containing the SNPs with the lowest P-values) were generated with the locusZoom (Pruim *et al.* 2010) software and are given in figure 26-33. Table 16 gives a summary of the individual SNPs with the lowest P-values. 14 of the candidate loci identified in this study were also identified in the study by Dolmans *et al*. 2011 (for comparison the p-values from the meta-analysis are given for these SNPs in table 16). A number of additional potential candidates for association are also listed in table 16. Among them for example rs703558 (figure 31) on chromosome 12q23.2 located upstream of the IGF1 gene showing a p-value of $2.0x10^{-5}$ and odds ratio of 1.52 and rs7714289 with a p-value of $9.2x10^{-5}$ and odds ratio of 0.69 located on 5q33.1 near the GPX3 gene. Another interesting candidate was rs2281146 on chromosome 20q11.23 with a p-value of $1.9x10^{-4}$ and odds ratio of 0.63 located near the CTNNBL1 gene.
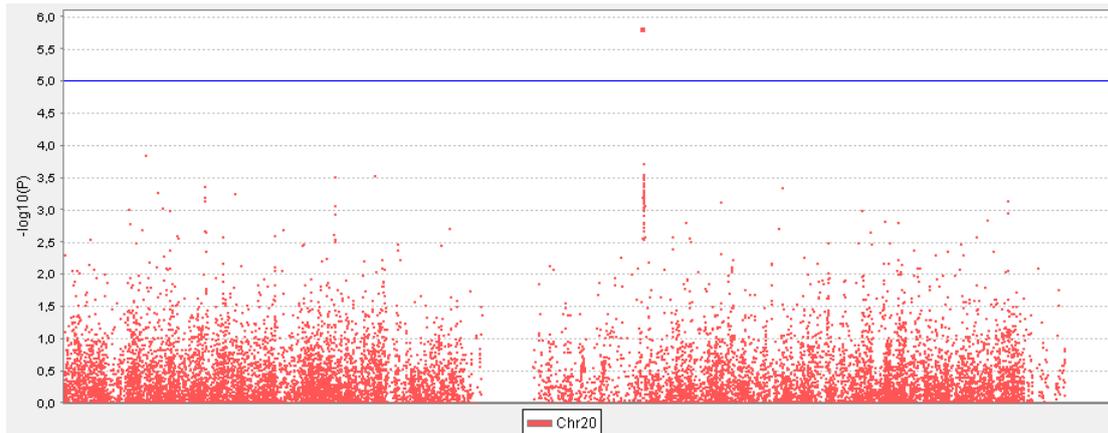
Figure 22. Manhattan plot showing the genomewide P-values (-log10) of chromosome 20 plotted against their respective chromosomal position. The horizontal blue line shows the suggestive genomewide significance threshold of 1×10^{-5}. The plot includes 359 DD cases and 1173 controls tested for 530,215 SNPs. P-values are those of a 2df test of logistic regression, which involves two variables representing an additive effect of allele dosage and a dominance deviation. The association test was corrected for the first four covariates of a multidimensional scaling analysis conducted with a selection of uncorrelated SNPs.
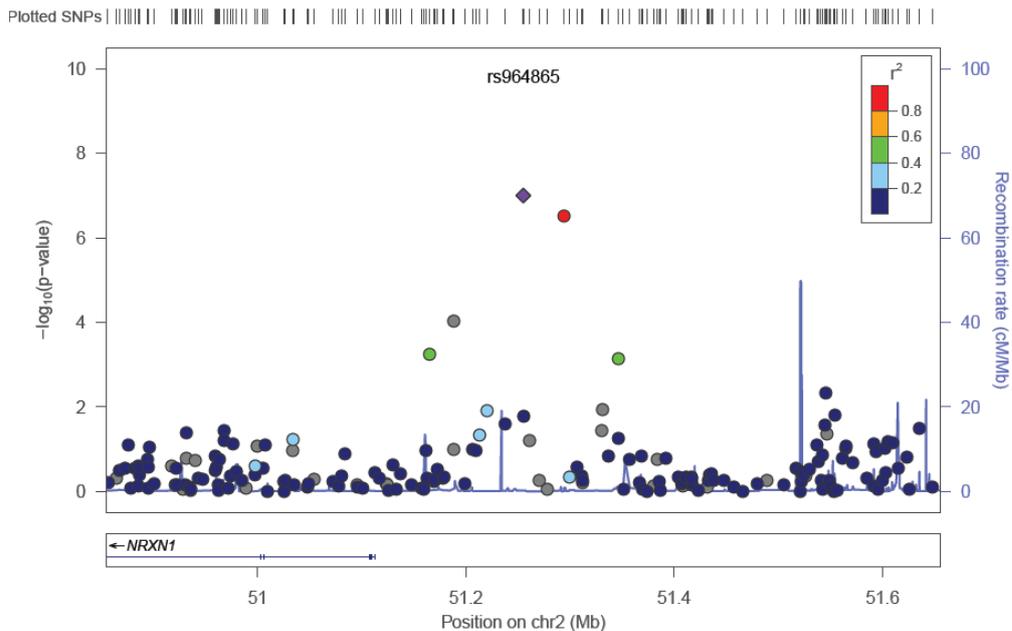
Figure 23. Regional plot of the identified candidate risk loci on 2p16.3. The P-values obtained using a 1-degree-of-freedom basic Chi-square allelic test (y-axis) were plotted against their chromosomal map positions (x-axis). The colour of each SNP spot reflects its r^2 value. Estimated recombination rates were plotted in blue. The gene NRXN1 is located near rs964865l.
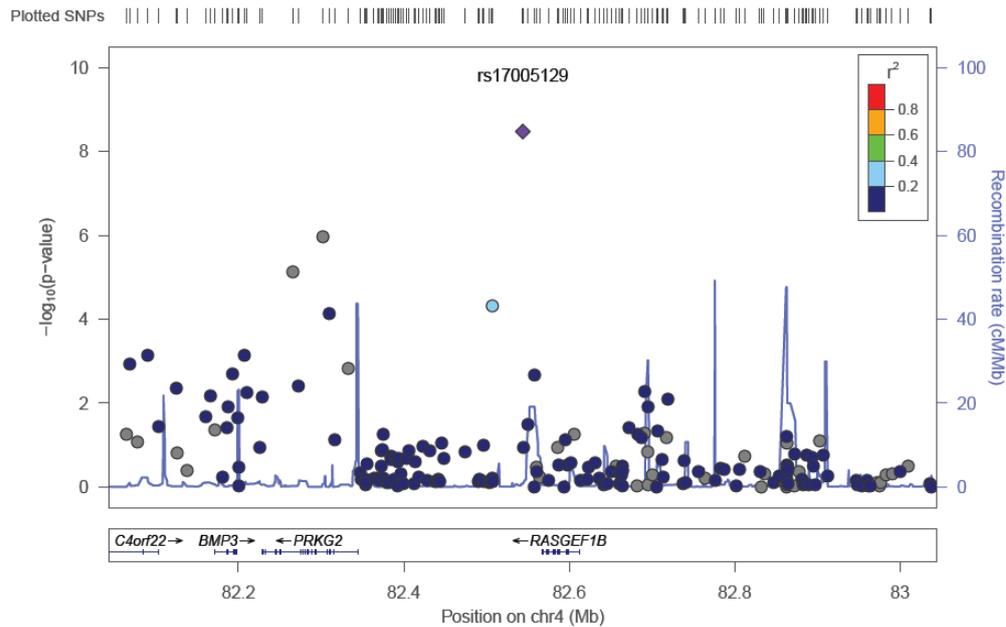
Figure 24. Regional plot of the identified candidate risk loci on 4q21.22. The P-values obtained using a 1-degree-of-freedom basic Chi-square allelic test (y-axis) were plotted against their chromosomal map positions (x-axis). The colour of each SNP spot reflects its r^2 value. Estimated recombination rates were plotted in blue. The SNP rs17005129 is located near the RASGEF1B gene.
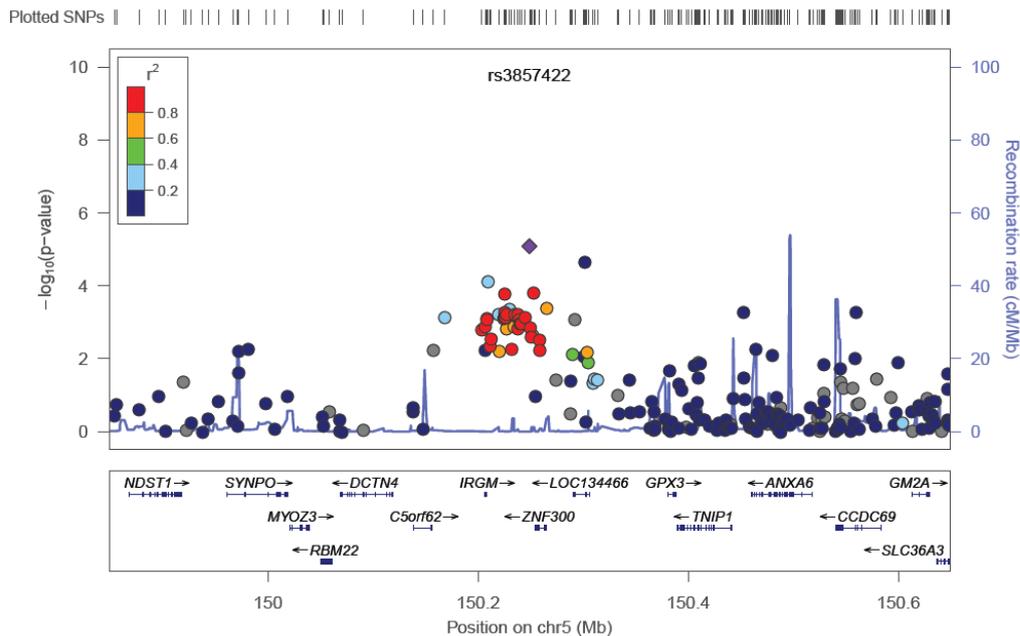
Figure 25. Regional plot of the identified DD risk loci on 5q33.1. The P-values obtained using a 1-degree-of-freedom basic Chi-square allelic test (y-axis) were plotted against their chromosomal map positions (x-axis). The colour of each SNP spot reflects its r^2 value. Estimated recombination rates were plotted in blue. The gene GPX3 (glutathione peroxidase 3) is located near rs3857422. The gene codes for a glutathione peroxidase, which functions in the detoxification of hydrogen peroxide.
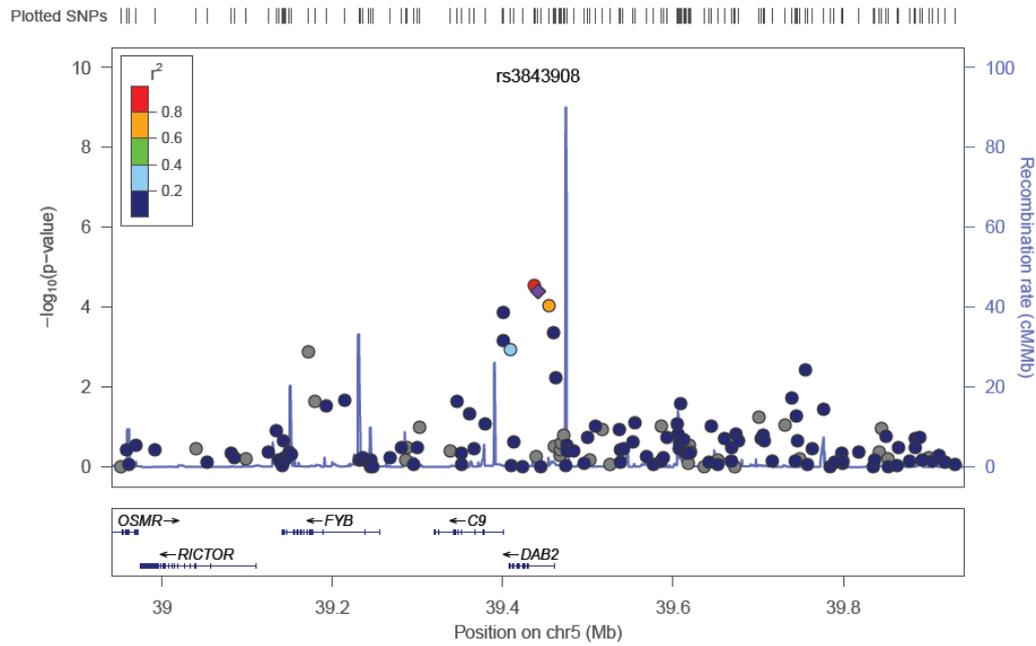
Figure 26. Regional plot of the identified DD candidate risk loci on 5p13.1. The P-values obtained using a 1-degree-of-freedom basic Chi-square allelic test corrected for genomic inflation (y-axis) were plotted against their chromosomal map positions (x-axis). The colour of each SNP spot reflects its r² value. Estimated recombination rates were plotted in blue. SNP rs3843908 is located intronic of the DAB2 gene. DAB2 was the only gene in this region expressed in disease and control tissue (Whole genome expression). This risk loci was also identified by Dolmans *et al.* 2011.
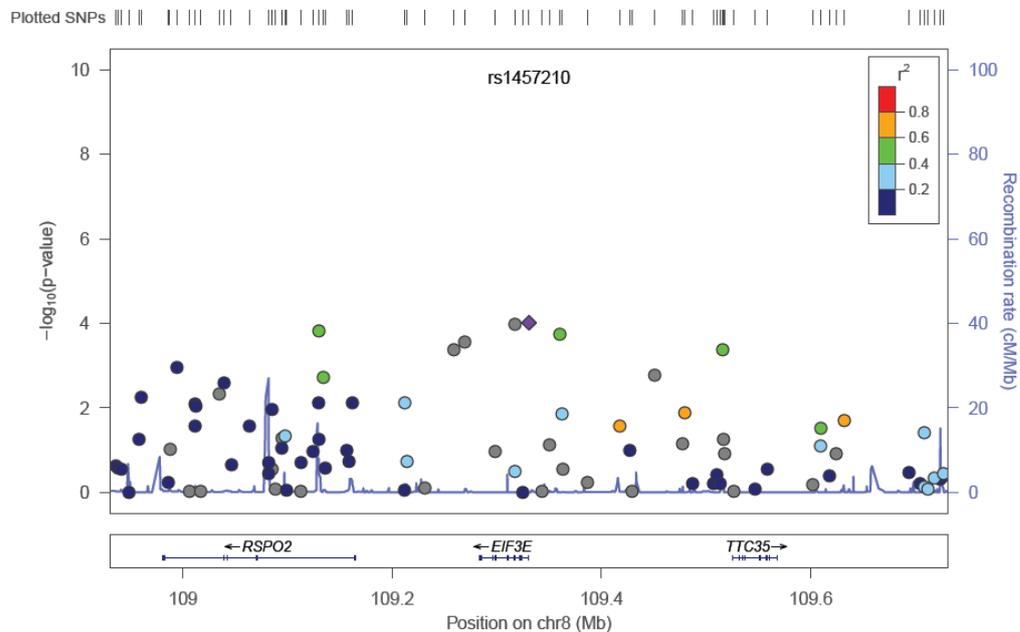
Figure 27. Regional plot of the identified DD candidate risk loci on 8q23.1. The P-values obtained using a 1-degree-of-freedom basic Chi-square allelic test corrected for genomic inflation (y-axis) were plotted against their chromosomal map positions (x-axis). The colour of each SNP spot reflects its r² value. Estimated recombination rates were plotted in blue. SNP rs1457210 is located near the genes EIF3E, RSPO2 and TTC35. This risk loci was also identified by Dolmans *et al.* 2011.
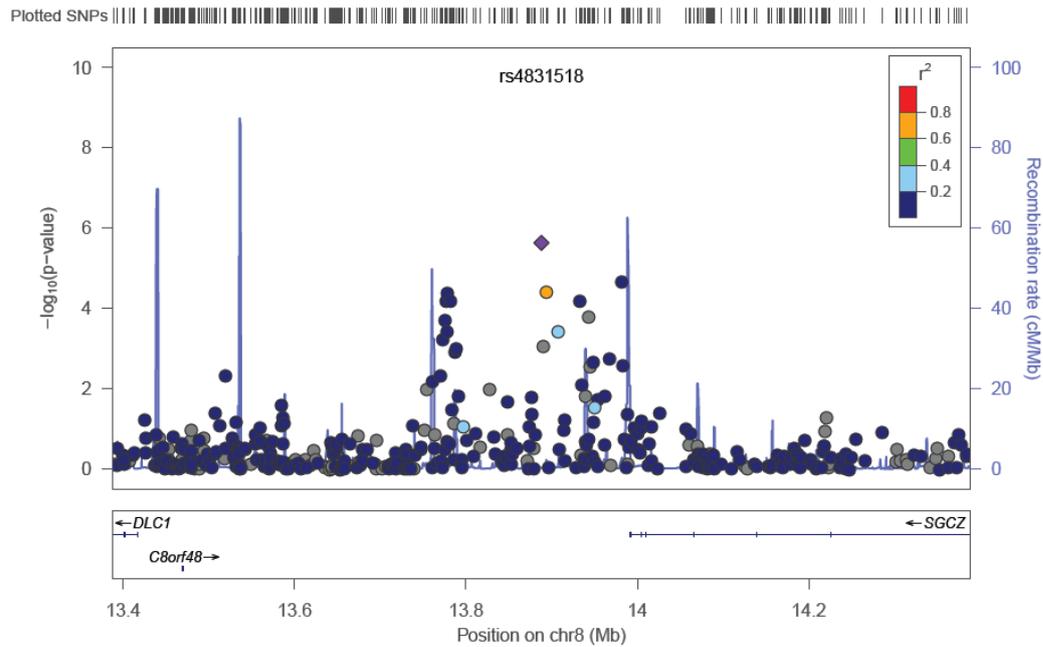
Figure 28. Regional plot of the identified DD candidate risk loci on 8p22. The P-values obtained using a 1-degree-of-freedom basic Chi-square allelic test corrected for genomic inflation (y-axis) were plotted against their chromosomal map positions (x-axis). The colour of each SNP spot reflects its r^2 value. Estimated recombination rates were plotted in blue. SNP rs4831518 is located downstream of the SGCZ gene.
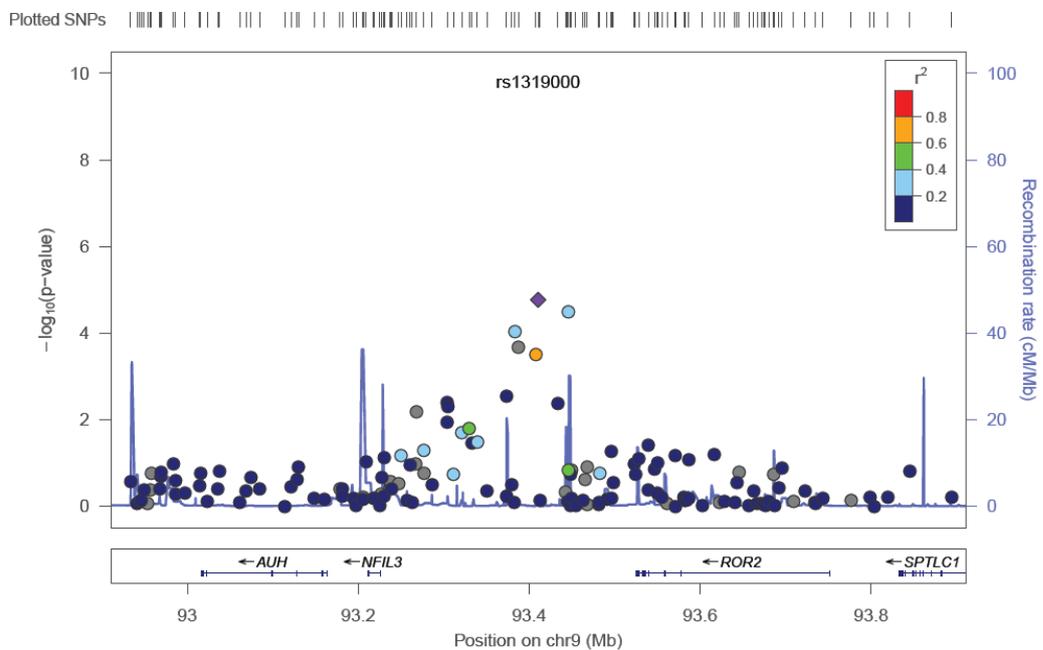
Figure 29. Regional plot of the identified DD candidate risk loci on 9q22.31. The P-values obtained using a 1-degree-of-freedom basic Chi-square allelic test corrected for genomic inflation (y-axis) were plotted against their chromosomal map positions (x-axis). The colour of each SNP spot reflects its r^2 value. Estimated recombination rates were plotted in blue. SNP rs1319000 is located intronic of the ROR2 gene. ROR2 is receptor for Wnt5a and is upreguated 10fold in DD primary tissue.
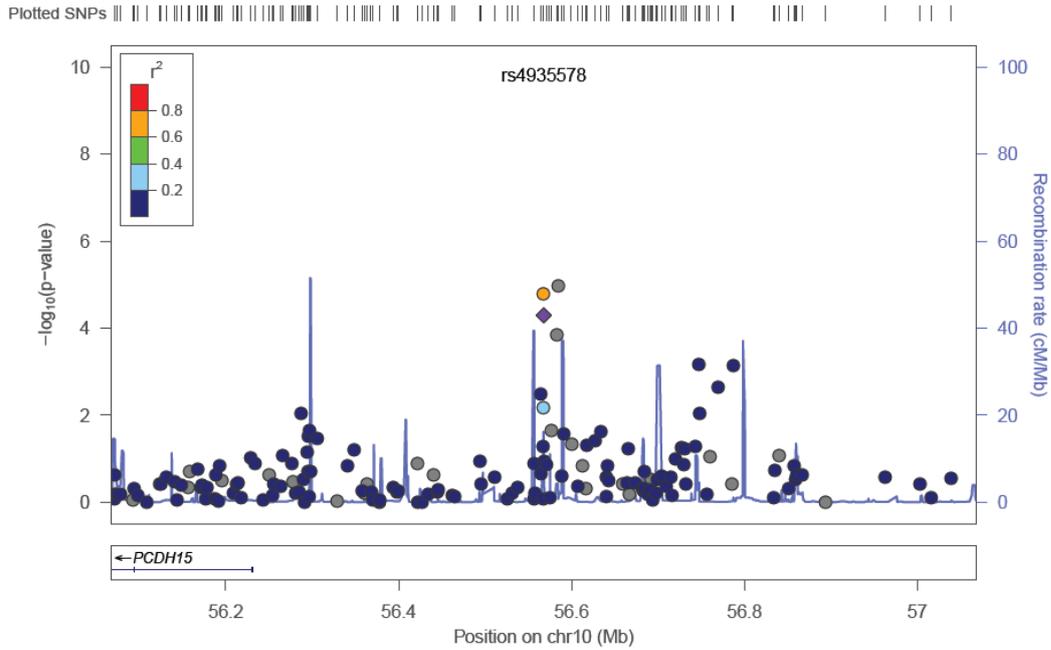
Figure 30. Regional plot of the identified DD candidate risk loci on 10q22.1. The P-values obtained using a 1-degree-of-freedom basic Chi-square allelic test corrected for genomic inflation (y-axis) were plotted against their chromosomal map positions (x-axis). The colour of each SNP spot reflects its r^2 value. Estimated recombination rates were plotted in blue. SNP rs4935578 is located intronic of the PCDH15 gene.
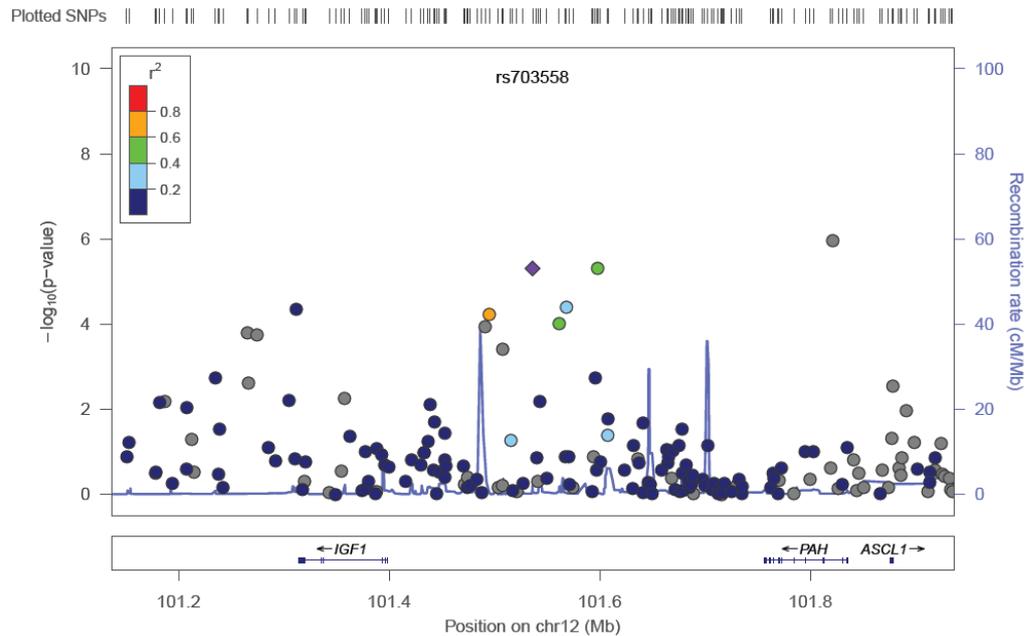
Figure 31. Regional plot of the identified DD candidate risk loci on 12q23.2. The P-values obtained using a 1-degree-of-freedom basic Chi-square allelic test corrected for genomic inflation (y-axis) were plotted against their chromosomal map positions (x-axis). The colour of each SNP spot reflects its r^2 value. Estimated recombination rates were plotted in blue. SNP rs703558 is located upstream of the IGF1 gene.
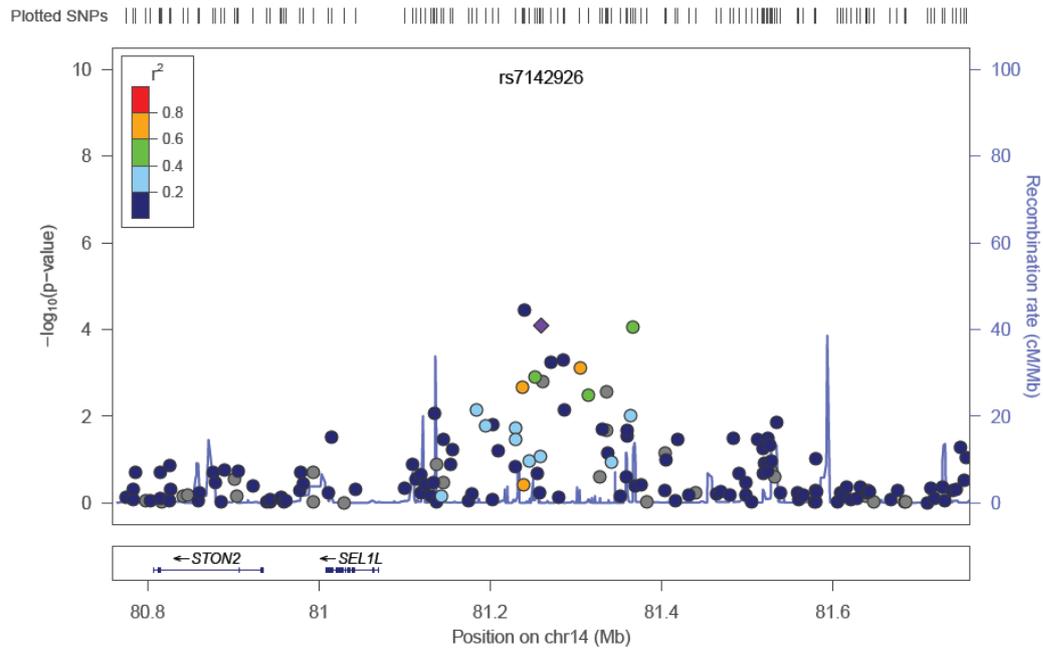
Figure 32. Regional plot of the identified DD candidate risk loci on 14q31.1. The P-values obtained using a 1-degree-of-freedom basic Chi-square allelic test corrected for genomic inflation (y-axis) were plotted against their chromosomal map positions (x-axis). The colour of each SNP spot reflects its r^2 value. Estimated recombination rates were plotted in blue. SNP rs7142926 is located upstream of the SEL1L gene.
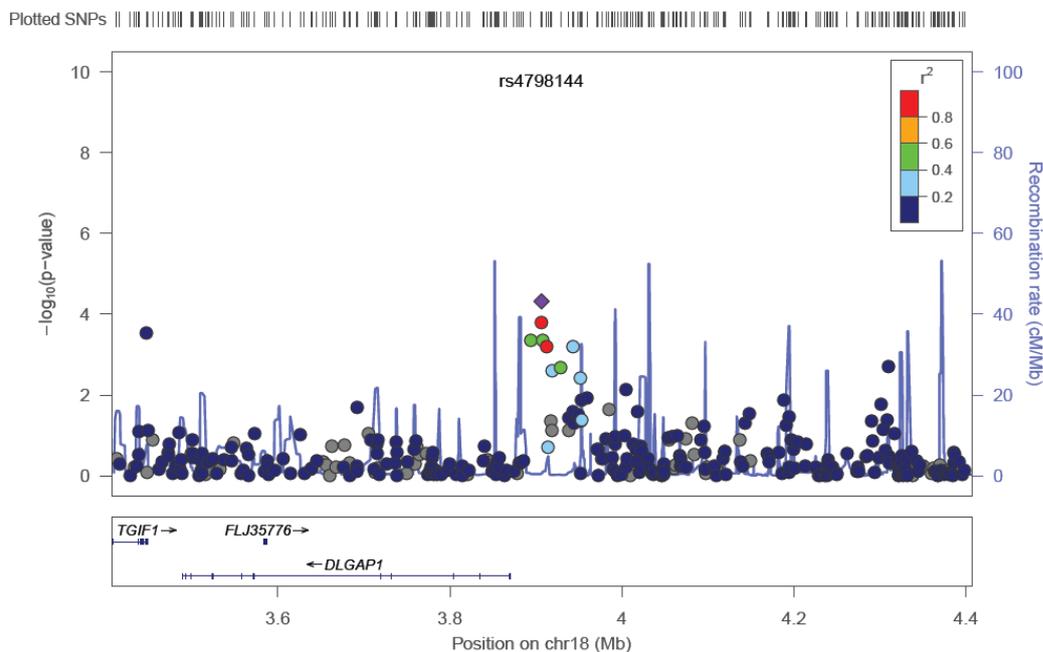

Figure 33. Regional plot of the identified DD candidate risk loci on 18p11.31. The P-values obtained using a 1-degree-of-freedom basic Chi-square allelic test corrected for genomic inflation (y-axis) were plotted against their chromosomal map positions (x-axis). The colour of each SNP spot reflects its r^2 value. Estimated recombination rates were plotted in blue. SNP rs7142926 is located downstream of the TGIF1 gene.
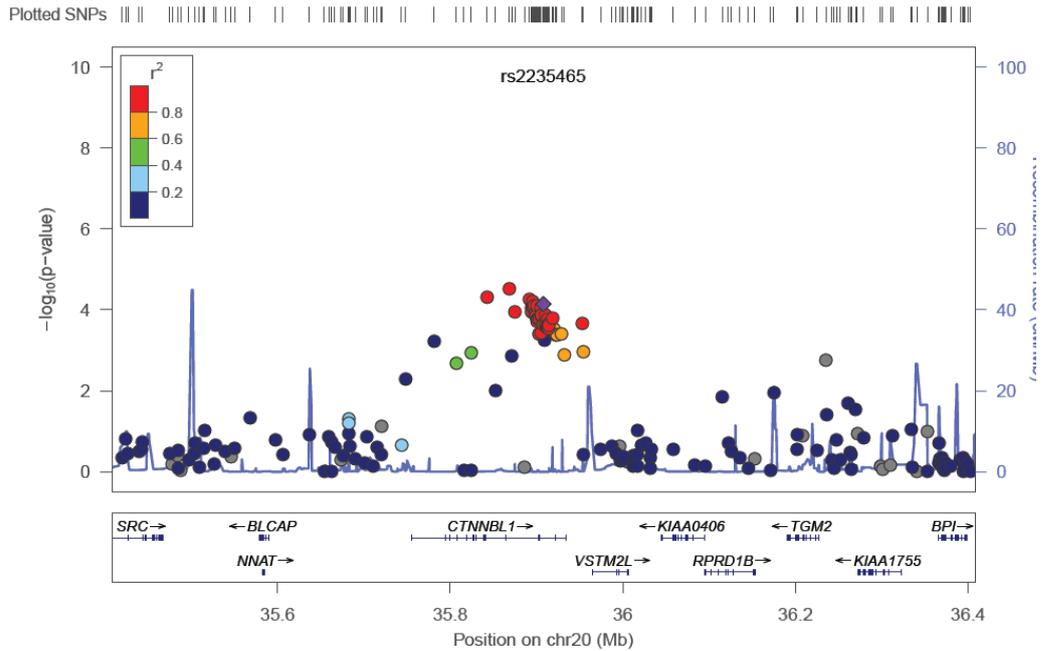
Figure 34. Regional plot of the identified DD candidate risk loci on 20q11.23. The P-values obtained using a 1-degree-of-freedom basic Chi-square allelic test corrected for genomic inflation (y-axis) were plotted against their chromosomal map positions (x-axis). The colour of each SNP spot reflects its r^2 value. Estimated recombination rates were plotted in blue. SNP rs2235465 is located intronic of the CTNNBL1 gene.
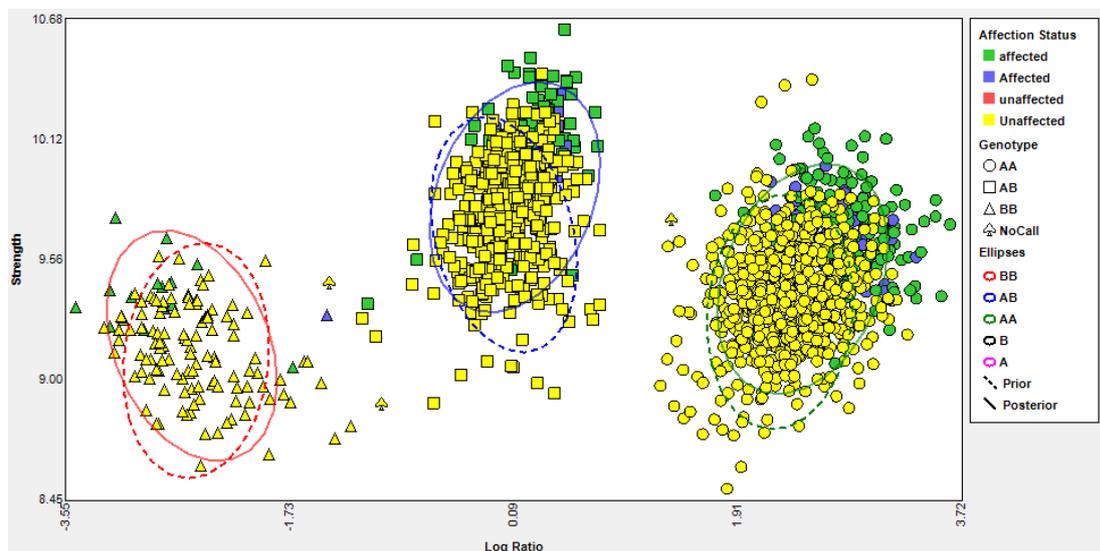
Figure 35. Clusterplot example for one SNP (rs4935578) with differences in signal strength between cases (green or blue) and controls (yellow). Note that all samples were annotated to the correct cluster.

Table 16. Axiom Genotyping Results

|		Axiom 2011 (359 cases 1173 controls)							Dolmans *et al.* 2011 Meta-analysis (2154 cases 9972 controls)				
NR	CHR	SNP	POSITION	A1	STAT	P-value	OR	GENE	SNP	POSITION	P-value	OR	GENE
1	1	rs7543680	22731269	A	21.09	2.63E-5	1.61	**WNT4**	rs7524102	22571034	**2.80E-09**	1.28	**WNT4**
2	2	rs964865	51401676	C	28.24	7.38E-7	0.46	NRXN1					
3	3	rs17686109	69692981	C	18.51	9.55E-5	1.81	PDZRN3	rs1123148	73973835	4.80E-04	0.87	PDZRN3
4	3	rs1550743	133411922	C	19.13	7.01E-5	1.41	CPNE4	rs1356802	133320767	1.60E-04	0.36	CPNE4
5	4	rs11722019	82083409	G	25.61	2.75E-6	2.58	RASGEF1B					
6	4	rs2639583	145602497	C	17.43	1.64E-4	1.68	HHIP					
7	4	rs17068670	180964374	C	18.56	9.30E-5	2.56	RP11-162G9	rs6824106	179038012	1.40E-04	0.12	RP11-162G9
8	5	rs2548170	39401620	T	16.31	2.87E-4	0.64	DAP2					
9	5	rs7714289	150321163	T	18.59	9.20E-5	0.69	IRGM, GPX3					
10	6	rs9276412	32710552	G	18.5	9.61E-5		HLA region					
11	6	rs9399674	149237452	C	14.14	8.48E-4		**TAB2**	rs2179367	149804230	2.50E-07	1.23	**TAB2**
12	7	rs17151317	25330508	C	17.4	1.67E-4	1.71	OSBPL3	rs4719773	24528683	0.02	0.89	OSBPL3
13	7	rs2290221	37987632	A	22.47	1.32E-5	1.73	**SFRP4**, EPDR1	rs16879765	37955620	**5.60E-39**	1.98	**SFRP4**, EPDR1
14	8	rs4831518	13843667	G	21.64	1.99E-5	1.83	SGCZ					
15	8	rs13266130	84319043	T	18.04	1.21E-4	1.92	RP11-51M18.1					
16	8	rs1457210	109261562	C	18.49	9.66E-5		**RSPO2**	rs611744	109297184	**7.90E-15**	0.75	**RSPO2**
17	9	rs1319000	94370675	T	18.3	1.06E-4	1.51	**ROR2**					
18	9	rs966155	118445627	T	20.2	4.11E-5	1.67	DEC1, PAPPA					
19	10	rs10825475	56914474	G	18.83	8.17E-5	0.67	PCDH15					
20	10	rs12572196	123707246	A	20.12	4.28E-5	1.99	NSMCE4A					
21	11	rs2256083	108430624	T	17.48	1.60E-4	1.46	EXPH5					
22	12	rs703558	103012080	C	21.63	2.01E-5	1.52	IGF1					
23	13	rs9529480	69571505	C	19.49	5.86E-5	1.51	RP11-501G6.1					
24	14	rs2031857	82169893	G	14.68	6.50E-4	1.90	SEL1L					
25	15	rs1509408	56286313	C	17.48	1.60E-4	1.51	MYO1E	rs2171286	57265777	7.50E-05	0.85	MYO1E
26	15	rs2469179	87135495	T	16.3	2.89E-4	1.49	ISG20	rs4932194	87046243	8.10E-07	0.82	ISG20
27	17	rs4591175	77658533	A	16.11	3.17E-4	0.55	RBFOX3					
28	18	rs4798144	3916561	G	14.79	6.13E-4	0.70	DLGAP1	rs1944967	37785137	4.10E-03	1.11	PIK3C3
29	19	rs17273603	57677373	G	15.71	3.89E-4	1.61	DUXA	rs11672517	62370006	**6.80E-14**	1.34	DUXA
30	20	rs2281146	36434857	T	17.1	1.93E-4	0.63	CTNNBL1					
31	22	rs16980831	26226840	G	18.1	1.17E-4	1.51	MYO18B	rs4820663	24684655	3.50E-03	1.20	MYO18B
32	22	rs7292297	46458123	G	15.26	4.87E-4		**WNT7B**	rs6519955	44800506	**3.20E-33**	1.54	**WNT7B**

GWA results: Given are the SNPs with the lowest P-value from each of the 32 regions that were associated with DD in the Axiom genotyping experiment. Results are compared with the replication SNPs from the meta-analysis by Dolmans *et al.* Significant P-values (<5.0x10-8) are given in bold. GENE: genes of interest located in the region of association; genes involved in Wnt-signalling are given in bold. STAT: P-values of the Axiom Data are those of a logistic regression corrected for the first four principal components (covariates). A1: minor allele; OR: odds ratio

3.2.2 GWAS Results: Imputed Data

The data from 186 cases genotyped with the Affymetrix 6.0 platform and 379 cases and 1219 controls genotyped with the Affymetrix Axiom platform was imputated with the Beagle v.3.3.2 software using the HapMap phase III Reference Panel. After quality control 543 cases and 1174 controls were included in the association testing. Again genomic inflation was in evidence because of the different geographic origin of cases and controls (figure 36). Based on the inflation factor, the first six components of a MDS analysis were included in the adjusted model of association testing. 5,204,451 SNPs reached an imputation score (Beagle's r^2) of >0.8 (resulting in a Bonferroni-Level: 9.6E-09). Figure 38 shows the Quantile-quantile plots under the adjusted model for different r^2 thresholds. Only SNPs with r^2>0.95 were considered here.
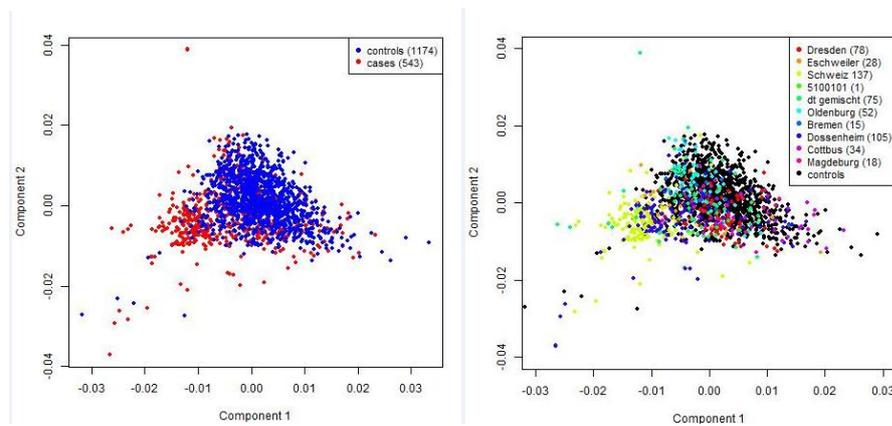
Figure 36. Scatterplots showing the first two components of a MDS analysis, for cases (red) and controls (blue) and for the different geographic origins of cases and controls. Based on this MDS analysis the first six components were included in the association testing in order to correct for genomic inflation.
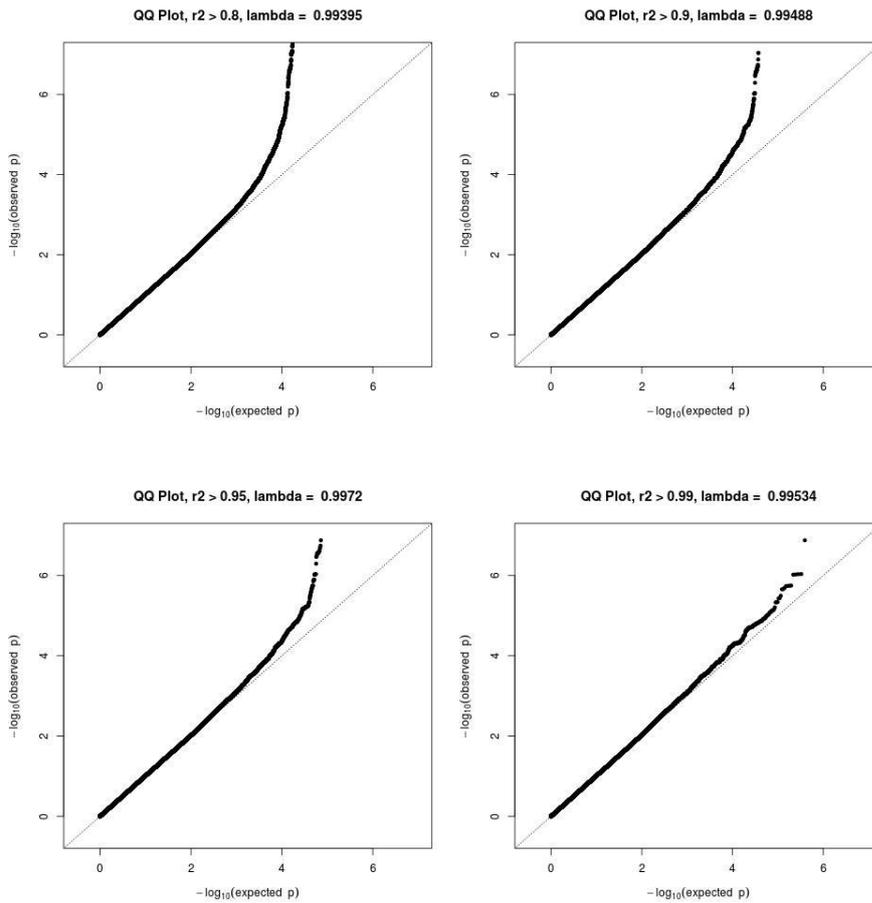
Figure 37. Quantile-quantile plot (qq-plot) of expected vs. observed P-values for a chi-square-test of association after correction for population stratification (adjusted model) for different imputation score thresholds (r^2).
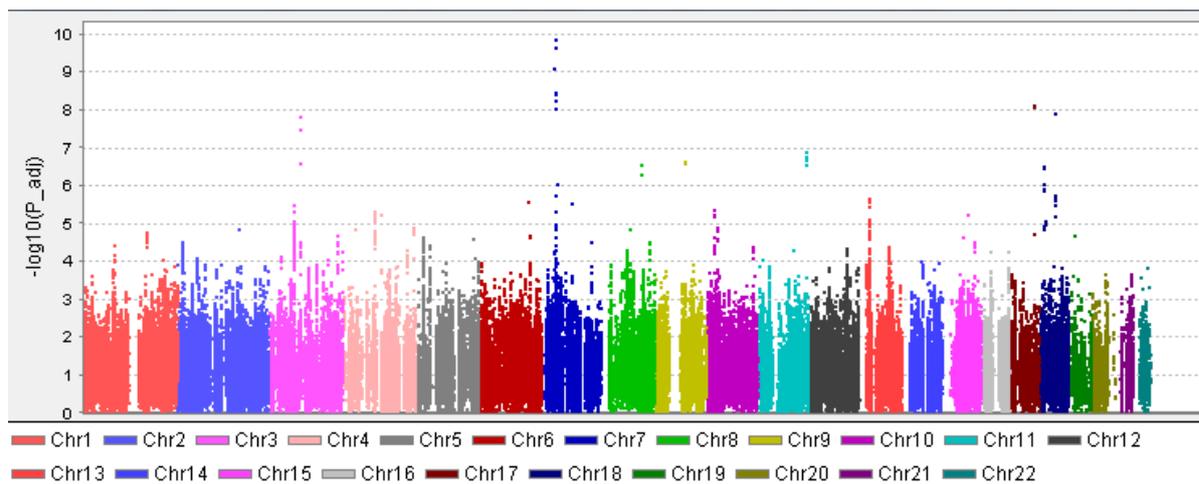
Figure 38. Manhattan plot showing the genomewide P-values (-log10) plotted against their respective chromosomal position. The plot includes 543 DD cases and 1174 controls tested for 5,204,451 SNPs. P-values are those of a 1df test of logistic regression, which takes into account an additive effect of allele dosage. The association test was corrected for the first six covariates of a multidimensional scaling (MDS). Gaps in chromosomes are non-imputed regions.

Figure 38 shows a Manhattan plot for the imputed data set. 21.1% (125 of 592 chunks, 5000bp each) of the genome could not be imputed. These are represented by gaps in the chromosomes (figure 38). The genomic region giving the strongest signal was the region on chromosome 7p14 already identified by Dolmans *et al*. 2011 (figure 39). 14 regions showed suggestive association. From these regions the SNPs showing the lowest p-values are summarised in table 17.

Table 17. Imputation GWAS results.

Chr	SNP	Position (bp)	A1	FRQ_A1	A2	P_adj	OR_adj	Beagle r^2	GENE
2	rs13388985	51393653	C	0.1418	T	9.63E-05	0.5921	0.989	NRXN1
3	rs13093477	86255678	C	0.2356	T	**1.47E-08**	0.5404	0.976	CADM2
3	rs9822103	181542324	T	0.0267	C	2.16E-05	3.1202	0.970	SOX2
4	rs1374657	30837143	C	0.1444	T	1.41E-05	1.6491	0.964	PCDH7
4	rs36007254	83875089	T	0.1891	G	7.36E-06	1.6212	0.996	LIN54
4	rs113075608	100240016	A	0.1625	G	6.91E-06	0.5644	*0.950*	ADH1B
7	rs2290221	37987632	G	0.1349	A	**2.21E-10**	2.1344	1.000	SFRP4
7	rs17172182	43285598	C	0.2037	G	9.40E-07	1.6663	0.994	HECW1
8	rs2981200	107850948	G	0.0927	A	2.74E-07	2.0331	0.966	ABRA
10	rs72785850	20236065	A	0.0659	G	4.58E-06	2.1051	0.991	PLXDC2
12	rs2946834	102787814	A	0.6802	G	4.51E-05	0.6915	0.997	IGF1
15	rs4640119	56195191	T	0.4868	C	2.38E-05	1.4436	0.975	MYO1E
17	rs16960070	64701109	G	0.021	A	**7.36E-09**	57.9719	0.963	PRKCA
18	rs56909423	12614456	C	0.0144	G	3.23E-07	49.8087	0.978	SPIRE1
18	rs8098349	39433420	A	0.4316	G	1.83E-06	1.4976	0.997	PIK3C3
22	rs2858477	37368878	C	0.26	T	0.0001442	0.675	0.971	TST, MPST

CHR: Chromosome, SNP: Single nucleotide polymorphism, A1: Allele 1, FRQ: Frequency of A1, from dosage data, OR: Odds ratio for association, P: p-value for association tests (adjusted for the first six covariates of a MDS analysis), Gene: genes of interest in this region.

Two of these SNPs feature p-values below 5×10^{-8}. Among these was rs2290221 on chromosome 7p14, showing the strongest association signal with a p-value of 2.2×10^{-10}, odds ratio of 2.13 and r^2 of 1. The other SNP was rs13093477 on chromosome 3p12.1 with a p-value of 1.5×10^{-8}, odds ratio of 0.54 and r^2 of 0.97. SNP rs13093477 is located downstream of the CADM2 gene. Four genomic regions showing suggestive association were also identified by Dolmans *et al*. 2011 (genomic regions around rs2290223 on chromosome 7p14, rs2981200 on 8q23.1, rs4640119 on 15q21.3 and rs8098349 on 18q12.3). SNPs from five genomic regions showed p-values comparable to those seen in the axiom data. The other loci identified in the axiom data had higher p-values in the imputed data.

3.2.3 SNPstream Genotyping

Selected SNPs were genotyped with the Genome Lap SNPstream 48-plex Genotyping System (Beckman Coulter GmbH, Germany) in order to replicate and validate GWAS findings. 48 SNPs were typed in 465 DD patients and 282 control samples (provided through the University of Essen). Four SNPs (rs2738694, rs1123148, rs1450843 and rs514839) failed in the analysis. Results were analysed with PLINK (http://pngu.mgh.harvard.edu/purcell/plink/). Association was tested with chi-square test and Fischer's exact test. Only results from the chi-square test are given. SNPs were typed in part to validate own GWAS results and in part to replicate GWAS findings from the University of Gröningen, the Netherlands (Dolmans *et al*. 2011) (see table 18). Results are given table 18. Seven additional SNPs all located on 7p14.1 showed no association (rs4719773, rs10261983, rs10250905, rs10276139, rs1802074, rs1802073, and rs1668357). These are not listed in table 18. The strongest SNP from the GWASs rs16879765 (P-value: 0.0007, OR: 1.69) on 7p14.1 also showed a strong association in the SNPstream analysis. rs423940 (P-value: $4x10^{-5}$, OR: 0.64) on chromosome 8, rs7863802 (P-value: $2x10^{-5}$, OR: 1.81) on chromosome 9 and rs6519955 (P-value: 0.0005, OR: 1.46) on chromosome 22 also showed significant association.

Table 18. SNP stream Genotyping Results. Comparing <u>465 patient</u> samples vs. <u>282 control</u> samples.

CHR	SNP	BP	A1	F_A	F_U	A2	CHISQ	P	OR	Group	Genes of interest
1	rs7524102	22698447	C	0.1850	0.1771	T	0.1422	0.7061	1.055	MCG	<u>WNT4</u>
3	rs11672517	73891145	A	0.2837	0.2463	G	2.3910	0.1221	1.212	MCG	RP11-20B7.1
3	rs1356802	131838077	C	0.3079	0.3040	A	0.0248	0.8748	1.019	MCG	CPNE4
4	rs6824106	178801018	C	0.3670	0.3907	T	0.8120	0.3675	0.904	MCG	RP11-162G9.1, AGA
5	rs12372139	36828019	G	0.0011	0	A	0.5973	0.4396	NA	MCG	SLC1A3
6	rs7747741	18301503	G	0.4305	0.4278	A	0.0099	0.9205	1.011	MCG	DEK, TPMT
6	rs237018	149743930	T	0.4814	0.5111	C	1.2010	0.2731	0.888	MCG	<u>MAP3K7IP2</u>
7	rs2722372	37890267	T	0.2357	0.2721	C	2.401	0.1213	0.8254	CCG/MCG	SFRP4, EPDR1
7	rs2722333	37892719	C	0.2307	0.2714	T	3.0150	0.0825	0.805	CCG/MCG	<u>SFRP4</u>, EPDR1
7	rs4720265	37944246	A	0.2818	0.2343	G	3.9430	0.0470	1.282	CCG/MCG	<u>SFRP4</u>, EPDR1
7	**rs16879765**	37989095	A	**0.1897**	0.1218	G	**11.420**	**0.0007**	**1.688**	CCG/MCG	**<u>SFRP4</u>, EPDR1**
7	rs6953285	38038637	C	0.4097	0.4430	T	1.5490	0.2134	0.873	CCG/MCG	<u>SFRP4</u>, EPDR1
7	rs6951125	116917118	A	0.4446	0.4357	G	0.1092	0.7411	1.037	MCG	<u>WNT2</u>
8	rs13269711	69979828	A	0.2555	0.2454	G	0.1839	0.6680	1.055	MCG	<u>SULF1</u>
8	rs2912522	69992380	G	0.2052	0.2463	A	3.3510	0.0672	0.790	MCG	<u>SULF1</u>
8	**rs423940**	109228008	T	**0.3896**	0.5000	C	**16.850**	**4.051E-005**	**0.638**	MCG	**<u>RSPO2</u>**
9	**rs7863802**	1199448	G	**0.2578**	0.1611	A	**18.290**	**1.899E-005**	**1.808**	MCG	**DMRT1-3**
9	rs10809650	1202371	G	0.2549	0.3125	A	5.6380	0.0176	0.753	MCG	DMRT1-3
9	rs10759289	111280824	C	0.3626	0.3309	T	1.5000	0.2207	1.151	CCG	ACTL7A, ACTL7B

Given are the SNPstream results for 465 patient samples and 282 controls. CHR: Chromosome, SNP: SNP identifier, BP: Physical position (base pair), A1: Minor allele name (based on whole sample), F_A: Minor allele frequency in cases, F_U: Minor allele frequency in controls, A2: Major allele name, CHISQ: Basic allelic test chi-square (1df), P: Asymptotic p-value, OR: Estimated odds ratio (for A1, i.e. A2 is reference), Group: Group that identified this SNP in initial GWAS: CCG: Cologne Centre for Genomics, MCG: Department of Genetics, University Medical Centre Gröningen and University of Gröningen, the Netherlands, Genes of interest: Genes that locate to these regions, underlined genes are involved in the Wnt signalling pathway, grey colour indicates SNPs with P-values below 0.1 and chi-square values above 3, SNPs in bold with P-value below 0.01.

Table 15 continued.

CHR	SNP	BP	A1	F_A	F_U	A2	CHISQ	P	OR	Group	Genes of interest
10	rs11188849	98364544	T	0.1396	0.1562	C	0.7614	0.3829	0.876	MCG	PIK3AP1
11	rs11216534	117628968	A	0.0691	0.0778	G	0.3826	0.5362	0.880	CCG	IL10RA-201
11	rs11216674	117879639	T	0.0615	0.0701	C	0.4123	0.5208	0.870	CCG	IL10RA-201
12	rs2073950	111894072	A	0.1872	0.2022	G	0.4905	0.4837	0.909	MCG	ATXN2
15	rs17302219	59478485	A	0.2077	0.2333	G	1.3100	0.2523	0.861	MCG	MYO1E
15	rs7168492	89238255	T	0.3180	0.3160	C	0.0062	0.9371	1.009	MCG	ISG20
16	rs1833203	5339095	C	0.0143	0.0126	G	0.0763	0.7823	1.139	CCG	Sweden
16	rs8052047	79812854	A	0.0394	0.0378	T	0.0243	0.8762	1.045	CCG	c-MAF
17	rs4789939	76881703	A	0.1689	0.1741	G	0.0651	0.7986	0.964	MCG	TIMP2
18	rs625896	39531139	C	0.3275	0.3764	T	3.5930	0.0580	0.807	MCG	PIK3C3
18	rs474605	39662517	G	0.4783	0.5268	A	3.2750	0.0703	0.8236	MCG	PIK3C3
19	rs11743146	57678194	A	0.1223	0.1237	C	0.0060	0.9383	0.987	MCG	several ZNFs
20	rs6093338	39028436	G	0.0824	0.0772	A	0.1250	0.7237	1.074	MCG	MAFB
20	rs742745	39313690	A	0.1258	0.1339	C	0.2044	0.6512	0.9307	MCG	MAFB
22	rs4820663	26354655	C	0.0826	0.0824	A	0.0001	0.9907	1.002	MCG	MYO18B
22	**rs6519955**	46440273	A	**0.4903**	0.3971	C	**12.120**	**0.0005**	**1.460**	MCG	**WNT7B**

Given are the SNPstream results for 465 patient samples and 282 controls. CHR: Chromosome, SNP: SNP identifier, BP: Physical position (base pair), A1: Minor allele name (based on whole sample), F_A: Minor allele frequency in cases, F_U: Minor allele frequency in controls, A2: Major allele name, CHISQ: Basic allelic test chi-square (1df), P: Asymptotic p-value, OR: Estimated odds ratio (for A1, i.e. A2 is reference), Group: Group that identified this SNP in initial GWAS: CCG: Cologne Centre for Genomics, MCG: Department of Genetics, University Medical Centre Gröningen and University of Gröningen, the Netherlands, Genes of interest: Genes that locate to these regions, underlined genes are involved in the Wnt signalling pathway, grey colour indicates SNPs with P-values below 0.1 and chi-square values above 3, SNPs in bold with P-value below 0.01.

The association of SNPs was tested for different patient subgroups. It was tested for patients with family predisposition and patients without or unknown family predisposition, and for patients affected early in life (Surgery before the age of 50 years.) and late and mild affected patients (Surgery after 50 years of age, or no surgery till collection date). Table 19 provides an overview for conducted data analyses.

Table 19. Summary of conducted analyses with SNPstream data.

N of patients	patient subgroup description	N controls	control subgroup description	Table
465	all typed with SNPstream	282	all typed with SNPstream	18
184	with positive fam. history	282	all typed with SNPstream	20
281	with negative or unknown fam. history	282	all typed with SNPstream	21
96	with age at first surgery <50yrs	282	all typed with SNPstream	text
369	with age at first surgery >50yrs	282	all typed with SNPstream	text
465	all typed with SNPstream	1972	all SNPstream + affy (1235 POPGEN; 455 KORA)	22
184	with positive fam. history	1972	all SNPstream + affy (1235 POPGEN; 455 KORA)	text
281	with negative or unknown fam. history	1972	all SNPstream + affy (1235 POPGEN; 455 KORA)	text
96	with age at first surgery <50yrs	1972	all SNPstream + affy (1235 POPGEN; 455 KORA)	text
369	with age at first surgery >50yrs	1972	all SNPstream + affy (1235 POPGEN; 455 KORA)	text

Given is an overview of compared patient and control datasets and the table in which their results are presented. N: number.

The 184 patients with family history for DD mostly contributed to the association of rs16879765 (P-value: 4.7×10^{-5}, OR: 2.08) (Table 20). For these 184 samples rs16879765 hat a minor allele frequency of 0.22 compared to 0.12 in controls and 0.17 in patients without or with unknown family predisposition (Table 21). rs423940 (P-value: 8.1×10^{-6}, OR: 0.54) on chromosome 8 also showed a stronger association for the subgroup of patients with family predisposition. More SNPs, rs11672517 (P-value: 0.09. OR: 1.29) on chromosome 3, rs237018 (P-value: 0.06. OR: 0.77) on chromosome 6, rs11216674 (P-value: 0.07. OR: 0.58) on chromosome 11, rs17302219 (P-value: 0.04. OR: 0.71) on chromosome 15, rs625896 (P-value: 0.01. OR: 0.70) and rs474605 (P-value: 0.05. OR: 1.30) on chromosome 18 tended towards an association, for the 184 DD samples with positive family history, compared to all 465 patient samples (table 16) and patients without family history (table 21). In contrast SNP rs7863802 (P-value: 1.5×10^{-5}. OR: 1.92) on chromosome 9 showed a stronger association in the subgroup of patients without a family history for DD (table 21) compared to those with family predisposition (P-value: 0.003. OR: 1.66).

Table 20. SNP stream Genotyping Results. Comparing <u>184 patient</u> samples with fam. predisposition vs. <u>282 control</u> samples.

CHR	SNP	BP	A1	F_A	F_U	A2	CHISQ	P	OR	Group	Genes of interest
1	rs7524102	22698447	C	0.1639	0.1771	T	0.2662	0.6059	0.9106	MCG	<u>WNT4</u>
3	rs11672517	73891145	A	0.2972	0.2463	G	2.8590	0.0909	1.2940	MCG	RP11-20B7.1
3	rs2323206	73951152	T	0.3785	0.3781	G	9.372e-005	0.9923	1.0010	MCG	RP11-20B7.1
3	rs1356802	131838077	C	0.3122	0.3040	A	0.0692	0.7925	1.0390	MCG	CPNE4
4	rs6824106	178801018	C	0.3667	0.3907	T	0.5307	0.4663	0.9027	MCG	RP11-162G9.1, AGA
5	rs12372139	36828019	0	0	0	A	NA	NA	NA	MCG	SLC1A3
6	rs7747741	18301503	G	0.4330	0.4278	A	0.0236	0.8779	1.0210	MCG	DEK, TPMT
6	rs237018	149743930	T	0.4472	0.5111	C	3.5300	0.0603	0.7739	MCG	<u>MAP3K7IP2</u>
7	rs2722372	37890267	T	0.232	0.2721	C	1.8270	0.1765	0.8085	CCG/MCG	<u>SFRP4</u>, EPDR1
7	rs2722333	37892719	C	0.225	0.2714	T	2.4560	0.1171	0.7795	CCG/MCG	<u>SFRP4</u>, EPDR1
7	rs4720265	37944246	A	0.2778	0.2343	G	2.1700	0.1408	1.2570	CCG/MCG	<u>SFRP4</u>, EPDR1
7	**rs16879765**	37989095	A	**0.2238**	0.1218	G	**16.580**	**4.668e-005**	**2.079**	CCG/MCG	**<u>SFRP4</u>, EPDR1**
7	rs6953285	38038637	C	0.4139	0.4430	T	0.7492	0.3867	0.8878	CCG/MCG	<u>SFRP4</u>, EPDR1
7	rs6951125	116917118	A	0.4438	0.4357	G	0.0582	0.8094	1.0340	MCG	<u>WNT2</u>
8	rs13269711	69979828	A	0.2806	0.2454	G	1.3930	0.2380	1.1990	MCG	<u>SULF1</u>
8	rs2912522	69992380	G	0.2099	0.2463	A	1.6150	0.2037	0.8131	MCG	<u>SULF1</u>
8	**rs423940**	109228008	T	**0.3492**	0.5000	C	**19.910**	**8.127e-006**	**0.5365**	MCG	**<u>RSPO2</u>**
9	**rs7863802**	1199448	G	**0.2417**	0.1611	A	**8.9880**	**0.0027**	**1.6590**	MCG	**DMRT1-3**

Given are the SNPstream results for 184 patient samples with family history for DD and 282 controls. CHR: Chromosome, SNP: SNP identifier, BP: Physical position (base pair), A1: Minor allele name (based on whole sample), F_A: Minor allele frequency in cases, F_U: Minor allele frequency in controls, A2: Major allele name, CHISQ: Basic allelic test chi-square (1df), P: Asymptotic p-value, OR: Estimated odds ratio (for A1, i.e. A2 is reference), Group: Group that identified this SNP in initial GWAS: CCG: Cologne Centre for Genomics, MCG: Department of Genetics, University Medical Centre Gröningen and University of Gröningen, the Netherlands, Genes of interest: Genes that locate to these regions, underlined genes are involved in the Wnt signalling pathway, grey colour indicates SNPs with P-values below 0.1 and chi-square values above 3, SNPs in bold with P-value below 0.01.

Table 20 continued:

CHR	SNP	BP	A1	F_A	F_U	A2	CHISQ	P	OR	Group	Genes of interest
9	rs10809650	1202371	G	0.2472	0.3125	A	4.5160	0.0336	0.7225	MCG	DMRT1-3
9	rs10759289	111280824	C	0.3481	0.3309	T	0.2866	0.5924	1.0800	CCG	ACTL7A, ACTL7B
11	rs11216674	117879639	T	0.0417	0.0701	C	3.1650	0.0752	0.5767	CCG	IL10RA-201
12	rs2073950	111894072	A	0.1750	0.2022	G	1.0360	0.3087	0.8369	MCG	ATXN2
15	rs17302219	59478485	A	0.1778	0.2333	G	4.0030	0.0454	0.7104	MCG	MYO1E
15	rs7168492	89238255	T	0.3028	0.3160	C	0.1757	0.6751	0.9401	MCG	ISG20
15	rs4932194	89245239	C	0.3118	0.3183	A	0.0431	0.8356	0.9701	MCG	ISG20
16	rs1833203	5339095	C	0.01944	0.01259	G	0.6822	0.4088	1.555	CCG	Sweden
16	rs8052047	79812854	A	0.05307	0.03777	T	1.219	0.2696	1.428	CCG	c-MAF
17	rs4789939	76881703	A	0.1722	0.1741	G	0.00517	0.9427	0.9871	MCG	TIMP2
18	rs625896	39531139	C	0.2972	0.3764	T	6.001	0.0143	0.7007	MCG	PIK3C3
18	rs474605	39662517	A	0.5385	0.4732	G	3.757	0.0526	1.299	MCG	PIK3C3
19	rs11743146	57678194	A	0.1093	0.1237	C	0.4384	0.5079	0.8696	MCG	several ZNFs
20	rs6093338	39028436	G	0.07263	0.07721	A	0.06498	0.7988	0.936	MCG	MAFB
20	rs742745	39313690	A	0.1346	0.1339	C	0.0008956	0.9761	1.006	MCG	MAFB
22	rs4820663	26354655	C	0.0663	0.08244	A	0.8135	0.3671	0.7903	MCG	MYO18B
22	**rs6519955**	46440273	A	**0.4890**	0.3971	C	7.554	**0.005987**	**1.453**	MCG	**WNT7B**

Given are the SNPstream results for 184 patient samples with family history for DD and 282 controls. CHR: Chromosome, SNP: SNP identifier, BP: Physical position (base pair), A1: Minor allele name (based on whole sample), F_A: Minor allele frequency in cases, F_U: Minor allele frequency in controls, A2: Major allele name, CHISQ: Basic allelic test chi-square (1df), P: Asymptotic p-value, OR: Estimated odds ratio (for A1, i.e. A2 is reference), Group: Group that identified this SNP in initial GWAS: CCG: Cologne Centre for Genomics, MCG: Department of Genetics, University Medical Centre Gröningen and University of Gröningen, the Netherlands, Genes of interest: Genes that locate to these regions, underlined genes are involved in the Wnt signalling pathway, grey colour indicates SNPs with P-values below 0.1 and chi-square values above 3, SNPs in bold with P-value below 0.01.

Table 21. SNP stream Genotyping Results. Comparing <u>281 patient</u> samples without fam. predisposition vs. <u>282 control</u> samples.

CHR	SNP	BP	A1	F_A	F_U	A2	CHISQ	P	OR	Group	Genes of interest
1	rs7524102	22698447	C	0.1996	0.1771	T	0.9014	0.3424	1.1590	MCG	WNT4
3	rs11672517	73891145	A	0.2757	0.2463	G	1.2150	0.2703	1.1650	MCG	RP11-20B7.1
3	rs2323206	73951152	T	0.3809	0.3781	G	0.0088	0.9253	1.0120	MCG	RP11-20B7.1
3	rs1356802	131838077	C	0.3043	0.3040	A	0.0002	0.9887	1.0020	MCG	CPNE4
4	rs6824106	178801018	C	0.3650	0.3907	T	0.7689	0.3806	0.8961	MCG	RP11-162G9.1, AGA
5	rs12372139	36828019	G	0.0018	0	A	0.9900	0.3198	NA	MCG	SLC1A3
6	rs7747741	18301503	G	0.4286	0.4278	A	0.0007	0.9789	1.0030	MCG	DEK, TPMT
6	rs237018	149743930	C	0.4982	0.4889	T	0.0941	0.7590	1.0380	MCG	MAP3K7IP2
7	rs2722372	37890267	T	0.2372	0.2721	C	1.7450	0.1865	0.8321	CCG/MCG	SFRP4, EPDR1
7	rs2722333	37892719	C	0.2335	0.2714	T	2.0620	0.1510	0.8177	CCG/MCG	SFRP4, EPDR1
7	rs4720265	37944246	A	0.2855	0.2343	G	3.7100	0.0541	1.3050	CCG/MCG	SFRP4, EPDR1
7	**rs16879765**	37989095	A	0.1679	0.1218	G	4.6750	0.0306	1.4550	CCG/MCG	**SFRP4, EPDR1**
7	rs6953285	38038637	C	0.4066	0.4430	T	1.4790	0.2239	0.8615	CCG/MCG	SFRP4, EPDR1
7	rs6951125	116917118	A	0.4467	0.4357	G	0.1342	0.7141	1.0460	MCG	WNT2
8	rs13269711	69979828	A	0.2400	0.2454	G	0.0431	0.8355	0.9711	MCG	SULF1
8	rs2912522	69992380	G	0.2029	0.2463	A	2.9680	0.0849	0.7788	MCG	SULF1
8	**rs423940**	109228008	T	**0.4158**	0.5000	C	**7.7780**	**0.0053**	**0.7116**	MCG	**RSPO2**
9	**rs7863802**	1199448	G	**0.2695**	0.1611	A	**18.750**	**1.489e-005**	**1.9210**	MCG	**DMRT1-3**
9	rs10809650	1202371	G	0.2591	0.3125	A	3.8110	0.0509	0.7695	MCG	DMRT1-3
9	rs10759289	111280824	C	0.3736	0.3309	T	2.1720	0.1405	1.2060	CCG	ACTL7A, ACTL7B

Given are the SNPstream results for 281 patient samples without or with unknown family history for DD and 282 controls. CHR: Chromosome, SNP: SNP identifier, BP: Physical position (base pair), A1: Minor allele name (based on whole sample), F_A: Minor allele frequency in cases, F_U: Minor allele frequency in controls, A2: Major allele name, CHISQ: Basic allelic test chi-square (1df), P: Asymptotic p-value, OR: Estimated odds ratio (for A1, i.e. A2 is reference, Group: Group that identified this SNP in initial GWAS: CCG: Cologne Centre for Genomics, MCG: Department of Genetics, University Medical Centre Gröningen and University of Gröningen, the Netherlands, Genes of interest: Genes that locate to these regions, underlined genes are involved in the Wnt signalling pathway, grey colour indicates SNPs with P-values below 0.1 and chi-square values above 3, SNPs in bold with P-value below 0.01.

Table 21 continued.

CHR	SNP	BP	A1	F_A	F_U	A2	CHISQ	P	OR	Group	Genes of interest
10	rs11188849	98364544	T	0.1374	0.1562	C	0.7762	0.3783	0.8599	MCG	PIK3AP1
11	rs11216534	117628968	A	0.0709	0.0778	G	0.1869	0.6655	0.9049	CCG	IL10RA-201
11	rs11216674	117879639	T	0.0748	0.0701	C	0.0898	0.7644	1.0730	CCG	IL10RA-201
12	rs2073950	111894072	A	0.1960	0.2022	G	0.0664	0.7966	0.9616	MCG	ATXN2
15	rs17302219	59478485	A	0.2263	0.2333	G	0.07651	0.7821	0.9609	MCG	MYO1E
15	rs7168492	89238255	T	0.3291	0.316	C	0.2138	0.6438	1.062	MCG	ISG20
15	rs4932194	89245239	C	0.3297	0.3183	A	0.1613	0.6879	1.053	MCG	ISG20
16	rs1833203	5339095	C	0.01099	0.01259	G	0.06056	0.8056	0.8714	CCG	Sweden
16	rs8052047	79812854	A	0.03069	0.03777	T	0.4212	0.5163	0.8065	CCG	c-MAF
17	rs4789939	76881703	A	0.1673	0.1741	G	0.08906	0.7654	0.9531	MCG	TIMP2
18	rs625896	39531139	C	0.3485	0.3764	T	0.9143	0.339	0.8864	MCG	PIK3C3
18	rs474605	39662517	A	0.509	0.4732	G	1.429	0.2319	1.154	MCG	PIK3C3
19	rs11743146	57678194	A	0.1313	0.1237	C	0.1461	0.7023	1.071	MCG	several ZNFs
20	rs6093338	39028436	G	0.08909	0.07721	A	0.5066	0.4766	1.169	MCG	MAFB
20	rs742745	39313690	A	0.1205	0.1339	C	0.4528	0.501	0.886	MCG	MAFB
22	rs4820663	26354655	C	0.09353	0.08244	A	0.4267	0.5136	1.148	MCG	MYO18B
22	rs6519955	46440273	A	**0.491**	0.3971	C	**9.934**	**0.001623**	**1.465**	MCG	**WNT7B**

Given are the SNPstream results for 281 patient samples without or with unknown family history for DD and 282 controls. CHR: Chromosome, SNP: SNP identifier, BP: Physical position (base pair), A1: Minor allele name (based on whole sample), F_A: Minor allele frequency in cases, F_U: Minor allele frequency in controls, A2: Major allele name, CHISQ: Basic allelic test chi-square (1df), P: Asymptotic p-value, OR: Estimated odds ratio (for A1, i.e. A2 is reference, Group: Group that identified this SNP in initial GWAS: CCG: Cologne Centre for Genomics, MCG: Department of Genetics, University Medical Centre Gröningen and University of Gröningen, the Netherlands, Genes of interest: Genes that locate to these regions, underlined genes are involved in the Wnt signalling pathway, grey colour indicates SNPs with P-values below 0.1 and chi-square values above 3, SNPs in bold with P-value below 0.01.

One SNP rs6519955 (P-value: 4.1×10^{-5}, OR: 1.99, minor allele frequency: 0.57) on chromosome 22 showed strongest association in the "young" DD patients (patients with age at first surgery < 50 years, see table 19) compared to the "old" patients (no surgery or first surgery after the age of 50 years) (P-value: 0.009, OR: 1.35, minor allele frequency: 0.47, (minor allele frequency in controls: 0.40)). This SNP was unfortunately not included in the POPGEN and KORA control data set, so that the comparison between young and old patients could not be repeated with the larger control set for this SNP. Analysing age at first surgery as a quantitative trait did not result in an association of rs6519955 (data not shown). The SNP with the best result in this analysis was rs6824106 on chromosome 4 with and regression coefficient of 3.7, r^2 of 0.02, and a P-value of 0.002.

The 465 patients typed with SNPstream where compared to all available control genotype data (table 22). Note that this could be done only for those SNPs that were included in the POPGEN and KORA data set, and therefore that not all SNPs from the SNPstream analysis were included in this comparison. Results are given in table 22. The SNP rs16879765 on chromosome 7 showed the strongest association (P-value: 5.8×10^{-10}, OR: 1.84). Two additional SNPs, from the initial GWAS with 186 DD patients, showed a suggestive association in this analysis: rs10759289 on chromosome 9 (P-value: 0.003, OR: 1.26), and rs8052047 on chromosome 16 (P-value: 0.04, OR: 1.48).

Again rs16879765 (Chr. 7) showed a stronger association in the subgroup of patients with a family predisposition for DD (P-value: 9.4×10^{-10}, OR: 2.26) compared to the patients without or unknown family history (P-value: 0.0003, OR: 1.57). The same tendency was true for SNP rs423940 on chromosome 8, which had a P-value of 1.3×10^{-6} and an odds ratio of 0.57 in patients with family history and a P-value of 0.003 and an odds ratio of 0.76 in patients without family predisposition. This tendency was also noted for SNP rs8052047 (Chr. 16) with a P-value of 0.005 (OR: 2.03) in patients with a family predisposition while no association was seen in patients without family history (P-value: 0.62, OR: 1.14). SNP rs11216674 showed a slight hint of association only in the cases with family history (P-value: 0.08, OR: 0.63). For two SNPs located to different regions on chromosome nine the opposite trend was observed: rs7863802 (P-value: 0.0002, OR: 1.48) and rs10759289 (P-value: 0.004, OR: 1.31) showed a stronger association in the subset of patients without a family history for DD than patients with family history (rs7863802: P-value: 0.05, OR: 1.28) and rs10759289 (P-value: 0.14, OR: 1.18).

Table 22. SNP stream Genotyping Results. Comparing <u>465 patient</u> samples vs. <u>1972 control</u> samples.

CHR	SNP	BP	A1	F_A	F_U	A2	CHISQ	P	OR	Group	Genes of interest
1	rs7524102	22698447	C	0.185	0.158	T	3.907	0.04808	1.21	MCG	WNT4
3	rs2323206	73951152	T	0.3791	0.3723	G	0.1443	0.704	1.029	MCG	RP11-20B7.1
3	rs1356802	131838077	C	0.3079	0.3358	A	2.602	0.1067	0.8798	MCG	CPNE4
4	rs6824106	178801018	C	0.367	0.3794	T	0.476	0.4903	0.9486	MCG	RP11-162G9.1, AGA
5	rs11743146	36844388	A	0.1223	0.125	C	0.04989	0.8233	0.9753	MCG	SLC1A3
6	rs237018	149743930	T	0.4814	0.5	C	1.021	0.3123	0.9281	MCG	MAP3K7IP2
7	rs10261983	37885121	T	0.3377	0.3358	C	0.01206	0.9125	1.009	CCG/MCG	SFRP4, EPDR1
7	rs2722372	37890267	T	0.2357	0.2536	C	1.246	0.2644	0.908	CCG/MCG	SFRP4, EPDR1
7	rs10250905	37907304	T	0.2522	0.2542	C	0.01621	0.8987	0.9892	CCG/MCG	SFRP4, EPDR1
7	**rs16879765**	37989095	A	**0.1897**	0.1131	G	**38.39**	**5.802e-010**	**1.836**	CCG/MCG	**SFRP4, EPDR1**
7	rs1668357	38004406	G	0.05531	0.05192	T	0.1715	0.6788	1.069	CCG/MCG	SFRP4, EPDR1
7	rs6951125	116917118	A	0.4446	0.4592	G	0.6278	0.4282	0.9427	MCG	WNT2
8	rs13269711	69979828	A	0.2555	0.2316	G	2.328	0.127	1.139	MCG	SULF1
8	**rs423940**	109228008	T	**0.3896**	0.4828	C	**25.5**	**4.422e-007**	**0.6838**	MCG	**RSPO2**
9	**rs7863802**	1199448	G	**0.2578**	0.1987	A	**15.27**	**9.326e-005**	**1.4**	MCG	**DMRT1-3**
9	rs10809650	1202371	G	0.2549	0.2937	A	5.379	0.02038	0.8231	MCG	DMRT1-3
9	**rs10759289**	111280824	C	**0.3626**	0.3108	T	**9.037**	**0.002645**	**1.262**	CCG	**ACTL7A, ACTL7B**
10	rs11188849	98364544	T	0.1396	0.16	C	2.335	0.1265	0.8513	MCG	PIK3AP1
11	rs11216534	117628968	A	0.06908	0.07067	G	0.02827	0.8665	0.9759	CCG	IL10RA-201
11	rs11216674	117879639	T	0.06154	0.06493	C	0.14	0.7083	0.9444	CCG	IL10RA-201

SNPstream results for 465 and 1972 controls. CHR: Chromosome, SNP: SNP identifier, BP: Physical position (base pair), A1: Minor allele name (based on whole sample), F_A: Minor allele frequency in cases, F_U: Minor allele frequency in controls, A2: Major allele name, CHISQ: Basic allelic test chi-square (1df), P: Asymptotic p-value, OR: Estimated odds ratio (for A1, i.e. A2 is reference, Group: Group that identified this SNP in initial GWAS: CCG: Cologne Centre for Genomics, MCG: Department of Genetics, University Medical Centre Gröningen and University of Gröningen, the Netherlands, Genes of interest: Genes that locate to these regions, underlined genes are involved in the Wnt signalling pathway, grey colour indicates SNPs with P-values below 0.1 and chi-square values above 3, SNPs in bold with P-value below 0.01.

Table 22 continued:

CHR	SNP	BP	A1	F_A	F_U	A2	CHISQ	P	OR	Group	Genes of interest
12	rs2073950	111894072	A	0.1872	0.1979	G	0.5282	0.4674	0.9337	MCG	ATXN2
15	rs17302219	59478485	A	0.2077	0.2192	G	0.5761	0.4479	0.9335	MCG	MYO1E
15	rs7168492	89238255	T	0.318	0.3536	C	4.109	0.04266	0.8524	MCG	ISG20
16	rs8052047	79812854	A	0.03939	0.02688	T	4.028	0.04475	1.484	CCG	c-MAF
18	rs625896	39531139	C	0.3275	0.3553	T	2.486	0.1148	0.8837	MCG	PIK3C3
18	rs474605	39662517	G	0.4783	0.4979	A	1.134	0.2869	0.9247	MCG	PIK3C3
20	rs6093338	39028436	G	0.08242	0.0757	A	0.4654	0.4951	1.097	MCG	MAFB
20	rs742745	39313690	A	0.1258	0.1365	C	0.7228	0.3952	0.9108	MCG	MAFB

SNPstream results for 465 and 1972 controls. CHR: Chromosome, SNP: SNP identifier, BP: Physical position (base pair), A1: Minor allele name (based on whole sample), F_A: Minor allele frequency in cases, F_U: Minor allele frequency in controls, A2: Major allele name, CHISQ: Basic allelic test chi-square (1df), P: Asymptotic p-value, OR: Estimated odds ratio (for A1, i.e. A2 is reference, Group: Group that identified this SNP in initial GWAS: CCG: Cologne Centre for Genomics, MCG: Department of Genetics, University Medical Centre Gröningen and University of Gröningen, the Netherlands, Genes of interest: Genes that locate to these regions, underlined genes are involved in the Wnt signalling pathway, grey colour indicates SNPs with P-values below 0.1 and chi-square values above 3, SNPs in bold with P-value below 0.01.

SNPs from four loci of the initial GWAS with 186 DD patients were included for validation in the SNPstream genotyping analysis. One SNP, rs16879765 on chromosome 7 was validated to be associated with DD. Two other SNPs, rs10759289 on chromosome 9 and rs8052047 on chromosome 16 showed suggestive association. Four SNPs (in addition to rs16879765) rs423940 on chromosome 8, rs7863802 and rs10809650 on chromosome 9, and rs6519955 on chromosome 22, typed in replication to the GWAS findings from the University of Gröningen (see Dolmans *et al*. 2011) were associated in the present sample set of 465 DD patients.

3.2.4 Sequencing of selected Candidate Genes

The SNP rs16879765 on 7p14.1 showed a strong association with DD in the GWA studies. The chromosomal region that showed association is relatively small with high recombination rates on both sides (see figure 39).
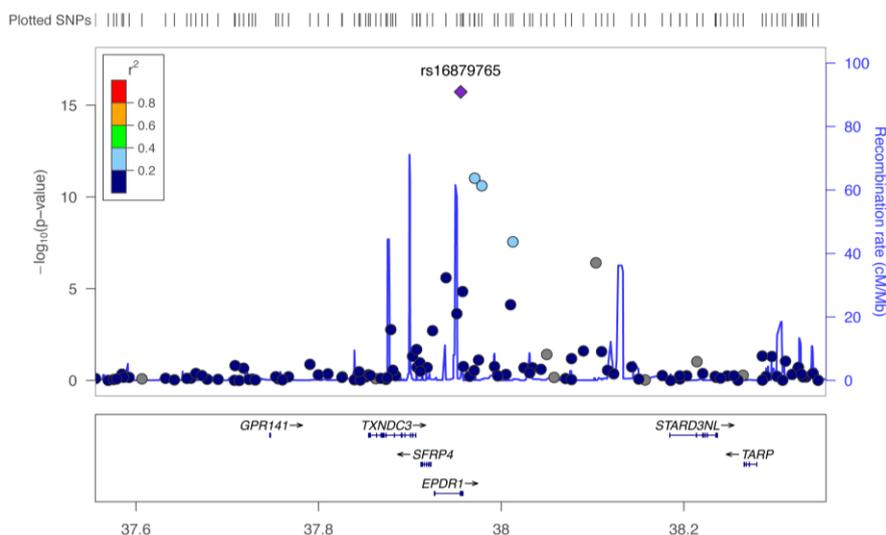
Figure 39. Regional plot of the identified DD risk loci on 7p14. The P-values, obtained using a 1-degree-of-freedom basic Chi-square allelic test corrected for genomic inflation (y-axis) were plotted against their chromosomal map positions (x-axis). The colour of each SNP spot reflects its r² value. Estimated recombination rates were plotted in blue. Region on chromosome 7, EPDR1 and SFRP4 are located near rs16879765. From Dolmans *et al.* 2011.

Three genes are located in this region: SFRP4, EPDR1 and TXNDC3. The SNP rs16879765 lies in the intron between exon 5 and 6 of the EPDR1 gene. TXNDC3 showed no signal in the expression analysis (see below) while SFRP4 and EPDR1 both were expressed in cases and controls. The exons of SFRP4 and EPDR1 were sequenced for mutations in the 26 patients that were homozygous for the minor allele of rs16879765. A few patients and controls with the other two genotypes were sequenced additionally. One patient (3011701) heterozygous for the SNP rs16879765, had a heterozygous mutation in exon 5 of the EPDR1

gene (7:37988478 T->C) changing the codon GTG to GCG which results in an amino acid change from valine to arginine at amino acid position 221 of the first transcript (ENST00000199448). Both EPDR1 and SFRP4 were expressed in fibroblasts of this patient. No other mutations were identified.

All patients homozygous for the minor allele of rs16879765 (A) were homozygous for the minor allele of two flanking SNPs rs2044831 (7:37988589) in exon 5 of the EPDR1 gene and rs1450851 (7:37989775) in exon 6 while patients heterozygous for rs16879765 (AG) were also heterozygous for these flanking SNPs in the exon sequence of EPDR1.

3.3   Expression analysis

3.3.1 Whole Genome Gene Expression Analysis

The Illumina HumanHT-12 v3 Expression BeadChip was used for whole genome expression analysis of 12 DD samples (primary disease tissue) and 12 matched controls (normal palmar fascia from control persons). The data was viewed with the Illumina genome studio software. Figure 40 shows the cluster diagram for analysed samples. Patients and controls cluster into two distinct groups with one female patient sample being different to both groups. No further sub-clustering of patient samples according to the sample characteristics noted in table 2 was observed. Interestingly female samples of neither patients nor controls clustered together.
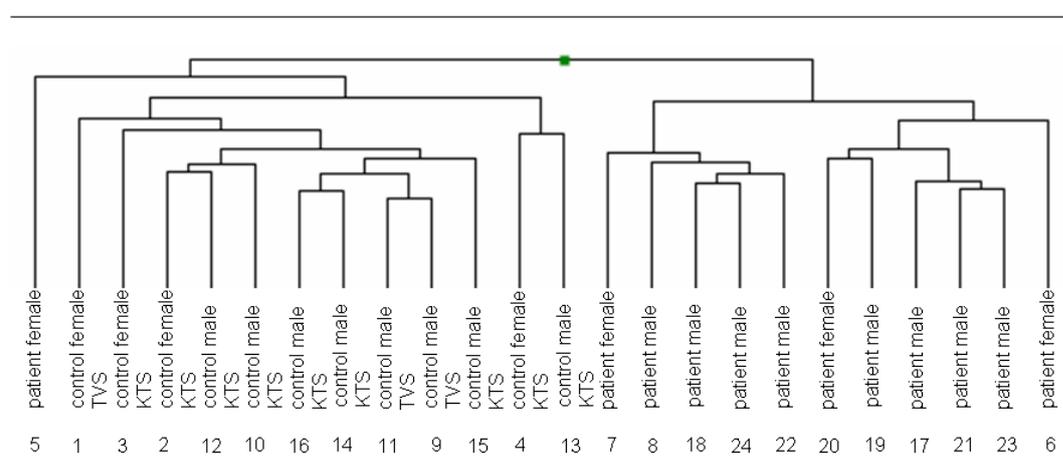
Figure 40. Cluster diagram for whole genome expression chip analysis. The dendrogram clearly demonstrates the differential agglomerative hierarchical profiling of disease versus control. Disease and control samples separate into two distinct clusters while one patient sample clusters somewhat different from the others. Numbers correspond to the sample numbers in table 2.

50 genes were significantly upregulated with a fold change of 5 to 52. All genes upregulated in this range are given in table 23. Among these were many genes coding for cell-adhesion molecules (e.g. THBS2, THBS4, TNC and CADM1), extra-cellular matrix components (e.g. COL14A1, COL1A1, COL7A1 and FNDC1) and cell signalling proteins (e.g. CDH11, SFRP2, FAP). Other genes, namely MAFB and SULF1 were implemented in a GWA study (see above). They locate to chromosomal regions associated with DD.

Table 23. Genes upregulated in DD patients.

SYMBOL	Signal cases	SD cases	Signal controls	SD controls	DiffScore	Fold Change
THBS4	11587.0	4139.5	222.5	217.1	51.0	**52.07**
TNC	3496.3	2638.4	113.8	105.8	23.0	**30.72**
RASL11B	892.0	501.9	50.0	59.7	32.0	**17.83**
LOC653499	596.3	1610.4	42.7	63.9	2.2	**13.96**
LGALS7	372.7	932.6	34.3	53.8	2.4	**10.88**
CADM1	1315.8	571.0	131.7	39.1	41.0	**9.99**
LOC728910	572.2	1401.5	57.9	80.3	2.4	**9.89**
NPTX2	447.4	402.5	48.4	22.2	14.7	**9.25**
ADAMTSL2	480.8	317.5	52.8	22.7	23.8	**9.11**
HLA-DRB5	477.6	593.1	54.9	194.7	7.3	**8.70**
CDH11	978.8	360.5	114.8	44.7	46.8	**8.52**
TMEM158	717.1	593.5	86.3	118.6	16.1	**8.31**
ANGPTL7	2464.2	2710.7	298.9	259.0	9.9	**8.24**
SCRG1	314.2	296.7	40.0	31.1	12.9	**7.85**
C5orf13	2752.8	1127.0	351.9	162.2	41.9	**7.82**
PGM2L1	351.8	274.6	47.6	27.3	17.6	**7.38**
SLCO2A1	647.6	288.8	88.2	45.2	37.8	**7.34**
THBS2	3741.2	1728.0	522.5	229.8	36.3	**7.16**
COL14A1	1047.7	461.6	147.6	114.9	37.3	**7.10**
FAM43B	278.1	191.5	39.6	52.7	20.2	**7.03**
MYO1D	924.3	381.7	133.3	46.8	40.7	**6.93**
TMEM45A	425.2	363.0	61.8	22.1	17.4	**6.88**
CYR61	1261.6	1009.7	193.0	108.1	16.3	**6.54**
FAM38B	456.3	222.6	71.6	121.4	28.3	**6.37**
CHSY3	305.3	186.3	48.0	18.8	24.6	**6.36**
NOV	1614.0	1343.7	255.1	147.1	15.1	**6.33**
COL7A1	583.7	613.3	93.1	109.3	9.8	**6.27**
FNDC1	3204.3	1215.4	533.6	593.9	38.8	**6.01**
MXRA5	6665.9	2527.2	1132.6	1021.4	40.1	**5.89**
FAP	1172.5	759.1	201.2	329.2	19.5	**5.83**
GJA1	1005.3	595.5	173.6	80.7	24.9	**5.79**
SFRP2	1486.9	763.0	257.5	180.4	29.6	**5.78**
COL1A1	15831.0	7355.9	2752.4	3207.5	31.1	**5.75**
SMOC2	367.7	74.3	64.8	36.9	64.2	**5.67**
LOX	431.1	170.3	76.9	33.6	40.3	**5.60**
AEBP1	3316.7	1026.0	592.1	212.1	49.7	**5.60**
COMP	10428.7	3964.3	1883.4	1509.8	39.8	**5.54**
SC65	349.3	194.7	63.2	43.9	26.1	**5.53**
COL5A2	5647.4	3542.2	1026.6	778.2	22.1	**5.50**
NT5DC2	1050.8	813.8	191.2	63.3	16.3	**5.50**
CRISPLD2	1789.2	648.4	328.7	157.4	43.4	**5.44**
RAI14	1481.2	532.2	276.5	97.7	44.1	**5.36**
CLEC11A	384.8	211.5	72.0	32.1	26.9	**5.34**
SLC16A3	413.0	227.1	78.2	110.3	23.4	**5.28**
SPON2	520.6	361.0	99.2	42.2	19.1	**5.25**
CHPF	661.7	337.4	126.3	29.7	29.9	**5.24**
GUCY1A3	653.3	279.6	124.8	52.9	36.7	**5.23**
SULF1	713.8	212.4	138.1	84.2	48.5	**5.17**
MAFB	3595.0	2645.9	699.6	292.2	17.3	**5.14**
LEPREL2	259.7	130.9	51.7	20.5	29.6	**5.02**

Given are the 50 most up regulated genes in DD patient samples sorted by fold change. The signal detection P-values for all genes and both cases and controls were 0. Diffscore: probability for cases and controls to differ in their expression (larger Diffscore = higher probability). Genes highlighted in grey have also been identified in other whole genome expression analyses.

Several novel genes were identified to be upregulated in DD primary disease tissue that were not identified in previous whole genome expression analysis, among them were e.g. thrombospondin 4 (THBS4), galectin 7 (LGALS7), cell adhesion molecule 1 (CADM1), neuronal pentraxin II (NPTX2), major histocompatibility complex, class II, DR beta 5 (HLA-DRB5), ADAMTS-like 2 (ADAMTSL2), scrapie responsive protein 1 (SCRG1), chromosome 5 open reading frame 13 (C5orf13), phosphoglucomutase 2-like 1 (PGM2L1), solute carrier organic anion transporter family, member 2A1 (SLCO2A1), family with sequence similarity 43, member B (FAM43B), myosin ID (MYO1D), transmembrane protein 45A (TMEM45A), cysteine-rich, angiogenic inducer, 61 (CYR61) and family with sequence similarity 38, member B (FAM38B).

Additionally 797 genes were upregulated with fold changes of 1.5 to 4.9 (Detection signal P-value = 0). Some additional genes were expressed in patient samples but reached no significant detection signal in control samples. Among these was e.g. POSTN which has been noted to be differentially expressed in DD in other expression studies (Shih *et al.* 2009).

Table 24 summarises the 46 genes down regulated with fold changes of -16 to -5. The table contains e.g. many genes that are involved in adipocyte metabolism e.g. LEP, LIPE, RBP4 and THRSP; some genes encoding for heat shock proteins e.g. HSPB7 and HSPB6 and pro-apoptotic genes like G0S2 and BOK.

Another 655 genes (detection signal P-value = 0) were down regulated with fold changes of -4.9 to -1.5. Of 226 nuclear encoded mitochondrial proteins 177 (78.3%) had fold changes below 1 compared to non-mitochondrial genes (46.2% with fold changes below 1, N = 5657, P-value of student's t-test = 1.74E-18).

Table 24. Most down regulated genes in DD patients.

SYMBOL	Signal cases	SD cases	Signal controls	SD controls	DiffScore	Ratio	Fold Change
G0S2	152.5	155.6	2391.8	1146.3	-38.2	0.064	**-15.68**
PPP1R1A	174.0	231.3	2514.3	953.7	-46.8	0.069	**-14.45**
LEP	108.8	132.9	1531.6	663.5	-40.7	0.071	**-14.07**
LIPE	103.2	106.5	1451.6	720.1	-36.4	0.071	**-14.07**
RBP4	50.8	41.5	705.7	238.3	-50.9	0.072	**-13.89**
THRSP	156.4	218.7	1986.3	837.3	-42.0	0.079	**-12.70**
TM7SF2	89.6	72.1	1130.4	434.0	-46.6	0.079	**-12.62**
TMEM37	64.9	41.3	797.0	650.9	-18.2	0.081	**-12.27**
TF	92.3	100.4	1010.2	928.2	-14.6	0.091	**-10.94**
PLIN	342.7	493.9	3723.3	1185.4	-50.2	0.092	**-10.86**
KIAA1881	1047.9	1058.8	11342.6	2624.9	-64.2	0.092	**-10.82**
HSPB7	113.7	57.7	1193.6	672.4	-30.3	0.095	**-10.50**
RDH5	177.6	214.5	1756.6	625.8	-46.8	0.101	**-9.89**
PNPLA2	195.1	112.0	1841.8	673.3	-46.8	0.106	**-9.44**
HSPB6	267.0	174.9	2511.3	2020.1	-17.7	0.106	**-9.41**
TIMP4	137.4	103.8	1158.4	508.2	-38.9	0.119	**-8.43**
CEBPA	418.3	295.0	3482.4	1535.0	-38.7	0.120	**-8.33**
LPL	157.4	192.4	1310.2	535.4	-40.1	0.120	**-8.32**
GPAM	340.4	573.5	2770.6	1298.9	-33.4	0.123	**-8.14**
MOSC1	141.1	248.7	1126.1	371.8	-43.7	0.125	**-7.98**
FAH	89.8	65.6	696.8	334.1	-34.8	0.129	**-7.76**
AGPAT2	131.0	43.1	998.5	522.5	-26.4	0.131	**-7.62**
RASD1	182.6	140.1	1372.0	574.5	-39.8	0.133	**-7.51**
SELENBP1	133.9	116.4	931.7	284.1	-49.7	0.144	**-6.96**
MAOA	605.9	682.4	3998.7	1043.5	-50.9	0.152	**-6.60**
ALDH2	516.5	340.9	3396.7	1150.3	-46.8	0.152	**-6.58**
C6	127.2	110.6	836.4	591.6	-19.6	0.152	**-6.57**
RARRES2	440.3	309.7	2732.5	1183.1	-37.0	0.161	**-6.21**
ADH1B	147.0	195.7	897.7	419.9	-30.9	0.164	**-6.11**
BOK	93.5	27.7	555.7	327.3	-25.5	0.168	**-5.94**
HOOK2	103.1	121.1	597.1	198.8	-42.2	0.173	**-5.79**
GPT2	177.3	141.5	1021.0	321.0	-46.8	0.174	**-5.76**
ADH1A	935.2	1180.9	5332.1	1628.7	-43.4	0.175	**-5.70**
ECHDC3	109.4	129.9	609.4	237.8	-36.3	0.180	**-5.57**
SCGB2A1	61.1	73.5	337.0	923.9	-1.7	0.181	**-5.51**
APOE	552.0	281.0	3009.6	1828.5	-23.4	0.183	**-5.45**
SLC19A3	153.9	326.2	822.7	373.4	-24.0	0.187	**-5.35**
ACSL1	101.8	60.9	542.1	155.4	-50.2	0.188	**-5.32**
FASN	803.9	277.2	4261.4	4017.4	-11.4	0.189	**-5.30**
IRX6	60.6	33.1	320.6	266.6	-14.2	0.189	**-5.29**
MMD	381.7	480.1	1990.9	782.1	-34.1	0.192	**-5.22**
HRASLS3	1033.8	1065.0	5298.4	1490.4	-45.9	0.195	**-5.13**
PECR	107.6	80.0	547.8	216.0	-37.8	0.196	**-5.09**
SNCG	63.3	37.3	321.0	146.5	-33.0	0.197	**-5.07**
SLC1A3	64.7	60.4	327.0	134.9	-34.6	0.198	**-5.06**

Given are the 46 most down regulated genes in DD patient samples sorted by fold change. The signal detection P-values for all genes and both cases and controls are 0. Diffscore – probability for cases and controls to differ in their expression (larger Diffscore – higher probability). Ratio

In order to access protein networks and signalling pathways of differentially expressed genes in DD, the IPA software tool was employed. Table 25 shows the molecules involved in the highest ranking networks and the molecules' primary functions related to these networks.

In Network 1 the majority of genes (P-value = 1.73E-03, N = 23) are involved in genetic disorders e.g. diabetes mellitus (P-value = 4.91E-02, N = 9), glucose metabolism disorder (P-value = 2.98E-02, N = 10), metabolic disorder (P-value = 4.07E-02, N = 11) and for example neuronal diseases (e.g. Huntington's disease, N = 5). Some molecules from network 1 are implemented in cell morphology (P-value = 2.88E-03, N = 10) like cell shape change, elongation, spreading, morphology and morphogenesis. The other tabulated networks are mainly associated with cell death and cell signalling. The functions of network 2 comprise among others: apoptosis (P-value = 6.49E-06, N = 21), quantity of cellular junctions (P-value = 6.65E-06, N = 8; and adherent junctions). Other functions in network 2 were e.g. cell cycle cell growth and migration and cellular assembly (aggregation of filaments).

Table 25. Top networks identified with the IPA software.

ID	Molecules in Network	Score	Focus Molecules	Top Functions
1	ACTG2 (includes EG:72), ACTN1, ADCY7, AKAP12, ALPL, ARHGAP1, ATP2A2, CAP2, CDC42EP4, CDK14, DHCR7, DHRS3, FLNC, FSH, GEM, HK2, ITGB5, KIDINS220, Lh, MAPK6, MAPRE2, NOL3, P4HA2, PDLIM3, PDXK, PHKA2, PLIN3, PPAP2A, RAB31, RAB5A, RGS5, TLN1, TRIB1, TUBA1A, TYRO3	26	33	Small Molecule Biochemistry, Drug Metabolism, Carbohydrate Metabolism
2	APP, BACE2, CDC42EP2, CDH1, CEBPB, CRABP2, CRYAB, DEGS1, DNM1, DSP, EZR, F Actin, GSN, IgG, KRT10, KRT16, LGALS7, LPAR1, PALLD, PIM1, PLS3, PPL, PTPRF, RAB11FIP5, RAPGEF3, SLC2A3, SNAI2, SPTBN1, STXBP1, TNFAIP2, TNFSF13B, TRIM21, TRIM29, UCHL1, ZMPSTE24	26	33	Cell Death, Cell-To-Cell Signalling and Interaction, Cellular Assembly and Organization
3	ACTL6A, Alpha tubulin, BMI1, CHRNA5, DR1, ETS2, FHL1, GADD45A, HERC5, HIF1A, Histone h4, Hsp70, HSPH1, HUWE1, LAMP2, LEP, MYC, MYCBP2, MYH11, MYO1B, NOX4, PERP, PI3K (complex), SMARCC1, SPAG9, STAT5B, TCF7L2, TFDP1, TRIP10, TUBB2C, TYMS, WAS, WIPF1, XBP1, ZNF217	22	31	Cell Death, Cell-mediated Immune Response, Cellular Development
4	A4GALT, ABCB1, ACSL3, BCAR1, BHLHE40, CD9, CD36, CD37, CD44, CD53, CD82, CD151, Collagen(s), CYR61, DYRK1B, ERK1/2, FCER1A, FCER1G, FGR, Focal adhesion kinase, FYN, GJA1, Integrin alpha 3 beta 1, ITGAV, JAK2, LYN, P38 MAPK, PDGFRB, PLAUR, RBP4, SERPINB5, SPP1, TGFB1I1, TP63, YES1	21	30	Cellular Movement, Cell Signalling, Post-Translational Modification
5	26s Proteasome, ACO1, AHR, B4GALT5, BCAP31, CD46, CD59, CSF1R, CTGF, CYP1B1, Eotaxin, ETS1, F10, F8A1, Fibrinogen, FOS, FOSB, FOXP1, FTH1, GAS1, IL12 (complex), IL7R, ITGA5, ITGAM, ITGB2, JUNB, LMNA, MMP2, Pkc(s), RAC2, SCD, TEK, TGFB3, THY1, TNC	21	30	Cell-To-Cell Signalling and Interaction, Inflammatory Response, Cellular Growth and Proliferation
6	BAZ1A, BCL2L13, CAV1, CAV2, CBX5, CDK2, COL1A2, CSF2RA (includes EG:1438), DEFB1, DNM2, E2f, EGR1, FLOT2, Hsp90, IGF1, IGFBP4, Interferon alpha, IRAK1, IRS1, IRS2, ISG20, Jnk, MAP3K11, p85 (pik3r), PCNA, PRKD1, PTGES, RFC4, SFN, SMARCA5, STAT5A, TICAM1, TLR5, TRIB2, ZNF160	21	30	Cellular Growth and Proliferation, Cell Death, Organismal Development

Given are the six highest ranking molecule interaction networks allocated by the IPA. © 2000-2011 Ingenuity Systems, Inc. All rights reserved.

Figure 41 exemplary depicts a graphical view of network 1 from table 25. In the centre stand two hormones, luteinizing hormone and follicle stimulating hormone that both are glycoprotein hormones secreted by the pituitary gland. In conjunction they induce egg and sperm production. Grouped around these are the other members in this network.


Figure 41. Graphical view of network one (from table 25). Upregulated genes are depicted in red, downregulated genes in green. The intensity of the colour corresponds to the fold change.


Figure 42. Graphical view of network one (from table 25). Upregulated genes are depicted in red, downregulated genes in green. The intensity of the colour corresponds to the fold change.

Figure 42 depicts network 2 of the IPA analysis (table 25). In its centre stands the immunoglobulin G (IgG), which is an antibody produced by b-cells in response to (bacterial) antigens. Next to it the 11fold upregulated galactoside-binding lectin 7 (LGALS7) catches the eye because of its red colour. The product of this gene is implicated in modulating cell-cell and cell-matrix interactions. It was originally cloned from epidermis (Magnaldo *et al*. 1995). The authors found by in situ hybridisation that it is expressed in keratinocytes and found mainly in stratified squamous epithelium. It expression is altered in cancer and LGALS7 was proposed as a biomarker in breast cancer (Demers *et al*. 2010) and esophageal squamous cell carcinoma (Zhu *et al*. 2010). It was found to induce the expression of matrix metalloproteinase 9 (MMP9) in HeLa cells (Park *et al*. 2010). In this study MMP9 was downregulated (-23fold, detection P-value in patients: 0.003, in controls: 0). LGALS7 is located on chromosome 19 with a gene duplicate adjacent to it on the other strand which was also upregulated (LOC728910 and LOC653499 in table 23). Keratin 10 and keratin 16 are found upregulated in this network while e.g. the small heat shock protein CRYAB is downregulated (fold change: -4.81).

Table 26. Top canonical pathways.

Name	P-value	Ratio
Mitochondrial Dysfunction	4,28E-14	83/127 (0.654)
Oxidative Phosphorylation	4,52E-12	84/140 (0.600)
Estrogen Receptor Signalling	4,55E-08	78/135 (0.578)
Valine, Leucine and Isoleucine Degradation	7,56E-08	45/63 (0.714)
Protein Ubiquitination Pathway	1,12E-07	138/270 (0.511)

Given are the five top canonical pathways as attributed by the IPA software. Ratio: number of deregulated genes/ number of genes in the network.

Table 26 summarises the highest ranking canonical pathways identified in the IPA analysis also graphical depicted in figure 43. Top ranks mitochondrial dysfunction followed by oxidative phosphorylation.
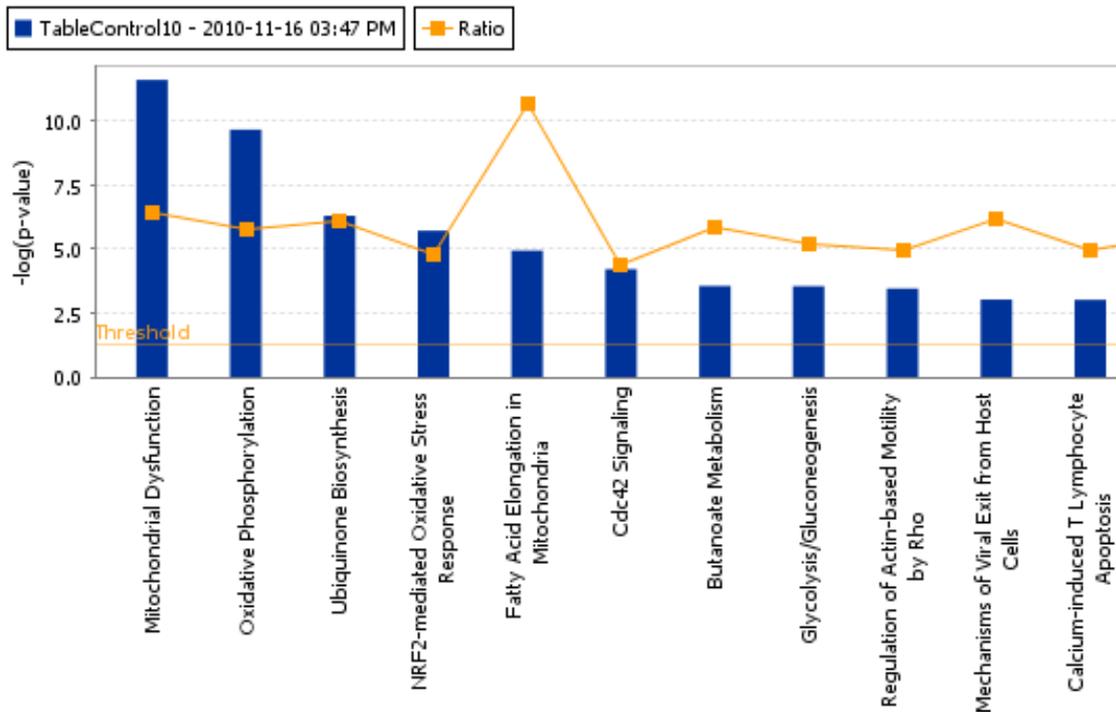
Figure 43. Graphical illustration of top canonical pathways with IPA. Given are P-values for each pathway (blue bars) and the ratio of the genes differentially expressed in this analysis divided by all genes in this pathway according to IPA used databases (yellow line). Note that network 5 (Fatty acid elongation in mitochondria) contains few (N = 5) genes compared to most other networks.

Figure 44 shows molecules involved in mitochondrial function and dysfunction and their localisation in the cell. Orbital spheres in the inner mitochondrial membrane represent the complexes I, III, and IV of the respiratory electron transporters chain. The majority of genes in this sketch appear to be downregulated (green colour). The main function of mitochondria is ATP production, which occurs during mitochondrial oxidative phosphorylation (see top canonical pathways, table 26). Reactive oxygen species (ROS) form as by-product of oxidative phosphorylation. ROS play an important role in cell signalling and create oxidative stress. Among the downregulated genes are those involved in the generation of, and response to ROS e.g. monoamine oxidase A (MAOA), catalase (CAT) and uncoupling protein 2 (UCP2).

Molecular Genetics of Dupuytren´s Disease
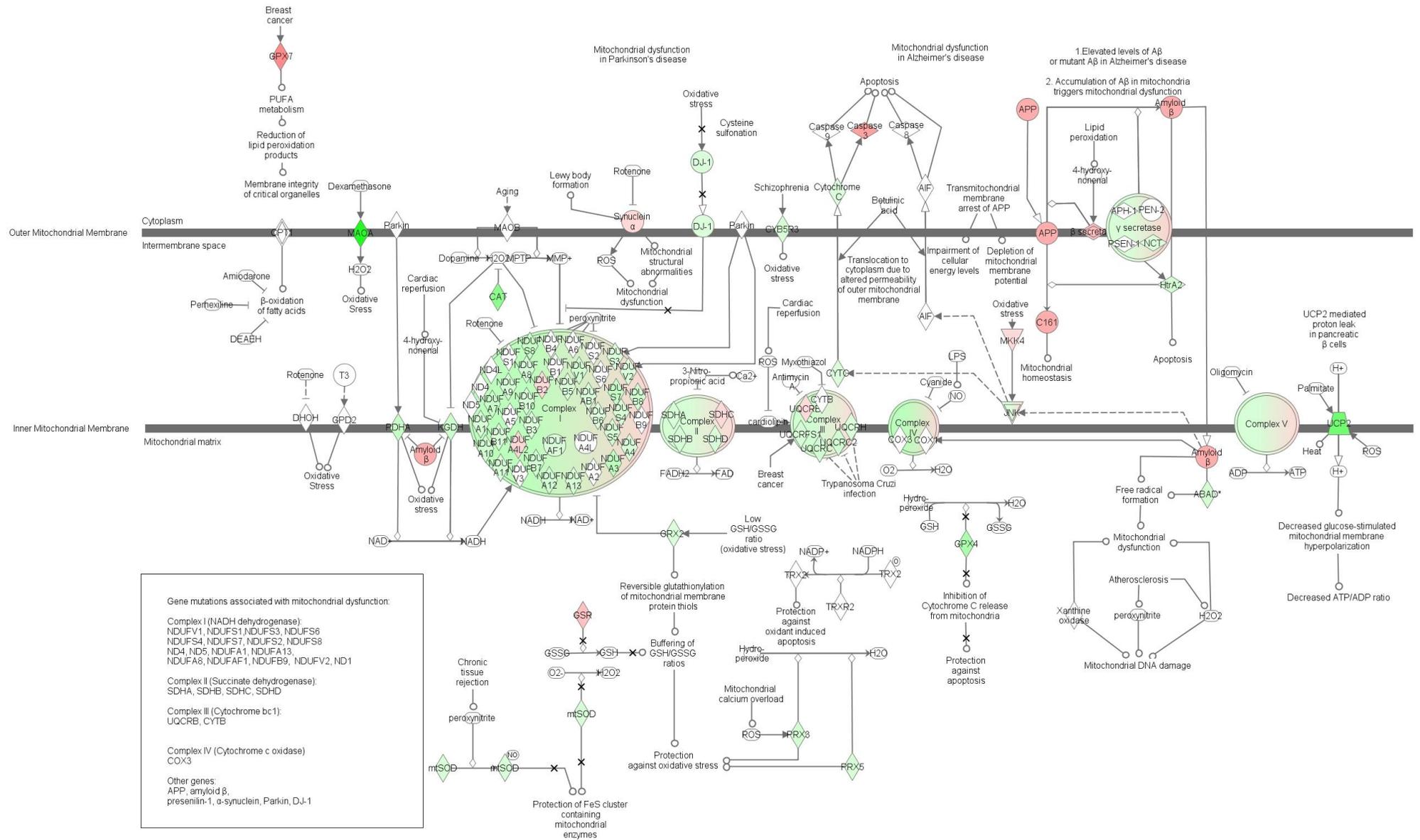
Figure 44. Mitochondrial dysfunction. Downregulated genes are highlighted in green, upregulated genes in red. Intensity in colour corresponds to fold change (source IPA).

Table 27 gives the top networks identified by IPA when only upregulated genes were considered in the analysis. Again genetic disease dominates the top functions allocated to the top networks. Together network 1 and 2 contained 38 molecules with functions and/or diseases allocated by IPA. 18 molecules are linked with cancer (P-value: 6.89E-05), 16 have been associated with genetic disorders (P-value: 6.89E-05) e.g. knuckle pads, non-insulin dependent diabetes mellitus, coronary artery disease and non-alcoholic fatty liver disease. Among allocated functions were e.g. cellular growth and proliferation (N = 15, P-value: 1.20E-03), cellular movement (N = 11, P-value: 9.38E-03 and cell death (N = 15, P-value: 3.33E-03). Network 1 and 2 are depicted in figure 45.

Table 27. Top networks upregulated genes only.

ID	Molecules in Network	Score	Focus Molecules	Top Functions
1	ARHGAP22, ATL1, CLEC11A, Cpla2, DPY19L1, FABP5, FJX1, GALNT4, GJB2, GJB6, Glutathione peroxidase, GMPPA, GMPPB, GPX2, GPX7, hCG, Ikb, IKK (complex), KDM5B, KLHL4, MAGED2, MPZL2, MTHFD1L, MUC1, MYO1B, RECQL, REEP1, SLC25A22, SPAG9, TMEM158, TNFRSF12A, TRO, TSC22D1, UCK2, ZNF217	37	30	Auditory Disease, Genetic Disorder, Neurological Disease
2	ABCC4, AMACR, CASP3, CKAP4, CLCA2 (includes EG:9635), CNN3, CRY1, DLG4, DUSP5, EIF4E2, EZH2, FMO1, FOXQ1, FRMD6, GEM, Insulin, KIF13B, LYN, MYCN, NUCB2, NUDT1, OMD, p85 (pik3r), PCGF2, PDGF BB, PHC3, PLEKHA1, PTEN, RYBP, STK38, TMED9, UBE2Q2, Ubiquitin, UNC5B, ZSWIM4	37	31	Cancer, Neurological Disease, Cellular Development
3	ADSS, BACH2 (includes EG:60468), CAMK2N1, Cbp, CCDC136, CDCA4, CXADR, DEGS1, DLK1, DSP, ERK, Fc gamma receptor, Fc receptor, FCER1A, FCGR1B, HES1, HEY2, HSD17B14, ID3, IgG, IgG1, KLF6, MAFB, MVP, PAQR3, PRSS23, SERPINH1, SMARCC1, SNAI2, SRGAP3, TCF12, TNFAIP1, ZFHX3, ZMPSTE24, ZNF408	35	29	Gene Expression, Cell Cycle, Cellular Development
4	ACPL2, BOP1, CDR2, CHPF, CHPF2 (includes EG:54480), CHSY1, CHSY3, CNOT6, FAM129A, FAM57A, GAR1, glucuronyl-N-acetylgalactosaminylproteoglycan beta-1,4-N-acetylgalactosaminyltransferase, GSR, IMPACT, LRRN1, MIR1, MIR101, MYC, N-acetylgalactosaminyl-proteoglycan 3-beta-glucuronosyltransferase, NOLC1, OAT, PAM, PERP, PGM2, Rfc, RFC4, RRM2B, SH3PXD2B, SLC16A9, SLC44A1, SNIP1, TAGLN2, TSPAN7, UST, Vla-4	35	29	Gene Expression, Infection Mechanism, Cellular Assembly and Organization
5	26s Proteasome, Angiotensin II receptor type 1, Arf, ARF4, C1QTNF5, Calcineurin A, COG6, FKBP2, FKBP7, FKBP9, FKBP10, FKBP11, Gsk3, KDELR2, KDELR3, LAMP2, LEPRE1, MGAT2, MYOZ3, NFATC1, peptidylprolyl isomerase, PPAP2A, PPAP2C, PPIC, PPP3CA, PRUNE2, RCN3, SDF2L1, SEC63, SEC24D, SRPRB, SURF4, TRAM1, XBP1, YIF1A	34	29	Genetic Disorder, Metabolic Disease, Cardiovascular Disease

Given are the five highest ranking molecule interaction networks allocated by the IPA software when only upregulated genes were considered in the analysis. © 2000-2011 Ingenuity Systems, Inc. All rights reserved.
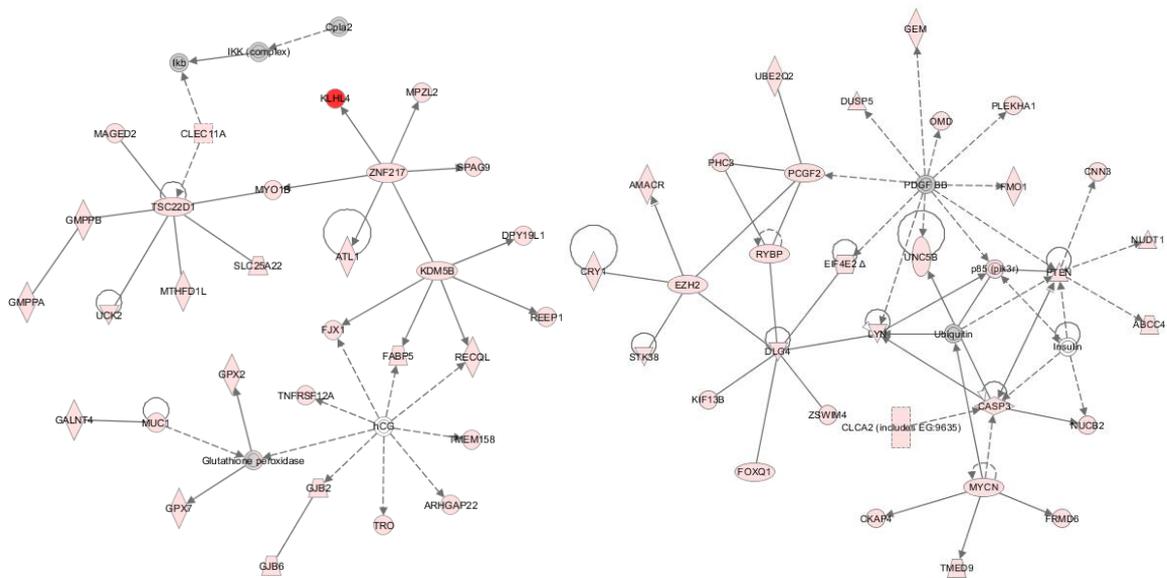
Figure 45. Network 1 and 2 upregulated genes only. Only upregulated genes were considered in the IPA analysis. The two top ranking networks, both with a score of 37 are depicted.

When only up regulated genes were considered in the IPA analysis (table 28, figure 46), Wnt/β-catenin signalling ranked top under the canonical pathways (P-value = 6.05E-07, ratio: 33/175 (0.189)), followed by p53 signalling (P-value = 4.04E-05, ratio: 22/99), axonal guidance signalling (P-value = 4.27E-04, ratio: 47/410) and Cdc signalling (P-value = 4.48E-04, ratio: 21/180).

Table 28. Top Signalling pathways upregulated genes only.

Pathway	P-value	Ratio
Wnt/β-catenin Signalling	6.05E-07	33/175 (0.189)
p53 Signalling	4.04E-05	20/99 (0.202)
Axonal Guidance Signalling	4.27E-04	47/410 (0.115)
Cdc42 Signalling	4.48E-04	21/180 (0.117)
Factors Promoting Cardiogenesis in Vertebrates	9.97E-04	16/95 (0.168)

Given are the five top canonical pathways as attributed by the IPA software. Ratio: number of upregulated genes/ number of genes in the network.
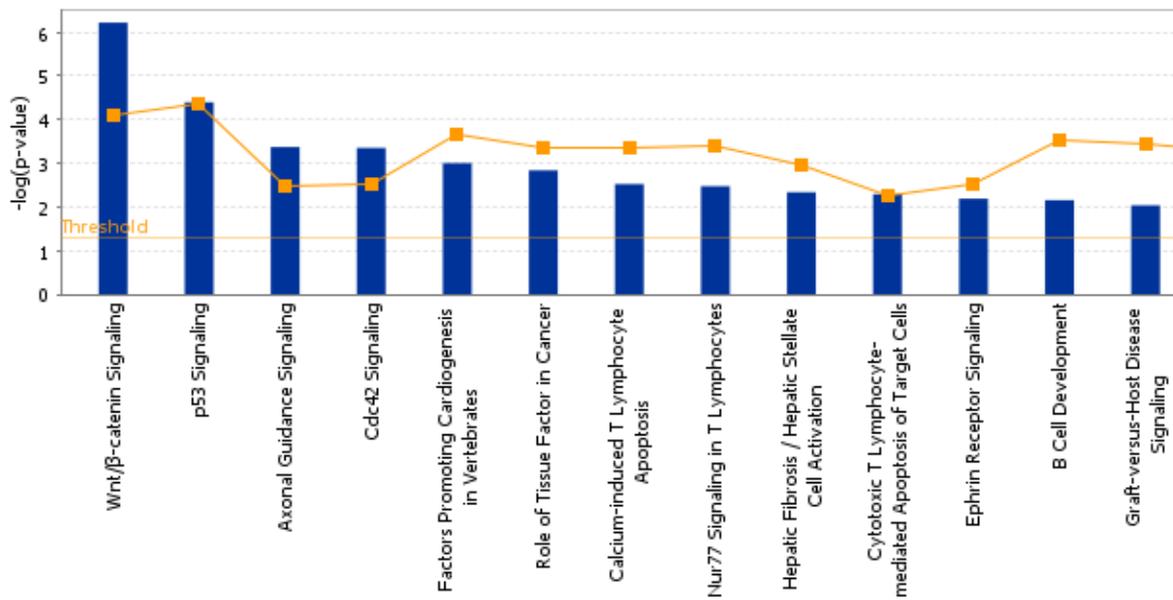
Figure 46. Graphical illustration of top canonical pathways with IPA for upregulated genes only. Given are P-values for each pathway (blue bars) and the ratio of the genes differentially expressed in this analysis divided by all genes in this pathway according to IPA used databases (yellow line). Note that network 5 (Fatty acid elongation in mitochondria) contains few (N = 5) genes compared to most other networks.

Table 34 of the appendix gives the genes involved in Wnt/β-catenin signalling (source IPA) that were expressed in the whole genome expression analysis. 40.9% (N = 110) of the genes were upregulated with fold changes above 1.5 and 11.8% genes were downregulated with fold change below -1.5). WNT11 was downregulated in patients with a fold change of -3.54. All other Wnt genes were poorly detected in the whole genome expression analysis or showed heterogeneous expression levels in patients and controls.

3.3.2 Quantitative Real-Time PCR

Quantitative real-time PCR (qPCR) was preformed for selected target genes in order to verify and refine whole genome expression analysis findings. Comparison was done for (1) patient and control tissue samples; (2) disease and control samples from the same patient; (3) patient and control fibroblasts and (4) patient fibroblasts treated with or without TGFβ1. Results are summarised in table 29.

Table 29. qPCR Results.

Nr.		Gene	Fold Change Chip	Tissue (P/C) P-value (sTTEST)	Fold Change	SD	Tissue (P/P) P-value (pTTEST)	Fold Change	SD	Cells (P/C) P-value (sTTEST)	Fold Change	SD	Cells (+/- TGFβ1) P-value (pTTEST)	Fold Change	SD
1	Ref.	ACTB	**1.228**	n.d.			n.d.			**2.02E-06**			**0.006**		
2	Ref.	EIF3H	**-1.008**	0.605			0.057			0.847			0.918		
3	Ref.	EIFC2C	**1.004**	0.834			0.150			0.363			0.289		
4	Ref.	GAPDH	**1.011**	0.333			0.106			0.057			**1.48E-04**		
5	Ref.	PCDH18	**1.001**	0.589			0.530			0.798			**0.009**		
6	Ref.	RN18S1	n.d.	n.d.			n.d.			0.860			**0.025**		
7	Ref.	RPS18	**1.081**	0.707			n.d.			0.877			0.251		
8	Ref.	TBP	**-1.146**	n.d.			n.d.			0.466			0.147		
1	Myo.	ACTA2	**1.221**	0.203	1.738	0.468	**0.024**	**3.795**	2.421	0.444	1.170	0.255	**0.001**	**17.696**	10.922
2	Oxi.	APP	**2.314**	**0.040**	**2.345**	0.510	**0.025**	**2.904**	1.672	0.703	1.022	0.156	**2.26E-04**	**1.801**	0.196
3	Oxi.	ATP5B	**-1.195**	n.d.			n.d.			0.616	-1.039	0.184	0.144	1.370	0.184
4	Oxi.	CASP3	**2.679**	0.098	2.060	0.410	0.053	2.166	1.453	0.769	1.057	0.387	**0.031**	**1.576**	0.415
5	Oxi.	CAT	**-3.372**	**3.04E-05**	**-2.968**	0.173	0.164	-2.465	0.221	0.844	1.083	0.366	0.796	1.174	0.177
6	Exp.	CDH1	**1.888**	n.d.			n.d.			**6.95E-05**	**2.113**	0.456	**0.048**	**9.239**	9.316
7	Oxi.	COX8A	**-1.357**	n.d.			n.d.			0.227	1.072	0.192	**0.022**	**1.576**	0.415
8	GWA	EPDR1	**-1.152**	n.d.			n.d.			**9.15E-04**	**-1.641**	0.225	**9.31E-05**	**2.014**	0.289
9	beta	FZD4	**-3.583**	n.d.			n.d.			**0.0098**	**-1.348**	0.233	0.185	-1.149	0.412
10	beta	GSK3β	**1.550**	n.d.			n.d.			0.592	-1.073	0.207	0.516	1.386	0.364
11	GWA	MAFB	**5.139**	**0.004**	**5.801**	3.823	**0.034**	**7.586**	7.115	0.584	-1.408	0.359	**0.001**	**-6.314**	0.127
12	Oxi.	MAOA	**-6.599**	**4.51E-07**	**-11.300**	0.052	**0.001**	**-7.059**	0.107	0.212	-1.125	0.453	0.858	1.134	0.385
13	GWA	RSPO2	1.682	**1.26E-04**	**26.587**	16.035	**0.005**	**20.423**	23.737	**8.47E-05**	**-7.122**	0.100	0.657	1.620	1.135
14	GWA	SFRP4	**2.678**	**0.003**	**5.224**	1.633	**0.004**	**7.272**	5.942	0.190	-1.382	0.720	0.073	1.840	0.668
15	Oxi.	SOD2	n.d.	0.634	-1.040	0.517	0.753	-1.753	0.481	**0.026**	**-1.698**	0.245	**0.019**	**-2.536**	0.159
16	Exp.	TGFß3	**4.964**	**9.95E-05**	**8.465**	2.026	**0.006**	**6.311**	4.734	0.130	1.200	0.393	0.102	-1.054	0.130
17	Exp.	THBS4	**52.070**	n.d.			n.d.			**0.010**	**-1.348**	0.233	**4.95E-04**	**9.867**	3.328
18	GWA	WNT2	-1.288	0.563	1.3049	0.6320	**0.033**	**1.730**	2.450	0.420	1.702	0.970	0.068	2.377	1.174
19	GWA	WNT4	1.973	n.d.			n.d.			**0.008**	**1.988**	0.844	0.059	12.398	13.444
20	GWA	WNT7B	4.193	n.d.			n.d.			**0.003**	**1.425**	0.239	**4.26E-04**	**4.634**	1.764

Given are the expression changes in 20 target genes detected with qPCR in total RNA samples derived from patient (P) and control (C) tissue and patient and control primary fibroblasts. P-values are those of paired t-test (pTTEST) and student's t-test (sTTEST). Type: Ref.: reference gene, beta: genes involved in the Wnt/β-catenin pathway, Exp.: genes of interest from the whole genome expression analysis, GWA: genes localised to regions found associated with DD in the GWAS, Oxi.: genes involved in oxidative stress and mitochondrial function; Fold change Chip: fold changes found in the whole genome expression analysis; SD: standard derivation. Significant P-values are given in bold (< 0.05). Fold changes with significant p-values are highlighted in colour. N.d.: not determined.

Reference gene expression was not significantly different between patient and control samples (table 29). Those reference genes for which the expression was significantly different between compared groups (e.g. ACTB) were excluded from the analysis.

Expression in Patient and Control Tissue Samples

The gene expression of 11 genes was compared in nine DD patients and nine controls. The patient samples were different ones from the ones used in the expression chip experiment. The control samples were different except two that were used before in the expression chip experiment. Results from the whole genome expression analysis could be verified in the qPCR experiment. For the genes: MAFB, APP, CASP3 and CAT fold changes were in the same range as determined in the whole genome expression analysis. For the genes TGFβ3, SFRP4 and MAOA fold changes were slightly higher than in the whole genome expression analysis. For RSPO2 signal detection failed in the whole genome expression analysis but a significant upregulation of this gene was observed in the qPCR experiment.

In addition the relative expression values of disease tissue were compared with those of macroscopically normal appearing tissue from the same patient. The control tissue was removed from adjacent to the disease tissue. This experiment was carried out for six DD patients. Most genes analysed (TGFβ3, MAFB, RSPO2, SFRP4, WNT2, ACTA2 (αSMA) and APP) showed a significant upregulation in disease tissue compared to control tissue from the same patient, while MAOA was significantly downregulated in the disease tissue. For CASP3, CAT and SOD2 no significant differences could be observed in control and disease tissue from the same patient.

Expression in Patient and Control Fibroblasts

DD and control derived primary fibroblast cell lines were harvested in passage three and the expression of target genes was compared for eleven patient cell lines and seven control cell lines. FZD4, CDH1, THBS4, EPDR1, RSPO2, and SOD2 showed significant expression differences in patient and control fibroblast RNA samples. For most of these genes the direction of deregulation was consisted with the expression patterns observed in tissue. But for RSPO2 a significant downregulation (fold change:-7.1) was observed in patient cells compared to control fibroblasts.

To assess the influence of TGFβ1 on target gene expression, the relative expression values of fibroblasts treated with TGFβ1 were compared to the same cell line not treated with TGFβ1. This was done for five DD patients and one control. When the expression of patient fibroblasts

stimulated with TGFβ1 was compared to the same patient cell line without TGFβ1 treatment, FZD4, THBS4, EPDR1, ACTA2, CASP3 and APP showed a significant upregulation and MAFB was downregulated in contrast to the expression of this gene in tissue samples.

Expression of WNT Genes

WNT2 was expressed in patient and control samples. The observed expression was heterogeneous in patient and control samples and no clear tendency for patient samples could be seen by comparing patient and control samples. But samples could be grouped into three groups according to the relative expression of WNT2. Three patient and three control samples showed a medium expression level, while five patient and three control samples showed a lower expression level and seven patient samples expressed a higher level of WNT2 than the other samples. The mean fold change for these last samples was 1.98 ± 0.49 (P-value: 1.68×10^{-5}) compared to the first group and 5.25 ± 1.29 (P-value: 4.12×10^{-8}) compared to the second group. WNT4 and WNT7B were significantly upregulated in patient fibroblasts and WNT7B was upregulated in fibroblasts treated with TGFβ1 (fold change: 4.63 ± 1.76, P-value: 4.26×10^{-4}).

Expression of EPDR1 and SFRP4

Patients that were homozygous for the major allele (GG) of SNP rs16879765 showed a significant downregulation (P-value: 0.0006) of the EPDR1 mRNA in fibroblasts compared to controls (mean fold change: -1.78 ± 0.11). The group of patients that carried the minor allele (A) for this marker showed a heterogeneous expression of EPDR1 in fibroblasts. Out of nine patient samples analysed two showed an upregulation (mean fold change: 1.73 ± 0.008), three a downregulation (mean fold change: -2.16 ± 0.12) while four samples showed no difference in their expression of EPDR1 compared to controls.

The same expression pattern was observed for the SFRP4 gene. As before patient samples with the GG genotype for rs16879765 showed a downregulation of SFRP4 mRNA compared to controls (P-value: 0.005, fold change: -1.5, N = 6 patient samples and 6 controls) and out of the nine patients with the minor allele the same two showed an upregulation and the same three samples a downregulation of the SFRP4 mRNA, while four samples showed no difference in their expression of SFRP4 compared to controls. For the samples carrying the minor allele down or upregulation could not be attributed to either homo- or heterozygous genotype. In total 11 samples with the minor allele for rs16879765 were analysed for SFRP4 expression. Two showed an upregulation, four a downregulation larger than the GG samples and five samples showed no change compared with controls. Control samples were not genotyped for rs16879765.

3.4 Cell culture and Immunohistological Staining

3.4.1 Functional Assays: Collagen Matrix Contraction Assay

Collagen contraction assays were carried out using DD and control primary cell cultures taken from diseased and normal fascia. Primary cultures (passages 3–6) were grown as three-dimensional fibroblast populated collagen lattices. Collagen lattices were cast in 24-well tissue culture trays with each well containing 500µl collagen. Patient cultures detached themselves from the bottom and wall of the culture dish within the first days and progressively contracted the collagen gel over 13 days (figure 47 and 48).
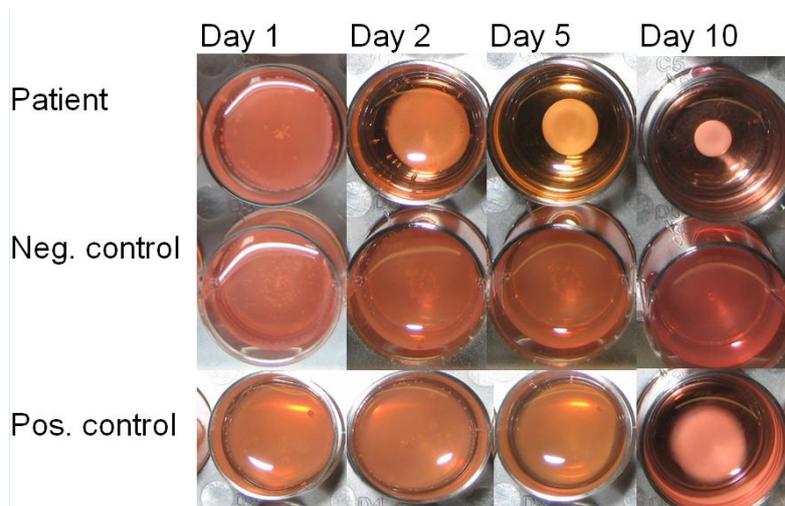
Figure 47. Contraction of fibroblast populated 3-dimensional collagen gels monitored over 10 days. Gel contraction for one patient cell line and one control (normal human fibroblasts) is shown. Patient cells rapidly contract the collagen gel visibly already at day two. The former attached gel detaches itself from the well wall within 24 hours. Control gels detach only after several days, while gels without cells (neg. control) do not contract.
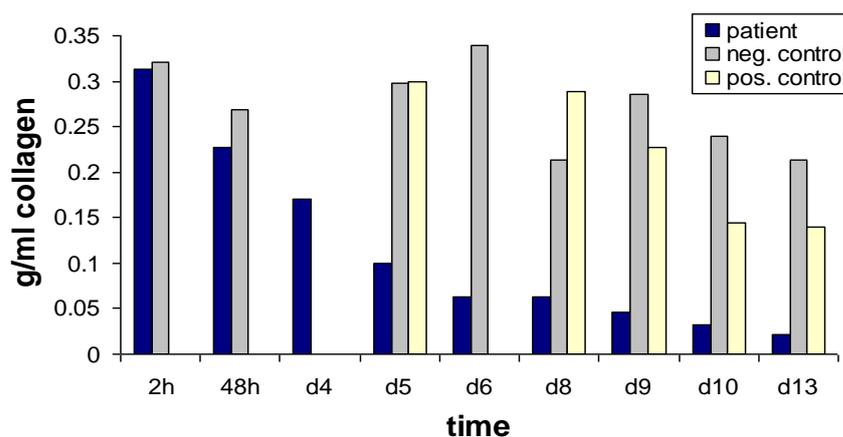
Figure 48. When the collagen gel contracts, water is excluded from the gel, making it lighter. The reduction in weight correlates to the amount of contraction. The weight of patient and control fibroblast populated gels was recorded over time and compared to the weight of empty gels.

3.4.2 Functional Assays: Oxidative Stress Enzyme Function

Whole genome expression analysis and qPCR revealed differences in catalase mRNA expression in disease and control tissue samples while no significant change in catalase mRNA levels was seen in cultured patient and control fibroblasts. To access enzyme activity in cultured fibroblast a catalase activity assay was preformed. Patient and control tissue derived fibroblasts were cultivated under described cell culture conditions at 37°C and 40.5°C. Cell homogenates of approximately 25,000 cells per sample were analysed in this assay. Within each run a standard curve was generated from known catalase concentrations (figure 49).
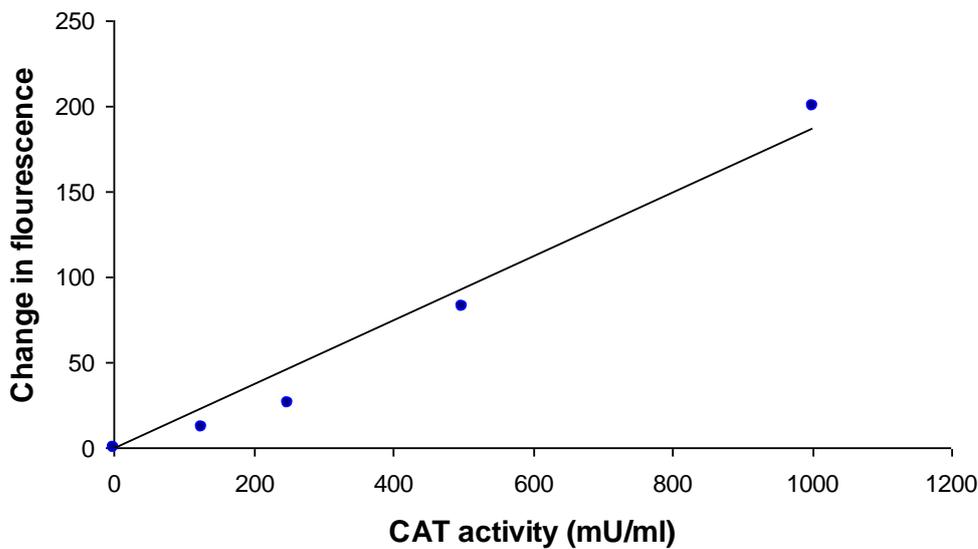
Figure 49. Catalase activity standard curve. Change in fluorescence is reported as observed fluorescence intensity subtracted from that of a non-catalase control. $r^2 = 0.96$.

The samples analysed for catalase activity separated into three distinct groups: Samples in group 1 showed the lowest catalase activity at 37°C (group 1 in figure 50). For these samples catalase activity remained also low at 40.5°C (group 1 in figure 51). Group 2 contained samples with medium catalase activity at 37°C (figure 50, group 2) and high catalase activity at 40.5°C (figure 51, group 2). Group 3 consisted of samples with high catalase activity both at 37°C and 40.5°C (group 3 (patients) and 4 (controls) in figure 50 and 51). Group 1 consisted of patients only. Group 2 consisted of three patients and two controls.
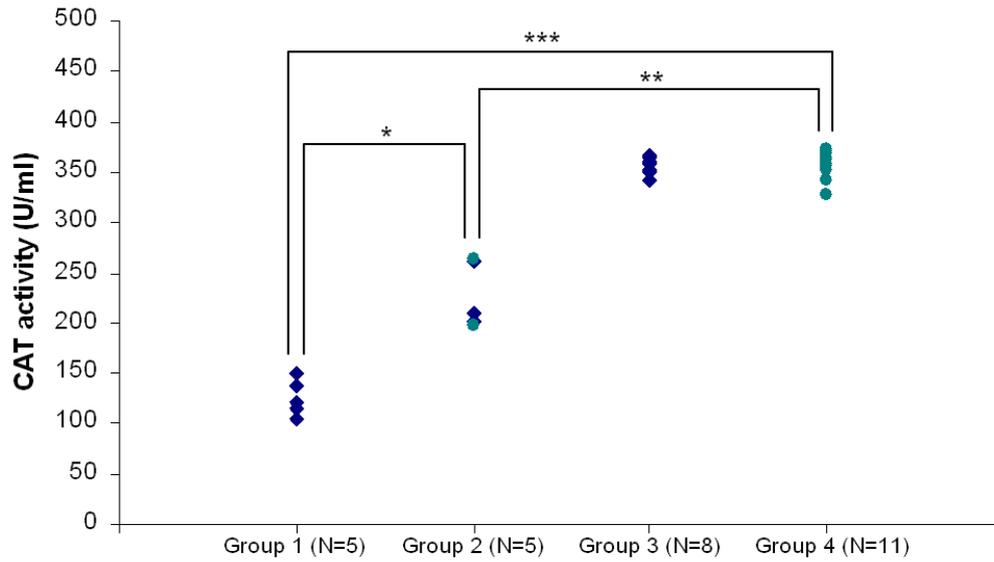
Figure 50. Catalase activity in patient and control fibroblasts cultivated at 37°C. Patient samples are depicted as blue diamonds, controls as green circles. P-value of two-tailed student's t-test: * 0.0003, ** 1.6E-08, * 9.4E-14.**
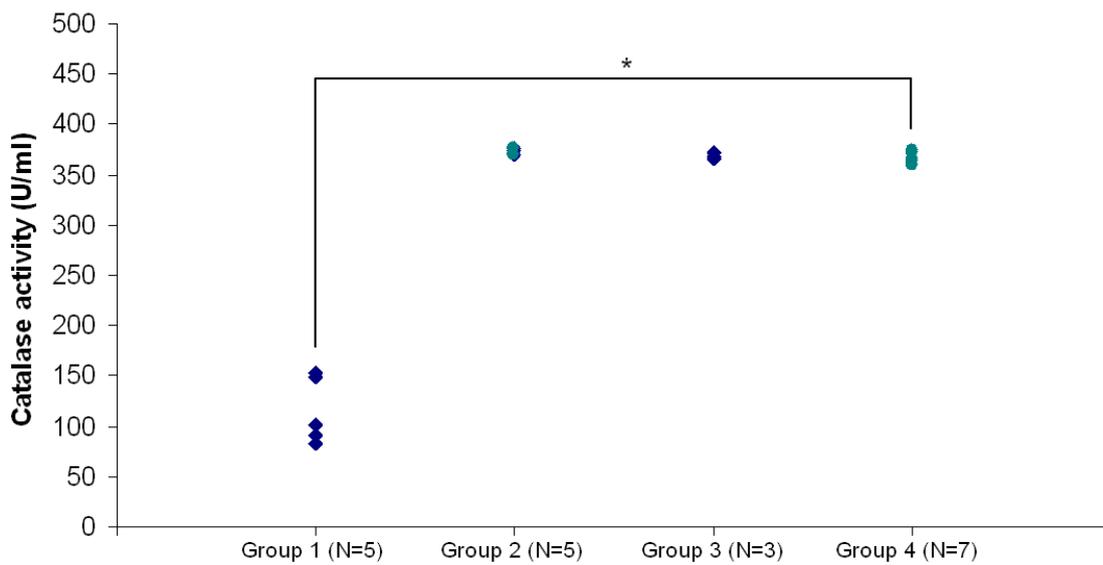
Figure 51. Catalase activity in patient and control fibroblasts cultivated at 40.5°C for 3 days. Patient samples are depicted as blue diamonds, controls as green circles. * P-value of two-tailed student's t-test: 2.6E-11.

Catalase activity was inversely correlated to the measured cell concentrations in the original samples before normalisation (figure 28, r^2 = 0.76) and positively correlated to the time interval between planting of cells and harvesting (r^2 = 0.77).
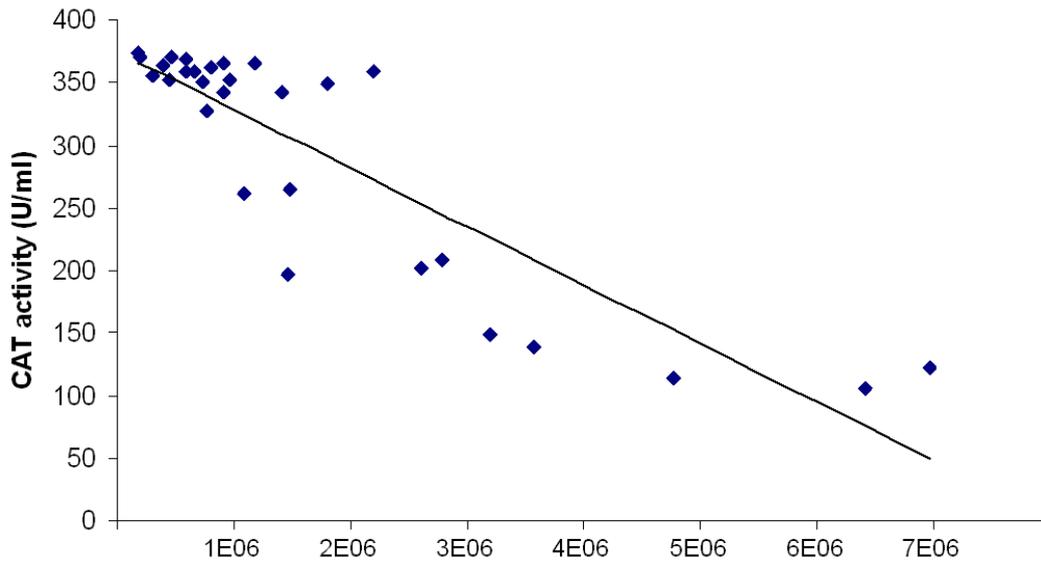
Figure 52. Catalase activity negatively correlated to cell numbers counted in the samples before normalisation.

3.4.3 Functional Assays: RNA interference

GWAS and whole genome expression experiments identified the Wnt/β-catenin signalling pathway to be potentially involved in DD pathology. One question was therefore whether Wnt could promote myofibroblast differentiation. The expression of αSMA as a marker for myofibroblast differentiation was measured in cells treated with Wnt. Patient cells were seeded onto collagen gels at day one in reduced serum medium (OptiMEM) and treated on day two with either Wnt3a (50ng/ml) or BIO (1μM). On day five cells were harvested, the RNA extracted and submitted to qPCR. Cells treated with Wnt3a showed a 2.5 fold upregulation of αSMA mRNA as determined by qPCR (figure 53) that was evident after 48 hours. Contrary cells treated with BIO, a GSK3β inhibitor, showed a 2.7 fold downregulation of αSMA expression after 48 hours.
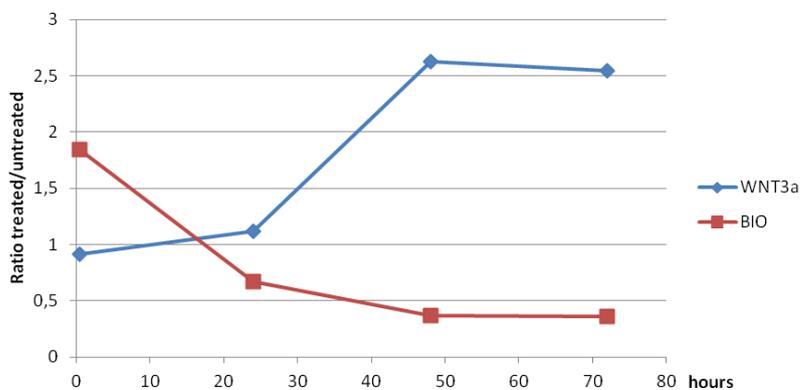
Figure 53. Expression of αSMA in patient cells either treated with 50ng/ml Wnt3a or 1μM BIO (GSK3β inhibitor). Expression was determined by relative quantification (qPCR), 0.5, 24, 48 and 72 hours after treatment.
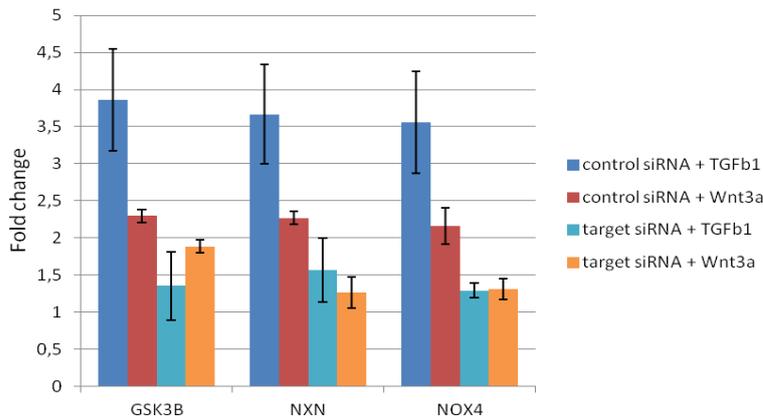
Figure 54. Relative αSMA expression in patient cells. 3 hours after addition of either control or target siRNA (GSK3β, NXN or NOX4) cells were treated with 2ng/ml TGFβ1 or 50ng/ml Wnt3a.

Similarly downregulation of GSK3β by RNAi resulted in downregulation of αSMA in cells treated with either TGFβ1 (2ng/ml) or Wnt3a (50ng/ml) (figure 55). RNAi mediated downregulation of nucleoredoxin, an inhibitor of Wnt/β-catenin signalling that interacts with dishevelled, likewise attenuated the upregulation of αSMA in cells treated with TGFβ1 or Wnt3a (figure 54). RNAi mediated downregulation of a third gene, NADPH oxidase 4 (NOX4) also prevented the upregulation of αSMA upon TGFβ1 or Wnt3a treatment (figure 54). NOX4 gene product is involved in mediating oxidative stress. RNAi experiments were done for two patients each. Further experiments with more patient and control cells are necessary to confirm these initial findings. Figure 55 shows the expression of GSK3β, NXN and NOX4 in tissue and cells.
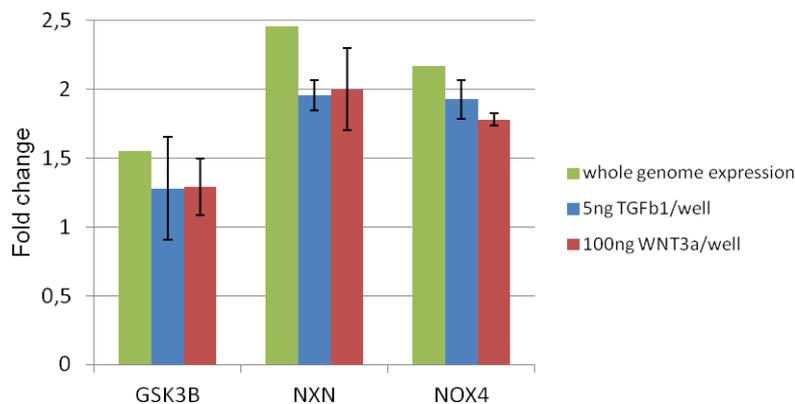
Figure 55. Relative expression of GSK3β, NXN and NOX4 in primary patient tissue compared to control tissue (whole genome expression) and in patient cells either treated with 2ng/ml TGFβ1 or 50ng/ml Wnt3a. Fold changes observed in treated cells are similar to those observed in the whole genome expression analysis.

3.4.4 Immunohistological Staining of Primary Tissue and Fibroblasts

Disease and control primary tissue was fixed in formalin, paraffin embedded, sectioned and HE stained. Disease tissue was rich in collagen fibres as evident from the red staining (figure 56). Disease tissue is characterised by cell rich (figure 56A) and cell poor (figure 56B) areas that alternate (figure 56C). Cell rich areas resemble nodules that contain high amounts of proliferating fibroblasts and fewer amounts of collagen fibres than the cell poor cord structures. The DD tissue is interspersed with blood vessels (figure 56, arrow). In comparison control fascia tissue is nearly devoid of cells and collagen fibres (figure 57).
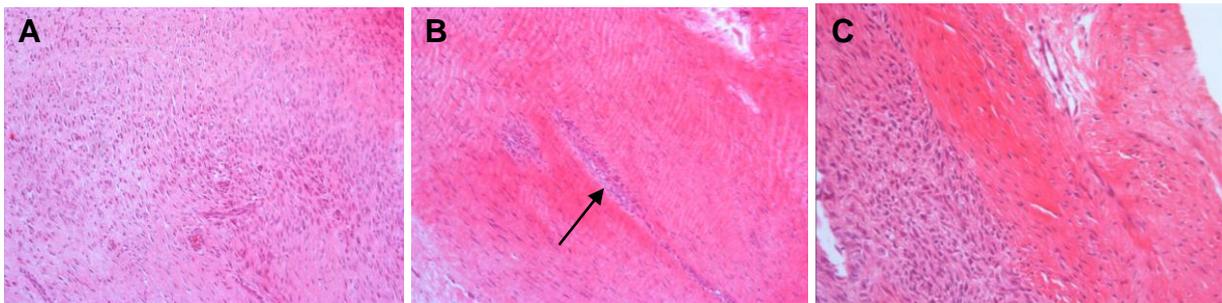
Figure 56. HE staining of DD tissue. The collagen (red staining) rich tissue consists of cell rich (A and C (blue stained nucleus)), and cell poor (B and C) areas. The arrow indicates a blood vessel longitudinally sectioned. 10 x magnification.
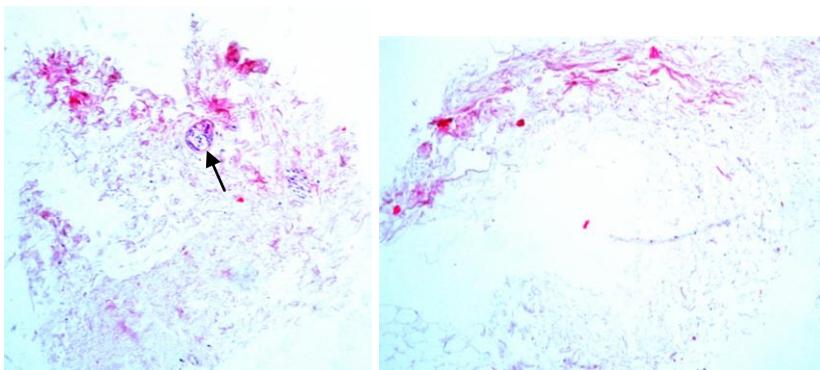
Figure 57. HE stainings of two control fascia samples from the palm. The tissue contains only few cells (nucleus stained in blue), few collagen fibres (red), and few small blood vessels (left picture, arrow). 10 x magnification.

Immunohistological staining of disease and control tissue for collagen IV revealed that control tissue predominantly consists of fat cells (figure 58B). Fat cells are also found around disease tissue (figure 58A). The cell and collagen rich areas that characterise disease tissue stained positive for collagen IV (figure 58A and B).
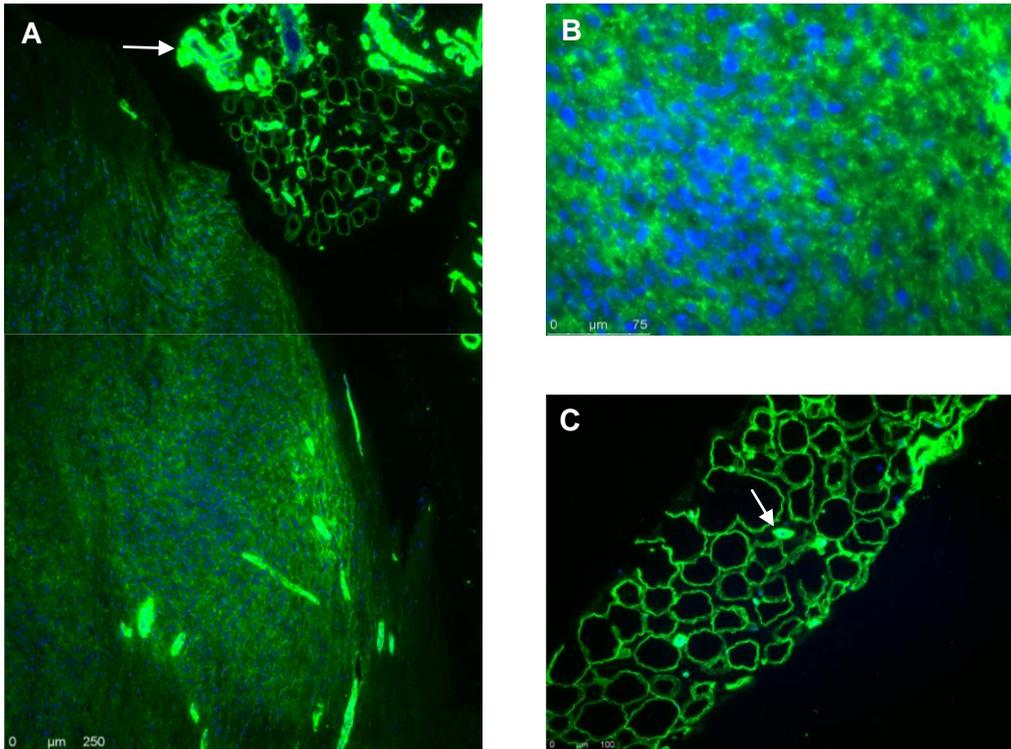
Figure 58. Depicted are disease (A and B) and control (C) tissue samples immunohistochemically stained for collagen 4 (green staining) and DAPI (blue staining of the nuclei). Highlighted are the basallamina in blood vessels (strong green staining, arrows), the outlining of fat cells (A (upper righthand corner) and C) and the collagen rich disease tissue (A and B only). A: 10x, B: 40x, C: 20x magnification.

Disease and control tissue samples were immunohistochemically stained for the presence of alpha smooth muscle actin (αSMA), a marker for myofibroblasts and also for vascular smooth muscle cells (VSMCs) that reside in the walls of blood vessels. Figure 59 shows the αSMA staining of control tissue. Only small blood vessels (figure 32C) within the tissue stain positive for αSMA. Figure 60 shows αSMA staining in primary disease tissue. αSMA is extensively present in the cell rich areas of the disease tissue.
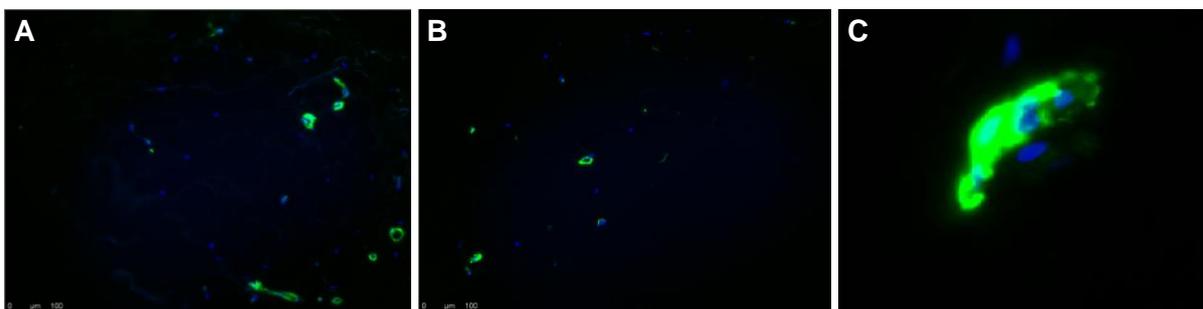
Figure 59. Immunohistochemical staining of control fascia tissue. A, B and C: αSMA staining (green) and DAPI (blue): vascular smooth muscle cells in small blood vessels are stained positive for αSMA. A and B: 20x magnification. C: ~40x magnification of a small blood vessel.
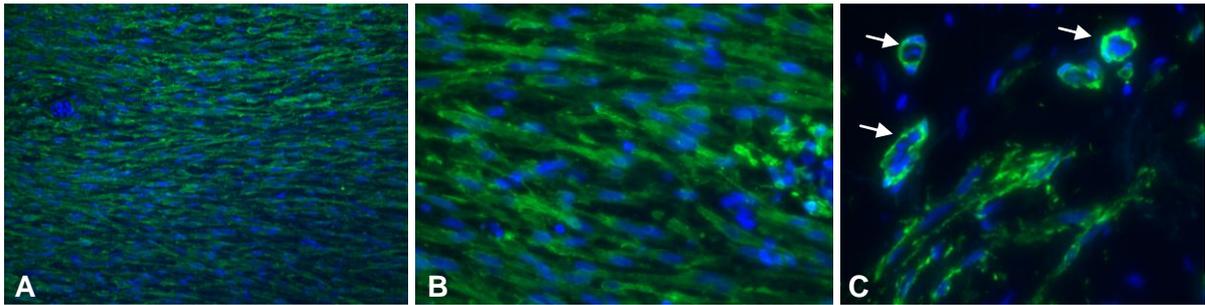
Figure 60. Immunohistochemical staining of disease tissue for αSMA (green) and DAPI (blue). Stained in green are myofibroblasts that constitute the disease tissue. Arrows in C indicate blood vessels that also stain positive for αSMA. A: 20x, B and C: 40x magnification.

Alpha Smooth Muscle Actin Staining in Fibroblasts

Patient and control fibroblasts were grown on different substrates (glass, poly-L-lysis, fibronectin and collagen) in the presence of TGFβ1 (2ng/ml) for three days. Cells were then immunohitochemically stained for αSMA. Both patient and control cells formed stress fibres upon TGFβ1 treatment. These are parallel sheets of actin fibres within the cytoskeleton of the cell (stained in red in figure 61, 62 and 63). Some cells additionally expressed αSMA (green staining). Both control and disease fibroblasts showed positive αSMA staining. The amount of αSMA varied within patient and control samples. While some patient cell lines exhibited relatively many αSMA positive cells (figure 62A) others had few αSMA positive cells (figure 61C).
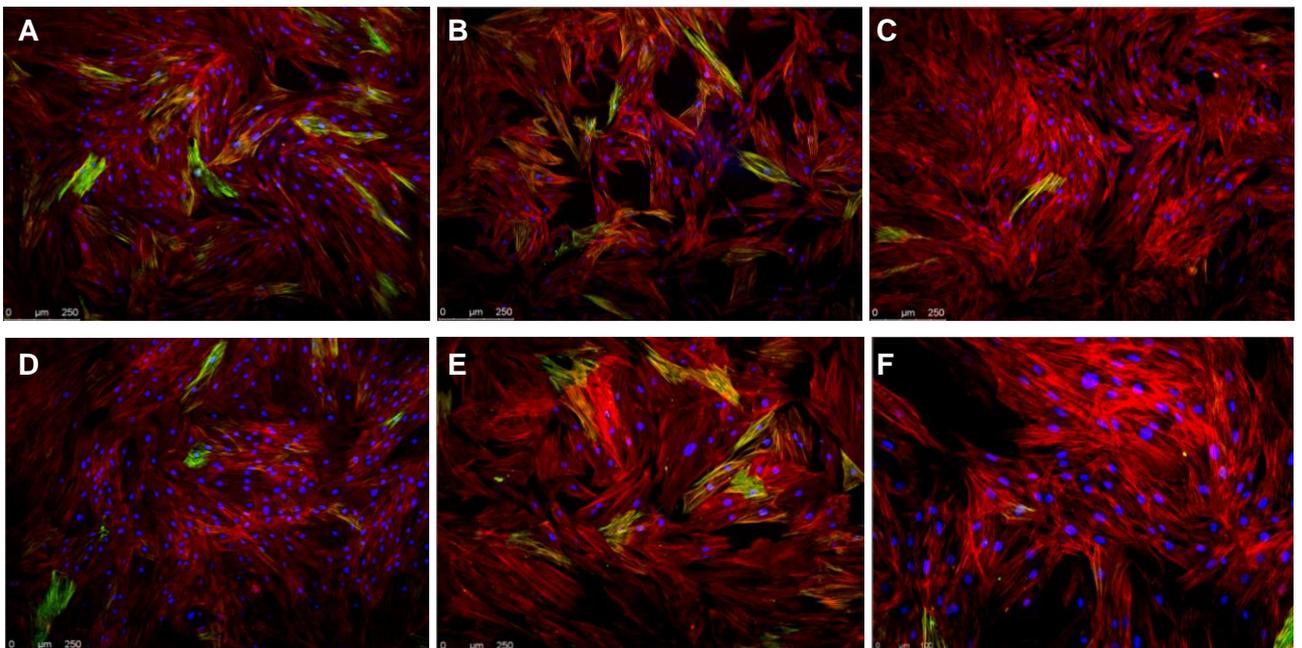
Figure 61. Immunohistochemical staining of primary fibroblast grown on <u>fibronectin</u> in the presents of TGFβ1 (2ng/ml) for three days. A-C: fibroblast derived from DD tissue (3 different patients), D-F: fibroblasts derived from healthy fascia of three controls. The nucleus is stained in blue (DAPI), the actin cytoskeleton is stained in red (Phalloidin) and αSMA is stained in green. A-D 10x, E and F 20x magnification.
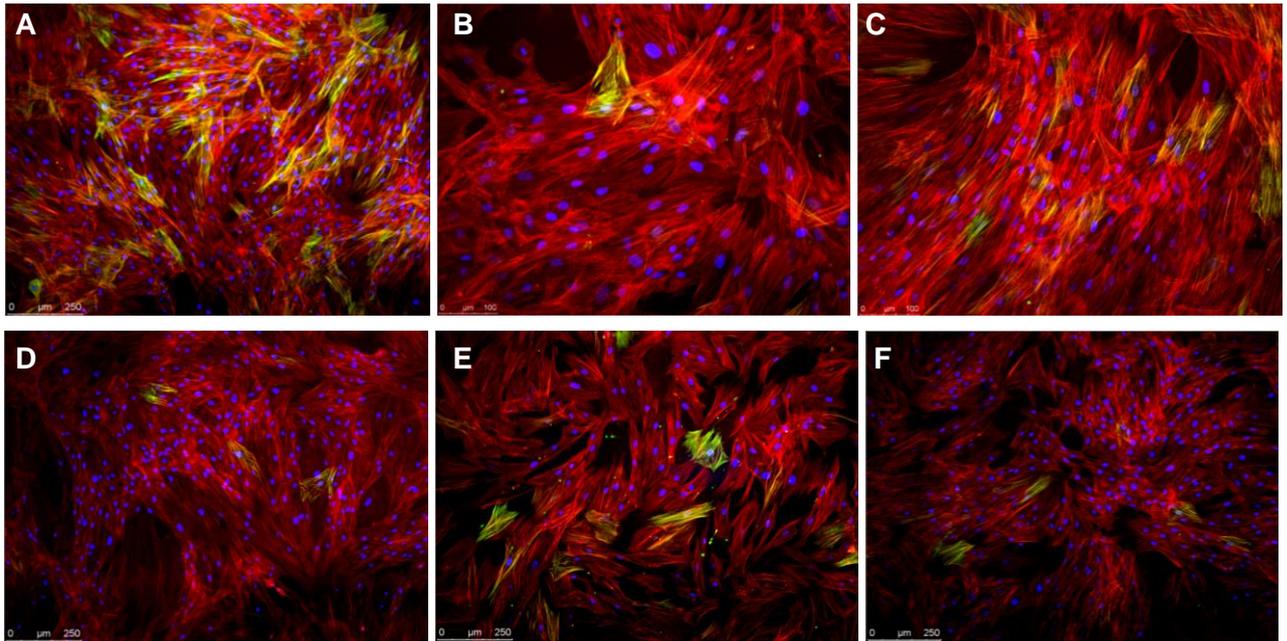
Figure 62. Immunohistochemical staining of primary fibroblast grown on <u>collagen</u> in the presents of TGFβ1 (2ng/ml) for three days. A-C: fibroblast derived from DD tissue (3 different patients), D-F: fibroblasts derived from healthy fascia of three controls. The nucleus is stained in blue (DAPI), the actin cytoskeleton is stained in red (Phalloidin) and αSMA is stained in green. A, D-F 10x, B and C 20x magnification.

Controls generally had few αSMA positive cells regardless of used substrates. Patient cells grown on collagen showed a trend towards more stress fibres and αSMA positive cells.
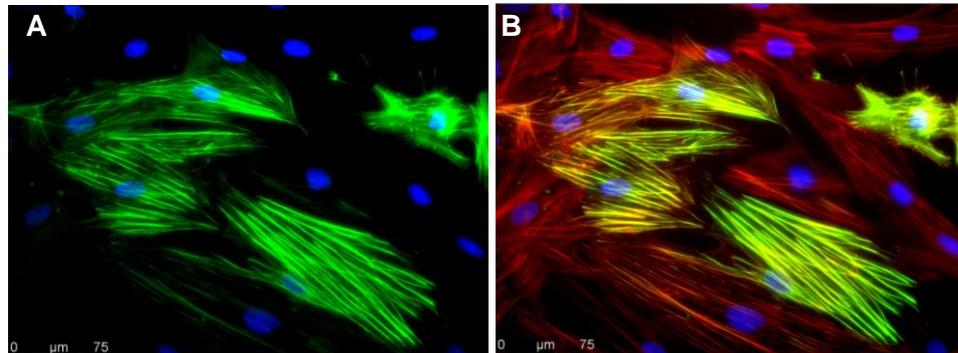
Figure 63. Immunohistochemical staining of primary disease fibroblasts grown on fibronectin. A: overlay DAPI (blue) and αSMA staining (green); B: overlay DAPI (blue), αSMA staining (green) and phallodin (red) staining. 40x magnification.

4 Discussion

4.1 Epidemiology

A questionnaire based survey of known risk factors and other parameters was conducted in order to characterise DD patients epidemiologically. This characterisation is desirable for the planning and interpretation of genetic and expression profile analyses. The survey itself can also give insights into the mechanisms that lead to DD. The questionnaire was completed by the attending physicians to ensure medical accuracy.

4.1.1 Heredity

Approximately 38.2% of patients reported a positive family history for DD, with one or more affected family members. In comparable studies observed family predisposition rates were conspicuously lower. These studies determined a family predisposition in 28% (Hakstian 1966), 27% (Coert *et al* 2006), 26% (Mäkelä *et al*. 1991), 14.8% (in men) (Early 1962), and 12.5% (Brenner *et al* 2001) of cases. In the present study patients were not selected for a family predisposition. However it is possible that patients with positive family history more readily agree to participate in a study investigating the genetic causes of this disease. Regional differences may also explain differences in family predisposition rates (see below).

It is possible that the overall rate of family predisposition noted in this study slightly underestimates the actual rate in German DD patients. Especially older patients may not have been able to indicate whether their parents or grandparents were affected by DD because those may not have presented at a clinic themselves. Within all investigated risk factors a family predisposition for DD had the largest impact on the mean age at first surgery. Patients were around five years younger, when they had affected family members. Coert *et al*. (2006) investigated the same parameter and found no difference in mean age in which patients were operated between those with and without family predisposition. This is maybe due to the smaller effective size (N = 261) in their study.

Additionally 3.3% of DD patients had affected family members in both of their parental lines. These patients were about 13 years younger than patients without positive family history when they underwent first surgery. This significant age differences could hint on additive genetic effects that lead to a stronger disease phenotype in these patients.

The rate of a family predisposition was highest in the younger patients and declined with age. This supports the observation that patients with a family predisposition are affected

earlier by the disease. On the other hand older patients are less likely to be able to indicate possibly affected family members due to the death of older relatives (e.g. parents).

The male-female ratio was highest in 40-49 year old patients, underlining that men are affected earlier. It was often reported that the observed male-female ratio is due to the later age of onset in female DD patients and that the ratio equals one for very old patients (Brenner *et al*. 2001). In this study more men than women underwent surgery for DD in all sampled age classes (decades of live). This was still true for 80-89 years old patients. The same tendency was noted by Loss *et al*. (2007).

4.1.2 Diabetes Mellitus

The mean age at the time of first surgery for Diabetes patients was significantly different in all patients and those with a familial predisposition for DD. Diabetes patients were three to four years older than non-diabetic patients when they first underwent surgery for DD. This tendency was also true for women and men separately. Diabetes mellitus itself is an ageing associated disease. It is therefore impossible to say whether the observed age differences are due to a described "milder phenotype" in diabetic DD patients or if the observed correlation with age is independent in both diseases. One could test for this e.g. by comparing the frequency of diabetes in DD patients to that of a collective of age matched controls.

4.1.3 Other Risk Factors (Smoking, Alcoholism, Epilepsy)

Smokers were on average slightly younger at the time of first surgery than non-smokers. This age difference was just not significant for all patients and patients without a familial predisposition for DD. In patients without familial predisposition the amount of consumed cigarettes per day did not correlate with the mean age at first surgery, while in men with familial predisposition there was an ~7 year difference in the mean age at first surgery for heavy smoker, who consumed more than twenty cigarettes per day and smokers who consumed less than five cigarettes per day (difference not significant). Heavy smoking may be a risk factor in DD. A larger sample collective would be desirable in order to test for this hypothesis. Loos *et al*. (2007) found no statistical correlation between heavy smoking (>20 cigarettes per day) and mean stage of disease after Iselin's classification. Brenner *et al*. (2001) noted a higher percentage of bilateral affected patients among heavy smokers compared to patients who consumed less than twenty cigarettes per day. In cohort or epidemiological case control studies a significant correlation between heavy smoking and the occurrence of DD was seen in the majority of studies e.g. An *et al*. (1988), Burge *et al*. (1997), Gudmundsson *et al*. (2000), Godtfredsen *et al*. (2004), and Burke *et al*. (2007) but

not seen in e.g. Zerajic and Finsen (2004). It could be advisable to subdivide patients into those with and without familiar predisposition when accessing the prevalence of heavy smoking or other suggestive risk factors in DD patients and correct for familial cases in cohort studies, respectively because family predisposition may be a strong risk factor for DD.

No correlation was seen between alcoholism and DD in this study. Only 0.9% of patients took antiepileptic drugs. Loos *et al*. (2007) and Brenner *et al*. (2001) both found 1.3% epilepsy patients in their respective patient collectives (2919 and 566 patients, respectively) and Coert *et al*. (2006) noted 1.9% epilepsy patients in a collective of 261 operated patients.

4.1.4 Occupational Exposure

Notable the prevalence of a family predisposition for DD was ≥50% in office workers, teachers and salesclerks. The family predisposition rate in manual workers was overall lower but for some profession groups it was still in the range or above the overall prevalence rate of 38.2%. It is possible that participants (and their physicians) who stated profession and hobby were in general more thoroughly when completing the questionnaire. This would explain the higher rate of family predisposition in all "workers", 40.5% (N = 454) compared to 35.1% (N = 348) in "non-workers" (participants with unknown profession). Still the higher frequency of familiar cases in office workers could hint indirectly that manual work or certain types of manual work are a risk factor for DD, so that the inherited form of DD is more prevalent in non-manual workers. Overall manual workers had a slightly lower mean age at first surgery than office clerks, teachers and salesclerks. Interestingly drivers had the lowest mean age at first surgery and the highest mean degree after Tubiana. Professional driving is not readily associated with heavy manual work but it is associated with e.g. hand-arm vibration syndrome (Åström *et al*. 2006). The eleven participants in this category were six truck drivers, two dredge drivers, one garbage truck driver, one crane driver and one driving instructor. Effective size was small in this category and results could be due to chance but they fit in with a recent publication by Descatha *et al*. (2011). The authors conducted a literature based meta-analysis on occupational exposure and DD and found that profession title alone was a poor parameter to access the association of manual work and DD. They found that studies investigating the duration and intensity of exposure to manual work and vibrations found positive associations between manual work and DD. Based on these findings the authors concluded that there is an association between DD and heavy manual labour and/or vibrations. Repetitive hand trauma and vibrations lead to nerve

disorders and fractures in the hands of race drivers (Masmejean *et al.* 1999, Mansfield and Marshall 2001). It is therefore important to inquire duration of manual work and exposure to vibrations including hobby and e.g. driving to place of work, when accessing occupational exposure in DD.

Age at first surgery is dependent on individual patients' needs and disease progression. Patients who's profession involves regular contact to customers e.g. salesclerks, will potentially present earlier for surgery than employees without customer contact e.g. laboratory technicians or pensioners. This could explain why carpenters had the highest mean age at first surgery compared to all other manual and non-manual workers. Disease progression can vary considerably from slow, surgery is not considered till late in life or not at all - to aggressively fast, surgery is required soon after first evidence of nodules. It therefore would be more adequate to compare the age of occurrence of the disease between different patient subgroups to access differences for professions and life styles. On the other hand stating the year of occurrence may be difficult for some DD patients because they may present at a clinic long time after first occurrence.

4.1.5 Inter-Centre Variance

The rate of family predisposition for DD varied between centres as did other parameters e.g. the prevalence of hypertension. The highest rate of a family predisposition between centres (and the lowest mean age of first surgery) had the group of patients that were recruited via the Dupuytren e.V. support community. These patients more actively participated in the study. They contacted the CCG via e-mail or telephone, got the material for blood collection and the questionnaire per post and went to their attending doctor, who took the blood sample. The sample was then sent back to the CCG by post. One can assume that patients who are not only affected themselves but are additionally confronted with DD in their family are more interested in this disease and its cause and are therefore more likely member of a support community and more willing to participate in studies investigating the genetic cause of DD. This centre, with only 71.7% patients with surgery for DD, has therefore to be treated somewhat separately when evaluating inter-centre variance. Sample collection in the other centres was not biased towards familiar cases. Nevertheless percentage of family predisposition ranged from 23.5% to 45.4% between different clinics. These differences could either be a function of regional differences e.g. one could hypothesise that there are more manual workers in rural vs. urban regions. Heavy manual work is a risk factor for DD and may account for a higher percentage of DD cases without family predisposition in rural

regions. Supporting this hypothesis there were 17.6% office worker among the patients from two centres from the north-east compared to 38.6% office workers in one centre in the south-west and e.g. 9.3% and 4.5% builders, respectively. Another possible explanation for the observed bias is the variability in persons who completed the questionnaire with the patients. Often more than one physician took the samples in each clinic. Dependent on work load they can be assumed to be more or less thoroughly in questioning the participant. A hint that observed differences may be at least partly due to regional differences is the prevalence of hypertension in DD patients from different centres. Interestingly the highest rates of hypertension ($\geq$ 50%) were found in the three clinics located in the east of Germany. Supporting that Meisinger *et al.* (2006) reported a 20% difference in the frequency of hypertension in a population in located in the north-east compared to one in the south-west of Germany.

4.1.6 Age at Menopause in Women

The mean age of natural menopause in women is generally given in the literature as 50 years of age (e.g. Shuster *et al.* 2010). Menopause between the ages 40-45 years is termed "early menopause" and "premature menopause" describes menopausal onset before the age of 40 years (Shuster *et al.* 2010). The mean age of menopause in this study was 48.2 years, marginally below the general mean. Jacobsen *et al.* (2002) analysed the relationship of menopausal onset and mortality rate in 19,731 Norwegian women and found a mean age at natural menopause of 48.4 years in women born in cohorts 1886 to 1926. The mean age of menopause in this study can therefore be considered to be normal. In the Norwegian survey 2.8% of women had natural menopause before the age of 40, and 1.6% stated natural menopause after the age of 55 years. Interestingly in this study 5.4% of women experienced natural menopausal onset before the age of 40, and 7.1% reported natural menopause after the age of 55 years while 21.4% were 50 years of age at menopausal onset. This may suggest a non normal distribution of menopausal age in women with DD. It would be of interest to investigate in a larger effective size whether these results are due to chance or not. A connection between menopausal onset and DD may point to the importance of aging associated factors in the pathogenesis of DD.

4.2   Genetic Association

Of all analysed risk factors, a genetic predisposition had the largest negative impact on the age of first surgery in DD patients. Genetic factors can be considered one of the major risk factors for DD. Accordingly the GWAS revealed several loci associated with DD. A study

combining the data sets from Germany, the Netherlands and UK identified nine loci for which association was significant on a genome wide level (Dolmans *et al.* 2011). They analysed the data from 2325 DD patients and 11,562 controls and found the following SNPs to be associated with DD with P-values (P) below 5.0×10^{-8}: rs16879765 (P = 5.6×10^{-39}; OR: 1.98) on 7p14.1, rs6519955 (P = 3.2×10^{-33}; OR: 1.54) and rs8140558 (P = 1.2×10^{-22}; OR: 1.39) on 22q13, and rs11672517 (P = 6.8×10^{-14}; rs2912522 (P = 2.0×10^{-13}; OR: 0.72) on 8q13 and rs8124695 ((P = 7.6×10^{-10}; OR: 1.48) on 20q11.2–q13.1, rs611744 (P = 7.9×10^{-15}; OR: 0.75) on 8q23.1, rs10809650 (P = 6.2×10^{-9}; OR: 0.80) and rs10809642 (P = 1.2×10^{-8}; OR: 1.35) on 9p24.3, and rs7524102 (P = 2.8×10^{-9}; OR: 1.28) on 1p36.23–p35.1.

Six of these nine loci contain genes involved in the Wnt/β-catenin signalling pathway: WNT4 (rs7524102) (P = 2.8×10^{-9}; OR: 1.28), SFRP4 (rs16879765) (P = 5.6×10^{-39}; OR: 1.98), WNT2 (rs4730775) (P = 3.0×10^{-8}; OR: 0.83), RSPO2 (rs611744) (P = 7.9×10^{-15}; OR: 0.75), SULF1 (rs2912522) (P = 2.0×10^{-13}; OR: 0.72), and WNT7B (rs6519955) (P = 3.2×10^{-33}; OR: 1.54). Together with the findings from the whole expression analysis (see below) this indicates that the Wnt/β-catenin pathway plays an important role in both the aetiology and the pathogenesis of DD. As described in the introduction the Wnt/β-catenin pathway is susceptible for aging associated changes (Marchand *et al.* 2011, Brack *et al.* 2007, Liu *et al.* 2007).

All six genes encode for proteins that function extracellulary by being either Wnt ligands (WNT2, WNT4 and WNT7B) or proteins that inhibit (SFRP4) or stimulate (RSPO2 and SULF1) Wnt signalling by interacting with Wnts, their receptors or other Wnt-signalling components in the ECM and the plasma membrane. Another locus associated with DD, although not on a genome wide level, rs237018 on 6q25.1 (P = 1.7×10^{-5}, OR: 0.86) contains the gene TAB2 (MAP3K7IP2) which is an activator of MAP3K7 and also involved in Wnt signalling (Dolmans *et al.* 2011).

Although the initial GWAS in the present study was quiet small, comparing only 186 DD samples with 1618 controls, it identified the strongest associated SNP rs16879765 on 7p14.1 that was replicated in the joint analysis (Dolman *et al.* 2011). Three other SNPs (out of four) showed a suggestive association in the verification analysis with SNPstream and 465 DD samples: rs10759289 on chromosome 9q31.2 (P-value: 0.003, OR: 1.26), and rs8052047 on chromosome 16q23.2 (P-value: 0.04, OR: 1.48, gene of interest: MAF) and rs11216674 on 11q23.3 (in cases with genetic predisposition only: P-value: 0.08, OR: 0.63).

379 cases and 1.219 controls were then genotyped with the Affymetrix Axiom platform. This data set was imputed together with the 186 cases genotyped with Affymetrix 6.0. The imputed data set considered 565 patients and 1219 controls analysed for 5 million SNPs. Again the strongest association signal was seen for the locus on chromosome 7p14.1 (SNP rs2290221, p-value of $2.2x10^{-10}$, odds ratio 2.13). This analysis also identified additional hits that need to be verified in subsequent experiments because some of the SNPs showing suggestive association were imputed. These need to be genotyped in cases and controls to confirm the association signal seen in the data.

No disease causing mutations have been identified so far and further efforts are required to unravel the genetic changes that underlie the genetic cause of DD. Several genes involved in Wnt signalling locate to different chromosomal regions associated with DD. Wnt signalling plays an important role during development and is also involved in many processes in the adult organism (see introduction). The genetic changes leading to DD apparently have no negative effects on early life. They are therefore rather not expected to abolish gene function completely, but may affect gene function in the context of aging associated changes in e.g. oxidative stress, tissue composition and immune response.

Differences in the gene expression patterns between carriers of the minor and major allele of rs16879765 on chromosome 7p14.1 were seen. While patients homozygous for the major allele showed downregulation of SFRP4 (and EPDR1) in disease derived fibroblasts, patients with the minor allele were heterogeneous in their expression of these genes. 11 samples with the minor allele for rs16879765 were analysed for SFRP4 expression. Two showed an upregulation, four a downregulation and five samples showed no change in SFRP4 expression compared to controls. SFRP4 has an inhibitory effect on Wnt/β-catenin signalling. Its expression is expected to be tightly regulated. Both over and under expression of SFRP4 may favour DD. In order to replicate observed differences, this expression analysis should be repeated in a larger sample set. In contrast to the downregulation of SFRP4 in fibroblasts from carriers of the major allele for rs16879765, SFRP4 was upregulated in primary tissue. Further analyses are required to investigate the relationship of genetic association and gene expression for this and other loci both in primary tissue samples and disease derived cells.

4.3   Expression and Function

A whole genome expression analysis was preformed comparing the expression profiles of 12 disease tissue samples with 12 matched controls. Most genes already identified in earlier whole genome expression analyses (Pan *et al*. 2002, Rehman *et al*. 2008, Satish *et al*. 2008, Zang *et al*. 2008), were also identified in this study, either the same gene other members of the same gene family were found to be deregulated in DD. A large number of additional genes not previously described were also identified. Given the large number of deregulated genes only some shall be discussed in the following. This discussion is divided into four paragraphs, (1) extra-cellular matrix components; (2) Wnt/β-catenin signalling pathway components; (3) genes involved in oxidative stress and mitochondrial dysfunction and (4) other deregulated genes (e.g. immune response). Genes involved in more than one of these processes are discussed only in one section, if appropriate.

4.3.1 Extra-Cellular Matrix Proteins overexpressed in DD

A number of extracellular matrix components were found to be highly upregulated in DD reflecting the high amount of extracellular matrix (ECM) found in the disease tissue. They function for example in matrix scaffolding, cell-matrix interaction, cell-cell signalling, cell migration and cell adhesion. Similar to processes involved in wound healing, fibroblasts in DD tissue heavily remodel the ECM including the deposition of collagens and other matrix proteins. The ECM not only provides a structural network but also facilitates migration of cells and cell signalling. ECM components therefore play important roles in the pathology of DD but it is not known whether they have any causative effect on its aetiology. Some examples for markedly upregulated ECM components are given in the following.

THBS4 was upregulated with a fold change of 52.07 and THBS2 was upregulated with a fold change of 7.16. Thrombospondins (THBS 1-5 gene products) are tri- or tetra-meric extracellular matrix glycoproteins (Adams *et al*. 2003). Each monomer contains at the cystin-rich c-terminus epidermal growth factor (EGF) - like modules, calcium-binding repeats, and a lectin-like C-terminal globe. THBS2 and 4 proteins (TSP2 and 4) differ in their module structure, calcium binding properties and inter-modular interactions (Misenheimer *et al*. 2005). THBSP4 is expressed by muscle interstitial cells and neurons, promotes neurite outgrowth, and accumulates at the neuromuscular junction (Arber and Caroni 1995). High levels of THBS4 mRNA have been detected in heart and skeletal muscles (Lawler *et al*. 1993), and human endothelial cells and vascular smooth muscle cells from brain blood vessels and coronary arteries have been shown to express THBS4 mRNA

(Stenina *et al*. 2003). The c-terminal domain of TSP4 binds to collagens I, II, III, and V as well as laminin-1, fibronectin, and matrilin-2 (Narouz-Ott *et al*. 2000). THBS4 is overexpressed in muscular dystrophies (Chen *et al*. 2000) and an A387P single nucleotide polymorphism of THBS4 was linked to susceptibility to myocardial infarction (Topol *et al*. 2001, Wessel *et al*. 2004) especially in older women (Cui *et al*. 2004), which could not be confirmed in a large case-control study (Koch *et al*. 2008). A polymorphism in the 3' untranslated region of THBS2 (rs8089) was likewise not confirmed to be associated with myocardial infarction in the meta-analysis of this study.

THBS2 protein (TSP2) binds LRP1 (low density lipoprotein receptor-related protein-1) which interacts with Notch3 and Jagged1 and also functions in Wnt signalling. TSP2 and LRP1 stimulate Notch activity by driving trans-endocytosis of the Notch ectodomain into the signal-sending cell (Meng *et al*. 2010). LRP1 was found to be downregulated (fold change: -1.54) in the present study.

TSP1 and -2 are similar in their structure (Misenheimer *et al*. 2005). They inhibit cell proliferation in endothelial cells (Jiménez *et al*. 2000, Nör *et al*. 2000). However, while TSP1 induces cell growth arrest through caspase activation and subsequent apoptosis, TSP2 proliferation inhibition does not involve induction of apoptosis (Armstrong *et al*. 2002). They also differ in their transcriptional regulation. The production of reactive oxygen species (ROS) specifically increases TSP2 mRNA levels, while TSP1 mRNA levels are not affected by ROS production (Lopes *et al*. 2003). The authors found that expression of Rac 1 leads to increased ROS production and subsequent TSP2 expression in human aortic endothelial cells and in vascular smooth muscle cells. THBS1 (fold change: +2.0) and THBS3 (fold change: +2.3) were also found to be upregulated in DD.

TSP1 and 2, tenascin-C (TCN) (fold change: +30.72), and SPARC (fold change: +1.57) induce the process of cellular de-adhesion. They induce the transition to an intermediate state of adhesiveness characterized by loss of actin-containing stress fibres and restructuring of the focal adhesion complexes with no effects on cell shape (Murphy-Ullrich 2001). This intermediate state is thought to be important during tissue remodelling processes like embryogenesis, wound healing, and inflammation where it facilitates cell migration and ECM remodelling.

TCN (fold change: +30.72) is a modular extracellular matrix glycoprotein composed of a series of epidermal growth factor-like repeats, fibronectin type 3-like repeats and a C-terminal fibrinogen-like globular domain (Jones and Jones 2000). Tenascin-C is highly

expressed in organogenesis and at sites of epithelial-mesenchymal transition (Ekblom and Aufderheide 1989). It is induced during wound healing, tumorigenesis, vascular hypertension and myocardial infarction (Chiquet-Ehrismann *et al*. 1995, Imanaka-Yoshida *et al*. 2001). TCN was not found to be differentially expressed in disease tissue and tissues adjacent to disease tissue (skin and fat) in DD patients (Shih *et al*. 2009).

Scrapie responsive protein 1 (SCRG1) is expressed in the developing brain (Dron *et al*. 1998) but is also expressed in cartilage where it locates to the extra-cellular matrix and is involved in chondrogenesis (Ochi *et al*. 2006).

The gene SULF1 locates to 8q13, a chromosomal region that was found to be significantly associated with DD (Dolmans *et al*. 2011). The heparan sulfate 6-O-endosulfatases (SULF1 (fold change: +5.17) and SULF2 (fold change: +3.6)) remove glucosamine-6S groups from specific regions of heparan sulfate (HS) chains at the cell surface (Dhoot *et al*. 2001, Morimoto-Tomita *et al*. 2002). HSs are complex glycans, found ubiquitously on the surface of nearly all animal cells (Esko and Lindahl 2001) where their sulfate groups form specific patterns, interacting with HS binding growth factors and their receptors (Lamanna *et al*. 2007). The activity of SULF1 promotes e.g. Wnt signalling: The removal of 6-O sulphate groups from HS chains favours the formation of low affinity HS–Wnt complexes that can functionally interact with Frizzled receptors to initiate Wnt signal transduction (Ai *et al*. 2003). Sulf activity also has an activating effect on BMP signalling (Viviano *et al*. 2004) and disrupts fibroblast growth factor 2 (FGF2) (Wang *et al*. 2004) and VEGF (Uchimura *et al*. 2006) receptor binding. Expression of SULF1 is induced by TGFβ1 (Yue *et al*. 2008).

4.3.2 Genes involved in Wnt/β-catenin Signalling

GWAS and whole genome expression analysis findings point to the Wnt/β-catenin signalling pathway as an important factor in the pathology of DD. Figure 64 depicts selected components of the Wnt/β-catenin signalling pathway that are deregulated in DD. In the absence of Wnt signal cytoplasmic β-catenin is either localised to cadherin-junctions at the intracellular side of the plasma membrane or bound in a complex with APC and Axin. The later is phosphorylated by casein kinase 1 (Ck1) and then glycogen synthase kinase 3 (Gsk3β). This leads to the ubiquitylation and proteasomal degradation of β-catenin. In the nucleus, prospective target genes of the pathway are kept in a repressed state by interacting with T-cell factor (TCF) and lymphoid enhancer-binding protein (LEF) transcription factors, with associated co-repressors. If Wnt signalling is active, β-catenin is translocated into the nucleus. Secreted frizzled-related proteins (SFRP) antagonize the Wnt pathway by binding to

either Wnts or Frizzled and thereby affecting receptor occupancy. Dickkopf (DKK) and KREMEN also inhibit Wnt signalling by binding to its receptors. Rspondin positively regulates β-catenin signalling by interacting with the Frizzled receptor and LDL-receptor-related protein (LRP5/6) and by competing with DKK (Moon *et al.* 2004, Kim *et al.* 2006). SULF also promotes Wnt signalling (Ai *et al.* 2003). The binding of Wnt to Frizzled leads to activation of the phosphoprotein Dishevelled (Dvl). The activation and membrane recruitment of Dvl probably recruits Axin and the destruction complex to the plasma membrane, where Axin directly binds to the cytoplasmic tail of LRP5/6. Axin is then degraded, which decreases β-catenin degradation (Tolwinski and Wieschaus 2004). The activation of Dvl also leads to the inhibition of GSK3β, which further reduces the phosphorylation and degradation of β-catenin, so that the post-translational stability of β-catenin, through WNT-dependent degradation of Axin and inhibition of GSK3β is increased. As β-catenin levels rise, it accumulates in the nucleus, where it interacts with DNA-bound TCF and LEF family members to activate the transcription of target genes.

The expression of WNT genes was heterogeneous in DD patients and controls. In the whole genome expression experiment the signal detection for most Wnt genes was poor, either because these Wnt genes were not expressed in analysed samples or because the assay failed for these genes. WNT11 was significantly downregulated (fold change: -3.5). O'Gorman *et al.* (2006) found WNT11 to be downregulated in DD tissue and patient derived fibroblasts compared to controls (fold change: ~ -5). They also found some Wnts (e.g. WNT10B) to be heterogeneous in their expression levels and concluded that Wnts are not particularly deregulated in DD. WNT11 is thought not to signal through the Wnt/β-catenin pathway but through other Wnt pathways (Pandur *et al.* 2002). WNT11 expression is induced through the interaction of β-catenin and estrogen-related receptor alpha (ESRRA) (fold change: -1.65). Transcriptional upregulation of WNT11 through β-catenin and ESRRA influences the migratory capacity of cancer cells and expression of ESRRA has been associated with a negative outcome in cancer (Dwyer *et al.* 2010). The observed high heterogeneity in the expression of Wnt ligands makes it difficult to evaluate their expression in patients and controls. In addition it was relative difficult to design specific qPCR primer for some Wnt genes, either because of the high sequence similarity within the Wnt gene family or because these genes were poorly expressed in analyzed samples. For the WNT2 gene the division of samples into expression groups revealed differences between patients and controls, while the comparison of all patients with all controls was less fruitful. Seven out of 15 analysed patient samples showed an upregulation of WNT2 (in fibroblasts) that was not seen in controls.

Especially for Wnt genes and other genes with heterogeneous expression levels the analysis of a large sample set is desirable to assess differences in patients and controls.
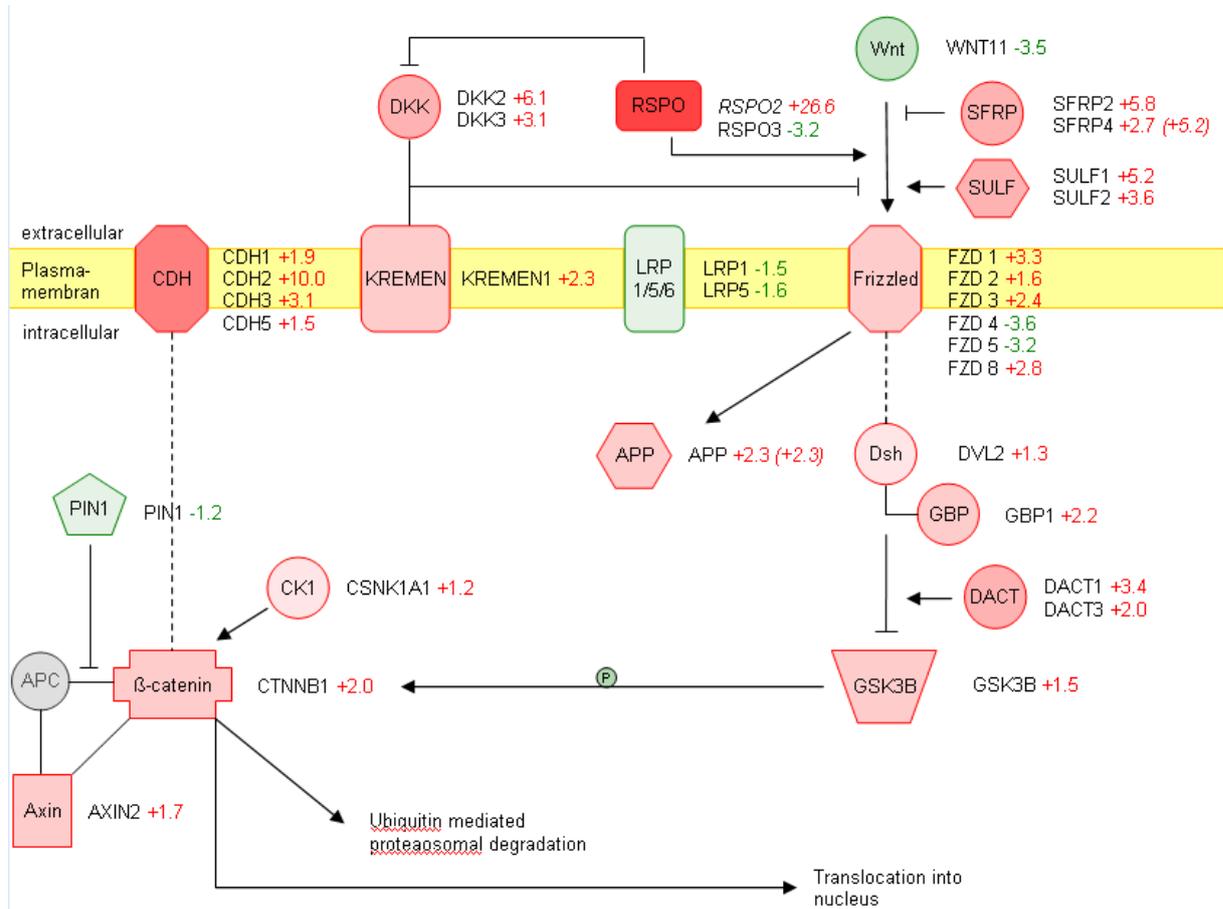
Figure 64. Wnt/β-catenin signalling pathway. Depicted are selected components of the Wnt/beta-catenin canonical pathway that are deregulated in DD. Red colour symbolises upregulated, green colour downregulated gene products. Each symbol stands for one molecule or a molecule group. The gene names are given next to the symbols and are tagged with the corresponding fold changes from the whole genome expression experiment (in green and red). Values in italics represent fold changes detected with qPCR.

The left hand side of figure 65 depicts the interaction partners of β-catenin in the nucleus. On the right hand side a selection of target genes that are upregulated by Wnt/β-catenin signalling are depicted. Prominent among these is WISP1 (not expressed in controls) a member of the WNT1 inducible signalling pathway (WISP) protein subfamily, which belongs to the connective tissue growth factor family (Pennica *et al.* 1998). Other members of this family are cysteine rich 61 (CYR61, fold change: +6.54), connective tissue growth factor (CTGF, fold change: +2.86), and nephroblastoma overexpressed (NOV, fold change: +6.33) which were also found to be significantly upregulated. WISP1 is a β-catenin responsive gene (Marchand *et al.* 2011). It is induced by Wnt1 and Wnt3a but not by Wnt4 (Königshoff *et al.* 2009) and it is also induced by TGFβ1 (Parisi *et al.* 2006). WISP protein is expressed at a high level in fibroblast cells and binds to decorin and biglycan, two

members of a family of small leucine-rich proteoglycans present in the extracellular matrix of connective tissue (Desnoyers *et al.* 2003) of which biglycan (BGN) was found to be upregulated in this study. The BGN protein contains two attached glycosaminoglycan chains. It plays a role in assembly of collagen fibrils and muscle regeneration. It interacts with several proteins among them collagen VI, and enhances vascular smooth muscle cell proliferation (Shimizu-Hirota *et al.* 2004). TGFβ induces the expression of biglycan (BGN).
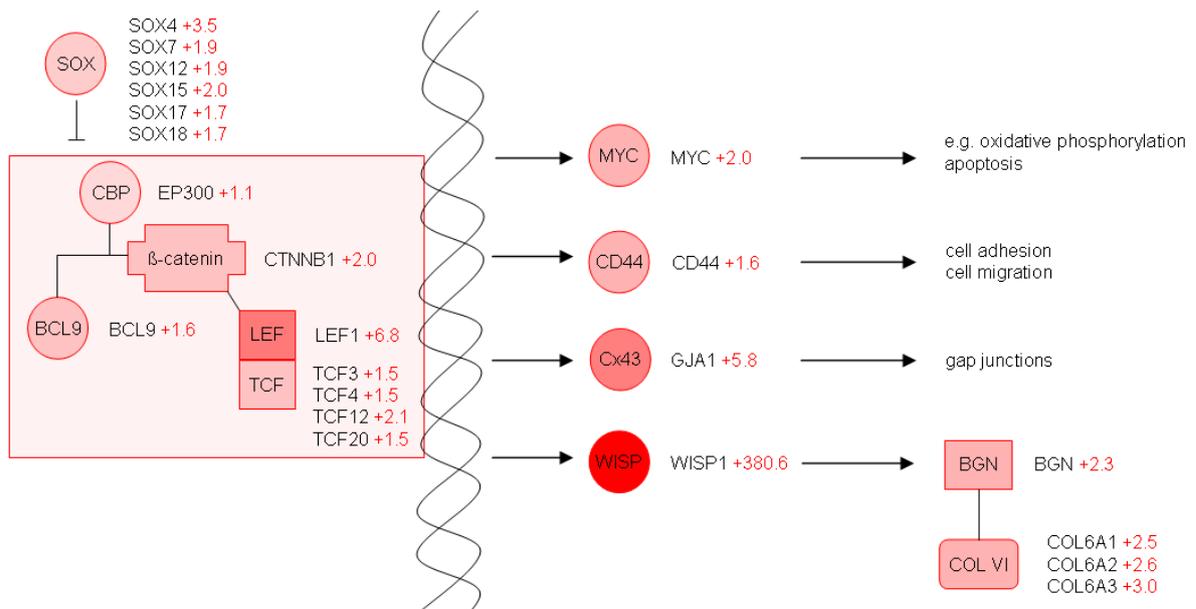
Figure 65. DNA bound β-catenin containing complex and selected target genes. Depicted are selected components of the Wnt/beta-catenin canonical pathway and its target genes that are deregulated in DD. Red colour symbolises upregulated gene products. Each symbol stands for one molecule or a molecule group. The gene names are given next to the symbols and are tagged with the corresponding fold change from the whole genome expression experiment.

Like WISP1 BGN was shown to be induced by TGFβ (Groth *et al.* 2005). The authors found that the TGFβ effect on BGN was dependent on cell adhesion and activated Rac1, which was presumed to acts through NADPH oxidases (NOXs). Deficiency of biglycan causes cardiac fibroblasts to differentiate into a myofibroblast phenotype (Melchior-Becker *et al.* 2011). GJA1 is a member of the connexin gene family (Cx). Cxs are the major component of gap junctions (Loewenstein 1981). Gap junctions are specialized intercellular channels that permit functional coupling of cells electrically and biochemically, allowing the selective diffusion of ions and metabolites between the cytoplasms of two adjacent cells (Kumar and Gilula 1996, Mroue *et al.* 2011). Additionally Cxs have diverse functions and interaction partners which are apparently channel-independent (e.g. Giepmans *et al.* 2001a, Giepmans *et al.* 2001b, Singh *et al.* 2005). Most interestingly Cx43 interacts with β-catenin, N-cadherin and NOV (member of the CTGF family, see above). Wnt1 induced Cx43 levels through β-catenin signalling. In response to Wnt signalling, the accumulating Cx43 colocalised with β-

catenin in the cell membrane of rat cardiomyocytes, thereby sequestering β-catenin to the cell membrane which in turn reduces β-catenin transcriptional activity (Ai *et al*. 2000). Cx43 also colocalises with N-cadherin in migrating neural crest cells (Xu *et al*. 2001). Analyses by immunohistochemistry, and coimmunoprecipitation and Western immunoblotting indicated that Cx43 and N-cadherin, and with them gap junctions and adhesion junctions, are coassembled in a large multiprotein complex. Consistent with this, siRNA-mediated knockdown of either Cx43 or N-cadherin resulted in the apparent loss of both proteins from the cell surface of neural cells (Wei *et al*. 2005). Likewise N-cadherin knockout cardiomyocytes are Cx43 gap junction-deficient (Luo and Radice 2003).

The cytoplasmic tail of Cx43 associates with NOV. NOV protein is down-regulated in the absence of Cx43 (but Cx43 protein levels are not affected by NOV absence). Overexpression of NOV increases the activity of the small GTPase Rac1, thereby revealing a pathway that links Cx43 directly to actin reorganization (Sin *et al*. 2009). Pannexins show similarities in their structure and topology with connexins and are thought to form channels as well (Dahl and Locovei 2006). Pannexin 1 (PANX1) was upregulated 2.51 fold.

CD44 is induced by Wnt/β-catenin signalling (Wielenga *et al*. 1999). CD44 is a cell-surface adhesion molecule and the major cell-surface receptor for the nonsulfated glycosaminoglycan hyaluronan (HA) (Aruffo *et al*. 1990). HA is a high-molecular-mass polysaccharide found in the extracellular matrix, especially of soft connective tissues (Laurent and Fraser 1992). CD44 plays a role in removal of extracellular matrix breakdown products after tissue injury response (Teder *et al*. 2002). Mast cells adhesion to bronchial smooth muscle cells in asthmatic patients involved collagen1, CD44, and integrin, alpha V (Girodet *et al*. 2010). Integrin, alpha V (ITGAV) was also found to be upregulated in this study (fold change: +3.25). CD44 therefore seems to be important for cell adhesion and motility in connective tissue.

V-myc myelocytomatosis viral oncogene homolog (avian) (MYC) expression is induced by the Wnt/β-catenin signalling pathway (He *et al*. 1998). The MYC protein is a multifunctional, nuclear phosphoprotein that functions as a transcription factor with over 2000 identified target genes. The c-Myc target gene database (http://www.myccancergene.org) and the literature were browsed to identify Myc target genes that were deregulated in DD.

Among the genes that are upregulated in response to Myc treatment were e.g. genes involved in cell adhesion: THBS4 (+ 52.07) (Mao *et al*. 2003), and apoptosis: APP (+2.31)

(Fernandez *et al*. 2003), CASP3 (+2.68) (Louro *et al*. 2002). One myc response gene downregulated in DD was the small heat shock protein, CRYAB (-4.81) (O'Connell *et al*. 2003, Guo *et al*. 2000). Direct Myc target genes identified by chromatin immunoprecipitation (ChIP) and promoter microarrays in human primary fibroblasts (Kim *et al*. 2008) are for example the actin binding proteins TAGLN (+1.50) (also called SM22α) and TAGLN2 (+2.09), homo sapiens superoxide dismutase 1 (SOD1, -1.40), SOX4 (+3.52), solute carrier family: SLC5A6 (sodium-dependent vitamin transporter, member 6: -3.29), SLC35B1 (+1.48), and DEAD (Asp-Glu-Ala-Asp) box polypeptide (DDX) 56 (-1.26). TAGLN has an expression pattern very similar to αSMA (Morgan and Gangopadhyay 2001).

Myc activates nuclear-encoded mitochondrial gene expression, and many direct targets of Myc are involved in mitochondrial function such as oxidative phosphorylation, metabolism, apoptosis, and glutamate metabolism. (Coller *et al*. 2000, Kim *et al*. 2008). The induction of proliferation and cell cycle progression by Myc may be in part due to its activation of mitochondrial biogenesis and oxidative phosphorylation (Li *et al*. 2005, Morrish *et al*. 2003).

Myc null rat fibroblasts have diminished mitochondrial mass and decreased number of normal mitochondria. Reconstitution of Myc expression in Myc null fibroblasts partially restored mitochondrial mass and function and normal-appearing mitochondria (Li *et al*. 2005). Nuclear-encoded mitochondrial target genes of Myc deregulated in DD are e.g. cytochrome c oxidase subunit Vb, COX5B (-1.50) and polymerase gamma, PLOG (-1.35).

CTCF-binding is required for protection from DNA methylation at the human MYC locus (Gombert and Krumm 2009).

Other target genes of β-catenin upregulated in DD include matrix metallopeptidase 7 (MMP7, fold change: +1.44) (Crawford *et al*. 1999, Brabletz *et al*. 1999) and matrix metallopeptidase 14 (MMP14, fold change: +10.08) (Takahashi *et al*. 2002). Proteins of the matrix metalloproteinase (MMP) family are involved in the breakdown of extracellular matrix. Most MMPs are secreted as inactive proproteins which are activated when cleaved by extracellular proteinases. The MMP7 enzyme degrades proteoglycans, fibronectin, elastin and casein and is involved in wound healing. MMP7 mediates cleavage of N-cadherin and promotes vascular smooth muscle cell apoptosis (Williams *et al*. 2010). While MMP9 (fold change: -23.22) promoted shedding of the extracellular portion of N-cadherin resulting in increased vascular smooth muscle cell proliferation via elevation of β-catenin signalling and cyclin D1 expression (Dwivedi *et al*. 2009). MMP2 was upregulated with a fold change of

+4.26. The MMP2 protein degrades collagen IV, and plays a role in endometrial menstrual breakdown, regulation of vascularisation and the inflammatory response.

Fibronectin, another extracellular matrix protein is upregulated by β-catenin signalling (Gradl *et al*. 1999) was upregulated with a fold change of +20.00 in DD. Collagen 1 is also a target of β-catenin signalling (Cheng *et al*. 2008). Although being a β-catenin target gene, the expression of cyclin D1 (CCND1) was not altered in DD compared to controls.

B-catenin signalling regulates the expression of its own effectors, e.g. Dickkopf 1 (DKK1) (Glinka *et al*., 1998) is itself a direct transcriptional target of β-catenin (Chamorro *et al*., 2005; Niida *et al*., 2004). Expression of Lef-1 (Hovanes *et al*. 2001) and TCF4 (Kolligs *et al*. 2002) is also promoted by β-catenin signalling. The expressions of SFRP2 (Lescher *et al*. 1998), FZD7 (Willert *et al*. 2002), axin2 (Yan *et al*. 2001), periostin (downregulated by Wnt) (Haertel-Wiesmann *et al*. 2000), are also affected by Wnt/β-catenin signalling.

The abundance of Wnt/β-catenin target genes underlines the importance of this pathway. In the future it will be crucial to determine the components and targets of this pathway that play a role in the pathology of DD. One first approach could be the comparison of DD derived fibroblasts with cells from young and old controls under different conditions e.g. stress or non-stress, and treatment with Wnts or knockdown of Wnt signalling components. In a recent study Wnt3A induced αSMA expression and stress fibre formation in mouse fibroblasts. This induction was dependant on β-catenin and TGFβ (Carthy *et al*. 2011).

Many genes involved in the Wnt/β-catenin canonical pathway were upregulated. Both promoting (RSPO, SULF) and repressing factors (SFRP, DKK) were upregulated. This may indicate that complex interactions with partly contradictory effects take place nevertheless resulting in the upregulation of the Wnt/β-catenin pathway. After renal epithelial injury Surendran *et al*. (2005) found an increase in Wnt/β-catenin signalling and at the same time increased expression of SFRP4 (Wnt inhibitor), while SFRP4 protein levels were not increased. Therefore expression levels must not necessarily correspond to protein levels. It could be desirable to test protein levels of selected in genes in DD samples and controls to further assess Wnt signalling in DD.

4.3.3 Mitochondrial Dysfunction and Oxidative Stress

The Illumina whole genome expression chip does not contain mitochondrial encoded genes. Transcripts of mitochondrial proteins encoded in the nucleus had an overall tendency to be downregulated in the whole genome expression analysis. Consequently IPA analysis highlighted mitochondrial dysfunction and oxidative stress as pathways significantly

affected and involved in the pathology of DD. Mitochondrial dysfunction and oxidative stress (ROS production) were associated with aging and aging associated diseases (e.g. Patti *et al*. 2003, Petersen *et al*. 2004, Lowell and Shulman 2005, Bowling and Beal 1995, Swerdlow and Khan 2004, Langston *et al*. 1983, Schapira *et al*. 1989, Bindoff *et al*. 1989, Kuwert *et al*. 1990, Kim *et al*. 2010). Among the most deregulated genes in these pathways were those involved in the generation of, and response to ROS e.g. monoamine oxidase A (MAOA) (fold change: -6.60), catalase (CAT) (fold change: -3.37), uncoupling protein 2 (UCP2) (fold change: -4.16), and glutathione peroxidase 4 (GPX4) (fold change: -2.44) were downregulated, while others were upregulated namely, glutathione peroxidase 7 (GPX7) (fold change: +3.34) and NADPH oxidase 4 (NOX4) (fold change: +2.17).

Catalase converts H_2O_2 to water and oxygen and thereby mitigates the toxic effects of H_2O_2. Mice overexpressing catalase had a ~45% decrease in H_2O_2 production in muscle. Compared to wild type controls, these mice showed no increase in mtDNA mutations or decrease of mitochondrial function (e.g. ATP production) with age (16 month) (Lee *et al*. 2010). Insulin resistance in muscle is associated with age and high fat diet. In another study reduction of H_2O_2 (antioxidant treatment or catalase overexpression) in mitochondria of muscle in mice, preserved insulin sensitivity despite a high fat diet (Anderson *et al*. 2009). Oxidative enzyme activity and protein levels of mitochondrial respiratory chain subunits were significantly elevated in mice fed on high fat diet for 5 or 20 weeks (Turner *et al*. 2007). This accelerated metabolism leads to mitochondria "exhaustion" in old animals. In mice insulin resistance proceeds oxidative damage and mitochondrial dysfunction (Bonnard *et al*. 2008).

TGFβ induced the expression of NOX4 and at the same time inhibited the expression of SOD2 and catalase in airway smooth muscle cells (Michaeloudes *et al*. 2011). TGFβ1 treatment reduced SOD2 expression in patient and control cells (fold change: -2.54). Changes of CAT expression were not seen upon TGFβ1 treatment in the present study. Moreover TGFβ induces αSMA expression via NOX4 in smooth muscle cells (Martin-Garrido *et al*. 2011). Transfection of human aortic smooth muscle cells with siRNA against NOX4 abolished TGFβ induced αSMA expression and stress fibre formation. Mitogen-activated protein kinase 1 MAPK1, serum response factor (SRF) and megakaryoblastic leukemia (translocation) 1 (MKL1) were also involved in this pathway (Martin-Garrido *et al*. 2011). Krause *et al*. (2011) found elevated MAPK1 phosphorylation upon TGFβ1 treatment in DD derived fibroblasts.

UCP2 is expressed in several tissues and shows highest expression in skeletal muscle. UCPs facilitate the transfer of anions (OH^-) from the mitochondria to the space between inner and outer mitochondrial membrane and the return transfer of protons (H^+). Thereby they reduce the mitochondrial membrane potential, separating oxidative phosphorylation from ATP synthesis. This process is also referred to as the mitochondrial proton leak (Rigoulet *et al.* 2011). UCP2 (and UCP3) are activated by ROS and do not catalyse proton leak in the absence of ROS (Esteves and Brand 2005).

Catalase Enzyme Activity Assay

A catalase activity assay was preformed to test for oxidative stress enzyme function in patient and control fibroblasts. Of 16 analyses patient samples 7 showed reduced catalase activity. Five patient samples had reduced catalase activity at 37°C and 40.5°C.

After planting fibroblasts in 225cm^2 cell culture flasks, populations reached confluence in six to twelve days. Most control cell lines showed slow growth while some patient cell lines grew extremely fast. Different growth behaviour was reflected in catalase activity. Fast growing patient cell lines had low enzyme activity compared with slow growing patient and control cell lines. Catalase overexpression is known to reduce cell population doubling times by prolonging the G0/G1 phase in the cell cycle (Onumah *et al.* 2009).

It is likely that observed growth rate differences due to catalase activity differences reflect the situation *in vivo*. At least for one patient included in the group of fast growing cell lines showing low catalase activity a very fast reoccurrence of the disease after surgery was observed.

Connections between Wnt/β-catenin and ROS

The Wnt/β-catenin signalling pathway was linked to ROS (Shin *et al.* 2004, Funato *et al.* 2006, Korswagen 2006). H_2O_2 induces a rapid increase in Wnt signalling that peaks around 20 min after stimulation (Funato *et al.* 2006), but signalling is reduced several hours after H_2O_2 treatment (Shin *et al.* 2004, Korswagen 2006). Influence of ROS on Wnt/β-catenin signalling is likely mediated via Disheveled (Dvl). Dvl interacts with nucleoredoxin (NXN) (Funato *et al.* 2006). NXN (+2.46) belongs to the family of thioredoxins. Thioredoxin (TXN) is a thiol oxidoreductase that is essential for DNA synthesis and for various redox signalling pathways (Holmgren 2000). TXN can scavenge ROS mainly by reducing various target proteins, including the H_2O_2-quenching enzyme peroxiredoxin (PRDX1-6) (Rhee *et al.* 2005). PRDX2 (-1.93), PRDX 3 (-1.28), PRDX 5 (-1.12) and PRDX 6 (-1.59) were by trend

downregulated, PRDX1 was not differentially expressed (fold change: 1.07), and PRDX4 was upregulated (fold change: 2.10). TRX also regulates stress signalling pathways (Fujino *et al*. 2006). TXN and related proteins compose a large heterogeneous family. Another gene similar to NXN is NXNL1 (Funato and Miki 2007) which was downregulated in DD (-7.08). NXN selectively affects Dvl function on β-catenin. NXN does not inhibit JNK activation by Dvl (Funato *et al*. 2006).

B-catenin interacts with E-cadherin, and the transcription factors Tcf/Lef, FOXO (FOXO1: -1.49), HIF1 (HIF1A: +2.11). These transcription factors are all regulated by ROS and the interaction with β-catenin enhances their activity, like was shown for the β-catenin/FOXO interaction (Esser *et al*. 2005). Under normal cellular conditions β-catenin, through Wnt signalling, is involved in cell proliferation and differentiation but under changed ROS conditions its function can shift to regulate transcription factors that support cell survival through increased stress resistance and ROS clearance. These findings may be taken to suggest that β-catenin is a pivot in reprogramming transcriptional activity following changes in ROS (Hoogeboom and Burgering 2011). SFRP4 treatment induced lower catalase activity and consequently higher H_2O_2 levels in cultured endothelial cells (Muley *et al*. 2010).

Oxidative stress and decline in mitochondrial function play an important role in aging and aging associated diseases. In how far they are a force that drives the aging process, as predicted by the free radical theory of aging, or are consequence of the aging process is not know. Nevertheless their association with DD emphasizes the importance of aging factors in the pathology of DD. Therefore DD can only be considered in the contest of aging.

Further experiments that investigate the role of oxidative stress in the pathology of DD are required. Disease tissue derived fibroblasts could be cultured under different stress conditions and analysed in terms of their contraction behaviour in collagen gels or their expression off target genes. Especially the relationship between oxidative stress and the Wnt/β-catenin signalling pathway should be considered in these experiments in order to determine whether this relationship plays a decisive role in DD.

Signalling Cascade that leads to Myofibroblast Differentiation

Wnt3A induced the expression of αSMA in (mouse) fibroblasts (Carthy *et al*. 2011). This induction was dependant on β-catenin, suggesting that the signal is transmitted through the Wnt/β-catenin signalling pathway. The induction of αSMA through Wnt3A was also dependant on TGFβ, suggesting that signal transmission requires TGFβ/SMAD signalling

(Carthy *et al*. 2011). As shown by e.g. Cucoranu *et al*. (2005), TGFβ induces the differentiation of fibroblasts into myofibroblasts. NOX4 is also required for αSMA induction through TGFβ (Martin-Garrido *et al*. 2011). NOX4 generates ROS (Babior 1999). Additionally TGFβ upregulation reduces the expression of CAT and SOD, which also leads to elevated ROS levels (Michaeloudes *et al*. 2011). Having established that this signalling cascade is present in DD fibroblasts the next step could be to determine whether αSMA expression is induced directly through smad DNA binding, as was shown for TAGLN (SM22α) (Shafer and Towler 2009) or if TGFβ/smad signalling leads to the upregulation of NOX4, which in turn induces αSMA expression through ROS signalling and the MAPK pathway, as shown by Martin-Garrido *et al*. (2011) for human aortic smooth muscle cells
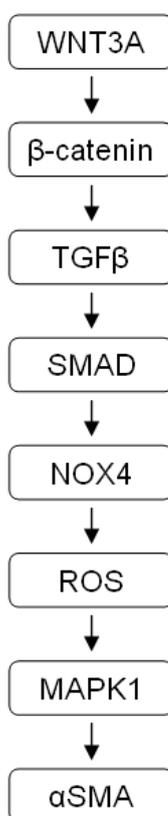
and by Bondi *et al*. (2010) for kidney fibroblasts (figure 66). In the later scenario the expression of αSMA would be sensitive to ROS. In this case it would be conceivable that elevated ROS levels may trigger myofibroblast differentiation even in the absence of Wnt/β-catenin signalling in the context of aging associated changes in ROS production. The TGFβ and MAPK pathways were upregulated in DD derived fibroblasts (Krause *et al*. 2011) and

NOX4 was upregulated in DD tissue in this study. NOX4 expression was induced by TGFβ1 and Wnt3a and NOX4 was required for αSMA induction through TGFβ1 or Wnt3a. These results support the hypothesis that the signalling cascade described for aortic smooth muscle cells and kidney fibroblasts (Martin-Garrido *et al*. 2011, Bondi *et al*. 2010) is also present in DD fibroblasts. Namely that TGFβ/smad signalling leads to the upregulation of NOX4 which in turn induces αSMA expression.

Figure 66. Proposed signalling cascade that leads to αSMA expression and myofibroblast differentiation.

In this study Wnt3a induced the expression of αSMA in patient cells. But inhibition of GSK3β or NXN (both Wnt/β-catenin signalling inhibitors) attenuated the upregulation of αSMA through TGFβ1 or Wnt3a. The inhibition of GSK3β in cells from asthma patients attenuated myofibroblast differentiation (Michalik *et al*. 2012). Michalik and colleges used lithium in their study. Lithium is a GSK3β inhibitor that is implemented in drugs for the treatment of psychiatric diseases. In these patients' lithium treatment coincided with the

remission of asthmatic symptoms (Nasr and Atkins 1977). More experiments are needed in order to unravel the signalling cascade that leads to myofibroblast differentiation in DD.

4.3.4 Other Genes Deregulated in DD

Among the other genes up- or downregulated in DD were a number of genes associated with the immune system, pointing to the possible infiltration of disease tissue by immune cells, e.g. macrophages (also see CD44 above).

HLA-DRB5 belongs to the HLA class II beta chain paralogues of DRB1. DRB5 encodes the beta chain of a heterodimer consisting of an alpha (DRA) and a beta (DRB) chain, both anchored in the membrane. It presents peptides derived from extracellular proteins and is expressed in antigen presenting cells (APC: B lymphocytes, dendritic cells, macrophages). DRB1 is expressed at a level five times higher than DRB5. The DRB5*1010 allele is linked with the *1501 allele of DRB1. HLA-DRB1*1010 has been associated with multiple sclerosis (MS) (Winchester et al. 1975). DRB5 e.g. attenuates MS severity (Caillier et al. 2008). The *1501 allele of HLA-DRB1 was also associated with DD (Brown et al. 2008).

Mason et al. (2011) found HLA-DRB5 to by differentially expressed in muscle tissue of healthy persons (N = 225). They proposed that bimodal expression (0.2% of the genes expressed in muscle) indicates important genes pointing to disease susceptibility. Interestingly, of the eight genes identified to have bimodal expression in their study six were found to be differentially expressed in this study (GSTM1: -2.69, HLA-DRB1: +2.30, ERAP2: +1.58, HLA-DRB5: +8.70, MAOA: -6.60, and THNSL2: -1.66).

CADM1 (fold change: +9.99) was described as a tumour suppressor gene in lung cancer (Kuramochi et al. 2001, Murakami et al. 2002). It encodes a member of the immunoglobulin (Ig) superfamily and shows significant homology in its extracellular domain with those of other Ig superfamily cell adhesion molecules (Masuda et al. 2002). It is expressed by cells of the immune system e.g. is expressed by human lung mast cells and promotes their interaction with airway smooth muscle cells (Hollins et al. 2008).

RASL11B (fold change: 17.83) is a member of the small GTPase protein family similar to RAS proteins. It is highly expressed in primary macrophages and coronary artery smooth muscle cells after TGFβ1 treatment (Stolle et al. 2007).

The gene MAFB locates to 20q11.2-q13.1, a chromosomal region that was found to be significantly associated with DD (Dolmans et al. 2011). Its expression was upregulated ~5 fold in DD primary tissue compared to controls and upregulated ~7 fold in disease tissue

compared with control tissue from the same patient. In contrast its expression was significantly downregulated ~7 fold in disease tissue derived fibroblasts treated with TGFβ1. Another gene from the same family, MAF locates to chromosome 16q23.2; a region that showed suggestive association with DD. MAF was not differentially expressed in DD and control tissue. The MAFB gene contains no introns. The encoded protein is a basic leucine zipper (bZIP) transcription factor. MAFB expression is regulated by the transcription factor TFE3 (Zanocco-Marani *et al*. 2009). Which was downregulated in DD (fold change: -1.79). MAFB is phosphorylated by GSK3β (Rocques *et al*. 2007). Transcriptional activation of MAF and MAFB in multiple myeloma (MM) leaded to upregulation of SFRP2 and downregulation of DKK1 (Zhan *et al*. 2006). Therefore MAFB may influence Wnt/β-catenin signalling by (indirectly) regulating two of its repressors. Another gene upregulated by MAFB expression in MM was secreted phosphoprotein 1 (SPP1), which itself induces β-catenin signalling via Akt activation and subsequent GSK3β inactivation (Robertson and Chellaiah 2010). SPP1 was downregulated in DD with a fold change of -19.56.

G0S2 (fold change: -15.68) was the strongest downregulated gene in the whole genome expression analysis (with both detection P-values = 0). It belongs to the genes involved in the G0/G1 switch, the switch from the G0 to the G1 phases of the cell cycle (Russell and Fordyke 1991). It shows highest expression in white and brown adipose tissue but it is also expressed in 3T3 fibroblasts (Zandbergen *et al*. 2005). There it is upregulated in growth arrested (confluent) 3T3 cells. Downregulation of G0S2 is either due to the higher fat content in control tissue or it also could reflect the high proliferating rate in DD fibroblasts. To exclude the first possibility one could compare the expression of G0S2 in fibroblast cell lines. Satish *et al*. (2008) compared the whole genome expression of DD tissue derived fibroblasts to control fibroblasts and found G0S2 to be downregulated four fold in disease fibroblasts.

In the table of genes downregulated in DD a large number of genes involved in adipose metabolism stand out. This is likely caused by the higher fat content in control tissue compared to DD tissue (figure 40). On the other hand keratins and other genes expressed in keratinocytes were upregulated in DD tissue. Outgrowth of keratinocytes from cultivated DD tissue samples was often observed, although all visible (epi-) dermal tissue was removed prior to cell culture. In the disease process the skin becomes attached to the nodules and gets invaginated into the underlying tissue. Some DD tissue samples therefore contain keratinocytes while keratinocytes will be few in the control tissue. Whether these keratinocytes are trapped accidentally or play an active part in the pathology of DD is not

known. Neighbouring skin and fat tissue was suspected to play a role in the pathogenesis of DD (Shih *et al*. 2009), but evidence for involved mechanisms is scarce. Spatial proximity of fascia, fat and skin in the palm suggest that interactions between these tissues take place both in normal and disease situations.
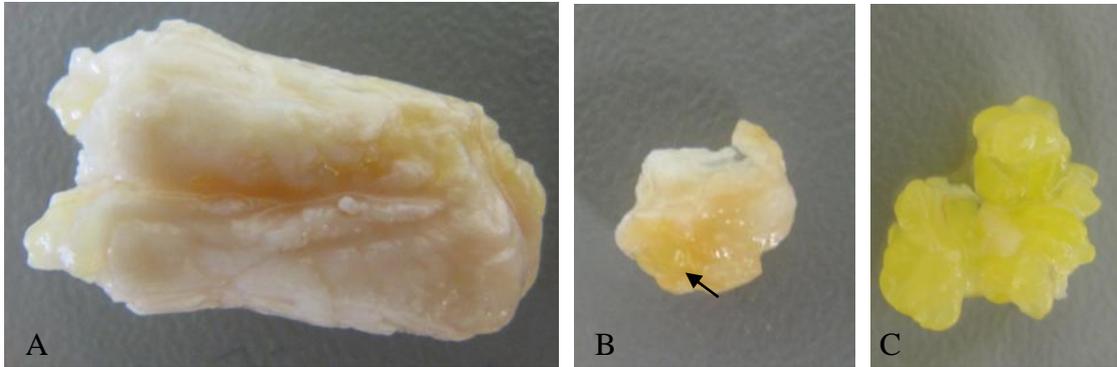
Figure 67. Pictures of one DD (A) and two control (B and C) tissue samples. The disease sample was hard and collagen rich. The depicted sample was about 1.3 cm long. The control samples contain more fat (arrow in B, yellow tissue). Control sample in C was not used for whole genome expression analysis. Fat tissue proved to be a very difficult tissue to isolate sufficient amounts of RNA for array analysis from. Therefore control samples consisting mainly of fat were not included in the whole genome expression analysis. Still the used control tissues had a higher fat content than DD tissue. Most control tissue samples were so tiny that only small amounts of total RNA were isolated.

5   Conclusions

DD is a progressive aging associated disease with a strong genetic basis. Although the underlying cause of this disease remains to be identified genetic association and expression analysis highlighted the Wnt/β-catenin pathway as a likely key player. Upregulation of the Wnt/β-catenin pathway in disease compared to control tissue shows that this pathway clearly is involved in the pathology of DD. At the same time genetic association of at least six chromosomal regions that contain Wnt/β-catenin signalling components suggests that these genes may harbour variants that contribute to the aetiology of DD. These assumed genetic variants most likely have no negative effect on development. And according to evolutionary theories of aging there was possibly no selection against them. The disease manifests itself only when changes in e.g. connective tissue composition or hormone signalling occur due to aging (and other factors such as disease, medicamentation, life style habits or (repetitive) hand trauma). The aging process is therefore likely to play a crucial role.

One future goal is the identification of disease-causing variants. This can be accomplished for example by next generation sequencing or exon sequencing of associated regions. For these approaches either a subgroup of very early or severely affected patients or several patients from one family could be selected.

As stated in the introduction, the aging process is characterised by conserved features because it is determined by conserved processes in most animals (e.g. reproduction and damage repair). That is not only true between different (model) organisms, but also between different aging associated diseases. The Wnt/β-catenin signalling pathway is involved in several aging associated diseases. The same applies for mitochondrial dysfunction and oxidative stress. When investigating aging associated diseases one has therefore to bear in mind which mechanisms are shared over different aging associated diseases. To identify these pathways and study their function is one approach to eventually access healthy aging in humans.

DD is particularly well suited to investigate the molecular mechanisms of aging associated diseases. Unlike many other aging associated diseases, e.g. neurodegenerative diseases, the abnormal tissue is easily accessible as it is removed during surgery. In support of genetic association studies one can thus perform expressions studies with primary tissue (as was done in this study). Additionally, questions, resulting from these analyses can be directly investigated *in vitro* in primary cells from DD patients.

6   References

Adams JC, Monk R, Taylor AL, Ozbek S, Fascetti N, Baumgartner S, Engel J. Characterisation of Drosophila thrombospondin defines an early origin of pentameric thrombospondins. J Mol Biol. 2003 Apr 25;328(2):479-94.

Ai X, Do AT, Lozynska O, Kusche-Gullberg M, Lindahl U, Emerson CP Jr. QSulf1 remodels the 6-O sulfation states of cell surface heparan sulfate proteoglycans to promote Wnt signaling. J Cell Biol. 2003 Jul 21;162(2):341-51. Epub 2003 Jul 14.

Ai Z, Fischer A, Spray DC, Brown AM, Fishman GI. Wnt-1 regulation of connexin43 in cardiac myocytes. J Clin Invest. 2000 Jan;105(2):161-71.

An HS, Southworth SR, Jackson WT, Russ B. Cigarette smoking and Dupuytren's contracture of the hand. J Hand Surg Am. 1988 Nov;13(6):872-4.

Anderson CA, Pettersson FH, Clarke GM, Cardon LR, Morris AP, Zondervan KT. Data quality control in genetic case-control association studies. Nat Protoc. 2010 Sep;5(9):1564-73.

van Amerongen R, Nusse R. Towards an integrated view of Wnt signaling in development. Development. 2009 Oct;136(19):3205-14.

Anderson EJ, Lustig ME, Boyle KE, Woodlief TL, Kane DA, Lin CT, Price JW 3rd, Kang L, Rabinovitch PS, Szeto HH, Houmard JA, Cortright RN, Wasserman DH, Neufer PD. Mitochondrial H2O2 emission and cellular redox state link excess fat intake to insulin resistance in both rodents and humans. J Clin Invest. 2009 Mar;119(3):573-81.

Andziak B, O'Connor TP, Buffenstein R. Antioxidants do not explain the disparate longevity between mice and the longest-living rodent, the naked mole-rat. Mech Ageing Dev. 2005 Nov;126(11):1206-12.

Arafa M, Steingold RF, Noble J. The incidence of Dupuytren's disease in patients with rheumatoid arthritis. J Hand Surg 1984;9B:165-6.

Arber S, Caroni P. Thrombospondin-4, an extracellular matrix protein expressed in the developing and adult nervous system promotes neurite outgrowth. J Cell Biol. 1995 Nov;131(4):1083-94.

Armstrong LC, Björkblom B, Hankenson KD, Siadak AW, Stiles CE, Bornstein P. Thrombospondin 2 inhibits microvascular endothelial cell proliferation by a caspase-independent mechanism. Mol Biol Cell. 2002 Jun;13(6):1893-905.

Aruffo A, Stamenkovic I, Melnick M, Underhill CB, Seed B. CD44 is the principal cell surface receptor for hyaluronate.Cell. 1990 Jun 29;61(7):1303-13.

Aström C, Rehn B, Lundström R, Nilsson T, Burström L, Sundelin G. Hand-arm vibration syndrome (HAVS) and musculoskeletal symptoms in the neck and the upper limbs in professional drivers of terrain vehicles--a cross sectional study. Appl Ergon. 2006 Nov;37(6):793-9.

Babior BM. NADPH oxidase: an update. Blood. 1999 Mar 1;93(5):1464-76.

Baird KS, Alwan WH, Crossan JF, Wojciak B. T-cell-mediated response in Dupuytren's disease. Lancet. 1993 Jun 26;341(8861):1622-3.

Barja, G. Mitochondrial oxygen radical generation and leak sites of production in states 4 and 3, organ specificity, and relation to aging and longevity. J. Bioenerg. Biomembr. 1999; 31: 347–366.

Bayat A, McGrouther DA. Management of Dupuytren's disease--clear advice for an elusive condition. Ann R Coll Surg Engl. 2006 Jan;88(1):3-8.

Bergamini E, Cavallini G, Donati A, Gori Z. The role of autophagy in aging: its essential part in the anti-aging mechanism of caloric restriction. Ann N Y Acad Sci. 2007 Oct;1114:69-78.

Bergenudd H, Lindgärde F, Nilsson BE. Prevalence of Dupuytren's contracture and its correlation with degenerative changes of the hands and feet and with criteria of general health. J Hand Surg Br. 1993 Apr;18(2):254-7.

Bernfield M, Götte M, Park PW, Reizes O, Fitzgerald ML, Lincecum J, Zako M. Functions of cell surface heparan sulfate proteoglycans. Annu Rev Biochem. 1999;68:729-77.

Bias WB, Nyberg LM Jr, Hochberg MC, Walsh PC. Peyronie's disease: a newly recognized autosomal-dominant trait. Am J Med Genet. 1982 Jun;12(2):227-35.

Bindoff LA, Birch-Machin M, Cartlidge NE, Parker WD Jr, Turnbull DM. Mitochondrial function in Parkinson's disease. Lancet. 1989 Jul 1;2(8653):49.

Blüher M, Kahn BB, Kahn CR. Extended longevity in mice lacking the insulin receptor in adipose tissue. Science. 2003 Jan 24;299(5606):572-4.

Bokov A, Chaudhuri A, Richardson A. The role of oxidative damage and stress in aging. Mech Ageing Dev. 2004 Oct-Nov;125(10-11):811-26.

Bondi CD, Manickam N, Lee DY, Block K, Gorin Y, Abboud HE, Barnes JL. NAD(P)H oxidase mediates TGF-beta1-induced activation of kidney myofibroblasts. J Am Soc Nephrol. 2010 Jan;21(1):93-102.

Bonnard C, Durand A, Peyrol S, Chanseaume E, Chauvin MA, Morio B, Vidal H, Rieusset J. Mitochondrial dysfunction results from oxidative stress in the skeletal muscle of diet-induced insulin-resistant mice. J Clin Invest. 2008 Feb;118(2):789-800.

Bowling AC, Beal MF. Bioenergetic and oxidative stress in neurodegenerative diseases. Life Sci. 1995;56(14):1151-71.

Brabletz T, Jung A, Dag S, Hlubek F, Kirchner T. Beta-catenin regulates the expression of the matrix metalloproteinase-7 in human colorectal cancer. Am J Pathol 1999;155:1033–1038.

Brack AS, Conboy MJ, Roy S, Lee M, Kuo CJ, Keller C, Rando TA. Increased Wnt signaling during aging alters muscle stem cell fate and increases fibrosis. Science. 2007 Aug 10;317(5839):807-10.

Browning BL and Browning SR. A unified approach to genotype imputation and haplotype phase inference for large data sets of trios and unrelated individuals. Am J Hum Genet 2009. 84:210-223.

Brenner P, Krause-Bergmann A, Van VH. Dupuytren contracture in North Germany. Epidemiological study of 500 cases. Unfallchirurg. 2001 Apr;104(4):303-11.

Brenner P and Rayan GM. Morbus Dupuytren - Ein chirurgisches Therapiekonzept. Springer, Wien, 2002

Burge P, Hoy G, Regan P, Milne R. Smoking, alcohol and the risk of Dupuytren's contracture. J Bone Joint Surg Br. 1997 Mar;79(2):206-10.

Brookes PS, Levonen AL, Shiva S, Sarti P, Darley-Usmar VM. Mitochondria: regulators of signal transduction by reactive oxygen and nitrogen species. Free Radic Biol Med. 2002 Sep 15;33(6):755-64.

Brown-Borg HM, Borg KE, Meliska CJ, Bartke A. Dwarf mice and the ageing process. Nature. 1996 Nov 7;384(6604):33.

Brown JJ, Ollier W, Thomson W, Bayat A.Positive association of HLA-DRB1*15 with Dupuytren's disease in Caucasians. Tissue Antigens. 2008 Aug;72(2):166-70.

Burge P, Hoy G, Regan P, Milne R. Smoking, alcohol and the risk of Dupuytren's contracture. J Bone Joint Surg Br. 1997 Mar;79(2):206-10.

Burke FD, Proud G, Lawson IJ, McGeoch KL, Miles JN. An assessment of the effects of exposure to vibration, smoking, alcohol and diabetes on the prevalence of Dupuytren's disease in 97,537 miners. J Hand Surg Eur Vol. 2007 Aug;32(4):400-6.

Cadigan KM, Nusse R. Wnt signaling: a common theme in animal development. Genes Dev. 1997 Dec 15;11(24):3286-305.

Caillier SJ, Briggs F, Cree BA, Baranzini SE, Fernandez-Viña M, Ramsay PP, Khan O, Royal W 3rd, Hauser SL, Barcellos LF, Oksenberg JR. Uncoupling the roles of HLA-DRB1 and HLA-DRB5 genes in multiple sclerosis. J Immunol. 2008 Oct 15;181(8):5473-80.

Cannizzo ES, Clement CC, Sahu R, Follo C, Santambrogio L. Oxidative stress, inflamm-aging and immunosenescence. J Proteomics. 2011 Jun 21.

Carrieri MP, Serraino D, Palmiotto F, Nucci G, Sasso F. A case-control study on risk factors for Peyronie's disease. J Clin Epidemiol. 1998 Jun;51(6):511-5.

Carthy JM, Garmaroudi FS, Luo Z, McManus BM. Wnt3a induces myofibroblast differentiation by upregulating TGF-β signaling through SMAD2 in a β-catenin-dependent manner. PLoS One. 2011;6(5):e19809. Epub 2011 May 18.

Cathcart MK. Regulation of superoxide anion production by NADPH oxidase in monocytes/macrophages: contributions to atherosclerosis. Arterioscler Thromb Vasc Biol. 2004 Jan;24(1):23-8.

Chamorro MN, Schwartz DR, Vonica A, Brivanlou AH, Cho KR, Varmus HE.FGF-20 and DKK1 are transcriptional targets of beta-catenin and FGF-20 is implicated in cancer and development. EMBO J. 2005 Jan 12;24(1):73-84.

Charlesworth B. Patterns of age-specific means and genetic variances of mortality rates predicted by the mutation-accumulation theory of ageing. J Theor Biol. 2001 May 7;210(1):47-65.

Chen YW, Zhao P, Borup R, Hoffman EP. Expression profiling in the muscular dystrophies: identification of novel aspects of molecular pathophysiology. J Cell Biol. 2000 Dec 11;151(6):1321-36.

Cheng, J.H., She, H., Han, Y.P., Wang, J., Xiong, S., Asahina, K., and Tsukamoto, H. (2008). Wnt antagonism inhibits hepatic stellate cell activation and liver fibrosis. Am. J. Physiol. Gastrointest. Liver Physiol. 294,G39–G49.

Cheon SS, Cheah AY, Turley S, Nadesan P, Poon R, Clevers H, Alman BA. beta-Catenin stabilization dysregulates mesenchymal cell proliferation, motility, and invasiveness and causes aggressive fibromatosis and hyperplastic cutaneous wounds. Proc Natl Acad Sci U S A. 2002 May 14;99(10):6973-8.

Cheon SS, Nadesan P, Poon R, Alman BA. Growth factors regulate beta-catenin-mediated TCF-dependent transcriptional activation in fibroblasts during the proliferative phase of wound healing. Exp Cell Res. 2004 Feb 15;293(2):267-74.

Chilosi M, Poletti V, Zamò A, Lestani M, Montagna L, Piccoli P, Pedron S, Bertaso M, Scarpa A, Murer B, Cancellieri A, Maestro R, Semenzato G, Doglioni C. Aberrant Wnt/beta-catenin pathway activation in idiopathic pulmonary fibrosis. Am J Pathol. 2003 May;162(5):1495-502.

Chiquet-Ehrismann R, Hagios C, Schenk S. The complexity in regulating the expression of tenascins. Bioessays. 1995 Oct;17(10):873-8.

Cho HY, Choi HJ, Sun HJ, Yang JY, An JH, Cho SW, Kim SW, Kim SY, Kim JE, Shin CS. Transgenic mice overexpressing secreted frizzled-related proteins (sFRP)4 under the control of serum amyloid P promoter exhibit low bone mass but did not result in disturbed phosphate homeostasis. Bone. 2010 Aug;47(2):263-71.

Clarke GM, Anderson CA, Pettersson FH, Cardon LR, Morris AP, Zondervan KT. Basic statistical analysis in genetic case-control studies. Nat Protoc. 2011 Feb;6(2):121-33.

Coert JH, Nérin JP, Meek MF. Results of partial fasciectomy for Dupuytren disease in 261 consecutive patients. Ann Plast Surg. 2006 Jul;57(1):13-7.

Coller HA, Grandori C, Tamayo P, Colbert T, Lander ES, Eisenman RN, Golub TR. Expression analysis with oligonucleotide microarrays reveals that MYC regulates genes involved in growth, cell cycle, signaling, and adhesion. Proc Natl Acad Sci U S A. 2000 Mar 28;97(7):3260-5.

O'Connell BC, Cheung AF, Simkevich CP, Tam W, Ren X, Mateyak MK, Sedivy JM. A large scale genetic analysis of c-Myc-regulated gene expression patterns. J Biol Chem. 2003 Apr 4;278(14):12563-73.

Coschigano KT, Clemmons D, Bellush LL, Kopchick JJ. Assessment of growth parameters and life span of GHR/BP gene-disrupted mice. Endocrinology. 2000 Jul;141(7):2608-13.

Crawford HC, Fingleton BM, Rudolph-Owen LA, Heppner Goss KJ, Rubinfeld B, Polakis P, Matrisian LM. The metalloproteinase matrilysin is a target of beta-catenin transactivation in intestinal tumors. Oncogene 1999;18:2883–2891.

Critchley EM, Vakil SD, Hayward HW, Owen VM. Dupuytren's disease in epilepsy: result of prolonged administration of anticonvulsants. J Neurol Neurosurg Psychiatry. 1976 May;39(5):498-503.

Couto-Gonzalez I, Brea-Garcia B, Taboada-Suárez A, González-Álvarez E. Aggressive Dupuytren's diathesis in a young woman. BMJ Case Rep. 2010 Sep 20;2010. doi:pii: bcr1220092592. 10.1136/bcr.12.2009.2592.

Cucoranu I, Clempus R, Dikalova A, Phelan PJ, Ariyan S, Dikalov S, Sorescu D. NAD(P)H oxidase 4 mediates transforming growth factor-beta1-induced differentiation of cardiac fibroblasts into myofibroblasts. Circ Res. 2005 Oct 28;97(9):900-7.

Cui J, Randell E, Renouf J, Sun G, Han FY, Younghusband B, Xie YG. Gender dependent association of thrombospondin-4 A387P polymorphism with myocardial infarction. Arterioscler Thromb Vasc Biol. 2004 Nov;24(11):e183-4.

Dahl G, Locovei S. Pannexin: to gap or not to gap, is that a question? IUBMB Life. 2006 Jul;58(7):409-19.

Dang CV, O'Donnell KA, Zeller KI, Nguyen T, Osthus RC, Li F. The c-Myc target gene network. Semin Cancer Biol. 2006 Aug;16(4):253-64.

Demers M, Rose AA, Grosset AA, Biron-Pain K, Gaboury L, Siegel PM, St-Pierre Y Am J. Overexpression of galectin-7, a myoepithelial cell marker, enhances spontaneous metastasis of breast cancer cells. Pathol. 2010 Jun;176(6):3023-31. Epub 2010 Apr 9.

Denkler K. Surgical complications associated with fasciectomy for dupuytren's disease: a 20-year review of the English literature. Eplasty. 2010 Jan 27;10:e15.

Desai SS, Hentz VR. The treatment of Dupuytren disease. J Hand Surg Am. 2011 May;36(5):936-42.

Desnoyers L, Arnott D, Pennica D. WISP-1 binds to decorin and biglycan. J Biol Chem. 2001 Dec 14;276(50):47599-607. Epub 2001 Oct 11.

Devlin B, Roeder K. Genomic control for association studies. Biometrics. 1999 Dec;55(4):997-1004.

Dolmans GH, Werker PM, Hennies HC, Furniss D, Festen EA, Franke L, Becker K, van der Vlies P, Wolffenbuttel BH, Tinschert S, Toliat MR, Nothnagel M, Franke A, Klopp N, Wichmann HE, Nürnberg P, Giele H, Ophoff RA, Wijmenga C; the Dutch Dupuytren Study Group, the German Dupuytren Study Group, the LifeLines Cohort Study, and the BSSH–GODD Consortium.Wnt Signaling and Dupuytren's Disease. N Engl J Med. 2011 Jul 6.

McDonald, JH. Handbook of Biological Statistics 2009 (2nd ed.). Sparky House Publishing, Baltimore, Maryland.

Doonan R, McElwee JJ, Matthijssens F, Walker GA, Houthoofd K, Back P, Matscheski A, Vanfleteren JR, Gems D. Against the oxidative damage theory of aging: superoxide dismutases protect against oxidative stress but have little or no effect on life span in Caenorhabditis elegans. Genes Dev. 2008 Dec 1;22(23):3236-41.

Dron M, Dandoy-Dron F, Guillo F, Benboudjema L, Hauw JJ, Lebon P, Dormont D, Tovey MG. Characterization of the human analogue of a Scrapie-responsive gene. J Biol Chem. 1998 Jul 17;273(29):18015-8.

Dwivedi A, Slater SC, George SJ. MMP-9 and -12 cause N-cadherin shedding and thereby beta-catenin signalling and vascular smooth muscle cell proliferation. Cardiovasc Res. 2009 Jan 1;81(1):178-86.

Dwyer MA, Joseph JD, Wade HE, Eaton ML, Kunder RS, Kazmin D, Chang CY, McDonnell DP. WNT11 expression is induced by estrogen-related receptor alpha and beta-

catenin and acts in an autocrine manner to increase cancer cell migration. Cancer Res. 2010 Nov 15;70(22):9298-308.

Early P. Population studies in Dupuytren's contracture. J Bone Joint Surg 1962;44B:602–13.

Ekblom P, Aufderheide E. Stimulation of tenascin expression in mesenchyme by epithelial-mesenchymal interactions. Int J Dev Biol. 1989 Mar;33(1):71-9.

Esko JD, Lindahl U. Molecular diversity of heparan sulfate. J Clin Invest. 2001 Jul;108(2):169-73.

Essers MA, de Vries-Smits LM, Barker N, Polderman PE, Burgering BM, Korswagen HC. Functional interaction between beta-catenin and FOXO in oxidative stress signaling. Science. 2005 May 20;308(5725):1181-4.

Esteves TC, Brand MD. The reactions catalysed by the mitochondrial uncoupling proteins UCP2 and UCP3. Biochim Biophys Acta. 2005 Aug 15;1709(1):35-44.

Falter E, Herndl E, Mühlbauer W. [Dupuytren's contracture. When operate? Conservative preliminary treatment?]. Fortschr Med. 1991 Apr 5;109(10):223-6.

Feissner RF, Skalska J, Gaum WE, Sheu SS. Crosstalk signaling between mitochondrial Ca2+ and ROS. Front Biosci. 2009 Jan 1;14:1197-218.

Fernandez PC, Frank SR, Wang L, Schroeder M, Liu S, Greene J, Cocito A, Amati B. Genomic targets of the human c-Myc protein. Genes Dev. 2003 May 1;17(9):1115-29. Epub 2003 Apr 14.

De Ferrari GV, Inestrosa NC. Wnt signaling function in Alzheimer's disease. Brain Res Brain Res Rev. 2000 Aug;33(1):1-12.

Flurkey K, Papaconstantinou J, Miller RA, Harrison DE. Lifespan extension and delayed immune and collagen aging in mutant mice with defects in growth hormone production. Proc Natl Acad Sci U S A. 2001 Jun 5;98(12):6736-41.

Freedman LP. Transcriptional targets of the vitamin D3 receptor-mediating cell cycle arrest and differentiation. J Nutr. 1999 Feb;129(2S Suppl):581S-586S.

Friedman DB, Johnson TE. A mutation in the age-1 gene in Caenorhabditis elegans lengthens life and reduces hermaphrodite fertility. Genetics. 1988 Jan;118(1):75-86.

De la Fuente M. Role of neuroimmunomodulation in aging. Neuroimmunomodulation. 2008;15(4-6):213-23.

De la Fuente M, Miquel J. An update of the oxidation-inflammation theory of aging: the involvement of the immune system in oxi-inflamm-aging. Curr Pharm Des. 2009;15(26):3003-26.

Fuerer C, Nusse R, Ten Berge D. Wnt signalling in development and disease. Max Delbrück Center for Molecular Medicine meeting on Wnt signaling in Development and Disease. EMBO Rep. 2008 Feb;9(2):134-8.

Fuerer C, Habib SJ, Nusse R. A study on the interactions between heparan sulfate proteoglycans and Wnt proteins. Dev Dyn. 2010 Jan;239(1):184-90.

Fujino G, Noguchi T, Takeda K, and Ichijo H. Thioredoxin and protein kinases in redox signaling. Semin Cancer Biol 26: 26, 2006.

Funato Y, Michiue T, Asashima M, Miki H. The thioredoxin-related redox-regulating protein nucleoredoxin inhibits Wnt-beta-catenin signalling through dishevelled. Nat Cell Biol. 2006 May;8(5):501-8.

Funato Y, Miki H. Nucleoredoxin, a novel thioredoxin family member involved in cell growth and differentiation. Antioxid Redox Signal. 2007 Aug;9(8):1035-57.

Garland CF, Comstock GW, Garland FC, Helsing KJ, Shaw EK, Gorham ED. Serum 25-hydroxyvitamin D and colon cancer: eight-year prospective study. Lancet. 1989 Nov 18;2(8673):1176-8.

Gerber RA, Perry R, Thompson R and Bainbridge C. Dupuytren's contracture: a retrospective database analysis to assess clinical management and costs in England. BMC Musculoskeletal Disorders 2011, 12:73

Ghosh S, Lertwattanarak R, Lefort N, Molina-Carrion M, Joya-Galeana J, Bowen BP, Garduno-Garcia JD, Abdul-Ghani M, Richardson A, Defronzo RA, Mandarino L, Van Remmen H, Musi N.Reduction in Reactive Oxygen Species Production by Mitochondria From Elderly Subjects With Normal and Impaired Glucose Tolerance. Diabetes. 2011 Jun 15.

Giepmans BN, Verlaan I, Hengeveld T, Janssen H, Calafat J, Falk MM, Moolenaar WH.Gap junction protein connexin-43 interacts directly with microtubules. Curr Biol. 2001a Sep 4;11(17):1364-8.

Giepmans BN, Hengeveld T, Postma FR, Moolenaar WH.Interaction of c-Src with gap junction protein connexin-43. Role in the regulation of cell-cell communication. J Biol Chem. 2001b Mar 16;276(11):8544-9.

van Gijn ME, Daemen MJ, Smits JF, Blankesteijn WM. The wnt-frizzled cascade in cardiovascular disease. Cardiovasc Res. 2002 Jul;55(1):16-24.

Giles RH, van Es JH, Clevers H. Caught up in a Wnt storm: Wnt signaling in cancer. Biochim Biophys Acta. 2003 Jun 5;1653(1):1-24.

Girodet PO, Ozier A, Trian T, Begueret H, Ousova O, Vernejoux JM, Chanez P, Marthan R, Berger P, Tunon de Lara JM. Mast cell adhesion to bronchial smooth muscle in asthma specifically depends on CD51 and CD44 variant 6. Allergy. 2010 Aug;65(8):1004-12.

Glinka A, Wu W, Delius H, Monaghan AP, Blumenstock C, Niehrs C. Dickkopf-1 is a member of a new family of secreted proteins and functions in head induction. Nature. 1998 Jan 22;391(6665):357-62.

Gloy J, Hikasa H, Sokol SY. Frodo interacts with Dishevelled to transduce Wnt signals. Nat Cell Biol. 2002 May;4(5):351-7.

Godtfredsen NS, Lucht H, Prescott E, Sørensen TI, Grønbaek M. A prospective study linked both alcohol and tobacco to Dupuytren's disease. J Clin Epidemiol. 2004 Aug;57(8):858-63.

Goldspink G, Fernandes K, Williams PE, Wells DJ. Age-related changes in collagen gene expression in the muscles of mdx dystrophic and normal mice. Neuromuscul Disord. 1994 May;4(3):183-91.

Gombert WM, Krumm A. Targeted deletion of multiple CTCF-binding elements in the human C-MYC gene reveals a requirement for CTCF in C-MYC expression. PLoS One. 2009 Jul 1;4(7):e6109.

González-Sancho JM, Aguilera O, García JM, Pendás-Franco N, Peña C, Cal S, García de Herreros A, Bonilla F, Muñoz A. The Wnt antagonist DICKKOPF-1 gene is a downstream target of beta-catenin/TCF and is downregulated in human colon cancer. Oncogene. 2005 Feb 3;24(6):1098-103.

Gordon MD, Nusse R. Wnt signaling: multiple pathways, multiple receptors, and multiple transcription factors. J Biol Chem. 2006 Aug 11;281(32):22429-33.

O'Gorman DB, Wu Y, Seney S, Zhu RD, Gan BS. Wnt expression is not correlated with beta-catenin dysregulation in Dupuytren's Disease. J Negat Results Biomed. 2006 Aug 30;5:13.

Gradl D, Kuhl M, Wedlich D. The Wnt/Wg signal transducer beta-catenin controls fibronectin expression. Mol Cell Biol 1999;19:5576–5587.

Groth S, Schulze M, Kalthoff H, Fändrich F, Ungefroren H. Adhesion and Rac1-dependent regulation of biglycan gene expression by transforming growth factor-beta. Evidence for oxidative signaling through NADPH oxidase. J Biol Chem. 2005 Sep 30;280(39):33190-9.

Gudmundsson KG, Arngrímsson R, Sigfússon N, Björnsson A, Jónsson T. Epidemiology of Dupuytren's disease: clinical, serological, and social assessment. The Reykjavik Study. J Clin Epidemiol. 2000 Mar 1;53(3):291-6.

Gudmundsson KG, Arngrímsson R, Sigfússon N, Jónsson T. Increased total mortality and cancer mortality in men with Dupuytren's disease: a 15-year follow-up study. J Clin Epidemiol. 2002 Jan;55(1):5-10.

Guğmundsson KG, Arngrímsson R, Sigfússon N, Jónsson T. Prevalence of joint complaints amongst individuals with Dupuytren's disease--from the Reykjavík study. Scand J Rheumatol. 1999;28(5):300-4.

Gumbiner BM. Regulation of cadherin adhesive activity. J Cell Biol. 2000 Feb 7;148(3):399-404.

Gunderson KL, Steemers FJ, Lee G, Mendoza LG, Chee MS. A genome-wide scalable SNP genotyping assay using microarray technology. Nat Genet. 2005 May;37(5):549-54.

Guo QM, Malek RL, Kim S, Chiao C, He M, Ruffy M, Sanka K, Lee NH, Dang CV, Liu ET. Identification of c-myc responsive genes using rat cDNA microarray. Cancer Res. 2000 Nov 1;60(21):5922-8.

Haertel-Wiesmann M, Liang Y, Fantl WJ, Williams LT. Regulation of cyclooxygenase-2 and periostin by Wnt-3 in mouse mammary epithelial cells. J Biol Chem. 2000 Oct 13;275(41):32046-51.

Hakstian RW. Long-term results of extensive fasciectomy. Br J Plast Surg. 1966 Apr;19(2):140-9.

The International HapMap Consortium. Integrating common and rare genetic variation in diverse human populations. Nature 467, 52-58. 2010.

He TC, Sparks AB, Rago C, Hermeking H, Zawel L, da Costa LT, Morin PJ, Vogelstein B, Kinzler KW. Identification of c-MYC as a target of the APC pathway. Science. 1998 Sep 4;281(5382):1509-12.

Hinz B, Celetta G, Tomasek JJ, Gabbiani G, Chaponnier C: Alphasmooth muscle actin expression upregulates fibroblast contractile activity. Mol Biol Cell 2001, 12:2730–2741

Hinz B: Masters and servants of the force: the role of matrix adhesions in myofibroblast force perception and transmission. Eur J Cell Biol 2006, 85:175–181

Hinz B, Pittet P, Smith-Clerc J, Chaponnier C, Meister JJ: Myofibroblast development is characterized by specific cell-cell adherens junctions. Mol Biol Cell 2004, 15:4310–4320

Hoang B, Moos M Jr, Vukicevic S, Luyten FP. Primary structure and tissue distribution of FRZB, a novel protein related to Drosophila frizzled, suggest a role in skeletal morphogenesis. J Biol Chem. 1996 Oct 18;271(42):26131-7.

Hollins F, Kaur D, Yang W, Cruse G, Saunders R, Sutcliffe A, Berger P, Ito A, Brightling CE, Bradding P. Human airway smooth muscle promotes human lung mast cell survival, proliferation, and constitutive activation: cooperative roles for CADM1, stem cell factor, and IL-6. J Immunol. 2008 Aug 15;181(4):2772-80.

Holmgren A. Antioxidant function of thioredoxin and glutaredoxin systems. Antioxid Redox Signal 2: 811–820, 2000.

Holzenberger M, Dupont J, Ducos B, Leneuve P, Géloën A, Even PC, Cervera P, Le Bouc Y. IGF-1 receptor regulates lifespan and resistance to oxidative stress in mice. Nature. 2003 Jan 9;421(6919):182-7.

Honda Y, Honda S. The daf-2 gene network for longevity regulates oxidative stress resistance and Mn-superoxide dismutase gene expression in Caenorhabditis elegans. FASEB J. 1999 Aug;13(11):1385-93.

Hovanes K, Li TW, Munguia JE, Truong T, Milovanovic T, Lawrence MJ, Holcombe RF, Waterman ML. Beta-cateninsensitive isoforms of lymphoid enhancer factor-1 are selectively expressed in colon cancer. Nat Genet 2001;28:53–57.

Howard JC, Varallo VM, Ross DC, Roth JH, Faber KJ, Alman B, Gan BS. Elevated levels of beta-catenin and fibronectin in three-dimensional collagen cultures of Dupuytren's disease cells are regulated by tension in vitro. BMC Musculoskelet Disord. 2003 Jul 16;4:16.

Hsieh JC, Kodjabachian L, Rebbert ML, Rattner A, Smallwood PM, Samos CH, Nusse R, Dawid IB, Nathans J. A new secreted protein that binds to Wnt proteins and inhibits their activities. Nature. 1999 Apr 1;398(6726):431-6.

Hurst LC, Badalamente MA, Hentz VR, Hotchkiss RN, Kaplan FT, Meals RA, Smith TM, Rodzvilla J; CORD I Study Group.Akelman E, Bear B, Belsky MR, Blazar P, Britton EN, Costas B, Frazier JL, Hentz V, Hotchkiss RN, Hurst LC, Badalamente MA, Kaplan FT, Lubahn J, McPherson S, Meals R, Peimer CA, Roeshot D. Injectable collagenase clostridium histolyticum for Dupuytren's contracture. N Engl J Med. 2009 Sep 3;361(10):968-79.

Imanaka-Yoshida K, Hiroe M, Nishikawa T, Ishiyama S, Shimojo T, Ohta Y, Sakakura T, Yoshida T. Tenascin-C modulates adhesion of cardiomyocytes to extracellular matrix during tissue remodeling after myocardial infarction. Lab Invest. 2001 Jul;81(7):1015-24.

International HapMap Consortium. The International Hap-Map Project. Nature. 2003;426:789 – 96.

International HapMap Consortium. A haplotype map of the human genome. Nature. 2005;437:1299 – 320.

Itasaki N, Jones CM, Mercurio S, Rowe A, Domingos PM, Smith JC, Krumlauf R. Wise, a context-dependent activator and inhibitor of Wnt signalling. Development. 2003 Sep;130(18):4295-305.

Jamora C, Fuchs E. Intercellular adhesion, signalling and the cytoskeleton. Nat Cell Biol. 2002 Apr;4(4):E101-8.

Jiménez B, Volpert OV, Crawford SE, Febbraio M, Silverstein RL, Bouck N.Signals leading to apoptosis-dependent inhibition of neovascularization by thrombospondin-1. Nat Med. 2000 Jan;6(1):41-8.

Jin T. The WNT signalling pathway and diabetes mellitus. Diabetologia. 2008 Oct;51(10):1771-80.

Jones FS, Jones PL. The tenascin family of ECM glycoproteins: structure, function, and regulation during embryonic development and tissue remodeling. Dev Dyn. 2000 Jun;218(2):235-59.

Kenyon C, Chang J, Gensch E, Rudner A, Tabtiang R. A C. elegans mutant that lives twice as long as wild type. Nature. 1993 Dec 2;366(6454):461-4.

Kimura KD, Tissenbaum HA, Liu Y, Ruvkun G. daf-2, an insulin receptor-like gene that regulates longevity and diapause in Caenorhabditis elegans. Science. 1997 Aug 15;277(5328):942-6.

Kirkwood TB, Austad SN. Why do we age? Nature. 2000 Nov 9;408(6809):233-8.

Klapholz-Brown Z, Walmsley GG, Nusse YM, Nusse R, Brown PO. Transcriptional program induced by Wnt protein in human fibroblasts suggests mechanisms for cell cooperativity in defining tissue microenvironments. PLoS One. 2007 Sep 26;2(9):e945.

Kim J, Lee JH, Iyer VR. Global identification of Myc target genes reveals its direct role in mitochondrial biogenesis and its E-box usage *in vivo*. PLoS One. 2008 Mar 12;3(3):e1798.

Kim J, Moody JP, Edgerly CK, Bordiuk OL, Cormier K, Smith K, Beal MF, Ferrante RJ. Mitochondrial loss, dysfunction and altered dynamics in Huntington's disease. Hum Mol Genet. 2010 Oct 15;19(20):3919-35.

Kim KA, Zhao J, Andarmani S, *et al*. R-Spondin proteins: a novel link to betacatenin activation. Cell Cycle 2006;5:23-6.

Kim KA, Wagle M, Tran K, Zhan X, Dixon MA, Liu S, Gros D, Korver W, Yonkovich S, Tomasevic N, Binnerts M, Abo A. R-Spondin family members regulate the Wnt pathway by a common mechanism. Mol Biol Cell. 2008 Jun;19(6):2588-96.

Koch W, Hoppmann P, de Waha A, Schömig A, Kastrati A. Polymorphisms in thrombospondin genes and myocardial infarction: a case-control study and a meta-analysis of available evidence. Hum Mol Genet. 2008 Apr 15;17(8):1120-6. Epub 2008 Jan 4.

Kolligs FT, Nieman MT, Winer I, Hu G, Van Mater D, Feng Y, Smith IM, Wu R, Zhai Y, Cho KR, Fearon ER. ITF-2, a downstream target of the Wnt/TCF pathway, is activated in human cancers with beta-catenin defects and promotes neoplastic transformation. Cancer Cell 2002;1:145–155.

Königshoff M, Kramer M, Balsara N, Wilhelm J, Amarie OV, Jahn A, Rose F, Fink L, Seeger W, Schaefer L, Günther A, Eickelberg O. WNT1-inducible signaling protein-1 mediates pulmonary fibrosis in mice and is upregulated in humans with idiopathic pulmonary fibrosis. J Clin Invest. 2009 Apr;119(4):772-87.

Korswagen HC. Regulation of the Wnt/beta-catenin pathway by redox signaling. Dev Cell. 2006 Jun;10(6):687-8.

Krause C, Kloen P, Ten Dijke P. Elevated transforming growth factor beta and mitogen-activated protein kinase pathways mediate fibrotic traits of Dupuytren's disease fibroblasts. Fibrogenesis Tissue Repair. 2011 Jun 28;4(1):14.

Krause KH. Tissue distribution and putative physiological function of NOX family NADPH oxidases. Jpn J Infect Dis. 2004 Oct;57(5):S28-9.

Kraytsberg Y, Simon DK, Turnbull DM, Khrapko K. Do mtDNA deletions drive premature aging in mtDNA mutator mice? Aging Cell. 2009 Aug;8(4):502-6.

Ku HH, Sohal RS. Comparison of mitochondrial pro-oxidant generation and anti-oxidant defenses between rat and pigeon: possible basis of variation in longevity and metabolic potential. Mech Ageing Dev. 1993 Nov;72(1):67-76.

Kumar NM, Gilula NB. The gap junction communication channel. Cell. 1996 Feb 9;84(3):381-8.

Kuramochi M, Fukuhara H, Nobukuni T *et al*. TSLC1 is a tumorsuppressor gene in human non-small-cell lung cancer. Nat Genet 2001;

27: 427–30.

Kuro-o M, Matsumura Y, Aizawa H, Kawaguchi H, Suga T, Utsugi T, Ohyama Y, Kurabayashi M, Kaname T, Kume E, Iwasaki H, Iida A, Shiraki-Iida T, Nishikawa S, Nagai R, Nabeshima YI. Mutation of the mouse klotho gene leads to a syndrome resembling ageing. Nature. 1997 Nov 6;390(6655):45-51.

Kuwert T, Lange HW, Langen KJ, Herzog H, Aulich A, Feinendegen LE. Cortical and subcortical glucose consumption measured by PET in patients with Huntington's disease. Brain. 1990 Oct;113 (Pt 5):1405-23.

Lamanna WC, Kalus I, Padva M, Baldwin RJ, Merry CL, Dierks T. The heparanome--the enigma of encoding and decoding heparan sulfate sulfation. J Biotechnol. 2007 Apr 30;129(2):290-307. Epub 2007 Feb 8.

Lambert AJ, Boysen HM, Buckingham JA, Yang T, Podlutsky A, Austad SN, Kunz TH, Buffenstein R, Brand MD. Low rates of hydrogen peroxide production by isolated heart mitochondria associate with long maximum lifespan in vertebrate homeotherms. Aging Cell. 2007 Oct;6(5):607-18. Epub 2007 Jun 27.

Lander ES, Linton LM, Birren B, Nusbaum C, Zody MC, Baldwin J, *et al*. Initial sequencing and analysis of the human genome. Nature. 2001;409:860 – 921.

Langston JW, Ballard P, Tetrud JW, Irwin I. 1983. Chronic Parkinsonism in humans due to a product of meperidine-analog synthesis. Science 219:979–980.

Larson D, Jerosch-Herold C. Clinical effectiveness of post-operative splinting after surgical release of Dupuytren's contracture: a systematic review. BMC Musculoskelet Disord. 2008 Jul 21;9:104.

Laurent TC, Fraser JR. Hyaluronan. FASEB J. 1992 Apr;6(7):2397-404.

Lawler J, Duquette M, Whittaker CA, Adams JC, McHenry K, DeSimone DW. Identification and characterization of thrombospondin-4, a new member of the thrombospondin gene family. J Cell Biol. 1993 Feb;120(4):1059-67.

Lee HY, Choi CS, Birkenfeld AL, Alves TC, Jornayvaz FR, Jurczak MJ, Zhang D, Woo DK, Shadel GS, Ladiges W, Rabinovitch PS, Santos JH, Petersen KF, Samuel VT, Shulman GI. Targeted expression of catalase to mitochondria prevents age-associated reductions in mitochondrial function and insulin resistance. Cell Metab. 2010 Dec 1;12(6):668-74.

Lee SS, Kennedy S, Tolonen AC, Ruvkun G. DAF-16 target genes that control C. elegans life-span and metabolism. Science. 2003 Apr 25;300(5619):644-7.

Lescher B, Haenig B, Kispert A. sFRP-2 is a target of the Wnt-4 signaling pathway in the developing metanephric kidney. Dev Dyn. 1998 Dec;213(4):440-51.

Li F, Wang Y, Zeller KI, Potter JJ, Wonsey DR, O'Donnell KA, Kim JW, Yustein JT, Lee LA, Dang CV. Myc stimulates nuclearly encoded mitochondrial genes and mitochondrial biogenesis. Mol Cell Biol. 2005 Jul;25(14):6225-34.

Liss GM, Stock SR. Can Dupuytren's contracture be work-related?: review of the evidence. Am J Ind Med. 1996 May;29(5):521-32.

Liu C, Li Y, Semenov M, Han C, Baeg GH, Tan Y, Zhang Z, Lin X, He X. Control of beta-catenin phosphorylation/degradation by a dual-kinase mechanism. *Cell.* 2002; 108: 837–847.

Liu H, Fergusson MM, Castilho RM, Liu J, Cao L, Chen J, Malide D, Rovira II, Schimel D, Kuo CJ, Gutkind JS, Hwang PM, Finkel T. Augmented Wnt signaling in a mammalian model of accelerated aging. Science. 2007 Aug 10;317(5839):803-6.

Livak KJ, Schmittgen TD. Analysis of relative gene expression data using real-time quantitative PCR and the 2-ΔΔCT method. Methods 2001;25:402–8.

Loeb LA, Wallace DC, Martin GM. The mitochondrial theory of aging and its relationship to reactive oxygen species damage and somatic mtDNA mutations. Proc Natl Acad Sci U S A. 2005 Dec 27;102(52):18769-70.

Loewenstein WR. Junctional intercellular communication: the cell-to-cell membrane channel. Physiol Rev. 1981 Oct;61(4):829-913.

Logan CY, Nusse R. The Wnt signaling pathway in development and disease. Annu Rev Cell Dev Biol. 2004;20:781-810.

Loos B, Puschkin V, Horch RE. 50 years experience with Dupuytren's contracture in the Erlangen University Hospital--a retrospective analysis of 2919 operated hands from 1956 to 2006. BMC Musculoskelet Disord. 2007 Jul 4;8:60.

Lopes N, Gregg D, Vasudevan S, Hassanain H, Goldschmidt-Clermont P, Kovacic H. Thrombospondin 2 regulates cell proliferation induced by Rac1 redox-dependent signaling. Mol Cell Biol. 2003 Aug;23(15):5401-8.

Louro ID, Bailey EC, Li X, South LS, McKie-Bell PR, Yoder BK, Huang CC, Johnson MR, Hill AE, Johnson RL, Ruppert JM.Comparative gene expression profile analysis of GLI and c-MYC in an epithelial model of malignant transformation. Cancer Res. 2002 Oct 15;62(20):5867-73.

Lowell BB, Shulman GI. (2005). Mitochondrial dysfunction and type 2 diabetes. Science 307:384–7.

Luck JV. Dupuytren's contracture; a new concept of the pathogenesis correlated with surgical management. J Bone Joint Surg Am. 1959 Jun;41-A(4):635-64.

Luo Y, Radice GL. Cadherin-mediated adhesion is essential for myofibril continuity across the plasma membrane but not for assembly of the contractile apparatus. J Cell Sci. 2003 Apr 15;116(Pt 8):1471-9.

De Magalhães JP, Church GM. Cells discover fire: employing reactive oxygen species in development and consequences for aging. Exp Gerontol. 2006 Jan;41(1):1-10.

Magnaldo T, Bernerd F, Darmon M.Galectin-7, a human 14-kDa S-lectin, specifically expressed in keratinocytes and sensitive to retinoic acid. Dev Biol. 1995 Apr;168(2):259-71.

Mäkelä EA, Jaroma H, Harju A, Anttila S, Vainio J. Dupuytren's contracture: the long-term results after day surgery. J Hand Surg Br. 1991 Aug;16(3):272-4.

Mammucari C, Rizzuto R. Signaling pathways in mitochondrial dysfunction and aging. Mech Ageing Dev. 2010 Jul-Aug;131(7-8):536-43.

Mansfield N J, Marshall J M. Symptoms of musculoskeletal disorders in stage rally drivers and co-drivers. Br J Sports Med 2001;35:314–320

Maravic M, Landais P. Dupuytren's disease in France – 1831 to 2001 – from description to economic burden. J Hand Surg [Br] 2005. 30B(5).

Marchand A, Atassi F, Gaaya A, Leprince P, Le Feuvre C, Soubrier F, Lompré AM, Nadaud S. The Wnt/beta-catenin pathway is activated during advanced arterial aging in humans. Aging Cell. 2011 Apr;10(2):220-32.

Martin GM, Austad SN, Johnson TE. Genetic analysis of ageing: role of oxidative damage and environmental stresses. Nat Genet. 1996 May;13(1):25-34.

Martin-Garrido A, Brown DI, Lyle AN, Dikalova A, Seidel-Rogol B, Lassègue B, San Martín A, Griendling KK. NADPH oxidase 4 mediates TGF-β-induced smooth muscle α-actin via p38MAPK and serum response factor. Free Radic Biol Med. 2011 Jan 15;50(2):354-62.

Martínez P, Blasco MA. Telomeric and extra-telomeric roles for telomerase and the telomere-binding proteins. Nat Rev Cancer. 2011 Mar;11(3):161-76.

Masmejean EH, Chavane H, Chantegret A, Issermann JJ, Alnot JY. The wrist of the formula 1 driver. Br J Sports Med. 1999 Aug;33(4):270-3.

Mason CC, Hanson RL, Ossowski V, Bian L, Baier LJ, Krakoff J, Bogardus C. Bimodal distribution of RNA expression levels in human skeletal muscle tissue. BMC Genomics. 2011 Feb 7;12:98.

Masuda M, Yageta M, Fukuhara H, Kuramochi M, Maruyama T, Nomoto A, Murakami Y. The tumor suppressor protein TSLC1 is involved in cell-cell adhesion. J Biol Chem. 2002 Aug 23;277(34):31014-9. Epub 2002 Jun 5.

Mao B, Wu W, Davidson G, Marhold J, Li M, Mechler BM, Delius H, Hoppe D, Stannek P, Walter C, Glinka A, Niehrs C. Kremen proteins are Dickkopf receptors that regulate Wnt/beta-catenin signalling. Nature. 2002 Jun 6;417(6889):664-7. Epub 2002 May 26.

Mao DY, Watson JD, Yan PS, Barsyte-Lovejoy D, Khosravi F, Wong WW, Farnham PJ, Huang TH, Penn LZ.Analysis of Myc bound loci identified by CpG island arrays shows that Max is essential for Myc-dependent repression. Curr Biol. 2003 May 13;13(10):882-6.

Medawar, P. B. An Unsolved Problem of Biology (Lewis, London, 1952).

Melchior-Becker A, Dai G, Ding Z, Schäfer L, Schrader J, Young MF, Fischer JW. Deficiency of biglycan causes cardiac fibroblasts to differentiate into a myofibroblast phenotype. J Biol Chem. 2011 May 13;286(19):17365-75.

Meng H, Zhang X, Lee SJ, Strickland DK, Lawrence DA, Wang MM. Low density lipoprotein receptor-related protein-1 (LRP1) regulates thrombospondin-2 (TSP2) enhancement of Notch3 signaling. J Biol Chem. 2010 Jul 23;285(30):23047-55. Epub 2010 May 14.

Mercurio S, Latinkic B, Itasaki N, Krumlauf R, Smith JC. Connective-tissue growth factor modulates WNT signalling and interacts with the WNT receptor complex. Development. 2004 May;131(9):2137-47.

Michaeloudes C, Sukkar MB, Khorasani NM, Bhavsar PK, Chung KF. TGF-β regulates Nox4, MnSOD and catalase expression, and IL-6 release in airway smooth muscle cells. Am J Physiol Lung Cell Mol Physiol. 2011 Feb;300(2):L295-304.

Michalik M, Wójcik KA, Jakieła B, Szpak K, Pierzchalska M, Sanak M, Madeja Z, Czyż J. Lithium Attenuates TGF-β(1)-Induced Fibroblasts to Myofibroblasts Transition in Bronchial Fibroblasts Derived from Asthmatic Patients. J Allergy (Cairo). 2012;2012:206109.

Misenheimer TM, Mosher DF. Biophysical characterization of the signature domains of thrombospondin-4 and thrombospondin-2. J Biol Chem. 2005 Dec 16;280(50):41229-35. Epub 2005 Oct 24.

Mitra A, Goldstein RY. Dupuytren's contracture in the black population: a review. Ann Plast Surg. 1994 Jun;32(6):619-22.

Moon RT, Kohn AD, Ferrari GVD, Kaykas A. WNT and beta-catenin signalling: diseases and therapies. Nat Rev Genet 2004;5:691-701.

Morgan KG, Gangopadhyay SS. Invited review: cross-bridge regulation by thin filament-associated proteins. J Appl Physiol. 2001 Aug;91(2):953-62.

Morimoto-Tomita M, Uchimura K, Werb Z, Hemmerich S, Rosen SD. Cloning and characterization of two extracellular heparin-degrading endosulfatases in mice and humans. J Biol Chem. 2002 Dec 20;277(51):49175-85. Epub 2002 Oct 3.

Morrish F, Giedt C, Hockenbery D. c-MYC apoptotic function is mediated by NRF-1 target genes. Genes Dev. 2003 Jan 15;17(2):240-55.

Mroue RM, El-Sabban ME, Talhouk RS. Connexins and the gap in context. Integr Biol (Camb). 2011 Apr;3(4):255-66.

Muley A, Majumder S, Kolluru GK, Parkinson S, Viola H, Hool L, Arfuso F, Ganss R, Dharmarajan A, Chatterjee S. Secreted frizzled-related protein 4: an angiogenesis inhibitor. Am J Pathol. 2010 Mar;176(3):1505-16.

Murakami Y. Functional cloning of a tumor suppressor gene, TSLC1, in human non-small cell lung cancer. Oncogene 2002; 21: 6936–48.

Murphy CT, McCarroll SA, Bargmann CI, Fraser A, Kamath RS, Ahringer J, Li H, Kenyon C. Genes that act downstream of DAF-16 to influence the lifespan of Caenorhabditis elegans. Nature. 2003 Jul 17;424(6946):277-83.

Murphy-Ullrich JE. The de-adhesive activity of matricellular proteins: is intermediate cell adhesion an adaptive state? J Clin Invest. 2001 Apr;107(7):785-90.

Naito AT, Shiojima I, Komuro I. Wnt signaling and aging-related heart disorders. Circ Res. 2010 Nov 26;107(11):1295-303.

Narouz-Ott L, Maurer P, Nitsche DP, Smyth N, Paulsson M. Thrombospondin-4 binds specifically to both collagenous and non-collagenous extracellular matrix proteins via its C-terminal domains. J Biol Chem. 2000 Nov 24;275(47):37110-7.

Nasr SJ, Atkins RW. Coincidental improvement in asthma during lithium treatment. Am J Psychiatry. 1977 Sep;134(9):1042-3.

Nelson WJ, Nusse R. Convergence of Wnt, beta-catenin, and cadherin pathways. Science. 2004 Mar 5;303(5663):1483-7.

Newsholme P, Haber EP, Hirabara SM, Rebelato EL, Procopio J, Morgan D, Oliveira-Emilio HC, Carpinelli AR, Curi R. Diabetes associated cell stress and dysfunction: role of mitochondrial and non-mitochondrial ROS production and activity. J Physiol. 2007 Aug 15;583(Pt 1):9-24.

Niida A, Hiroko T, Kasai M, Furukawa Y, Nakamura Y, Suzuki Y, Sugano S, Akiyama T. DKK1, a negative regulator of Wnt signaling, is a target of the beta-catenin/TCF pathway. Oncogene. 2004 Nov 4;23(52):8520-6.

Nusse R. Wnt signaling in disease and in development. Cell Res. 2005 Jan;15(1):28-32.

Noble J, Heathcote JG, Cohen H. Diabetes mellitus in the aetiology of Dupuytren's disease. J Bone Joint Surg Br. 1984 May;66(3):322-5.

Nör JE, Mitra RS, Sutorik MM, Mooney DJ, Castle VP, Polverini PJ. Thrombospondin-1 induces endothelial cell apoptosis and inhibits angiogenesis by activating the caspase death pathway. J Vasc Res. 2000 May-Jun;37(3):209-18.

Ochi K, Derfoul A, Tuan RS. A predominantly articular cartilage-associated gene, SCRG1, is induced by glucocorticoid and stimulates chondrogenesis *in vitro*. Osteoarthritis Cartilage. 2006 Jan;14(1):30-8. Epub 2005 Sep 26.

Ogg S, Paradis S, Gottlieb S, Patterson GI, Lee L, Tissenbaum HA, Ruvkun G. The Fork head transcription factor DAF-16 transduces insulin-like metabolic and longevity signals in C. elegans. Nature. 1997 Oct 30;389(6654):994-9.

Onumah OE, Jules GE, Zhao Y, Zhou L, Yang H, Guo Z. Overexpression of catalase delays G0/G1- to S-phase transition during cell cycle progression in mouse aortic endothelial cells. Free Radic Biol Med. 2009 Jun 15;46(12):1658-67.

Pálmer HG, González-Sancho JM, Espada J, Berciano MT, Puig I, Baulida J, Quintanilla M, Cano A, de Herreros AG, Lafarga M, Muñoz A. Vitamin D(3) promotes the differentiation of colon carcinoma cells by the induction of E-cadherin and the inhibition of beta-catenin signaling. J Cell Biol. 2001 Jul 23;154(2):369-87.

Pan D, Watson HK, Swigart C, Thomson JG, Honig SC, Narayan D. Microarray gene analysis and expression profiles of Dupuytren's contracture. Ann Plast Surg 2003, 50:618-622.

Pandur P, Läsche M, Eisenberg LM, Kühl M. Wnt-11 activation of a non-canonical Wnt signalling pathway is required for cardiogenesis. Nature. 2002 Aug 8;418(6898):636-41.

Papaconstantinou J. Insulin/IGF-1 and ROS signaling pathway cross-talk in aging and longevity determination. Mol Cell Endocrinol. 2009 Feb 5;299(1):89-100.

Paravicini TM, Touyz RM. Redox signaling in hypertension. Cardiovasc Res. 2006 Jul 15;71(2):247-58.

Parisi MS, Gazzerro E, Rydziel S, Canalis E.Expression and regulation of CCN genes in murine osteoblasts. Bone. 2006 May;38(5):671-7.

Park JB. Phagocytosis induces superoxide formation and apoptosis in macrophages. Exp Mol Med. 2003 Oct 31;35(5):325-35.

Park JE, Chang WY, Cho M. Induction of matrix metalloproteinase-9 by galectin-7 through p38 MAPK signaling in HeLa human cervical epithelial adenocarcinoma cells. Oncol Rep. 2009 Dec;22(6):1373-9.

Park JI, Venteicher AS, Hong JY, Choi J, Jun S, Shkreli M, Chang W, Meng Z, Cheung P, Ji H, McLaughlin M, Veenstra TD, Nusse R, McCrea PD, Artandi SE. Telomerase modulates Wnt signalling by association with target gene chromatin. Nature. 2009 Jul 2;460(7251):66-72.

Patti ME, Butti AJ, Crunkhorn S, Cusi K, Berria R, Kashyap S, Miyazaki Y, Kohane I, Costello M, Saccone R, *et al* (2003). Coordinated reduction of genes of oxidative metabolism in humans with insulin resistance and diabetes: Potential role of PGC1 and NRF1. Proc Natl Acad Sci USA 100:8466–71.

Peña-Silva RA, Miller JD, Chu Y, Heistad DD. Serotonin produces monoamine oxidase-dependent oxidative stress in human heart valves. Am J Physiol Heart Circ Physiol. 2009 Oct;297(4):H1354-60.

Pendás-Franco N, Aguilera O, Pereira F, González-Sancho JM, Muñoz A. Vitamin D and Wnt/beta-catenin pathway in colon cancer: role and regulation of DICKKOPF genes. Anticancer Res. 2008 Sep-Oct;28(5A):2613-23.

Pendás-Franco N, García JM, Peña C, Valle N, Pálmer HG, Heinäniemi M, Carlberg C, Jiménez B, Bonilla F, Muñoz A, González-Sancho JM. DICKKOPF-4 is induced by TCF/beta-catenin and upregulated in human colon cancer, promotes tumour cell invasion and angiogenesis and is repressed by 1alpha,25-dihydroxyvitamin D3. Oncogene. 2008 Jul 24;27(32):4467-77.

Pennica D, Swanson TA, Welsh JW, Roy MA, Lawrence DA, Lee J, Brush J, Taneyhill LA, Deuel B, Lew M, Watanabe C, Cohen RL, Melhem MF, Finley GG, Quirke P, Goddard AD, Hillan KJ, Gurney AL, Botstein D, Levine AJ. WISP genes are members of the connective tissue growth factor family that are up-regulated in wnt-1-transformed cells and aberrantly expressed in human colon tumors. Proc Natl Acad Sci U S A. 1998 Dec 8;95(25):14717-22.

Pérez VI, Bokov A, Van Remmen H, Mele J, Ran Q, Ikeno Y, Richardson A. Is the oxidative stress theory of aging dead? Biochim Biophys Acta. 2009 Oct;1790(10):1005-14.

Perls TT, Alpert L, Fretts RC. Middle-aged mothers live longer. Nature. 1997 Sep 11;389(6647):133.

Petersen KF, Dufour S, Befroy D, Garcia R, Shulman GI. (2004). Impaired mitochondrial activity in the insulin-resistant offspring of patients with type 2 diabetes. New Eng J Med 350:664–71.

Pruim RJ*, Welch RP*, Sanna S, Teslovich TM, Chines PS, Gliedt TP, Boehnke M, Abecasis GR, Willer CJ. (2010) LocusZoom: Regional visualization of genome-wide association scan results. Bioinformatics 2010 September 15; 26(18): 2336.2337.

Purcell S, Neale B, Todd-Brown K, Thomas L, Ferreira MA, Bender D, Maller J, Sklar P, de Bakker PI, Daly MJ, Sham PC. PLINK: a tool set for whole-genome association and population-based linkage analyses. Am J Hum Genet. 2007 Sep;81(3):559-75.

Qian A, Meals RA, Rajfer J, Gonzalez-Cadavid NF.Comparison of gene expression profiles between Peyronie's disease and Dupuytren's contracture. Urology. 2004 Aug;64(2):399-404.

Rao TP, Kühl M. An updated overview on Wnt signaling pathways: a prelude for more. Circ Res. 2010 Jun 25;106(12):1798-806.

Rayan GM. Clinical presentation and types of Dupuytren's disease. Hand Clin. 1999 Feb;15(1):87-96, vii.

Rhee SG, Chae HZ, and Kim K. Peroxiredoxins: a historical overview and speculative preview of novel mechanisms and emerging concepts in cell signaling. Free Radic Biol Med 38:1543–1552, 2005.

Rigoulet M, Yoboue ED, Devin A. Mitochondrial ROS generation and its regulation: mechanisms involved in H(2)O(2) signaling. Antioxid Redox Signal. 2011 Feb 1;14(3):459-68.

van Rijssen AL, Gerbrandy FS, Ter Linden H, Klip H, Werker PM. A comparison of the direct outcomes of percutaneous needle fasciotomy and limited fasciectomy for Dupuytren's disease: a 6-week follow-up study. J Hand Surg Am. 2006 May-Jun;31(5):717-25.

Robertson BW, Chellaiah MA. Osteopontin induces beta-catenin signaling through activation of Akt in prostate cancer cells. Exp Cell Res. 2010 Jan 1;316(1):1-11.

Rocques N, Abou Zeid N, Sii-Felice K, Lecoin L, Felder-Schmittbuhl MP, Eychène A, Pouponnot C. GSK-3-mediated phosphorylation enhances Maf-transforming activity. Mol Cell. 2007 Nov 30;28(4):584-97.

Rozen WM, Edirisinghe Y, Crock J (2012) Late Complications of Clinical *Clostridium Histolyticum* Collagenase Use in Dupuytren's Disease. PLoS ONE 7(8): e43406. doi:10.1371/journal.pone.0043406

Russell L, Forsdyke DR. A human putative lymphocyte G0/G1 switch gene containing a CpG-rich island encodes a small basic protein with the potential to be phosphorylated. DNA Cell Biol. 1991 Oct;10(8):581-91.

Sanz A, Fernández-Ayala DJ, Stefanatos RK, Jacobs HT. Mitochondrial ROS production correlates with, but does not directly regulate lifespan in Drosophila. Aging (Albany NY). 2010 Apr;2(4):200-23.

Schapira AH, Cooper JM, Dexter D, Jenner P, Clark JB, Marsden CD. Mitochondrial complex I deficiency in Parkinson's disease. Lancet. 1989 Jun 3;1(8649):1269.

Schmittgen TD, Livak KJ. Analyzing real-time PCR data by the comparative CT method. Nat Protocols 2008;3:1101–8.

Sgrò CM, Partridge L. A delayed wave of death from reproduction in Drosophila. Science. 1999 Dec 24;286(5449):2521-4.

Semënov M, Tamai K, He X. SOST is a ligand for LRP5/LRP6 and a Wnt signaling inhibitor. J Biol Chem. 2005 Jul 22;280(29):26770-5.

Shafer SL, Towler DA. Transcriptional regulation of SM22alpha by Wnt3a: convergence with TGFbeta(1)/Smad signaling at a novel regulatory element. J Mol Cell Cardiol. 2009 May;46(5):621-35.

Shih B, Brown JJ, Armstrong DJ, Lindau T, Bayat A. Differential gene expression analysis of subcutaneous fat, fascia, and skin overlying a Dupuytren's disease nodule in comparison to control tissue. Hand (N Y). 2009 Sep;4(3):294-301.

Shih B, Bayat A. Scientific understanding and clinical management of Dupuytren disease. Nat Rev Rheumatol. 2010 Dec;6(12):715-26.

Shimizu-Hirota R, Sasamura H, Kuroda M, Kobayashi E, Hayashi M, Saruta T. Extracellular matrix glycoprotein biglycan enhances vascular smooth muscle cell proliferation and migration. Circ Res. 2004 Apr 30;94(8):1067-74. Epub 2004 Mar 18.

Shin SY, Kim CG, Jho EH, Rho MS, Kim YS, Kim YH, Lee YH. Hydrogen peroxide negatively modulates Wnt signaling through downregulation of beta-catenin. Cancer Lett. 2004 Aug 30;212(2):225-31.

Sin WC, Tse M, Planque N, Perbal B, Lampe PD, Naus CC. Matricellular protein CCN3 (NOV) regulates actin cytoskeleton reorganization. J Biol Chem. 2009 Oct 23;284(43):29935-44.

Singh D, Solan JL, Taffet SM, Javier R, Lampe PD. Connexin 43 interacts with zona occludens-1 and -2 proteins in a cell cycle stage-specific manner. J Biol Chem. 2005 Aug 26;280(34):30416-21. Epub 2005 Jun 26.

Slattery D. Review: Dupuytren's disease in Asia and the migration theory of Dupuytren's disease. ANZ J Surg. 2010 Jul-Aug;80(7-8):495-9.

Smith SP, Devaraj VS, Bunker TD. The association between frozen shoulder and Dupuytren's disease. J Shoulder Elbow Surg. 2001 Mar-Apr;10(2):149-51.

Sohal RS, Sohal BH, Orr WC. Mitochondrial superoxide and hydrogen peroxide generation, protein oxidative damage, and longevity in different species of flies. Free Radic Biol Med. 1995 Oct;19(4):499-504.

Steemers FJ, Chang W, Lee G, Barker DL, Shen R, Gunderson KL. Whole-genome genotyping with the singlebase extension assay. Nat Methods. 2006;3:31 − 3.

Stenina OI, Desai SY, Krukovets I, Kight K, Janigro D, Topol EJ, Plow EF. Thrombospondin-4 and its variants: expression and differential effects on endothelial cells. Circulation. 2003 Sep 23;108(12):1514-9. Epub 2003 Sep 2.

Stolle K, Schnoor M, Fuellen G, Spitzer M, Cullen P, Lorkowski S.Cloning, genomic organization, and tissue-specific expression of the RASL11B gene. Biochim Biophys Acta. 2007 Jul-Aug;1769(7-8):514-24. Epub 2007 Jun 6.

Sugimura R, Li L. Noncanonical Wnt signaling in vertebrate development, stem cells, and diseases. Birth Defects Res C Embryo Today. 2010 Dec;90(4):243-56.

Surendran K, Schiavi S, Hruska KA. Wnt-dependent beta-catenin signaling is activated after unilateral ureteral obstruction, and recombinant secreted frizzled-related protein 4 alters the progression of renal fibrosis. J Am Soc Nephrol. 2005 Aug;16(8):2373-84.

Swerdlow RH, Khan SM. A "mitochondrial cascade hypothesis" for sporadic Alzheimer's disease. Med Hypotheses. 2004;63(1):8-20.

Tahara EB, Navarete FD, Kowaltowski AJ. Tissue-, substrate-, and site-specific characteristics of mitochondrial reactive oxygen species generation. Free Radic Biol Med. 2009 May 1;46(9):1283-97.

Takada R, Satomi Y, Kurata T, Ueno N, Norioka S, Kondoh H, Takao T, Takada S. Monounsaturated fatty acid modification of Wnt protein: its role in Wnt secretion. Dev Cell. 2006 Dec;11(6):791-801.

Takahashi M, Tsunoda T, Seiki M, Nakamura Y, Furukawa Y. Identification of membrane-type matrix metalloproteinase-1 as a target of the beta-catenin/Tcf4 complex in human colorectal cancers. Oncogene 2002;21:5861–5867.

Teder P, Vandivier RW, Jiang D, Liang J, Cohn L, Puré E, Henson PM, Noble PW. Resolution of lung inflammation by CD44. Science. 2002 Apr 5;296(5565):155-8.

Terman A, Gustafsson B, Brunk UT. The lysosomal-mitochondrial axis theory of postmitotic aging and cell death. Chem Biol Interact. 2006 Oct 27;163(1-2):29-37.

Tolwinski, N. S. & Wieschaus, E. Rethinking WNT signaling. Trends Genet. 20, 177–181 (2004).

Tomasek JJ, Gabbiani G, Hinz B, Chaponnier C, Brown RA: Myofibroblasts and mechano-regulation of connective tissue remodeling. Nat Rev Mol Cell Biol 2002, 3:349–363

Topol EJ, McCarthy J, Gabriel S, Moliterno DJ, Rogers WJ, Newby LK, Freedman M, Metivier J, Cannata R, O'Donnell CJ, Kottke-Marchant K, Murugesan G, Plow EF, Stenina O, Daley GQ. Single nucleotide polymorphisms in multiple novel thrombospondin genes may be associated with familial premature myocardial infarction. Circulation. 2001 Nov 27;104(22):2641-4.

Trifunovic A, Wredenberg A, Falkenberg M, Spelbrink JN, Rovio AT, Bruder CE, Bohlooly-Y M, Gidlöf S, Oldfors A, Wibom R, Törnell J, Jacobs HT, Larsson NG. Premature ageing in mice expressing defective mitochondrial DNA polymerase. Nature. 2004 May 27;429(6990):417-23.

Tubiana R. Evaluation of deformities in Dupuytren's disease. Ann Chir Main. 1986;5(1):5-11.

Tunn S, Gurr E, Delbrück A, Buhr T, Flory J. The distribution of unsulphated and sulphated glycosaminoglycans in palmar fascia from patients with Dupuytren's disease and healthy subjects. J Clin Chem Clin Biochem. 1988 Jan;26(1):7-14.

Turner N, Bruce CR, Beale SM, Hoehn KL, So T, Rolph MS, Cooney GJ Excess lipid availability increases mitochondrial fatty acid oxidative capacity in muscle: evidence against a role for reduced fatty acid oxidation in lipid-induced insulin resistance in rodents.

Diabetes. 2007 Aug;56(8):2085-92.

Uchimura K, Morimoto-Tomita M, Bistrup A, Li J, Lyon M, Gallagher J, Werb Z, Rosen SD. HSulf-2, an extracellular endoglucosamine-6-sulfatase, selectively mobilizes heparin-bound growth factors and chemokines: effects on VEGF, FGF-1, and SDF-1. BMC Biochem. 2006 Jan 17;7:2.

Uematsu K, He B, You L, Xu Z, McCormick F, Jablons DM. Activation of the Wnt pathway in non small cell lung cancer: evidence of dishevelled overexpression. Oncogene. 2003 Oct 16;22(46):7218-21.

Varallo VM, Gan BS, Seney S, Ross DC, Roth JH, Richards RS, McFarlane RM, Alman B, Howard JC. Beta-catenin expression in Dupuytren's disease: potential role for cell-matrix interactions in modulating beta-catenin levels *in vivo* and *in vitro*. Oncogene. 2003 Jun 12;22(24):3680-4.

Veeman MT, Axelrod JD, Moon RT. A second canon. Functions and mechanisms of beta-catenin-independent Wnt signaling. Dev Cell. 2003 Sep;5(3):367-77.

Venter JC, Adams MD, Myers EW, Li PW, Mural RJ, Sutton GG, *et al*. The sequence of the human genome. Science. 2001;291:1304 – 51.

Wei CJ, Francis R, Xu X, Lo CW.Connexin43 associated with an N-cadherin-containing multiprotein complex is required for gap junction formation in NIH3T3 cells. J Biol Chem. 2005 May 20;280(20):19925-36. Epub 2005 Feb 28.

Werner S, Grose R: Regulation of wound healing by growth factors and cytokines. Physiol Rev 2003, 83:835–870

Wessel J, Topol EJ, Ji M, Meyer J, McCarthy JJ. Replication of the association between the thrombospondin-4 A387P polymorphism and myocardial infarction. Am Heart J. 2004 May;147(5):905-9.

van de Wetering M, Sancho E, Verweij C, de Lau W, Oving I, Hurlstone A, van der Horn K, Batlle E, Coudreuse D, Haramis AP, Tjon-Pon-Fong M, Moerer P, van den Born M, Soete G, Pals S, Eilers M, Medema R, Clevers H. The beta-catenin/TCF-4 complex imposes a crypt progenitor phenotype on colorectal cancer cells. Cell. 2002 Oct 18;111(2):241-50.

Whitelock JM, Iozzo RV. Heparan sulfate: a complex polymer charged with biological activity. Chem Rev. 2005 Jul;105(7):2745-64.

Wielenga VJ, Smits R, Korinek V, Smit L, Kielman M, Fodde R, Clevers H, Pals ST. Expression of CD44 in Apc and Tcf mutant mice implies regulation by the WNT pathway. Am J Pathol. 1999 Feb;154(2):515-23.

Wilbrand S, Ekbom A, Gerdin B. Cancer incidence in patients treated surgically for Dupuytren's contracture. J Hand Surg Br. 2000 Jun;25(3):283-7.

Willert J, Epping M, Pollack JR, Brown PO, Nusse R. A transcriptional response to Wnt protein in human embryonic carcinoma cells. BMC Dev Biol. 2002 Jul 2;2:8.

Willert K, Brown JD, Danenberg E, Duncan AW, Weissman IL, Reya T, Yates JR 3rd, Nusse R. Wnt proteins are lipid-modified and can act as stem cell growth factors. Nature. 2003 May 22;423(6938):448-52.

Williams GC. Pleiotropy, natural selection and the evolution of senescence. Evolution 11, 398–411 (1957).

Williams H, Johnson JL, Jackson CL, White SJ, George SJ. MMP-7 mediates cleavage of N-cadherin and promotes smooth muscle cell apoptosis. Cardiovasc Res. 2010 Jul 1;87(1):137-46.

Winchester R, Ebers G, Fu SM, Espinosa L, Zabriskie J, Kunkel HG.B-cell alloantigen Ag 7a in multiple sclerosis. Lancet. 1975 Oct 25;2(7939):814.

Woodruff MJ, Waldram MA. A clinical grading system for Dupuytren's contracture. J Hand Surg Br. 1998 Jun;23(3):303-5.

Wurster-Hill DH, Brown F, Park JP, Gibson SH. Cytogenetic studies in Dupuytren contracture. Am J Hum Genet. 1988 Sep;43(3):285-92.

Xiao NM, Zhang YM, Zheng Q, Gu J. Klotho is a serum factor related to human aging. Chin Med J (Engl). 2004 May;117(5):742-7.

Xu X, Li WE, Huang GY, Meyer R, Chen T, Luo Y, Thomas MP, Radice GL, Lo CW. J Modulation of mouse neural crest cell motility by N-cadherin and connexin 43 gap junctions. Cell Biol. 2001 Jul 9;154(1):217-30.

Yan D, Wiesmann M, Rohan M, Chan V, Jefferson AB, Guo L, Sakamoto D, Caothien RH, Fuller JH, Reinhard C, Garcia PD, Randazzo FM, Escobedo J, Fantl WJ, Williams LT. Elevated expression of axin2 and hnkd mRNA provides evidence that Wnt/beta -catenin signaling is activated in human colon tumors. Proc Natl Acad Sci U S A. 2001 Dec 18;98(26):14973-8.

Yi F, Sun J, Lim GE, Fantus IG, Brubaker PL, Jin T. Cross talk between the insulin and Wnt signaling pathways: evidence from intestinal endocrine L cells. Endocrinology. 2008 May;149(5):2341-51.

Yoon JC, Ng A, Kim BH, Bianco A, Xavier RJ, Elledge SJ. Wnt signaling regulates mitochondrial physiology and insulin sensitivity. Genes Dev. 2010 Jul 15;24(14):1507-18.

Zandbergen F, Mandard S, Escher P, Tan NS, Patsouris D, Jatkoe T, Rojas-Caro S, Madore S, Wahli W, Tafuri S, Müller M, Kersten S. The G0/G1 switch gene 2 is a novel PPAR target gene. Biochem J. 2005 Dec 1;392(Pt 2):313-24.

Zanocco-Marani T, Vignudelli T, Parenti S, Gemelli C, Condorelli F, Martello A, Selmi T, Grande A, Ferrari S. TFE3 transcription factor regulates the expression of MAFB during macrophage differentiation. Exp Cell Res. 2009 Jul 1;315(11):1798-808.

Zerajic D, Finsen V. Dupuytren's disease in Bosnia and Herzegovina. An epidemiological study. BMC Musculoskelet Disord. 2004 Mar 29;5:10.

Zhan F, Huang Y, Colla S, Stewart JP, Hanamura I, Gupta S, Epstein J, Yaccoby S, Sawyer J, Burington B, Anaissie E, Hollmig K, Pineda-Roman M, Tricot G, van Rhee F, Walker R, Zangari M, Crowley J, Barlogie B, Shaughnessy JD Jr. The molecular classification of multiple myeloma. Blood. 2006 Sep 15;108(6):2020-8.

Zhang DY, Wang HJ, Tan YZ. Wnt/β-Catenin Signaling Induces the Aging of Mesenchymal Stem Cells through the DNA Damage Response and the p53/p21 Pathway. PLoS One. 2011;6(6):e21397.

Zhu X, Ding M, Yu ML, Feng MX, Tan LJ, Zhao FK. Identification of galectin-7 as a potential biomarker for esophageal squamous cell carcinoma by proteomic analysis. BMC Cancer. 2010 Jun 15;10:290.

7 Appendix

7.1 Questionnaires and Informed Consent Forms

Prof. Dr. Peter Nürnberg
Cologne Center for Genomics
Universität zu Köln
Weyertal 115b
50931 Köln

Dr. Hans Christian Hennies
Cologne Center for Genomics
Universität zu Köln
Weyertal 115b
50931 Köln

DUPUYTREN'SCHE ERKRANKUNG: KLINISCHE DATEN

Name, Vorname: _____

Geburtsdatum: _____

Barcode-Etikett

Geschlecht: weiblich ○   männlich ○

ethnische/geografische Herkunft: deutsch ○   andere: _____

Tätigkeit/bes. manuelle Belastung: _____

Dupuytren'sche Erkrankung:

Rechts: ○   Rezidiv ○   Erste OP (Jahr):_____   Stadium nach Tubiana: _____
                                                              (0, 1, 2, 3, 4)
Links: ○   Rezidiv ○   Erste OP (Jahr):_____   Stadium nach Tubiana: _____
                                                              (0, 1, 2, 3, 4)

Dupuytren nach Trauma oder OP?: ○ ja   ○ nein   Sudeck-Dystrophie: ○ _____

Ektopisch (z.B. Morbus Ledderhose): _____

Familienanamnese: _____
(ggf. Stammbaum beifügen)

Krankheiten:

Diabetes mellitus: Ja ○   nein ○   _____

Rheumatoide Arthritis: Ja ○   nein ○   _____

Epilepsie: Ja ○   nein ○   _____

andere Krankheiten: _____

Bei Frauen: Eierstock-OP: Ja ○   nein ○   _____

               Hormone: Ja ○   nein ○   _____

               Alter bei Menopause: _____

Lebensgewohnheiten:

Nikotin: ○ <5 Z./d   ○ <20 Z./d   ○ >20 Z./d   ○ nie   ○ ja ehemals bis: _____

Alkohol: ○ gelegentlich   ○ regelmäßig   ○ nie   ○ ja ehemals bis: _____

Medikamenteneinnahme:

Antiarrhythmica: ○ ja   Antihypertensiva: ○ ja   Antiepileptica: ○ ja

Andere Medikamente: _____

Arzt: _____

Figure 68. Latest version of the questionnaire filled out by Dupuytren patients participating in the study.

Dr. Hans Christian Hennies
Cologne Center for Genomics
Universität zu Köln
Zülpicher Str. 47
50674 Köln

Prof. Dr. Peter Nürnberg
Cologne Center for Genomics
Universität zu Köln
Zülpicher Str. 47
50674 Köln

DUPUYTREN'SCHE ERKRANKUNG: KLINISCHE DATEN

Name, Vorname:

Geburtsdatum:

Geschlecht: ◯ männlich ◯ weiblich

ethnische/geografische Herkunft:

Dupuytren'sche Erkrankung:

Alter bei erster OP:

Stadium nach Tubiana: ◯ 0 ◯ 1 ◯ 2 ◯ 3 ◯ 4

Familienanamnese:

ektopisch:

Krankheiten:

Diabetes mellitus: ◯ ja ◯ nein

Rheumatoide Arthritis: ◯ ja ◯ nein

Epilepsie: ◯ ja ◯ nein

andere Autoimmunerkrankungen: ◯ ja ◯ nein

andere Krankheiten:

Lebensgewohnheiten:

Nikotin: ◯ nein ◯ ja: ◯ <5 Z./d ◯ <20 Z./d ◯ >20 Z./d

Alkohol: ◯ nein ◯ ja: ◯ gelegentlich ◯ regelmäßig

weitere Kommentare:

Figure 69. First version of the questionnaire filled out by Dupuytren patients participating in the Study

Prof. Dr. Peter Nürnberg
Cologne Center for Genomics
Universität zu Köln
Weyertal 115b
50931 Köln

Dr. Hans Christian Hennies
Cologne Center for Genomics
Universität zu Köln
Weyertal 115b
50931 Köln

DUPUYTREN´SCHE ERKRANKUNG: EINWILLIGUNGSERKLÄRUNG
Blutprobe zur Gewinnung von DNS
Gewebeprobe zur Gewinnung von RNS und Zellen

Über die Verfahren zur Entnahme einer Blutprobe und der Gewinnung von Erbsubstanz (DNS) aus dieser Blutprobe und zur Entnahme einer Gewebeprobe, der Gewinnung von Zellen aus dieser Gewebeprobe und der Kultivierung dieser Zellen in künstlichen Medien bin ich hinreichend aufgeklärt worden.

Ich bin mit der Teilnahme an der Studie einverstanden. Die Teilnahme an der Studie erfolgt freiwillig. Die Studienleiter haben mir versichert, dass diese Einwilligung ohne Angabe von Gründen jederzeit zurückgezogen werden kann. Ich verzichte auf ein Entgelt dafür, dass ich die Proben für Forschungszwecke zur Verfügung gestellt habe.

	Ja	Nein
Ich bin damit einverstanden, dass meine Proben für die genetische Erforschung der Dupuytren'schen Erkrankung untersucht werden.	☐	☐
Ich möchte, dass meine Proben nach Abschluss der genetischen Untersuchung vernichtet werden.	☐	☐
Meine Proben sollen vernichtet werden, wenn ich später erklären sollte, dass ich nicht mehr an der Untersuchung teilnehmen möchte.	☐	☐
Ich bin damit einverstanden, dass auch im Fall der Vernichtung der Proben die Ergebnisse der Untersuchung weiter verwendet werden.	☐	☐
Ich bin damit einverstanden, dass meine Proben auch für andere genetische Forschungen verwendet werden.	☐	☐
Ich bin damit einverstanden, dass die Studienleiter oder von ihnen bestimmte Personen in der Zukunft mit mir Kontakt aufnehmen.	☐	☐

Name des Spenders/der Spenderin: _____, geboren am _____

Datum und Unterschrift (Spender): _____

Name des aufklärenden Arztes: _____

Für die Richtigkeit: Datum und Unterschrift (Arzt): _____

Figure 70. Informed consent form filled out by Dupuytren patients participating in the Study.

Prof. Dr. Peter Nürnberg
Cologne Center for Genomics
Universität zu Köln
Weyertal 115b
50931 Köln

Dr. Hans Christian Hennies
Cologne Center for Genomics
Universität zu Köln
Weyertal 115b
50931 Köln

DUPUYTREN'SCHE ERKRANKUNG: KLINISCHE DATEN FÜR KONTROLLEN:

Name, Vorname: _____

Barcode-Etikett

Geburtsdatum: _____

Geschlecht: ◯ weiblich ◯ männlich

ethnische/geografische Herkunft: ◯ deutsch andere: _____

Art der OP/Herkunft des entnommenen Bindegewebes: _____

Dupuytren'sche Erkrankung:

Liegt vor: ◯ ja ◯ nein

Familienanamnese: ◯ negativ ◯ positiv: _____

Dupuytren'sche Erkrankung:

Liegt vor: ◯ ja ◯ nein

Familienanamnese: ◯ negativ ◯ positiv: _____

EINWILLIGUNGSERKLÄRUNG:

Über das Verfahren zur Entnahme einer Gewebeprobe, der Gewinnung von RNA und Proteinen aus dieser Gewebeprobe bin ich hinreichend aufgeklärt worden.

Ich bin mit der Teilnahme an der Studie einverstanden. Die Teilnahme an der Studie erfolgt freiwillig. Die Studienleiter haben mir versichert, dass diese Einwilligung ohne Angabe von Gründen jederzeit zurückgezogen werden kann. Ich verzichte auf ein Entgelt dafür, dass ich die Proben für Forschungszwecke zur Verfügung gestellt habe.

Ich bin damit einverstanden, dass meine Proben für die genetische
Erforschung der Dupuytren'schen Erkrankung untersucht werden. ◯ ja ◯ nein

Datum und Unterschrift: _____

Kommentare: _____

_____

Arzt: _____

Figure 71. Questionnaire and informed consent form fillt out by control persons participating in the Dupuytren Study.

7.2 Primer Sequences

Table 30. Primer for sequencing of the SFRP4 gene.

primer name	primer sequence	product size (bp)
SFRP4_1_F	TGCATTTGCAAAGTAGTGACG	542
SFRP4_1_R	CAGAGTTTGTAACTCTCAAGTT	
SFRP4_2_F	GAAGGCTTGAGTCCACACTGATAC	379
SFRP4_2_R	CTCTGTGGTCTCTTTCTGTCTGGA	
SFRP4_3-1_F	GGTGATGTCACCGCTTCTGCAC	456
SFRP4_3-1_R	CACAGCGCCACTAGGATGGAGAGG	
SFRP4_3-2_F	GCGCTTTCTGTCTGCCGGGGTCG	556
SFRP4_3-2_R	CAGTTCTCGATTGGCAGCCACAGC	
SFRP4_4+5_F	CCAGCTGGGTGAACAGACCAAATC	356
SFRP4_4+5_R	CCAGCTTTGTAATGAACCAAGTCTC	
SFRP4_6_F	CTTTAAGAGAGGCTCAGAAGTTG	351
SFRP4_6_R	CTGAGATTGAGGTCTTCCTAACAGTG	
SFRP4_7_F	GCAGATCAGCAGATCATCTCAATAC	333
SFRP4_7_R	GAAATCTGTTATGTGCACTTACATC	
SFRP4_8-1_F	CACATTAGCTGAGCACCATAAAGGG	521
SFRP4_8-1_R	GTTACTCTGAATGCAATGCAATAAGCC	
SFRP4_8-2_F	GCAGCATTTTTCTTAAGGCTATGC	389
SFRP4_8-2_R	CCTTCTGCAGACCATAAACACATAAAG	
SFRP4_8-3_F	GCTTCTAAGAAGGAACAGTAGTGG	610
SFRP4_8-3_R	GATTAAAGTATCCCAACTGTCAAG	
SFRP4_8-4_F	CTTTGCCTAAATACATGTGAGAGGAG	634
SFRP4_8-4_R	CAAATGTATCCCAAGGTACTAATGAAG	

Table 31. Primer for sequencing of the EPDR1 gene.

primer name	primer sequence	product size (bp)
EPDR1_1_F	TGAGGTTTTATGGTCTGTTGACATTC	297
EPDR1_1_R	GATTCTGAATTAGGACTATGCCAAC	
EPDR1_2_F	GAATCGCCAGTATGTGCAGTTTG	348
EPDR1_2_R	CATTGTGTAATTACTGTCATTGGCAAAC	
EPDR1_3-1_F	CTTGCCCCTCCCTGTGTGATTACC	468
EPDR1_3-1_R	CGTCCTGGCATCGCGGTCAGCCTT	
EPDR1_3-2_F	GAGCCGGCGGGAGCCACTCTGATC	457
EPDR1_3-2_R	GCAAGGGGCCGGAAAGAGTTACAG	
EPDR1_4_F	CCTGCAAGAGGTACAGGTCATCG	426
EPDR1_4_R	GTGCCTCTCTAGCAGATGTCTCTAG	
EPDR1_5_F	GATTGCCTAGCTAGTAATTTCTTTC	471
EPDR1_5_R	CCTGCAGACCTAAGTGGAGGCT	
EPDR1_6-1_F	ACCACCATAAGAAAAAATATGAACTTC	448
EPDR1_6-1_R	TCTGTAAACAGAGCTTGAGTAGTCA	
EPDR1_6-2_F	CAGCTGGAGATGGATATGAGACTAG	404
EPDR1_6-2_R	GGGCATTCTCTGCAGGGAATTTAAGA	
EPDR1_6-3_F	AGAAGTTTGCCTTGGCAGCAAGTATT	420
EPDR1_6-3_R	GCACATACATCAATACTCTTGCATAG	
EPDR1_6-4_F	GGCAGTTTAGAGAATCCTAATGTCT	450
EPDR1_6-4_R	GTACCCAAGGAGCTCACAGCCAAGAT	
EPDR1_6-5_F	GTTGCACCTTGCATCTTGAGCATGCAT	373
EPDR1_6-5_R	AATATAGGTGTCACACATTTCTCCTGG	
EPDR1_6-6_F	CTATTCTAGATGCTTCTACTGTTATG	356
EPDR1_6-6_R	AAATGGATCAAGAATGACTTGGAAGC	

Table 32. Primer for qPCR.

primer name	primer sequence	product size (bp)
ACTA2_F	ccgcaaatgcttctaaaacac	70
ACTA2_R	tccacaggacattcacagttg	
APP_F	tggaagaggtggttcgagtt	60
APP_R	acttgtcaacggcatcagg	
ATP5B_F	cagcagattttggcaggtg	70
ATP5B_R	cttcaatgggtcccaccata	
CASP3_F	ctggttttcggtgggtgt	88
CASP3_R	ccactgagttttcagtgttctcc	
CAT_F	ccatcgcagttcggttct	64
CAT_R	gggtcccgaactgtgtca	
CDH1_F	cgactaggggactcgagaga	73
CDH1_R	accaccagcaacgtgatttc	
COX8A_F	ggaagcttgggatcatgga	95
COX8A_R	ggtctccaggtgtgacagg	
EIF2C2_F	AGAACGAGCGGGGGACAAGCA	121
EIF2C2_R	GTGCAGCGCACGTAGGTGTGA	
EIF3H_F	GATGCGGAGCCTTCGCCATGT	95
EIF3H_R	CCAGGAGTGCCCGGGTAACG	
EPDR1_F	agaggaaggcgctgatcc	90
EPDR1_R	tggtggcttggtcaatctg	
FZD4_F	ttcacaccgctcatccagta	76
FZD4_R	tgcacattggcacataaaca	
GSK3B_F	AGGTCCTGGGAACTCCAACAAGGG	118
GSK3B_R	GGAGTTCGGGGTCGGAAGACCTT	
MAFB_F	agggaagctgccaagctc	67
MAFB_R	atttgaccataagacaaggctgt	
MAOA_F	aacccaaaacagaatcttacgc	113
MAOA_R	cccgaaatggatatgttttcc	
MnSOD_F	tgtgctttctcgtcttcagc	61
MnSOD_R	gagcccagatacccaaag	
PCDH18_F	aaccacgtgccagagaattt	77
PCDH18_R	gaaagaagctgagagacctgct	
RPL19_F	GGGCCCGAGCGAGCTCTTTCCTT	102
RPL19_R	TTCTTGCCACAGCGGAGGACACT	
RSPO2_F	ccatccgggtactatggaca	74
RSPO2_R	gaatcacagttttctattctgcatctt	
SFRP4_F	gcctgaagccatcgtcac	68
SFRP4_R	ccatcatgtctggtgtgatgt	
SOD1_F	ccatgttcatgagtttggagataa	73
SOD1_R	tctggatagaggattaaagtgagga	
THBS4_F	gctccagcttctacgtggtc	125
THBS4_R	ccctggacctgtcttagacttc	
WNT2_F	tttggcagggtcctactcc	87
WNT2_R	cctggtgatggcaaatacaa	
WNT7B_F	CCATCTGCCAGAGTCGGCCCGATG	110
WNT7B_R	GGCAGAGCAGTTCCAGCGTCCGAAG	

7.3 GWAS detailed Results

Table 33. GWAS detailed results 186 cases compared with 1618 controls.

CHR	SNP	POSITION	UNADJ	GC	QQ	BONF	HOLM	SIDAK_SS	SIDAK_SD	FDR_BH	FDR_BY
1	rs1890024	162,115,263-162,116,263	1.30E-10	1.14E-09	7.49E-02	9.26E-05	9.26E-05	9.26e-08	9.26E-05	1.72E-06	2.41E-05
1	rs12126332	162,600,414-162,601,414	3.90E-07	1.86E-06	0.0001672	0.0002785	0.0002785	0.0002785	0.0002784	2.31E-03	3.25E-02
1	rs6674453	19,433,112-19,434,112	1.74E-07	8.82E-07	0.0001434	0.0001246	0.0001246	0.0001246	0.0001246	1.21E-06	1.70E-02
1	rs7554574	81,460,797-81,461,797	1.71E-06	7.26E-06	0.0002022	0.001219	0.001219	0.001219	0.001218	8.41e-06	0.0001182
1	rs11586072	81,986,661-81,987,661	6.67e-06	1.52E-02	0.0004135	1	1	0.9915	0.9915	0.01611	0.2264
1	rs10913320	177,364,005-177,365,005	4.16E-10	3.34E-09	8.05E-02	2.98E-04	2.98E-04	2.98E-04	2.98E-04	5.13E-06	7.21E-05
1	rs6540808	214,103,271-214,104,271	3.47E-07	1.67E-06	0.000163	0.0002478	0.0002477	0.0002477	0.0002477	2.12E-03	2.98E-02
1	rs1833040	216,771,072-216,772,072	5.21E-03	1.21E-02	0.0004023	1	1	0.9759	0.9759	0.01294	0.1818
1	rs11117808	217,396,292-217,397,292	3.37E-03	8.09E-03	0.0003771	1	1	0.9098	0.9097	0.008908	0.1252
1	rs17047589	218,475,630-218,476,630	1.93E-04	5.74E-04	0.0002903	0.1377	0.1377	0.1287	0.1286	0.0006621	0.009307
1	rs16849180	229,044,392-229,045,392	7.34E-10	5.64E-09	8.19E-02	5.25E-04	5.25E-04	5.25E-04	5.25E-04	8.89E-06	1.25e-07
2	rs17046473	24,906,139-24,907,139	1.21E-08	7.48E-08	0.000107	8.62E-03	8.62e-06	8.62E-03	8.62e-06	1.12E-07	1.57E-03
2	rs13392392	42,053,778-42,054,778	3.80E-10	3.07E-09	7.63E-02	2.72E-04	2.72E-04	2.71E-04	2.71E-04	4.94E-06	6.94E-05
2	rs4510173	160,660,607-160,661,607	2.45E-06	1.01E-05	0.0002106	0.001749	0.001748	0.001747	0.001747	1.16E-02	0.0001628
2	rs12617336	162,848,812-162,849,812	5.45E-09	3.59E-08	9.31E-02	3.89E-03	3.89E-03	3.89E-03	3.89E-03	5.81E-05	8.17E-04
2	rs2060198	166,244,730-166,245,730	9.07E-04	2.40E-03	0.0003365	0.6482	0.648	0.477	0.4769	0.00269	0.03781
2	rs41376445	171,427,778-171,428,778	2.02E-05	7.12E-05	0.0002442	0.01441	0.0144	0.0143	0.0143	8.23e-05	0.001157
2	rs10803852	171,665,209-171,666,209	3.35E-03	8.05E-03	0.0003757	1	1	0.9088	0.9087	0.008903	0.1252
2	rs7601760	177,647,997-177,648,997	3.17E-11	3.10E-10	7.21E-02	2.27E-05	2.27E-05	2.27E-05	2.27E-05	4.36E-07	6.13E-06
2	rs6731229	239,315,047-239,316,047	4.75e-14	4.50E-10	7.35E-02	3.40E-05	3.40E-05	3.40E-05	3.40E-05	6.41E-07	9.00E-06
3	rs17582553	21,985,331-21,986,331	1.39E-12	1.73E-11	6.51E-02	9.96E-07	9.96E-07	1.03E-06	1.03E-06	2.12E-08	2.98E-07
3	rs11718264	109,472,195-109,473,195	1.41E-06	6.07E-06	0.0001966	0.001004	0.001004	0.001004	0.001003	7.12E-03	0.0001001
3	rs16856504	109,950,602-109,951,602	1.06e-07	3.30E-04	0.0002777	0.07575	0.07573	0.07295	0.07293	0.0003796	0.005336

CHR: chromosom; SNP: single nucleotide polymorphism identifier; POSITION: chromosomal localisation of the SNP (base pair position); UNADJ: unadjusted P-value, GC: ; QQ: ; BONF: P-value after Bonferroni correction; HOLM: P-value after Holm-Bonferroni correction; SIDAK: P-value after Šidák correction; FDR: .

Table 33 continued.

CHR	SNP	POSITION	UNADJ	GC	QQ	BONF	HOLM	SIDAK_SS	SIDAK_SD	FDR_BH	FDR_BY
4	rs16839778	7,174,191-7,175,191	7.36E-08	3.98E-07	0.0001266	5.26E-02	5.26E-02	5.26E-02	5.26E-02	5.78E-04	8.12E-03
4	rs10213406	7,906,827-7,907,827	1.11E-05	4.11e-08	0.0002358	0.007955	0.007953	0.007923	0.007921	4.71E-02	0.0006616
4	rs6825629	12,572,878-12,573,878	3.92E-10	3.16E-09	7.77E-02	2.8e-07	2.8e-07	2.8e-07	2.8e-07	5.00E-06	7.03E-05
5	rs36791	109,329,695-109,330,695	8.24E-04	2.2e-06	0.0003337	0.589	0.5888	0.4451	0.445	0.002465	0.03464
5	rs17131910	109,630,471-109,631,471	3.81E-06	1.53E-05	0.0002148	0.002724	0.002723	0.00272	0.002719	1.77E-02	0.0002486
6	rs478791	10,774,946-10,775,946	1.77E-03	4.45E-03	0.0003533	1	1	0.7169	0.7168	0.004988	0.07011
6	rs6936890	10,784,763-10,785,763	9.68E-03	2.15e-05	0.000447	1	1	0.999	0.999	0.02163	0.304
6	rs9366776	31,256,130-31,257,130	7.40E-03	1.68E-02	0.0004205	1	1	0.995	0.995	0.01758	0.2471
6	rs2068204	33,058,218-33,059,218	9.89E-06	3.69E-05	0.0002302	0.007071	0.007069	0.007046	0.007044	4.29E-02	0.0006024
6	rs929052	36,714,194-36,715,194	2.07E-08	1.23E-07	0.000114	1.48E-02	1.48E-02	1.48E-02	1.48E-02	1.80E-04	2.53E-03
6	rs12661480	37,962,808-37,963,808	3.28E-04	9.39E-04	0.0003043	0.2347	0.2346	0.2092	0.2091	0.001076	0.01513
7	rs10085558	37,984,780-37,985,780	5.11E-05	1.68E-04	0.0002609	0.03653	0.03652	0.03587	0.03586	0.0001953	0.002746
7	rs16879765	37,988,595-37,989,595	8.54E-04	2.27E-03	0.0003351	0.6102	0.61	0.4568	0.4566	0.002542	0.03574
7	rs2044830	38,023,904-38,024,904	3.76E-03	8.95E-03	0.0003883	1	1	0.9317	0.9316	0.009655	0.1357
7	rs17171240	38,024,074-38,025,074	8.07E-03	1.82E-02	0.0004274	1	1	0.9969	0.9969	0.01885	0.265
8	rs13260434	3,225,724-3,226,724	4.60E-03	1.08E-02	0.0003925	1	1	0.9626	0.9626	0.0117	0.1644
8	rs2623668	3,644,185-3,645,185	1.66E-04	4.99E-04	0.0002861	0.1185	0.1185	0.1118	0.1117	0.0005781	0.008126
8	rs11777623	75,897,198-75,898,198	6.25E-14	9.83E-13	6.23E-02	4.47E-08	4.47E-08	7.94E-08	7.93E-08	9.92E-10	1.40E-08
8	rs10875382	136,800,559-136,801,559	6.66E-07	3.05E-06	0.0001784	0.0004762	0.0004761	0.0004761	0.000476	3.72e-06	5.23e-05
9	rs7032394	2,159,878-2,160,878	2.04E-05	7.19e-08	0.000247	0.01457	0.01456	0.01446	0.01446	8.23E-05	0.001157
9	rs7032831	2,160,192-2,161,192	3.03E-05	1.04E-04	0.000254	0.02168	0.02168	0.02145	0.02144	0.0001191	0.001675

CHR: chromosom; SNP: single nucleotide polymorphism identifier; POSITION: chromosomal localisation of the SNP (base pair position); UNADJ: unadjusted P-value, GC: ; QQ: ; BONF: P-value after Bonferroni correction; HOLM: P-value after Holm-Bonferroni correction; SIDAK: P-value after Šidák correction; FDR: .

Kerstin Becker

Table 33 continued.

CHR	SNP	POSITION	UNADJ	GC	QQ	BONF	HOLM	SIDAK_SS	SIDAK_SD	FDR_BH	FDR_BY
9	rs10963171	17,635,927-17,636,927	1.12e-11	6.99E-08	0.0001056	8.00E-03	8.00E-03	8.00E-03	8.00E-03	1.05E-04	1.48e-06
9	rs7851959	20,307,666-20,308,666	4.04E-10	3.25E-09	7.91E-02	2.89E-04	2.89E-04	2.89E-04	2.89E-04	5.07E-06	7.12E-05
9	rs35517812	110,970,886-110,971,886	8.37E-03	1.88E-02	0.000433	1	1	0.9975	0.9975	0.0193	0.2713
9	rs7849991	111,278,442-111,279,442	9.46E-03	2.11E-02	0.0004428	1	1	0.9988	0.9988	0.02134	0.2999
9	rs10759289	111,280,824-111,281,824	8.91E-03	1.99e-05	0.0004358	1	1	0.9983	0.9983	0.02041	0.2869
9	rs10759290	111,280,841-111,281,841	6.42E-03	1.47E-02	0.0004107	1	1	0.9899	0.9898	0.01562	0.2195
9	rs7863555	123,185,097-123,186,097	2.58E-12	3.05e-14	6.79E-02	1.84E-06	1.84E-06	1.83E-06	1.83E-06	3.76E-08	5.29E-07
10	rs16924545	24,597,740-24,598,740	2.36E-12	2.81E-11	6.65E-02	1.69E-06	1.69E-06	1.67E-06	1.67E-06	3.51E-08	4.94E-07
10	rs745947	106,532,460-106,533,460	5.03E-04	1.39E-03	0.0003169	0.3597	0.3596	0.3021	0.302	0.001585	0.02227
10	rs1349624	106,830,602-106,831,602	5.00E-06	1.96E-05	0.0002176	0.003576	0.003575	0.003569	0.003568	2.29E-02	0.0003222
10	rs12415432	129,743,645-129,744,645	3.89e-16	5.32E-12	6.37E-02	2.78e-10	2.78e-10	3.17E-07	3.17E-07	6.05E-09	8.50E-08
11	rs501560	111,395,783-111,396,783	2.06E-03	5.13E-03	0.0003575	1	1	0.7701	0.7699	0.005742	0.08071
11	rs10891927	116,080,697-116,081,697	5.12E-03	1.19E-02	0.0003995	1	1	0.9742	0.9741	0.01278	0.1797
11	rs11216534	117,628,968-117,629,968	1.21e-10	6.30E-07	0.0001322	8.65E-02	8.65E-02	8.65E-02	8.64E-02	9.10E-04	1.28E-02
11	rs11216674	117,879,639-117,880,639	5.67E-04	1.56E-03	0.0003211	0.4053	0.4052	0.3333	0.3332	0.001762	0.02477
11	rs12225323	117,920,077-117,921,077	3.03E-04	8.71E-04	0.0003015	0.2164	0.2163	0.1946	0.1945	0.001002	0.01408
12	rs12321570	69,161,743-69,162,743	1.16E-11	1.22E-10	6.93E-02	8.29E-06	8.29E-06	8.25E-06	8.25E-06	1.66E-07	2.33e-09
15	rs9806619	47,471,900-47,472,900	7.49e-09	2.85e-08	0.0002218	0.005353	0.005352	0.005339	0.005337	3.37E-02	0.0004732
15	rs16960559	48,379,619-48,380,619	4.17E-05	1.39E-04	0.0002567	0.02978	0.02977	0.02934	0.02934	0.0001619	0.002275
15	rs8029891	50,439,732-50,440,732	1.55E-06	6.64e-09	0.000198	0.001107	0.001107	0.001106	0.001106	7.80E-03	0.0001096
15	rs6493942	57,962,582-57,963,582	2.00E-09	1.42E-08	8.89E-02	1.43E-03	1.43E-03	1.43E-03	1.43E-03	2.23E-05	3.14E-04
15	rs16944662	62,127,757-62,128,757	1.25E-06	5.45E-06	0.0001938	0.000894	0.0008938	0.0008936	0.0008934	6.43E-03	9.04e-05
15	rs4390546	63,208,686-63,209,686	9.51E-06	3.55E-05	0.0002274	0.006795	0.006794	0.006772	0.006771	4.17E-02	0.000586
15	rs1385951	65,215,457-65,216,457	5.76E-22	3.76E-20	4.27E-02	4.12E-16	4.12E-16	INF	INF	1.33E-17	1.87E-16
15	rs11856313	73,859,989-73,860,989	2.30E-11	2.30E-10	7.07E-02	1.65E-05	1.65E-05	1.64E-05	1.64E-05	3.23E-07	4.54e-06

CHR: chromosom; SNP: single nucleotide polymorphism identifier; POSITION: chromosomal localisation of the SNP (base pair position); UNADJ: unadjusted P-value, GC: ; QQ: ; BONF: P-value after Bonferroni correction; HOLM: P-value after Holm-Bonferroni correction; SIDAK: P-value after Šidák correction; FDR: .

Table 33 continued.

CHR	SNP	POSITION	UNADJ	GC	QQ	BONF	HOLM	SIDAK_SS	SIDAK_SD	FDR_BH	FDR_BY
16	rs1833203	53,390,957-53,391,957	5.61E-08	3.10E-07	0.0001238	4.01E-02	4.01E-02	4.01E-02	4.01E-02	4.51E-04	6.33E-03
16	rs2077576	78,338,264-78,339,264	2.51E-03	6.17E-03	0.0003617	1	1	0.8339	0.8338	0.006931	0.09743
16	rs2738694	78,518,357-78,519,357	4.40E-16	1.01E-14	5.25E-02	3.14E-10	3.14E-10	INF	INF	8.27E-12	1.16E-10
16	rs8052047	79,812,854-79,813,854	2.41E-209	5.29E-193	3.50E-03	1.72E-203	1.72E-203	INF	INF	5.75E-204	8.08E-203
16	rs41338245	80,834,241-80,835,241	3.20E-04	9.16e-07	0.0003029	0.2284	0.2283	0.2042	0.2041	0.001052	0.01479
16	rs804902	81,104,465-81,105,465	2.09E-08	1.25E-07	0.0001154	1.50E-02	1.50E-02	1.50E-02	1.50E-02	1.80E-04	2.53E-03
16	rs8058531	83,103,555-83,104,555	1.60E-07	8.16E-07	0.0001406	0.0001145	0.0001145	0.0001145	0.0001145	1.13E-03	1.59E-02
17	rs3744171	76,993,397-76,994,397	6.21E-05	2.02E-04	0.0002637	0.04441	0.0444	0.04344	0.04343	0.000235	0.003303
23	rs6421524	2,010,440-2,011,440	3.69E-03	8.80E-03	0.0003841	1	1	0.9284	0.9283	0.009575	0.1346
23	rs5982585	2,357,640-2,358,640	9.34E-04	2.47e-06	0.0003379	0.6675	0.6673	0.487	0.4869	0.002758	0.03877
23	rs311100	2,660,593-2,661,593	6.47e-07	1.76E-03	0.0003225	0.4624	0.4622	0.3702	0.3701	0.001994	0.02803
23	rs7889262	32,007,938-32,008,938	2.96e-07	8.53E-04	0.0002987	0.2115	0.2115	0.1907	0.1906	0.0009885	0.01389
23	rs553369	154,962,939-154,963,939	1.96E-04	5.82E-04	0.0002931	0.1398	0.1398	0.1305	0.1305	0.0006658	0.009359

CHR: chromosom; SNP: single nucleotide polymorphism identifier; POSITION: chromosomal localisation of the SNP (base pair position); UNADJ: unadjusted P-value, GC: ; QQ: ; BONF: P-value after Bonferroni correction; HOLM: P-value after Holm-Bonferroni correction; SIDAK: P-value after Šidák correction; FDR: .

7.4 Whole Genome Expression Analysis detailed Results

Table 34. Wnt/β-catenin signalling pathway components.

SYMBOL	case Signal	case STDEV	case Pval	Control Signal	control STDEV	control Pval	DiffScore	Fold change	CHR
WNT11	24.7	17.5	0.0079	87.5	31.4	0	33.94	-3.54	11
RSPO3	131.7	176.3	0	420.6	196.9	0	17.40	-3.19	6
SOX8	77.5	62.1	0	226.1	136.2	0	14.78	-2.92	16
TLE1	42.2	24.8	0.0026	105.3	21.3	0	38.15	-2.50	9
TCF7L1	50.4	24.1	0	111.2	39.8	0	22.82	-2.21	2
FRAT1	9.1	3.5	0.0017	16.7	8.8	0.0002	9.72	-1.83	10
TCF7L2	55.6	33.9	0	99.7	30.8	0	13.99	-1.79	10
SFRP1	1548.9	1440.2	0	2567.3	971.6	0	5.59	-1.66	8
SOX9	158.8	142.6	0	256.2	227.0	0	2.37	-1.61	17
LRP5	164.9	82.6	5.55E-05	258.3	64.9	8.68E-07	10.80	-1.57	11
TLE3	41.7	19.9	0.0026	64.9	32.7	0	5.92	-1.55	15
LRP1	126.2	43.6	0	194.1	63.6	0	11.95	-1.54	12
VEGFA	19.3	8.1	0.1214	29.2	12.1	0.0832	9.23	-1.51	6
MARK2	10.9	6.7	0.0082	16.1	7.9	0.0006	2.63	-1.47	11
VEGFB	817.5	132.6	0.0370	1192.8	281.2	0.0305	11.15	-1.46	
BTRC	6.9	4.4	0.0099	10.0	3.9	0.0072	2.00	-1.44	10
TGFBR3	1763.6	731.5	0	2497.2	398.4	0	11.97	-1.42	1
SOX13	148.9	65.4	0	195.8	80.6	0	3.43	-1.32	1
WNT2	23.6	13.1	0.0079	30.4	30.0	0.0013	1.02	-1.29	7
MAP4K1	14.8	7.0	0.0004	18.9	13.4	0.0001	1.53	-1.28	19
TLE2	176.6	78.6	0	218.6	96.7	0	2.11	-1.24	19
MAP4K2	201.7	54.1	0	244.6	35.0	0	7.07	-1.21	11
SOX10	27.6	25.2	0.0053	32.6	34.7	0.0013	0.48	-1.18	22
PIN1	909.3	191.2	0	1060.0	184.8	0	5.24	-1.17	19
MAP3K7IP1	29.2	11.4	0.0231	34.0	8.7	0.0013	4.67	-1.16	22
TCF15	7.6	4.4	0.0303	8.8	5.5	0.0250	0.77	-1.15	20
WNT16	6.5	2.4	0.0099	7.4	3.7	0.0173	0.66	-1.13	7
PPARD	18.2	5.1	0.0013	20.5	8.1	0.0018	0.56	-1.13	6
LRP6	16.4	7.0	0.0105	18.4	13.0	0.0092	0.58	-1.12	12
SRC	87.5	28.9	0.1364	92.0	34.9	0.0617	0.75	-1.05	20
NR5A2	17.3	8.0	0.0199	18.1	6.1	0.0096	0.43	-1.05	1
CCND1	2075.3	628.2	0	2171.5	990.7	0	0.31	-1.05	11
UBB	6503.8	981.1	0	6796.1	1076.2	0	1.17	-1.04	17
DVL3	287.0	79.4	0	298.6	85.3	0	0.38	-1.04	3
WNT2B	10.7	4.8	0.0006	11.1	6.3	0.0005	0.11	-1.03	1
TCF25	704.1	196.3	0	721.1	179.7	0	0.23	-1.02	16
AKT1	818.8	224.1	9.99E-05	832.7	129.4	0.0031	-0.53	-1.02	14
SOX14	8.2	3.6	0.0224	8.3	4.3	0.0264	0.05	-1.01	3
UBC	8910.0	647.0	7.50E-06	8820.6	699.1	2.44E-05	-0.98	1.01	12
MAP4K3	55.7	18.5	0	54.9	19.4	0	-0.09	1.01	2

Given is a selection of genes involved in or affected by the Wnt/β-catenin canonical pathway and expressed in DD (case) and control connective tissue. Signal: detection signal mean, STDEV: standard derivation from signal mean (N = 12), Pval: detection p-value. Genes are sorted by expression fold change, genes with the lowest fold change at the top.

Table 34 continued.

SYMBOL	case Signal	case STDEV	case Pval	Control Signal	control STDEV	control Pval	DiffScore	Fold change	CHR
AXIN1	147.6	16.3	0.0113	144.0	20.2	0.0098	-0.11	1.03	16
RUVBL2	149.5	45.4	0	143.0	74.8	0	-0.28	1.05	19
DVL1	8.3	6.4	0.0446	7.9	6.2	0.0572	-0.50	1.06	1
NFKB1	1008.7	149.0	0	917.0	147.4	0	-3.25	1.10	4
APPL1	35.4	9.6	0.0040	32.0	7.8	0.0013	-1.48	1.10	3
NLK	7.3	4.6	0.0316	6.6	5.3	0.0290	-0.39	1.11	17
EP300	173.9	47.1	0	157.1	56.4	0	-1.17	1.11	22
HDAC1	728.3	128.1	0	657.0	115.7	0	-2.94	1.11	1
TGFBRAP1	124.0	61.9	0	110.1	56.8	0	-0.75	1.13	2
ILK	763.6	163.5	0.0025	674.2	110.8	0.0224	-2.01	1.13	11
MAP3K7IP2	6.1	3.1	0.0064	5.3	2.3	0.0048	-1.07	1.16	6
RARA	135.4	50.9	0.1332	112.9	50.0	0.0321	0.14	1.20	17
TCFL5	258.9	76.2	0	211.4	37.5	0	-5.11	1.22	20
CSNK1A1	77.9	17.9	1.05E-06	63.4	10.5	1.05E-06	-4.67	1.23	5
TGFBR2	1419.2	430.7	1.95E-07	1125.5	261.7	8.23E-08	-3.64	1.26	3
DVL2	139.1	16.1	0	109.5	16.2	0	-22.59	1.27	17
JUN	1040.6	541.8	0	770.2	233.2	0	-3.53	1.35	1
WNT5B	53.0	25.2	0.3166	36.9	18.3	0.4120	-2.75	1.43	12
MMP7	383.4	473.6	0	266.0	362.8	0	-0.95	1.44	11
MAP3K7	204.4	63.4	3.47E-06	141.2	25.4	7.81E-06	-10.42	1.45	6
TCF3	143.1	41.6	0	98.4	31.3	0	-11.47	1.46	19
WISP2	1426.6	1009.7	0	977.0	473.6	0	-2.81	1.46	20
TCF20	79.1	8.0	0.0010	53.8	9.8	0.0009	-13.92	1.47	22
FRAT2	239.0	38.2	0	162.1	37.9	0	-26.00	1.47	10
CDH5	697.2	307.5	0	469.7	113.6	0	-7.71	1.48	16
APPL2	719.3	209.0	0	468.8	143.2	0	-14.69	1.53	12
TCF4	798.8	159.5	0	519.0	89.5	0	-28.63	1.54	18
GSK3B	165.1	70.8	0	106.5	34.4	0	-8.77	1.55	3
PPP2R4	140.4	58.7	0.0060	90.3	16.7	0.0150	-4.42	1.55	9
BCL9	89.7	27.4	0	56.9	9.9	0	-18.23	1.58	1
CD44	2037.1	313.5	3.05E-09	1251.3	504.8	0	-12.80	1.63	11
SOX17	55.8	19.3	0	33.6	13.9	0.0013	-13.26	1.66	8
AXIN2	486.7	113.7	0	291.9	90.3	0	-23.78	1.67	17
RSPO2	23.4	14.0	0.0008	13.9	5.7	0.4638	-5.89	1.68	8
TGFB1I1	152.3	72.8	0	87.0	44.1	8.68E-07	-7.27	1.75	16
SOX18	1485.9	1002.7	0	847.8	337.6	0	-5.91	1.75	20
WNT5A	44.2	30.6	0.0026	24.5	13.5	0.0040	-5.59	1.80	3
CDH1	266.5	381.4	0	141.1	204.6	0	-1.65	1.89	16
TLE4	109.6	29.8	2.17E-05	57.7	11.0	7.03E-05	-22.80	1.90	9
SOX7	101.7	77.9	5.55E-05	52.8	21.9	8.68E-05	-4.40	1.92	8
SOX12	16.6	14.0	0.0105	8.6	4.0	0.0237	-4.95	1.93	20
MAP4K5	112.1	32.3	4.25E-05	57.8	22.7	0.0004	-18.93	1.94	14
WNT4	11.6	14.1	0.0171	5.9	5.9	0.0329	-2.48	1.97	1
MYC	217.4	100.7	3.47E-06	109.5	20.9	1.39E-05	-14.92	1.99	8

Given is a selection of genes involved in or affected by the Wnt/β-catenin canonical pathway and expressed in DD (case) and control connective tissue. Signal: detection signal mean, STDEV: standard derivation from signal mean (N = 12), Pval: detection p-value. Genes are sorted for expression fold change, genes with the lowest fold change at the top.

Table 34 continued.

SYMBOL	case Signal	case STDEV	case Pval	Control Signal	control STDEV	control Pval	DiffScore	Fold change	CHR
SOX15	119.3	68.1	0	59.9	37.4	0	-9.24	1.99	17
CTNNB1	61.2	28.3	0.0038	30.4	9.7	0.0096	-5.05	2.01	
TP53	45.0	23.7	0.0026	22.2	19.6	0.0053	-8.70	2.03	17
TCF12	242.6	74.5	3.96E-05	112.9	17.6	0.0005	-22.13	2.15	15
KREMEN1	40.1	21.5	0.0002	17.6	9.1	0.0004	-9.21	2.28	22
APP	1185.6	448.2	0	512.3	174.1	2.44E-08	-21.62	2.31	21
WNT3	23.7	15.8	0.0079	9.6	8.5	0.0224	-9.77	2.47	17
UBD	36.5	30.5	0.0026	14.0	11.4	0.0119	-7.65	2.61	6
VEGFC	123.6	34.4	0	47.4	19.0	0	-38.21	2.61	4
MAP4K4	295.7	74.2	0.0009	111.8	18.9	0.0053	-30.38	2.65	2
SFRP4	1557.9	506.2	4.25E-05	581.9	730.9	0.0009	-16.71	2.68	7
TGFBR1	6.4	3.5	0.0369	2.2	5.0	0.1594	-7.32	2.87	9
DKK3	1502.4	343.6	0.0016	491.0	453.5	0.0164	-22.09	3.06	11
CDH3	67.8	48.4	0	22.0	32.8	0.0040	-9.66	3.08	16
SOX4	110.6	44.0	0	31.4	15.0	0.0013	-32.88	3.52	6
TGFBI	9670.5	5813.0	0	2352.2	1504.2	0	-20.69	4.11	5
WNT7B	10.7	12.9	0.1201	2.5	2.6	0.3283	-4.58	4.19	22
TGFB3	1300.1	494.9	0	261.9	143.4	0	-39.82	4.96	14
SFRP2	1486.9	763.0	0	257.5	180.4	0	-29.56	5.78	4
GJA1	1005.3	595.5	0	173.6	80.7	0	-24.88	5.79	6
DKK2	21.9	15.4	0.0001	3.6	2.7	0.1156	-18.96	6.06	4
LEF1	58.6	36.5	3.47E-06	8.6	3.3	0.0115	-23.18	6.79	4
CDH2	174.7	175.7	0	17.4	7.5	0.0092	-12.30	10.03	18
TGFB2	133.2	93.5	0	12.0	9.9	0.0145	-22.42	11.12	1
SOX21	27.2	58.7	0.0053	1.8	3.3	0.2240	-3.18	15.25	13
WISP1	125.6	75.7	0.0001	0.3	5.3	0.4437	-28.66	380.60	8

Given is a selection of genes involved in or affected by the Wnt/β-catenin canonical pathway and expressed in DD (case) and control connective tissue. Signal: detection signal mean, STDEV: standard derivation from signal mean (N = 12), Pval: detection p-value. Genes are sorted for expression fold change, genes with the lowest fold change at the top.

8   Erklärung

Ich versichere, dass ich die von mir vorgelegte Dissertation selbständig angefertigt, die benutzten Quellen und Hilfsmittel vollständig angegeben und die Stellen der Arbeit – einschließlich Tabellen, Karten und Abbildungen –, die anderen Werken im Wortlaut oder dem Sinn nach entnommen sind, in jedem Einzelfall als Entlehnung kenntlich gemacht habe; dass diese Dissertation noch keiner anderen Fakultät oder Universität zur Prüfung vorgelegen hat; dass sie – abgesehen von unten angegebenen Teilpuplikationen – noch nicht veröffentlicht worden ist sowie, dass ich eine solche Veröffentlichung vor Abschluss des Promotionsverfahrens nicht vornehmen werde.

Die Bestimmungen dieser Promotionsordnung sind mir bekannt. Die von mir vorgelegte Dissertation ist von Herrn Prof. Dr. Peter Nürnberg betreut worden.

Nachfolgend genannte Teilpublikationen liegen vor:

Wnt Signaling and Dupuytren's Disease. Dolmans GH, Werker PM, Hennies HC, Furniss D, Festen EA, Franke L, Becker K, van der Vlies P, Wolffenbuttel BH, Tinschert S, Toliat MR, Nothnagel M, Franke A, Klopp N, Wichmann HE, Nürnberg P, Giele H, Ophoff RA, Wijmenga C; the Dutch Dupuytren Study Group, the German Dupuytren Study Group, the LifeLines Cohort Study, and the BSSH–GODD Consortium. N Engl J Med. 2011 Jul 6.

Ich versichere, dass ich alle Angaben wahrheitsgemäß nach bestem Wissen und Gewissen gemacht habe und verpflichte mich, jedmögliche, die obigen Angaben betreffenden Veränderungen, dem Dekanat unverzüglich mitzuteilen.

…………………………………   …………………………………….

Datum   (Kerstin Becker)